SC

FILTRATION OF NON-NEWTONIAN FLUIDS

by

A. R. Koteswara RAO

A thesis submitted in partial fulfillment
of the requirement for the degree of

Doctor of Philosophy

in the

DEPARTMENT OF CHEMICAL ENGINEERING
UNIVERSITY OF OTTAWA

Ottawa, Canada March, 1970

Research Director

Candidate

ABSTRACT

In view of increasing usage and importance of non-Newtonian fluids in the chemical industries and in scientific research, an investigation into the filtration of non-Newtonian fluids was undertaken. During the course of the present investigation, filtration equipment was designed and constructed to conduct experiments to substantiate the theoretical analysis for the filtration of incompressible, time independent non-Newtonian fluids. The fundamental relationship formulated for filtration in the course of this investigation, which incorporates recent modifications of Tiller and Shirato[4] and of Shirato et al.[5, 6], accounting for the variation of the superficial velocity of the liquid through the cake and the velocity of the particles of the cake associated with cake compaction, was experimentally verified and confirmed. Also experimental data were obtained to establish the viability and efficiency of an improved method of treatment[84, 85] in which the filtration is considered to be comprised of an initial stage and the main filtration stage yielding a convenient means of characterization of the initial stage of filtration and of its effects on filter medium and cake characteristics. Further, the usefulness of the concepts and relationships developed for filtration in the interpretation and processing of experimental data is demonstrated utilizing the data collected in the constant pressure and constant rate filtration of slurries of calcium carbonate in water and in hydroxyethyl cellulose (Natrosol 250) solutions. The filtration area of the apparatus was 4.51×10^{-2} sq. ft. and the calcium carbonate content of the slurries was 2.5 per cent by weight. The applied filtration pressure and flow rate in the constant pressure and constant rate experiments ranged between 50 to 350 psi and 2.24×10^{-4} to 3.29×10^{-3} ft./sec., respectively.

ACKNOWLEDGEMENT

The author is deeply indebted to his supervisor, Professor William Kozicki, for the advice, guidance, encouragement and personal understanding throughout the course of this research. He also wishes to acknowledge other faculty members of the Chemical Engineering Department, particularly Dr. B. C. -Y. Lu, for their interest in this work.

The author wishes to express his gratitude to Dr. Carlos Tiu and Mr. S. N. Pasari for their assistance from time to time. Further, he is thankful to Mr. C. P. Khulbe for his ready help in conducting the experiments and preparing the drawings.

Author's appreciation is also extended to Mr. G. Gasperetti for his willing assistance in the design and construction of equipment.

TABLE OF CONTENTS

page

LIST OF TABLES

TABLE page

LIST OF FIGURES

FIGURE page

FIGURE page

FIGURE page

FIGURE page

FIGURE page

NOMENCLATURE

A = cross-sectional area of the filter bed

A = quantity defined by Equation (117)

B = quantity defined by Equation (118)

A_1 = empirical constant defined in m-p correlation

B_1 = empirical constant defined in m-p correlation

D = diameter of capillary tube

e = $\varepsilon/(1-\varepsilon)$, local void ratio

g_c = conversion factor

h = vertical distance from a horizontal datum plane

I = unit tensor

J_R = correction factor for the conventional filtration resistance α_R for Newtonian fluids

J_{Rn} = correction factor, defined by the integral on the right side of Equation (94), for the conventional filtration resistance α_R for non-Newtonian fluids

K = characteristic value of the fluid consistency index

K = function defined by Equation (26)

K_r = constant defined by Equation (42)

k = permeability defined in Darcy's equation; bold letter denotes permeability tensor

k_i = impermeability factor

m = moisture ratio, ratio of mass of wet to dry cake

m_o = empirical constant defined by Equation (114)

N = function defined by Equation (109)

N = number of experimental points

n = characteristic value of flow behaviour index

n_o = empirical constant defined in α-p correlation

n' = flow behaviour index defined by equation $n' = \dfrac{d\left(\ln \dfrac{D\Delta P}{4L}\right)}{d(\ln 8\langle U\rangle/D)}$

n_o = empirical constant defined in α_T-p correlation

n_o = empirical constant defined in λ-p correlation

n_1 = empirical constant defined in n-p correlation

p = applied filtration pressure

p_s = solids compressive pressure

p_1 = hydraulic pressure at the filter medium and cake interface

p' = $p + \rho gh/g_c$, potential function

q = instantaneous local superficial velocity vector of the liquid in cake; bold letter denotes velocity vector

q_s = effective superficial surface velocity of the liquid; bold letter denotes velocity vector

q_x = local superficial velocity of the liquid at distance x from the medium

q_1 = superficial velocity of the filtrate at the exit of the cake

R_m = filter medium resistance

R_h = hydraulic radius defined by Equation (5)

r = instantaneous local superficial velocity of solid particle; bold letter denotes velocity vector

r_o = empirical constant defined in α-p correlation

r_x = local superficial velocity of solids at distance x from the medium

S_o = specific surface per unit volume of solid particles

s = mass fraction of solids in the slurry

T = tortuosity of the filter bed

u = instantaneous local velocity of the liquid in the cake

$\langle u \rangle$ = average velocity of the liquid in the cake void space

u_p = instantaneous local velocity of solid particles; bold letter denotes velocity vector

$\bar{u}_s$ = average effective surface velocity of the liquid

V = cumulative filtrate volume

V_o = initial effective cumulative filtrate volume

v = cumulative filtrate volume per unit area

v_i = filtrate volume interval of initial stage

v_o = initial effective volume of filtrate per unit area

v_o = function defined by Equation (27)

w = mass of cake solids per unit area

w_x = mass of cake solids per unit area in distance x from the medium

x = distance from the medium

X = $\log (p - p_l)$

Y = $\log (\theta + \theta_c)$

GREEK LETTERS

α = average specific filtration resistance

α_R = conventional average specific cake resistance defined by Equation (21)

α_T = total specific cake resistance defined by Equation (96)

α_x = local specific cake resistance defined by Equation (13)

γ = rate of deformation tensor

ϵ = local value of porosity of the filter cake

ϵ_x = local value of porosity at distance x from the medium

ξ = aspect factor

$\mathbb{K}$ = function defined by Equation (101)

λ = function defined by Equation (112)

λ_o = empirical constant in λ-p correlation

η = non-Newtonian viscosity

η_{ap} = apparent viscosity; bold letter denotes apparent viscosity tensor; η_{ij}, component of the apparent viscosity tensor

μ = viscosity of the liquid

θ = time

θ_o = effective time of commencement of filtration defined by Equation (32)

θ_i = time interval of initial transient stage of constant rate filtration

θ_c = v_o/q_1, time correction term

ρ = density of the liquid

ρ_s = density of solid particles

$\bar{\sigma}^2$ = $\frac{1}{N}\sum^{N} (Y_{expt} - Y_{calc})^2$, variance. Here N denotes the number of experimental points

τ = shear stress tensor

$\bar{\tau}_w$ = average shear stress at the solid surface

$\bar{\tau}_y$ = yield stress

Φ = mapping tensor defined by Equation (71)

∇ = del operator

SUBSCRIPTS

i,j = 1, 2, 3 refer to the components of vector and tensor quantities

α = refers to the component along the α-principal axis, e.g., α = x, y, z in Cartesian coordinates

x = refers to the quantity evaluated at distance 'x' from the filter medium

CHAPTER I

INTRODUCTION

Filtration is the operation in which a heterogeneous mixture of fluid and particles of solid are separated by a filter medium which permits the flow of the fluid but retains the particles of solid. By means of a pressure difference applied between the slurry inlet and the filtrate outlet, filtrate is forced through the equipment. The solid particles are trapped within the pores of the membrane and build up as a layer on the surface of this membrane. The fluid, which may be either gas or liquid, passes through the bed of solids and through the retaining filter medium.

Industrial filtrations range from simple to highly complex separations. The fluid may be a liquid or gas, the solid particles may be coarse or fine, rigid or plastic, round or elongated, separate individuals or aggregate. Therefore a multitude of filters has been developed to meet the different problems. However, the underlying basic principles of filtration in all these cases inherit their origin from the flow of fluids through the porous materials, possessing either compressible or incompressible characteristics. Most of the early studies were confined to the flow of Newtonian fluids through these porous materials thereby indirectly resulting in the development of filtration of only Newtonian fluids. This confinement to investigations involving only to Newtonian fluids is not because of the materials, whose flow behaviour in shear can not be characterized by Newtonian relationship, being less important in processing industries and elsewhere. At the early stages, attempts were not made to investigate the flow of non-Newtonian fluids through the porous media because of the mathematical complications involved, in addition

to the insufficient understanding of the behaviour of these fluids under different conditions of shear stress.

Industries in which non-Newtonian fluid behaviour is encountered include those dealing with the following: Rubber, plastics and synthetic fibers, petroleum, soap and detergents, pharmaceuticals, biological fluids, atomic energy, cement, foods, paper pulp, paint, light and heavy chemicals, fermentation processes, oil field operations, ore processing and printing. It is evident therefore that an understanding of non-Newtonian flow may enable substantial economic improvement to be made in a wide diversity of processing techniques. Hence, the flow of non-Newtonian fluids through packed bed and porous media has received considerable attention recently. Despite the large number of investigations devoted to the flow of rheologically complex fluids through packed beds and porous media in the past decade, which have been described in a recent comprehensive paper by Savins[60], relatively little work providing the fundamental information has been undertaken concerning the flow of these complex fluids through anisotropic compressible porous media. Such information is pertinent to the study of the filtration of the non-Newtonian fluids, a subject of great importance to the chemical industry because of the constantly increasing proportion of fluids with non-Newtonian flow characteristics being manufactured industrially.

In view of the increasing usage and importance of non-Newtonian fluids in the chemical industries and in scientific research, an investigation into the filtration of non-Newtonian fluids was undertaken for this thesis research work. In the initial part of this work, filtration studies were conducted with slurries of calcium carbonate in water and in dilute carboxy methyl cellulose (CMC) solutions to provide the guide lines for modification of the equations derived in

the first attempts at analysis and formulation of the problem and to incorporate the necessary alterations in the final design of the filtration equipment. The details pertaining to this part of the work are presented elsewhere[1] and so are not included in this thesis.

During the course of the present investigation, filtration equipment was designed and constructed to conduct experiments to substantiate the theoretical analysis for the filtration of incompressible, time independent non-Newtonian fluids. The fundamental relationship formulated for filtration in the course of this investigation, which incorporates recent modifications of Tiller and Shirato[4] and of Shirato et al.[5], accounting for the variation of the superficial velocity of the liquid through the cake and the velocity of the particles of the cake associated with cake compaction, was experimentally verified and confirmed. Also, experimental data were obtained to establish an improved method of treatment[84, 85] in which the filtration was considered to be comprised of an initial stage and main filtration stage to yield a convenient means of characterization of the initial stage of filtration and of its effects on the filter medium and cake characteristics. Further, the usefulness of the concepts and relationships developed[84, 85, 86] for filtration in the interpretation and processing of experimental data is demonstrated utilizing the data collected in the constant pressure and constant rate filtration of slurries of calcium carbonate in water and of slurries of calcium carbonate in hydroxyethyl cellulose (Natrosol 250) solutions.

CHAPTER II

LITERATURE SURVEY

Single and multiple phase fluid flow through particulate beds occurs on a universal scale in both natural and man directed operations. In spite of its basic importance in widely divergent fields, relatively little emphasis has been placed on experimental and theoretical investigations in comparison to such fields as mass and heat transfer. Several obstacles have impeded progress in filtration and flow through porous media. First, the complexity of even the most simple model discourages the investigators from attempting solutions. Secondly, the nature of the particles and precipitates forming the filter beds is such that reproducibility becomes a serious problem. The researcher finds that he must not only deal with the difficult flow problem but must also contend with the vagaries of crystal formation and flocculation. In spite of the relatively little emphasis that has been placed on the field because of the obstacles, fairly good progress has been made in the recent past.

The equation governing filtration originated in the work of Almy and Lewis[7], who filtered chromium hydroxide in a small plate and frame press at a series of constant pressures. Subsequently, Sperry's equation[8, 9] was deduced from theoretical considerations. These equations had been prompted by the anology between the filtration process and the flow of ground water through soil. The essential difference between Lewis' and Sperry's equations was the manner in which the effect of filter-base resistance was treated. Because of the fact that Sperry's treatment led to a more formidable expression, the Lewis equation had been generally

accepted for engineering purposes. Though there were many attempts[10, 11, 12] reported in the literature to improve these filtration equations, the success achieved was not outstanding. Significant advances were achieved by Ruth and coworkers[13, 14, 15] in the theory of filtration. They postulated that the resistance of a filter cake could be expressed as a linear function of pressure, a form which possessed decided advantages over the accepted Lewis equation. In the course of the work performed in their laboratories, a modified equation governing filtration had been developed and a number of methods were worked out for analysing the data of filter tests. The success of their work had been attributed in large measure to the new conceptions of the specific cake resistance and the methods of treatment. For slightly compressible materials they claimed superiority of constant rate filtration over constant pressure filtration for a number of specified reasons[13]. In continuation of his work in the field of filtration, Ruth[2] established the mathematical background for treatment of constant rate and constant pressure filtration that was used with complete satisfaction for several years. Mathematical simplicity in relation to the engineering requirements of analysis and design had been the prime objective of this development, yet neither the accuracy nor correctness of concept had been sacrificed in its attainment. The fundamental axiom of filtration with its essential postulate that filter septum resistance may be expressed in terms of filtrate volume had served as the basis for constant pressure filtration. In contrast, it was found just as essential to the simple treatment of constant rate filtration that the concept be discarded and septum resistance be expressed as a pressure drop. Further, Ruth[16] focused his attention on the nature of fluid flow through filter septa and its importance in the filtration equation. At this stage of development, Carman[17]

introduced the application of the Kozeny equation[18] to filtration, which gained universal importance. The Kozeny-Carman equation was derived for viscous flow in granular beds on the assumption of perfectly random packing of discrete particles and through the use of the mean hydraulic pore diameter expressed in terms of the void fraction and particle specific surface. Carman[19] and later Sullivan and Hertel[20], Sullivan[21, 22], and Coulson[23] had experimentally demonstrated that the constant in the Kozeny-Carman equation is a function of both particle shape and orientation (i. e. the shape of cross section available for flow), and the ratio of the length of actual flow path to cake thickness for beds with oriented packings. For random packing of incompressible beds (i. e. beds or cakes having a constant cross section porosity from top to bottom), the same constant had been calculated from experimental data for spherical and nonspherical particles by Carman[24, 25], Fair and Hatch[26], Hatch[27], Lea and Nurse[28], and Blain[29]. The experimental difficulties in applying this approach to compressible cakes of small particles, using data collected from actual filtrations, were considerible. Those difficulties arose from the fact that in filtration of compressible cakes the mechanical pressure stress on cake particles varies through the cake depth, causing variation in cake porosity and specific resistance through the depth of the deposited cake[2, 17, 30]. In view of these factors, a method whereby compressible filter cakes having uniform porosity through their depth could be formed and their permeability and pressure measured as a function of mechanical pressure stress appeared to be a practical approach to the application of granular bed theory to compressible filter cakes. This approach was suggested by Heertjes[31], Miller[32] and Ruth[33], and the latter employed this attack in a study of cakes of a single

material. The specific filtration resistance of finely divided solids and chemical precipitates was generally greater than could be accounted for on the basis of the Kozeny equation. A modification[33] was proposed in which abnormal resistance to passage of liquids was explained by the assumption that a portion of a measured void volume was unused or "dead". In the same report, a method was described for experimentally distinguishing the resistance contribution of dead void volume from that of particle size and shape by means of permeability tests on solids subjected to increasing degrees of mechanical compression. It was further advocated that the hypothesis of dead void volume had physical basis as a region adjoining the capillary wall in which electro-osmosis, induced by streaming potential generation, opposed the flow caused by the hydrostatic pressure difference.

B. F. Ruth[33] and Carman[17, 25] introduced the consolidometer or the compression permeability cell to investigate the local filter cake conditions for estimating the overall filter cake characteristics after deriving an approximate theoretical expression relating the average specific resistance of cake to local value of specific cake resistance. One of the most important assumptions in predicting filtration characteristics from the result obtained by the compression-permeability experiment, is that the local value of porosity and the local specific filtration resistance of filter cake, in dynamic state, are equivalent to the values obtained for the compressed cake, in a static equilibrium state, in a consolidometer. Experimental work on cakes of seventeen materials of subsieve and submicron ultimate particle size was reported by Grace[34] initiating a direct attack on the nature of variation of specific cake resistance through the development and extensive application of compression-

permeability technique for studying cake properties. Application of Kozeny-Carman and other similar relationships to the data was considered, and the limitations of these relationships were stated where particle flocculation was a controlling factor. During the course of these investigations, Grace[34] disproved the hypothesis of Ruth[33] that a back electro-osmosis or electro-viscous effect might account for the increased resistance, in the light of the theoretical work by Booth[35] and Elton[36]. Calculations based on the formulas developed for predicting the magnitude of this effect showed that at the electrolyte concentration employed, the effect would be negligible even if a back electro-osmosis or electro-viscous effect existed. Experimental work of Dobry[37] had indicated that this postulated effect could not be realised in practice. The controlling role of particle flocculation with the compressible cakes was further defined by Grace[38] through the application of microscopic and light transmission techniques for characterizing the degree of particle flocculation in the feed suspension and the correlation of the degree of flocculation with values of average specific cake resistance for resulting filter cakes. Further, the utility of the compression-permeability method in sizing pressure or vacuum filters for compressible cakes was confirmed.

Based on the Kozeny law relating the rate of flow to the porosity, Tiller[39] developed a method for determining (i) the pressure drop versus the depth, and the flow versus the applied pressure in a fixed bed of solids; (ii) the volume versus time relationship in constant pressure filtration. He assumed that porosity is solely a function of the pressure on solids, thus eliminating solids such as certain naturally occurring clays in which application of pressure causes only a slow approach to the equilibrium

porosity. Further, Tiller correlated the per cent voids to the pressure by a power function with powers ranging from 0.01 to 0.05 for applied pressures up to 100 psi for such materials as Kaolin, calcium carbonate, carbon black, diatomaceous earth, and mixtures of these materials. Numerical methods were used as a tool for the calculation of constant rate and constant pressure filtration. Based on the graphical methods[39], Tiller[40] later developed analytical equations which were similar to the empirical equations used by Coimbra[41] and Luke[42]. The proposed equations were valid for the substances studied by Grace for pressures up to 100 psi except for the more highly compressible materials. Kottwitz and Boylan[43] conducted filtration tests at constant pressure on commercial-scale equipment using pearl corn-starch and noticed that the specific filtration resistance predicted from the compression-permeability test data agreed very well with the actual specific filtration resistance of the prefilt leading to the conclusion that filtration theory can be satisfactorily used in the industrial practice.

Till this stage of development, virtually all the filtration literature was concerned with constant rate or constant pressure, with greater emphasis on the latter. The operation of most of the pressure filters is usually constant rate during the early stages and constant pressure during much later stages of the cycle because of the characteristics of the centrifugal pump, which is generally used for feeding the slurry. Recently, Tiller[44] developed methods for predicting pressure-volume-time relationships in variable-pressure-variable-rate operation.

The introduction of the new theory[3] of variation of flow rate with respect to distance through a filter cake revolutionised the

filtration theory by pointing out that certain assumptions which had previously served as basis for conventional equations employed in constant pressure filtration were in error. New partial differential equations were presented for flow through compressible media in which flow rate varies with cake thickness and the conventional constant pressure equations were modified to satisfy the new theory. Tiller and Huang[3] attempted to develop equations describing filtration in terms of gross measurable parameters taking into consideration the new theory. It was observed[45] that under conditions where superficial flow rate through the cake was constant and the medium pressure could be neglected, local porosity and hydraulic pressure were functions of fractional cake distance. Shirato[46] and coworkers carried on investigations on the filtration behaviour of two slurries and concluded that, when the particle size distribution of the precipitates of two slurries are approximately the same, the equilibrium porosity of the mixed sludge is nearly equal to the simple additive value, and, when the particle size distributions are considerably different, the equilibrium porosity of the mixed sludge is less than the additive value. A new definition of filtration resistance was presented[4] in view of the new theory[45, 47] showing that the filtration resistance depends upon slurry concentration as well as applied pressure. Shirato and Sambuichi[48] conducted experimental and theoretical studies on constant pressure filtration of thick slurries and arrived at a conclusion that the modern theory was able to cover various practical aspects of filtration processes. Further, the conventional expressions for hydraulic pressure distribution were revised[49] in view of this theory of variation of flow rate with respect to distance through a filter cake. Good agreement was noticed in the observed values of the hydraulic

pressure distributions when compared with the new theoretical values predicted from the compression-permeability data and with an analytic approximate expression derived[49]. Recently, attention was diverted to multi-dimensional filtration and many reports [50, 51, 52, 53, 54] on this subject are available in literature.

Before 1963, the literature is confined only to Newtonian filtration indicating the lack of development in the field of non-Newtonian flow through porous media. The flow of non-Newtonian fluids through packed beds and porous media has received considerable attention recently[55, 56, 57, 58, 59]. An excellent interpretive review of the published literature on this subject has been presented by Savins[60] at a recent conference. Kozicki and coworkers[1] conducted a study of non-Newtonian flow through porous materials and eventually applied their concepts to the problem of non-Newtonian filtration. At the present time, no other reports appear to be available in the literature on the filtration of non-Newtonian fluids.

CHAPTER III

THEORETICAL ANALYSIS

In the first section of this chapter, the theoretical analysis pertaining to the improved method of treatment of filtration data of Newtonian fluids, developed in the course of this investigation[84, 85] is presented. The analysis presented considers the filtration to be comprised of an initial stage and main filtration stage, yielding a convenient means of characterization of the initial stage of filtration conducted at constant pressure or constant rate. In the second section, an appropriate discussion of rheology of non-Newtonian fluids is given. In the third and the last section of this chapter, the formulation of Darcy's law for the flow of incompressible time independent non-Newtonian fluids through anisotropic compressible porous media is presented. The equations derived[86] for the constant pressure and constant rate filtration of non-Newtonian fluids, based upon the Darcy's law, are also presented. The derivation of these equations takes into consideration the improved method of treatment of filtration operation. The analysis of filtration, presented in sections 1 and 3, incorporates the recent modifications of Tiller and Shirato[4] and of Shirato et al.[5] accounting for the variation of the superficial velocity of the liquid through the cake and the velocity of the particles of the cake associated with cake compaction.

SECTION 1

FILTRATION OF NEWTONIAN FLUIDS

The Kozeny equation relating the rate of flow through a bed of solids can be derived from the following modified form of the Poiseuille equation.

$$g_c \left(\frac{dp_x}{dx}\right) = - \frac{k_i \mu}{R_h^2} u \qquad (1)$$

where k_i is the dimensionless constant, u is the linear velocity, μ is the viscosity, R_h is the hydraulic radius, p_x is the pressure and x is the distance. The hydraulic radius is given by

$$R_h = \frac{\text{(Flow area)}}{\text{(Wetted perimeter)}} \times \frac{\text{(Length of path)}}{\text{(Length of path)}} = \frac{\text{(Void volume)}}{\text{(Surface area of solids)}} \qquad (2)$$

since the value $\frac{\epsilon}{(1-\epsilon)}$ represents the ratio of void volume to the volume of solids, the void volume is given by

$$\text{void volume} = \left[\frac{\epsilon}{(1-\epsilon)}\right] \text{(volume of solids)} \qquad (3)$$

substituting Equation (3) in Equation (2) yields

$$R_h = \frac{\epsilon \text{ (volume of solids)}}{(1-\epsilon) \text{ (Surface area of solids)}} \qquad (4)$$

The surface area of the solids per cubic foot of solids (exclusive of voids) is termed the specific surface, S_o which can be substituted in Equation (4) to yield

$$R_h = \frac{\epsilon}{(1-\epsilon) S_o} \qquad (5)$$

The true velocity 'u' in the interstices of the solids is given by the superficial velocity q divided by the percent voids

$$u = \frac{q}{\epsilon} \qquad (6)$$

Making substitutions in the modified Poiseuille equation leads to

$$\frac{d p_x}{dx} = \frac{k_i}{g_c} \mu \frac{(1-\epsilon)^2 S_o^2}{\epsilon^3} q \qquad (7)$$

The minus sign usually appearing in the pressure gradient term has been dropped since x is measured from the filter medium, i.e., in the direction opposite to the direction of flow, as indicated in Figure 1. Tiller and Shirato[4] clearly indicated the necessity to measure distance from the fixed medium rather than the moving cake surface.

Referring to Figure 1, the mass dw_x of solids in the filter cake layer of thickness dx is given by

$$dw_x = \rho_s (1-\epsilon) A \, dx \qquad (8)$$

per unit area

$$dw_x = \rho_s (1-\epsilon) \, dx \qquad (9)$$

therefore

$$dx = \frac{dw_x}{\rho_s (1-\epsilon)} \qquad (10)$$

As liquid flows frictionally through a bed of compressive solids, viscous drag on the particles produces an accumulative compressive pressure which causes the porosity to decrease as the supporting medium is approached. For point contact between solids, the following relation holds[34, 39, 40]

$$dp_s + dp_x = 0 \qquad (11)$$

where p_x is the hydraulic pressure at a distance x from the surface of the cake and p_s is the solid compressive pressure. Writing dp_x in terms of dp_s in Equation (7) gives rise to

$$g_c \frac{dp_s}{dw_x} = - \mu \, q_x \frac{k_i S_o^2 (1-\epsilon)}{\epsilon^3 \rho_s} \qquad (12)$$

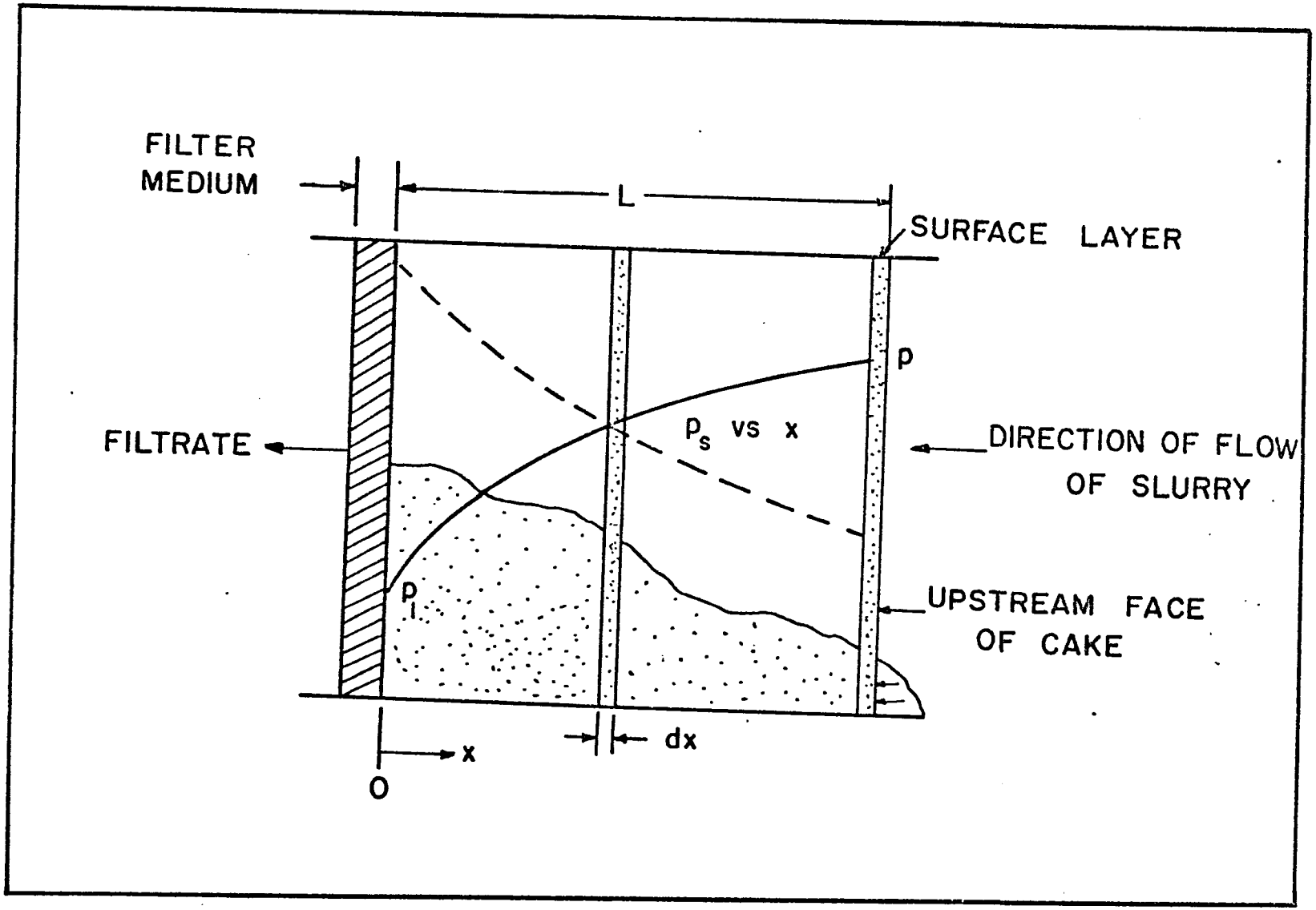

Fig. 1 Section through filter medium and cake, showing the pressure profiles.

In classical filtration theory, it is convenient to lump those parameters which are functions only of the pressure drop across the filter bed together in a single quantity α_x, called the local specific cake resistance[45, 61]. Mathematically, α_x is defined by

$$\alpha_x = \frac{k_i}{R_h^2 \rho_s \varepsilon (1 - \varepsilon)} = \frac{k_i (1 - \varepsilon) S_o^2}{\varepsilon^3 \rho_s} \tag{13}$$

with the aid of Equation (13), Equation (12) can be written as

$$g_c \frac{dp_s}{dw_x} = - \mu \alpha_x q_x \tag{14}$$

This basic differential equation for filtration rests upon the assumption that the liquid moves past the stationary solid particles. The solids move towards the septum as the cake is compressed during filtration, and it is false to assume that the solid velocity is zero. As a practical matter the velocity of solids is important for highly concentrated slurries. Equation (14) must be modified where the velocity of solids is comparable to the velocity of the liquid. A concentrated slurry is roughly defined as one in which the solid content in the slurry contains about 50 to 75% of the solid concentration at the cake surface [6].

It should be recognized that the internal flow rates of liquid, q_x, and solids r_x, are not constant throughout the thickness of the cake due to the continuous compression of the cake.

If ε_x is the porosity at x, the true average velocity of the liquid is represented by q_x/ε_x, and the true average velocity of the solids is given by $r_x/(1 - \varepsilon_x)$. Therefore the true average relative velocity, u_x, of liquids to solids is represented by[6]

$$u_x = \frac{q_x}{\epsilon_x} - \frac{r_x}{(1-\epsilon_x)} \tag{15}$$

Multiplying the Equation (15) by the local porosity, ϵ_x, yields the apparent relative flow rate of liquid to solids based upon unit cross sectional area

$$\epsilon_x u_x = q_x - \frac{\epsilon_x}{(1-\epsilon_x)} r_x = q_x - e_x r_x \tag{16}$$

where e_x is the local void ratio. This method of treatment was first introduced by Shirato et al.[5] to account for the movement of the solid particles in the cake associated with cake compaction. Now, replacing the flow rate of liquid by relative flow rate of the liquid to the solids in Equation (14) leads to

$$g_c \frac{dp_s}{dw_x} = -\mu \alpha_x (q_x - e_x r_x) \tag{17}$$

when flow takes place through a fixed, compressible bed in which the solids are not moving, r_x is zero and q_x is constant (although the average liquid velocity q_x/ϵ_x may vary).

The superficial liquid and solid velocities in the cake have been shown by Shirato[5, 6] to be simply related to the superficial velocity of the filtrate at the exit of the cake by

$$q_x + r_x = q_1 \tag{18}$$

When Equation (17) is integrated across the entire thickness of the cake, the following result is obtained[5, 6] which is an improvement of the previous result of Tiller and Shirato[4] in which only the variation of the superficial velocity q_x with respect to the distance was considered:

$$q_1 = \frac{dv}{d\theta} = \frac{g_c (p - p_1)}{\mu J_R \alpha_R w} = \frac{g_c p}{\mu (J_R \alpha_R w + R_m)} \tag{19}$$

The pressure at the filter medium - cake interface, p_1 in Equation (19), is related to the flow rate q_1 at the exit of the cake by

$$g_c p_1 = \mu q_1 R_m \tag{20}$$

and α_R is the conventional filtration resistance defined by Carman[17] and Ruth[33] as

$$\alpha_R = \frac{p - p_1}{\int_0^{p-p_1} \frac{dp_s}{\alpha_x}} \tag{21}$$

The coefficient α_R is also known as the average specific cake resistance. As the name suggests, it is an average quantity for the entire cake and as indicated by McCabe and Smith[61], it must be measured experimentally for each sludge. For a particular sludge, it is a function of only pressure drop across the cake. The dimensions of α_R and LM^{-1}, and it is measured in feet per pound.

R_m, the filter medium resistance, can be defined by analogy with Equation (21) as given by Equation (20).

The dimension of R_m is L^{-1}, and the units are expressed in reciprocal feet. It is generally observed[61] that the magnitude of the filter medium resistance depends on the pressure drop and perhaps on the flow rate and also an old, used filter medium offers more resistance to flow than a new, clear one. Since the medium resistance plays an important role only during the early stages of filtration, it is satisfactorily assumed to be constant during any filtration and is

usually determined from experimental data. The magnitude of R_m is reported to be varying from experiment to experiment even for the same sludge and filter.

J_R is a correction factor for α_R resulting from the variation of q_x with x and the movement of solids as a result of compaction of the cake. Originally, J_R is defined by Tiller and Shirato[4] as

$$J_R = \int_0^1 \left(\frac{q_x}{q_1}\right) \, d\left(\frac{w_x}{w}\right) \tag{22}$$

A relationship for evaluation of J_R obtained recently by Shirato[5, 6] indicates that J_R depends mainly upon slurry concentration and to a lesser extent on filtration pressure. For computational purposes J_R is placed in the form[6]

$$J_R = \int_0^1 \left[1 - \frac{(\varepsilon_x - \varepsilon_{avg\,x})\,(m - 1)}{(1 - \varepsilon_x)\,\varepsilon_{avg}\,(1 - m\,s)} \; s\left(\frac{x}{L}\right)\right] d\left(\frac{w_x}{w}\right) \tag{23}$$

It has been found that α_R is a good approximation for the average filtration resistance $\alpha = J_R \; \alpha_R$ when the slurry is dilute. For example, values for J_R reported by Shirato et al.[48] for slurries of clay, cement material and ignition plug indicate a value of J_R between 0.99 and unity for the slurry concentrations used in the present investigation.

Making use of the following relationship,

$$w = \frac{\rho\, s}{(1 - m\, s)} \; v \tag{24}$$

Equation (19) may be written in terms of the volume of the filtrate in the following manner:

$$q_1 = \frac{dv}{d\theta} = \frac{K}{2(v+v_o)} \tag{25}$$

where

$$K = \frac{2 g_c p (1 - m s)}{\mu \alpha s \rho} \tag{26}$$

and

$$v_o = \frac{R_m (1 - m s)}{\alpha s \rho} \tag{27}$$

Filtration at Constant Pressure

For purposes of mathematical treatment and convenient industrial practice, filtration operations are classified according to the variation of the pressure and the flow rate with time. The different catagories into which the filtration operations are classified are the following:

(i) Constant pressure filtration:- During this operation the applied pressure is held constant resulting in the variation of flow rate with time.

(ii) Constant rate filtration:- In this process, the volumetric rate of filtrate is maintained constant by gradually increasing the applied pressure with time.

(iii) Variable - pressure - variable - rate filtration:- As the name suggests, both pressure and flow rate vary during this operation. The use of a centrifugal pump can result in the rate varying with the back pressure on the pump.

(iv) Stepped pressure filtration:- For experimental purposes, it is possible to manually increase pressure during a filtration and simulate various pumping conditions.

Of the above mentioned classifications, constant pressure and constant rate filtrations are very commonly and widely used in the laboratories as well as in the industries. The combination of these two types of filtration is well utilized in industries by conducting the filtration at constant rate till the maximum pressure is attained and then by carrying on at constant pressure to the extent desired. Hence, the investigations reported here are confined to filtrations at constant pressure and constant rate. The following analysis pertains to the constant pressure filtration of Newtonian fluids and closely follows the treatment presented in a recent report[84].

When a filter cake of appreciable thickness has been deposited, the pressure at the medium - cake interface p_1 becomes small in comparison to the pressure at the cake surface, and α_R and consequently α assume a constant value which is a function of the pressure p. Experimentally it is also observed that m is effectively constant after a relatively short interval. Hence K and v_o in Equation (25) will take on constant values in constant pressure filtration, after some initial period of filtration.

During the initial stage of the filtration, when the cake thickness is small and p_1 is not insignificant compared to p, α_R becomes a function of $(p - p_1)$ and varies continuously with an increase in the amount of filtrate v. Variations in the pressure in the early part of the initial stage and the variation of m ascribable to the initial stage are additional possible sources of variation superimposed on K and v_o in the initial stage.

To perform the integration of Equation (25), allowance for the variation of K and v_o in the initial stage of the filtration is conveniently made by rewriting Equation (25) in the following equivalent form:[84],

$$\frac{d\theta}{dv} = \frac{2}{K}(v + v_o) + F(v) \qquad F(v) \neq 0, \quad 0 \leq v < v_i$$
$$F(v) = 0, \qquad v \geq v_i \tag{28}$$

Here K and v_o denote the eventual constant values assumed by these quantities subsequent to the initial period. The initial stage interval of the filtration in which variations in K and v_o are assumed localized is represented in quantitative terms by the filtrate volume v_i. F(v) is a function of filtrate volume serving as a correction term yielding the correct $d\theta/dv$ in the initial period. As indicated, the correction is zero beyond the initial stage where $v > v_i$. Similar characterization of initial period of filtration of non-Newtonian fluids is presented on the Page (54) in Section III.

Equation (28) can be rewritten

$$d\theta = \frac{2}{K}(v+v_o)\, d\,(v+v_o) + F(v)\, dv \tag{29}$$

and integrated, applying the limits $v = 0$ at $\theta = 0$ and $v = v > v_i$ at $\theta = \theta$, as follows

$$\theta = \frac{2}{K}\int_{v_o}^{v+v_o} (v + v_o)\, d\,(v + v_o) + \int_0^{v_i} F(v)\, dv \tag{30}$$

to obtain,

$$\theta = \frac{1}{K}(v^2 + 2vv_o) + \theta_o \tag{31}$$

where the constant represented by the integral on the right side of Equation (30) has been replaced according to

$$\theta_o = \int_0^{v_i} F(v)\, dv \tag{32}$$

Setting v equal to zero in Equation (31) yields the result that

$\theta = \theta_o$ which is appropriately termed the effective time of commencement of filtration.

Differentiation of Equation (31) with respect to v yields the familiar result

$$\frac{d\theta}{dv} = \frac{2}{K}(v + v_o) \tag{33}$$

which is the basis for the previous method of evaluation of K and v_o from experimental constant pressure filtration data. The disadvantage of this method concerns the quantity $d\theta/dv$ which cannot be evaluated conveniently with any accuracy.

This difficulty is conveniently circumvented by the use of Equation (31) which can be fitted to experimental data collected during the main filtration stage by the method of least squares. This statistical method proceeds by evaluating the constants in the analytical expression chosen to represent the data in a manner which makes the variance a minimum. This gives the best values of 1/K, v_o and θ_o in the Equation (31). Thus, a good fit of the data can be achieved with relative ease. Further, the method is based on an analysis in which explicit consideration was given to the variation of K and v_o in the initial filtration stage.

Filtration at Constant Rate

The analysis presented for constant rate filtration in this section is based on the theory developed in this laboratory to account for the variation in the filtrate flow rate during the initial stage and closely resembles the analysis given in a recent report[85].

The rate of flow of filtrate in a constant rate filtration can be represented in the following manner:

$$\frac{dv}{d\theta} = q_1 + f(\theta) \qquad f(\theta) \neq 0, \quad 0 < \theta < \theta_i$$
$$f(\theta) = 0, \qquad \theta \geq \theta_i \tag{34}$$

Here θ_i denotes the time interval of the initial transient stage of the filtration, when the filtrate flow rate is varying. The function of time $f(\theta)$, which depends upon the actual filtrate flow rate versus time history of the initial period, is a correction term yielding the filtrate rate at any instant of time. This rate differs from the value of q_1 in the constant rate period. As indicated, the correction is zero when the elapsed time is greater than the time interval θ_i.

The volume of filtrate collected in the elapsed time $\theta > \theta_i$ is thus given by

$$v = \int_0^{\theta} \frac{dv}{d\theta} \, d\theta = q_1\theta + \int_0^{\theta_i} f(\theta) \, d\theta \tag{35}$$

This equation for v is linear in θ, since the integral expression on the right side is a constant. At θ equal to zero, the equation yields the result that v is equal to the value of the integral $\int_0^{\theta_i} f(\theta) \, d\theta$, which is appropriately termed the initial effective volume of filtrate and designated as v_o.

Hence, the filtrate volume can be represented by

$$v = q_1\theta + v_o \tag{36}$$

The initial effective volume of filtrate v_o can be readily evaluated, according to Equation (36), as the v intercept of the straight line obtained in a plot of v versus θ, extrapolated back to the initial condition, $\theta = 0$. The additional information required to use this new method of treatment of the data collected during constant rate filtration is the filtration rate - time history of the initial stage.

Equation (19) may be rewritten in terms of the volume of the filtrate, using the relationship given by Equation (24)

$$w = \frac{\rho s}{(1 - m s)} v \tag{24}$$

as follows

$$g_c (p - p_1) = \frac{\mu q_1 J_R \alpha_R \rho s}{(1 - m s)} v \tag{37}$$

Substitution of the expression for v given by Equation (36) in Equation (37) yields

$$(\theta + \frac{v_o}{q_1}) = \frac{g_c (1 - m s)}{\mu q_1^2 J_R \alpha_R \rho s} (p - p_1) \tag{38}$$

Making use of the assumption, investigated by Luke[42] and Coimbra[41], that the filtration resistance may be expressed as a power function of the pressure drop across the cake $(p - p_1)$,

$$\alpha = J_R \alpha_R = r_o (p - p_1)^{n_o} \tag{39}$$

leads to

$$(\theta + \theta_c) = \frac{g_c (1 - m s)}{\mu q_1^2 \rho s r_o} (p - p_1)^{1 - n_o} \tag{40}$$

where θ_c is a time correction given by $\theta_c = v_o / q_1$.

With reference to the fact that Equation (39) incorrectly predicts a zero filtration resistance when the pressure drop $(p - p_1)$ is zero, we simply note our requirement that Equation (39) give the actual representation of the filtration resistance in the time interval $\theta_i \leq \theta \leq \theta$, under consideration.

Taking the logarithm of each side of Equation (40) results in

$$\log(\theta + \theta_c) = (1 - n_o)\log (p - p_1) - \log K_r \qquad (41)$$

where

$$K_r = \frac{\mu q_1^2 \rho s r_o}{g_c (1 - m s)} \qquad (42)$$

Since Equation (41) is linear (with $Y = \log (\theta + \theta_c)$ and $X = \log (p - p_1)$), a simple linear regression analysis, utilizing a computer, may be carried out to give p_1, $(1 - n_o)$ and $\log K_r$. The procedure used is the following. First, p_1 is determined approximately by plotting $(\theta + \theta_c)$ versus p on rectangular coordinates and extrapolating the smooth curve drawn through the points to the pressure axis, where $(\theta + \theta_c) = 0$. The p-intercept determined is used as a guide in selection of trial values for p_1. A number of individual values in the neighbourhood of this reference p_1 value are then assigned to p_1 and a set of values of $(1 - n_o)$ and $\log K_r$, corresponding to each value of p_1 selected, are determined by computation, using the method of least squares. The variance between the experimental data points and the equation resulting for each set of values of p_1, $(1 - n_o)$ and $\log K_r$ is also computed. A plot on rectangular graph paper of the variance versus p_1 is then constructed, and the p_1 and corresponding $(1 - n_o)$ and $\log K_r$ values yielding the minimum variance are taken as yielding the equation with the best fit of the experimental data.

In passing, it should be pointed out that the computational program just described may also be utilized to obtain the values of p_1, $(1 - n_o)$, and $\log K_r$, yielded by the previous method and required for comparison purposes, by simply replacing $(\theta + \theta_c)$ by θ in Equation (41) and in the claculations.

SECTION 2

RHEOLOGY OF NON-NEWTONIAN FLUIDS

Before presenting the actual analysis of filtration of Non-Newtonian fluids, it is felt necessary to discuss in brief the rheology of non-Newtonian fluids.

Fluids which do not exhibit a linear relationship between the shear stress (τ_{yx}) and shear rate (dv_x/dy) are called non-Newtonian fluids.

The subject of non-Newtonian flow is a subdivision of rheology, "The science of deformation and flow of matter". In order to take account of the nature of different fluids, one introduces a rheological equation of state, or constitutive equation, which identifies the basic characteristics of fluids. In particular one must specify a relation between the viscous part of the momentum flux tensor τ and the rate of deformation tensor γ (with cartesian components $\gamma_{ij} = \frac{\partial v_i}{\partial x_j} + \frac{\partial v_j}{\partial x_i}$).

Generalised Newtonian Fluid

A most useful and practical constitutive relation is that for the so called "Generalised Newtonian Fluid"[63].

$$\tau = - \eta \gamma \tag{43}$$

where η is the viscosity. This relation is analogous to Newton's law except that the non-Newtonian viscosity η, a scalar, is a function of γ (or a function of τ) as well as of temperature and pressure whereas viscosity of a Newtonian fluid depends on the local pressure and temperature but not on τ or γ.

This relation is a simplification of the Reiner-Rivlin-Prager relation[64]

$$\tau_{ij} = -\eta\,\gamma_{ij} - \eta_c \sum_k \gamma_{ik}\,\gamma_{kj} \tag{44}$$

where η and the cross viscosity η_c are, in general, functions of scalar invariants of rate of deformation tensor γ. Equation (44) is the most general relation between τ and γ which does not involve space or time derivatives of either τ or γ. The exclusion of time effects restricts the relation to inelastic fluids. One other restriction on Equation (44) is that the net entropy production rate must be nonnegative[65, 66].

In order for η to be a scalar function of the tensor γ, it must depend only on the "invariants" of γ. The invariants are those special combinations of the components of γ that transform as scalars under a rotation of coordinate system:

$$\text{I} = (\gamma : \delta) = \sum_i \gamma_{ii} \tag{45}$$

$$\text{II} = (\gamma : \gamma) = \sum_i \sum_j \gamma_{ij}\,\gamma_{ji} \tag{46}$$

$$\text{III} = \det \gamma = \sum_i \sum_j \sum_k \varepsilon_{ijk}\,\gamma_{1i}\,\gamma_{2j}\,\gamma_{3k} \tag{47}$$

where δ_{ij} and ε_{ijk} are the Kronecker delta and Alternating unit tensor respectively, which are used to express the formulas more compactly.

The reduction of Equation (44) to Equation (43) depends upon several assumptions. First in all cases, the fluid will be considered incompressible. Here the first invariant I is identically equal to zero from the equation of continuity. Second, the cross viscosity

effects will be neglected, i. e. $\eta_c = 0$. There is little known about the cross viscosity effects. Third, it will be assumed that there exists no functional dependence of the viscosity η on the third invariant III. There is little known about the effect of III on fluid flow. In simple flow geometries, e. g. flow through tube or slit, the third invariant is identically zero. In more complex geometries this is generally not true. Slattery and Bird[67] were able to correlate data for flow of non-Newtonian fluids about a sphere without the incorporation of third invariant leading to the suggestion that its contribution is small. It is adequate, therefore, for many cases, to use the generalised Newtonian relation as

$$\tau = - \eta(II)\, \gamma \qquad (48)$$

which, in summary, describes an inelastic, incompressible fluid for which the effects of cross viscosity and third invariant are ignored.

Specific Rheological Equations of State

Numerous empirical functions of the form of Equation (48) have been presented in the literature. Equations representing various models are given in a tabular form in a recent text book[71]. Any proposed rheological model should represent the actual behaviour of fluid with accuracy, convenience and simplicity. No known model describes the behaviour of all non-Newtonian fluids with a reasonable number of constants. Different models may be necessary to describe different fluids, or even the same fluid under different conditions. The "best" relationship for a given fluid is not necessarily known until an experiment is made on the fluid to relate τ and γ. It is known a priori, however, that if the model is to be a reasonable approximation to reality, certain conditions should apply.

(a) The viscosity should approach a constant value at low shear stress, i.e. a "lower limiting viscosity", η_o.

(b) The viscosity should approach a constant value at high shear stresses i.e. an "upper limiting viscosity", η_∞.

Condition (a) is of special importance. A fluid may be expected to exhibit a constant viscosity at the lowest flow rates which are generally encountered in the flow of viscous fluids through porous media. The fulfillment of condition (b) is not critical. The upper limiting viscosity usually requires severe flow conditions which are not likely found in most flow systems.

Four representative models for non-Newtonian fluids are summarized below. Each of these equations contains empirical positive parameters, which can be evaluated numerically to fit data on τ_{yx} versus (dv_x/dy) at constant temperature and pressure.

The Bingham Model

$$\tau = -\left[\mu_o + \frac{\tau_o}{\sqrt{\frac{1}{2}(\gamma:\gamma)}}\right]\gamma \quad \text{For } \tfrac{1}{2}(\tau:\tau) > \tau_o^2 \tag{49}$$

$$\gamma = 0 \quad \text{For } \tfrac{1}{2}(\tau:\tau) < \tau_o^2 \tag{50}$$

A substance that follows this two parameter model is called a Bingham plastic: it remains rigid when the shear stress is of smaller magnitude than the yeild stress τ_o but flows somewhat like a Newtonian fluid when the shear stress exceeds τ_o. This model has been found reasonably accurate for many fine suspensions and pastes.

The Ostwald - De Waele Model

This rheological model is very widely used and is also known

as the Power-law model.

$$\tau = -\left[K \left| \sqrt{\tfrac{1}{2}(\gamma : \gamma)} \right|^{n-1}\right] \gamma \qquad (51)$$

where K and n are two positive fluid parameters determinable from viscometric measurements. When n = 1 and K = μ, the model represents the Newtonian fluid. This model does not describe either the lower limiting viscosity η_o or the upper limiting viscosity η_∞. It is also subject to Reiner's[62] "dimension objection" since the dimension of K will vary with the value of n. Nonetheless, the model generally gives an adequate description of fluid behaviour over an intermediate range of shear rates. More important, other useful empirical models are simple extensions of the power-law model. Because of its mathematical simplicity, Equation (51) has been used extensively by investigators.

The Ellis Model

Ellis and more recently, Gee and Lyon[68] proposed an extension of the power-law model with three constants for plastic melts:

$$\gamma = -\left[\varphi_o + \varphi_1 \left(\tfrac{1}{2}(\gamma : \gamma)\right)^{\frac{\alpha-1}{2}}\right] \tau \qquad (52)$$

where φ_o, φ_1 and α are the fluid parameters. The Ellis model does not describe the upper limiting viscosity, η_∞, but more important, for polymer solutions, it does describe the lower viscosity $\eta_o = 1/\varphi_o$.

The Reiner-Philippoff Model

$$\tau = -\left[\mu_\infty + \frac{\mu_o - \mu_\infty}{1+\frac{\frac{1}{2}(\tau:\tau)}{\tau_o^2}}\right]\gamma \qquad (53)$$

This model contains three adjustable positive parameters: μ_o, μ_∞ and τ_o. Since Newtonian behaviour has often been observed both at very low and very high shearing rates, Equation (53) has been set up to reduce to Newton's law of viscosity with $\mu = \mu_o$ and $\mu = \mu_\infty$, respectively, in these two limiting cases. The plot of τ_{yx} versus (dv_x/dy) has inflection points located at $\tau_{yx} = \pm \tau_o \sqrt{3\mu_o/\mu_\infty}$.

The values of the parameters used in these models for various solutions are tabulated and presented in a text book[63]. It is important to remember that these equations are nothing more than empirical curve fitting formulas, and it is hazardous to apply them beyond the range of available data. Also, the parameters of any of these models are functions of temperature, pressure, composition, and, usually, of the range of (dv_x/dy) over which the equation is fitted. Therefore, the conditions of measurement must be carefully specified in reporting rheological parameters.

Under unsteady state conditions, a number of additional types of non-Newtonian behaviour are possible. For example, fluids that show a limited decrease in η with time under a suddenly applied constant stress are called thixotropic, whereas those show an increase in η with time are called rheopectic.

Viscoelastic Fluids

Fluids that partially return to their original form when the applied stress is released are called viscoelastic. In a purely

Hookean elastic solid the stress corresponding to a given strain is independent of time, whereas for viscoelastic substances the stress will gradually dissipate. In contrast to purely viscous liquids, on the other hand, viscoelastic fluids flow when subjected to stress but part of their deformation is gradually recovered upon removal of the stress.

Oldroyd[69] derived a differential equation relating shear stress to shear rate in viscoelastic emulsions which is the same as an equation derived earlier by Frohlich and Sack[70] for an incompressible and dilute dispersion of equal-sized, elastic-solid spheres in a Newtonian fluid. The equation gives a linear relation between the shear stress τ, the rate of shear γ, and their time rates of change, as follows:

$$\tau + \lambda_1 \frac{d\tau}{dt} = \frac{\mu^*}{g_c} \left[\gamma + \lambda_2 \frac{d\gamma}{dt} \right] \qquad (54)$$

The expression contains three constants, a viscosity μ^*, and two "relaxation times" λ_1 and λ_2. The relaxation times obviously have the physical significance that if the motion is suddenly stopped, the shear stress decays as $\exp(-t/\lambda_1)$, and if the stress is removed the rate of strain decays as $\exp(-t/\lambda_2)$. The quantity μ^* is Newtonian viscosity observed in the fluid at the very low rates of shear. Equation (54) reduces to the Newtonian fluid ($\lambda_1 = \lambda_2 = 0$) and to the Maxwell fluid ($\lambda_2 = 0$) as special cases. A more detailed review of the flow behaviour of these materials is presented in some text books[71, 72]. The quantitative study of these and other types of time-independent behaviour is an important and largely undeveloped area of fluid mechanics.

Effective Slip Near Solid Boundary

Among the important properties of some non-Newtonian fluids, worthy of a special mention is their anomalous behaviour near a solid boundary. It has been observed that some non-Newtonian fluids show anomalous behaviour near a solid boundary, due to a preferred orientation of particles or molecules caused by the presence of wall. This effect can be shown clearly with a suspension of paper pulp. When this material flows through a transparent pipe a clear water annulus is observed adjacent to the wall. The fluid in this region has a lower viscosity and this gives rise to an effective velocity of slip at the wall.

Hence, in the region close to the wall (say within a normal distance of ϵ) the rate of shear will not be a function of shear stress alone. If the shear stress near the wall y = 0 is τ, the rate of shear will differ from the value $f(\tau)$ which it would have remote from a boundary by an amount which depends upon y, the normal distance from the wall,

$$\text{i. e.} \quad (du/dy) = f(\tau) + g(\tau, y) \tag{55}$$

$$\text{where} \quad g(\tau, y) = 0 \quad \text{when} \quad y > \epsilon \tag{56}$$

The velocity u just outside the region of anomalous flow is then

$$u = f(\tau)\, y + \int_0^{\epsilon} g(\tau, y)\, dy \tag{57}$$

in other words

$$u - s(\tau) = f(\tau)\, y \tag{58}$$

where

$$s(\tau) = \int_0^{\epsilon} g(\tau, y)\, dy \qquad (59)$$

$s(\tau)$ is the value of u when y is zero, and is the effective velocity of slip at the wall; it is dependent on the local shear stress, τ. This approach has been presented by Oldroyd[73]. A report of an extensive study on the anomalous behaviour of the polymer solutions used in the filtration experiments is in press[74]. In this report, a method of evaluating "critical shear stress", which denotes the value of wall shear stress marking the transition from a negative effective velocity at the wall, attributable to gel formation and polymer adsorption, to a positive effective velocity of slip, ascribable to the formation of a thin layer at the wall with properties those of the solvent,is also presented.

SECTION 3

FILTRATION OF NON-NEWTONIAN FLUIDS

The filtration equations presented in this section are derived from the extension of Darcy's law for the flow of an incompressible time independent non-Newtonian fluid in a compressible porous medium exhibiting anisotropy. Hence, it is very much relevant to discuss briefly some characteristics of porous media and Darcy's law.

The interconnected porosity in a porous solid provides tortuous passages through which fluid can flow. The geometry of these passage ways is complex, and it would be a hopeless task to predict flow by considering the individual channels. However, since the number of channels is large enough that average properties have meaning, a porous medium is generally treated as a continuous medium having certain average properties rather than as an assemblage of discrete passages[77].

Permeability

Permeability is that property of porous material which characterizes the ease with which a fluid may be made to flow through the material by an applied pressure gradient. Also it is sometimes referred to as the fluid conductivity of the porous material. It is obvious that permeability must be determined by the geometry of the porous structure in a more or less statistical fashion. Many attempts have been made to construct a theory which relates this structure to permeability. A rather complete review of such theories is given by Scheidegger[87]. The theory of Kozeny[88] treats the porous medium as a bundle of capillary tubes of equal length. These tubes are not necessarily of circular cross section. Numerous modifications of Kozeny equation have been proposed. One such modification is proposed

to account for the fact that the tubes of flow in a porous medium are not straight, and hence the path length of flow is greater than the length of the sample of the porous material. Thus, tortuosity, T, is defined as the ratio of the flow-path length to sample-path length. Other modifications are discussed by Brooks and Purcell[89].

Another approach to the relation between the pore structure and permeability is also based on a capillary tube model. This is the calculation of the permeability from "pore-size distribution". In this scheme, the porous material is treated as a bundle of capillary tubes having equal lengths and circular cross sections with a distribution of radii. Since the flow through each tube is given by the Hagen-Poiseuille law, the flow through the system can be related to the radius distribution function, which, in turn, yields an expression for permeability. Burdine, Gournay and Reichertz[90] have applied this theory with pore size distributions determined by the mercury injection method rather successfully to sedimentary rocks.

Without going further into discussion of the various structural theories of permeability, certain general conclusions are possible[91]. Permeability must be proportional to some sort of mean square pore diameter, or radius squared, and the spread of pore size must also be an important factor in the determination of the permeability. Of course, these factors also determine the specific surface of the material and hence the Kozeny theory also relates to pore size distribution.

Since fluids have mass it follows from Newton's second law of motion that forces must be exerted on a fluid to change either the direction or magnitude of fluid velocity. When a fluid flows through a porous medium the velocity of a fluid element changes rapidly from

point to point along its tortuous flow path. The forces which produce these changes in velocity vary rapidly from point to point.

However, in a naturally porous material the porous structure and hence the multitude of flow paths have a random character. It is reasonable to suppose that the random variations in flow path for any particular fluid element are uniformly distributed. Also the variations in magnitude of velocity can be expected to be distributed uniformly with mean zero. Thus, for steady laminar flow the lateral forces associated with the microscopic random variations in velocity can be expected to average to zero over any macroscopic volume. However, the inertial forces in the direction of flow will not average to zero and hence will only be negligible for low flow rates.

Darcy's Law

For isotropic porous media, Darcy's law presents simple proportionalities between the components of the volumetric flux and the corresponding components of the gradient of low potential. Thus,

$$q_x = -\frac{k}{\mu}\frac{\partial p'}{\partial x_i}, \qquad i = 1, 2, 3 \tag{60}$$

where k is the permeability and μ is the viscosity of the fluid. By the definition of isotropic porous medium it is implied that the porous medium has the same permeability to flow in all directions. The permeability may well be a function of position. If the medium is not isotropic, the permeability is a function of direction and the situation is more complicated. Many porous materials exhibit a distinct anisotropic character, particularly fibrous materials, such as wood as well as some sedimentary rocks. Thus the fluid transmissibility in such materials is not the same in all directions. To take this

characteristic of porous media into account, it requires a further generalization of the laws of flow. This extension is achieved by heuristic reasoning just as the extensions from the fundamental experimental law were made. The correctness of such extension can be established only by appeal to the experiments for confirmation of predictions based on such extensions. The most general linear relationship between q_i and the components $\frac{\partial p'}{\partial x_i}$ that can be postulated takes the form

$$q_i = -\frac{1}{\mu}\left(k_{i1}\frac{\partial p'}{\partial x_1} + k_{i2}\frac{\partial p'}{\partial x_2} + k_{i3}\frac{\partial p'}{\partial x_3}\right) \quad i = 1, 2, 3 \tag{61}$$

Here the nine quantities, k_{ij} ($i = 1, 2, 3$; $j = 1, 2, 3$) form the elements of a tensor.

The generalization of Darcy's law postulated here retains a linear dependence of q_i upon the components of potential gradient, which is a heuristic reason for assuming this form. The three equations given in Equation (61) can be written as the single matrix equation

$$\begin{pmatrix} q_1 \\ q_2 \\ q_3 \end{pmatrix} = -\frac{1}{\mu}\begin{pmatrix} k_{11} & k_{12} & k_{13} \\ k_{21} & k_{22} & k_{23} \\ k_{31} & k_{32} & k_{33} \end{pmatrix}\begin{pmatrix} \frac{\partial p'}{\partial x_1} \\ \frac{\partial p'}{\partial x_2} \\ \frac{\partial p'}{\partial x_3} \end{pmatrix} \tag{62}$$

Then, if a rotation of the coordinate axis is considered, the manner in which the k-matrix transforms under such a rotation can be investigated. Such an investigation shows that, if the k-matrix is symmetric, then rotation of the axes to a particular orientation produces a diagonal k-matrix.

Thus, if

$$k_{ij} = k_{ji} \qquad i = 1, 2, 3; \quad j = 1, 2, 3 \tag{63}$$

then for a particular set of rectangular axis, x_i', i = 1, 2, 3 (i.e., a particular orientation of the coordinate system) the k-matrix takes the form (denoted as the k'-matrix)

$$(k'\text{-matrix}) = \begin{pmatrix} k_1 & 0 & 0 \\ 0 & k_2 & 0 \\ 0 & 0 & k_3 \end{pmatrix} \tag{64}$$

The directions of the particular set of coordinate axis to which this k'-matrix corresponds are called the principal axes of the porous medium. It is to be noted that these principal axes are orthogonal to each other. Thus, the converse statement is also correct, for a porous medium having orthogonal principal axes the k-matrix is symmetric for any orientation of the coordinate system, and is diagonal for a coordinate system congruent with the principal axes.

For the coordinate axes oriented parallel to the principal axes of the porous medium having orthogonal principal axes, the postulated form of Darcy's law becomes

$$q_i = -\frac{k_i}{\mu}\left(\frac{\partial p'}{\partial x_i}\right) \qquad i = 1, 2, 3 \tag{65}$$

Thus each component of q is proportional to the corresponding component of the potential gradient but the constants of proprotionality are not equal since the k_i are not equal.

It should be noted that this rotation of axes also requires a change in the form of p'. Thus, since, in general, not one of the primed coordinates is parallel to the vertical (direction of the gravita-

tional force), p' must be written as

$$p' = g \sum_{i=1}^{3} x_i' \cos a_i + \int_{p_o'}^{p'} \frac{dp'}{p'} \tag{66}$$

Here the a_i, i = 1, 2, 3 are the angles between the respective primed axes, x_i', i = 1, 2, 3 and x_3 which is assumed vertical.

It has been experimentally demonstrated that some anisotropic porous media can be described by a permeability matrix as presented above[92]. Furthermore, the particular materials investigated possessed orthogonal principal axes. However, it can not be expected that all anisotropic porous media would have orthogonal principal axes.

Darcy's Law for non-Newtonian Flow

Darcy's law for the flow of an incompressible time independent non-Newtonian fluid in a compressible porous medium exhibiting anisotropy can be represented by[1, 75]

$$\eta_{ap} \cdot (\mathbf{q}) = - \mathbf{k} \cdot \nabla p' \tag{67}$$

As pointed out in an earlier section dealing with the filtration of Newtonian fluids, it was proved by Shirato[5, 6] that the solids move towards the septum as the cake is compressed during filtration, and it is false to assume that the velocity of solids is zero. Hence, it is necessary to introduce the relative velocity of the liquid to the velocity of solids in equation to account for the movement of the particles associated with cake compaction. In view of this fact Equation (67) can be written as

$$\eta_{ap} \cdot (\mathbf{q} - \varepsilon \mathbf{u}_p) = - \mathbf{k} \cdot \nabla p' \tag{68}$$

where u_p is the instantaneous local velocity vector ascribable to the centre of mass of solid particles of the cake undergoing compaction.

As discussed in Section 2 of this chapter, it has been observed that some non-Newtonian fluids show anomalous behaviour near a solid boundary, due to a preferred orientation of particles or molecules due to the presence of the solid. Some evidence of the anomalous surface effects in the filtration of the non-Newtonian slurries is reported in literature[1]. Hence, the effective superficial surface velocity q_s arising from the anomalous behaviour of the fluid is to be included in the equation representing Darcy's law. For example, polymer adsorption - gel formation at a solid surface is characterized by a superficial velocity vector which is oppositely directed to the fluid velocity vector. The electro-kinetic effect or electro-osmosis associated with the streaming potential generation and retardation of flow of liquids through small capillary[33] can be similarly characterized. Taking all these facts into consideration, Equation (68) can be transformed into

$$\eta_{ap} \cdot (\mathbf{q} - \varepsilon \mathbf{u}_p - \mathbf{q}_s) = -\mathbf{k} \cdot \nabla p' \qquad (69)$$

It might be in order to make a brief mention of streaming potential and electro-osmosis at this stage. When two chambers containing water are separated by a plate of porous material and a difference of electrical potential between the chambers is maintained with a battery or a power supply by two metal electrodes on each side of the porous plate, a flow of water occurs from one side to the other. This phenomenon is called electro-osmosis. Liquids other than water also exhibit this behaviour. Conversely, when water or other liquid is forced through a porous plate by a pressure differential, an electrical potential difference across the plate is observed.

This potential is called the streaming potential. Generally, electro kinetic phenomena are of little significance in most problems of fluid flow through porous media. The magnitude of these electro-kinetic effects are discussed by Glasstone[93].

Filtration Equations for non-Newtonian Fluids

In filtration, the gradient of hydrostatic potential, which for an incompressible fluid is related to the fluid pressure by $p' = p + \rho gh/g_c$, can be conveniently replaced by pressure gradient, the error involved being negligible because of small hydrostatic heads.

In view of this assumption, Darcy's law can be rewritten in the following convenient form for use in filtration.

$$\eta_{ap} \cdot (\mathbf{q} - e\mathbf{r} - \mathbf{q}_s) = \mathbf{k} \cdot \nabla p \qquad (70)$$

where r is the superficial velocity of the particles based on the entire cross section[5.6], without regard for the void space, and e is the local void ratio defined earlier in Equation (16). The subsequent analysis closely follows the theory developed by Kozicki et al., which is presented in a recent report[86].

The formulation of the Equation (70) is based on the assumption that a tensor $\bar{\Phi}$ can be determined which maps the vectors on the left sides into the vectors on the right sides of the equations as follows

$$\nabla p = +\bar{\Phi} \cdot (\mathbf{q} - e\mathbf{r} - \mathbf{q}_s) \qquad (71)$$

The apparent viscosity tensor of the fluid can thus be determined from a knowledge of the permeability tensor k for the anisotropic medium and the mapping tensor $\bar{\Phi}$ in accordance with the

relationship

$$\eta_{ap} = \mathbf{k} \cdot \bar{\Phi} \tag{72}$$

In the simplest case of flow in an isotropic medium, if we set $\mathbf{k} = kI$ and $\bar{\Phi} = \bar{\Phi}I = (\eta_{ap}/k)I$, with

$$k = \frac{\varepsilon R_h^2}{k_i} = \frac{\varepsilon^3}{k_i S_o^2 (1-\varepsilon)^2} \tag{73}$$

and η_{ap} given by

$$\eta_{ap} = \frac{\bar{\tau}_w}{(1+\xi) \int_{\tau_y}^{\bar{\tau}_w} \frac{\tau^{\xi}}{\eta^{T}} d\tau} \frac{1+\xi}{} \tag{74}$$

Equation (69) reduces to the following relationship consistent with one found previously[1] for the case in which the solid particles are stationary:

$$\mathbf{q} = \varepsilon \mathbf{u}_p + \mathbf{q}_s - \frac{\mathbf{k}}{\eta_{ap}} \nabla p' \tag{75}$$

In Equations (73) and (74), k_i and ξ are the impermeability and aspect factors, respectively, which characterize the flow geometry of the isotropic porous medium. The quantity $\bar{\tau}_w$, which represents the contour-integrated average value of the shear stress along the solid boundary of a non-circular capillary, is evaluated in this instance as

$$\bar{\tau}_w = R_h \left| \nabla p' \right| = R_h \left| \nabla p \right|$$

where the hydraulic radius is given typically by the relation

$$R_h = \frac{\varepsilon}{(1-\varepsilon)\, S_o} \tag{76}$$

η in Equation (74) is the non-Newtonian viscosity, which is discussed in an earlier section.

For the purpose of the discussion to follow, Equation (70) is rewritten in terms of the following equivalent matrix equation:

$$\begin{pmatrix} \eta_{11} & \eta_{12} & \eta_{13} \\ \eta_{21} & \eta_{22} & \eta_{23} \\ \eta_{31} & \eta_{32} & \eta_{33} \end{pmatrix} \begin{pmatrix} q_1 - er_1 - q_{s1} \\ q_2 - er_2 - q_{s2} \\ q_3 - er_3 - q_{s3} \end{pmatrix}$$

$$= -\begin{pmatrix} k_{11} & k_{12} & k_{13} \\ k_{21} & k_{22} & k_{23} \\ k_{31} & k_{32} & k_{33} \end{pmatrix} \begin{pmatrix} \frac{\partial p}{\partial x_1} \\ \frac{\partial p}{\partial x_2} \\ \frac{\partial p}{\partial x_3} \end{pmatrix} \tag{77}$$

By reference to the manner of formation of a filter cake, by deposition of the particles and compaction, in conjunction with a compressive force, it can be conceived that the permeability tensor for a filter cake is symmetric, that is $k_{ji} = k_{ij}$, as discussed earlier a set of orthogonal axes x, y, z can be found (with one of these axes being colinear with the $(\mathbf{q} - \mathbf{er} - \mathbf{q}_s)$ vector) with respect to which the k-matrix becomes a diagonal matrix. The same intuitive and physical considerations coupled with the expectation that when the $(\mathbf{q} - \mathbf{er} - \mathbf{q}_s)$ vector is successively considered colinear with each of the principal axes, the mapping indicated by Equation (71) in each case will yield a pressure gradient ∇p which is colinear with the mapped vector $(\mathbf{q} - \mathbf{er} - \mathbf{q}_s)$, lead to the result that the mapping tensor $\bar{\Phi}$ is also a diagonal matrix with respect to the same set of principal axes. Further, in

view of Equation (72), the important and significant result is found that the apparent viscosity tensor η_{ap} is also representable by a diagonal matrix with the same set of principal axes as the permeability tensor.

Hence for a filter cake, Equation (77), depicting Darcy's law, can be expressed in the simpler form

$$\begin{pmatrix} \eta_{ap,x} & 0 & 0 \\ 0 & \eta_{ap,y} & 0 \\ 0 & 0 & \eta_{ap,z} \end{pmatrix} \begin{pmatrix} q_x - er_x - q_{sx} \\ q_y - er_y - q_{sy} \\ q_z - er_z - q_{sz} \end{pmatrix}$$

$$= -\begin{pmatrix} k_x & 0 & 0 \\ 0 & k_y & 0 \\ 0 & 0 & k_z \end{pmatrix} \begin{pmatrix} \frac{\partial p}{\partial x} \\ \frac{\partial p}{\partial y} \\ \frac{\partial p}{\partial z} \end{pmatrix} \qquad (78)$$

which leads to the set of simultaneous equations given by

$$q_\alpha = er_\alpha + q_{s\alpha} - \frac{k_\alpha}{\eta_{ap,\alpha}} \frac{\partial p}{\partial x_\alpha} \qquad \alpha = x, y, z \qquad (79)$$

These contain the implicit assumption, also involved in Equations (74) and (75), that ϵ and e are only functions of position, i. e., $\epsilon = \epsilon(x, y, z)$, etc.

The set of Equations (79) leads to results consistent with expectation for the corresponding one-dimensional flow problems along either of the principal axes if the respective quantities **k** and η_{ap}, are given by the following relationships, analogous to Equations (73) and (74), respectively,

$$k_a = \frac{\epsilon R_{h_a}^2}{k_{ia}} = \frac{\epsilon^3}{k_{ia} S_{oa}^2 (1-\epsilon)^2} \tag{80}$$

and

$$\eta_{ap,a} = \frac{\bar{\tau}_{wa}^{\,1+\xi_a}}{(1+\xi_a)\int_{\tau_y}^{\bar{\tau}_{wa}} \frac{\tau^{\xi_a}}{\eta}\, d\tau\; T_a} \tag{81}$$

The a-subscript designation in the above equations refers to the values of the respective quantities applicable for flow in the direction along the a-principal axis. For example, R_{ha} refers to the hydraulic radius to flow along the a-principal axis and similarly S_{oa} is the surface area per unit volume with reference to flow in the a direction. It is noted that allowance is made for the variation of the impermeability factor k_i and the aspect factor ξ, characterizing the flow geometry of the voids, and the tortuosity T, with respect to the principal axis. In other words, the values of these quantities may be different for flow in each of the three directions determined by the principal x, y and z-axes, respectively. The quantity $\bar{\tau}_{wa}$ in Equation (81) is similarly evaluated from

$$\bar{\tau}_{wa} = R_{ha} \frac{\partial p}{\partial x_a} \tag{82}$$

For the analysis of the one-dimensional problem in Cartesian coordinates presently undertaken, we select the orthogonal principal x, y, z axes as our reference frame with the principal x-axis colinear with the $(\mathbf{q} - e\mathbf{r} - \mathbf{q}_s)$ vector. Thus Equations (79) representing Darcy's law reduce to a single non-trivial equation, which is written in the appropriate form

$$q_x = e_x r_x + q_{sx} + \frac{k_x}{\eta_{ap,x}} \frac{dp_x}{dx} \tag{83}$$

where the minus sign usually appearing before the pressure gradient term has been dropped since x now represents the distance measured from the filter medium, i. e., in the direction opposite to the direction of flow as already explained on Page 14 , in the analysis of the filtration of Newtonian fluids. An x-subscript has also been added to the void ratio e to emphasize that this quantity, in addition to the others, is a function of the position variable x.

Introduction of the solids compressive pressure given by Equation (11) in the analysis of Newtonian filtration as

$$p_s = p' - p_x' = p - p_x, \tag{84}$$

with the equality on the extreme right valid in filtration, into Equation (83) gives

$$q_x = e_x r_x + q_{sx} - \frac{k_x}{\eta_{ap,x}} \frac{dp_s}{dx} \tag{85}$$

or,

$$q_x = e_x r_x + q_{sx} - \frac{\rho_s (1 - \epsilon_x) k_x}{\eta_{ap,x}} \frac{dp_s}{dw_x} \tag{86}$$

where dw_x gives the mass of solids in a thickness dx of filter cake, in accordance with the Equation (9).

Equation (86) on rearrangement yields the basic differential equation for filtration of non-Newtonian fluids,

$$\frac{dp_s}{dw_x} = \frac{1}{\rho_s (1 - \epsilon_x)} \frac{dp_s}{dx} = - \eta_{ap,x} \alpha_x (q_x - e_x r_x - q_{sx}) \tag{87}$$

where

$$\alpha_x = \frac{1}{k_x \rho_s (1 - \epsilon_x)} = \frac{k_{ix}}{R_{hx}^2 \rho_s \epsilon_x (1 - \epsilon_x)}$$

$$= \frac{S_{ox}^2 k_{ix} (1 - \epsilon_x)}{\epsilon_x^3 \rho_s} \qquad (88)$$

It is interesting to note that Equation (87) reduces to Equation (17), the basic differential equation for filtration of Newtonian fluids, on replacing the non-Newtonian viscosity by Newtonian viscosity and equating q_s to zero because of the absence of surface effects in case of Newtonian fluids.

The subsequent development involves the introduction of a fluid model equation incorporating fluid parameters which characterize the viscous characteristics of the fluid. The Ostwald de-Waele or power-law fluid model equation, for which $1/\eta = (1/k)^{1/n} \tau^{(1/n) - 1}$, is chosen for its simplicity and usefulness in representation of fluid behaviour. The development, however, is not restricted to Ostwald-de-Waele fluids but applicable to time-independent viscous fluids in general since the variation of the flow behaviour parameters with the second invariant of the stress tensor τ or of the rate of deformation tensor γ is taken into consideration.

The expression thus obtained for the apparent viscosity is

$$\eta_{ap,x} = \frac{(\xi_x + 1/n_x)}{(1 + \xi_x)} (K_x)^{1/n_x} \bar{\tau}_{wx}^{1-(1/n_x)} \qquad (89)$$

When the defining relationship for the apparent viscosity extended to account for the movement of the solids associated with cake compaction,

$$\bar{\tau}_{wx} = \eta_{ap,x} k_{ix} \frac{(\langle u \rangle_x - u_{px} - \bar{u}_{sx})}{R_{hx}}$$

$$= \eta_{ap,x} k_{ix} \frac{(q_x - e_x r_x - q_{sx})}{\epsilon_x R_{hx}} \qquad (90)$$

is substituted for $\bar{\tau}_{wx}$ in Equation (89), there results

$$\eta_{ap,x} = K_x \left[\frac{(\xi_x + 1/n_x)}{(1+\xi_x)}\right]^{n_x} \left(\frac{k_{ix}}{\epsilon_x R_{hx}}\right)^{n_x - 1} (q_x - e_x r_x - q_{sx})^{n_x - 1} \qquad (91)$$

A comment might be in order, at this stage, with reference to the manner of selection of n_x and K_x at a section of the cake corresponding to a particular x. It has been found[71, 76, 77] that the power law fluid equation yields a good representation of the actual relationship between pressure gradient and average velocity if the fluid parameters n and K, which in general are functions of shear stress, evaluated at the wall shear stress are used. In the present case, n_x and K_x are similarly designated as the values of the fluid parameters n and K corresponding to the value of the second invariant τ given by the value $\bar{\tau}_{wx} = R_{hx}\,(dp/dx)$, applicable at the section.

The substitution of $\eta_{ap,x}$ as given by Equation (91) into the basic differential equation for filtration, Equation (87), gives, after some rearrangement,

$$\frac{dp_s}{a_x} = -K_x \left[\frac{(\xi_x + 1/n_x)}{(\xi_x + 1)}\right]^{n_x} \left(\frac{k_{ix}}{\epsilon_x R_{hx}}\right)^{n_x - 1} (q_x - e_x r_x - q_{sx})^{n_x} \, dw_x \qquad (92)$$

which is integrated as follows:

$$\int_{o}^{p-p_1} \frac{dp_s}{a_x} = -\int_{w}^{o} K_x \left[\frac{(\xi_x + 1/n_x)}{(\xi_x + 1)}\right]^{n_x} \left(\frac{k_{ix}}{\epsilon_x R_{hx}}\right)^{n_x - 1} (q_x - e_x r_x - q_{sx})^{n_x} \, dw_x$$

$$= w \int_{o}^{1} K_x \left[\frac{(\xi_x + 1/n_x)}{(\xi_x + 1)}\right]^{n_x} \left(\frac{k_{ix}}{\epsilon_x R_{hx}}\right)^{n_x - 1} (q_x - e_x r_x - q_{sx})^{n_x} \, d\left(\frac{x}{w}\right) \tag{93}$$

According to the mean value theorem, the integral on the right side of Equation (93) can be equated to the value of the integrand evaluated at an appropriate intermediate position within the cake, $0 < w_x/w < 1.0$. The net dimensions of the integral will thus be those of the dimensions of the integrand evaluated at this intermediate position. We designate the values assumed by n_x and K_x at this intermediate position as n and K, respectively, and introduce these parameters on the right side of Equation (93) which then becomes

$$\int_{o}^{p-p_1} \frac{dp_s}{a_x} = K q_1^{\,n} \, w \int_{o}^{1} \frac{K_x q_x^{\,n_x}}{K q_1^{\,n}} \left[\frac{(n\,\xi_x + n/n_x)}{n(\xi_x + 1)}\right]^{n(n_x/n)} \left(\frac{k_{ix}}{\epsilon_x R_{hx}}\right)^{n(n_x/n)-1}$$

$$(1 - e_x r_x/q_x - q_{sx}/q_x)^{n(n_x/n)} \, d\left(\frac{w_x}{w}\right) \tag{94}$$

It is presumed that the various quantities including $(K_x q_x^{\,n_x}/K q_1^{\,n})$, $(k_{ix}/\epsilon_x R_{hx})$, ξ_x, n_x/n, etc., appearing in the integral expression on the right side of Equation (94) can be specified as functions of the position variable w_x/w. Shirato[5, 6] derived a relationship between r_x/q_1 and w_x/w after Tiller and Shirato[4] had previously derived one between q_x/q_1 and w_x/w. Since $r_x/q_x = (r_x/q_1)(q_1/q_x)$, it is reasonable to expect that a relationship between r_x/q_x and w_x/w also exists in the present case.

The integral on the right side of Equation (94), which reduces to the simpler expression of Shirato[5, 6] given by Equation (23) for a Newtonian fluid, for which $n_x/n = n = 1$, is similarly designated as J_{Rn}. In general, it may be expected that J_{Rn} will be a function of n, as well as of the slurry concentration and pressure drop across the cake found for Newtonian fluids by Tiller and Shirato[4]. It is allowed that the flow behaviour index n will vary with the pressure drop across the cake $(p - p_1)$ as well as the concentration and composition of the polymer solution. For a given solution and slurry composition, however, the flow behaviour index n will depend upon the imposed pressure drop. It is clear from the earlier discussion that the net dimensions of J_{Rn} are L^{1-n}. For the situation in which n is found to be unity, as in the case of a Newtonian fluid, J_{Rn} will be dimensionless.

Thus Equation (94) may be represented in the simpler form

$$q_1^n = \left(\frac{dv}{d\theta}\right)^n = \frac{(p - p_1)}{K\, \alpha_R\, J_{Rn}\, w} = \frac{(p - p_1)}{K\, \alpha_T\, w} \qquad (95)$$

where α_R is the traditional filtration resistance as defined earlier by Equation (21)

$$\alpha_R = \frac{p - p_1}{\int_0^{p-p_1} \frac{dp_s}{\alpha_x}} \qquad (21)$$

and α_T the total specific resistance of the cake related to the resistance defined by Ruth by

$$\alpha_T = J_{Rn}\, \alpha_R \qquad (96)$$

The total filter medium resistance R_m is defined similarly in accordance with the relationship

$$p_1 = K q_1^n R_m \tag{97}$$

This expression may be utilized to rewrite Equation (95) in the form

$$q_1^n = \left(\frac{dv}{d\theta}\right)^n = \frac{p}{K(\alpha_R J_{Rn} w + R_m)} \tag{98}$$

Making use of the expression $w = \rho s v/(1 - m s)$, relating the weight of the filter cake to the volume of filtrate collected, we obtain

$$\left(\frac{d\theta}{dv}\right)^n = \frac{K \alpha_T \rho s}{p(1 - m s)} \left[v + \frac{R_m (1 - m s)}{\alpha_T \rho s}\right] \tag{99}$$

or, finally,

$$d\theta = \frac{n+1}{n\mathbb{K}} (v + v_o)^{1/n} dv \tag{100}$$

where

$$\mathbb{K} = \frac{n+1}{n} \left[\frac{p(1 - m s)}{K \alpha_T \rho s}\right]^{1/n} \tag{101}$$

and

$$v_o = \frac{R_m (1 - m s)}{\alpha_T \rho s} \tag{102}$$

The validity of these Equations (100, 101 and 102) is confirmed by their reducing to Equations (25, 26 and 27) respectively, on appropriate substitution of properties of Newtonian fluids.

Filtration at Constant Pressure

As pointed out earlier in the Newtonian filtration section, it is convenient to consider the constant pressure filtration as effectively consisting of two stages:

(1) the initial stage, of relatively short duration, in which p_1 is appreciable in relation to p so that α_R, n, J_{Rn} and therefore α_T will vary continuously; it is also considered that the effects of variation in the moisture content of the cake determined by m as well as of variations in p with time which may be encountered to varying extents during the commencement of the filtration are effectively confined to the initial stage,

(2) the main filtration stage of primary interest in which p_1 is negligible compared to p and the quantities α_R, n, J_{Rn} and α_T are effectively constant.

The relationship of the primary variables of both stages can thus be conveniently represented by the following relationship:

$$d\theta = \left[\frac{n+1}{n\mathbb{K}} (v + v_o)^{1/n} + F(v)\right] dv \qquad (103)$$

$$F(v) \neq 0, \quad 0 \leq v < v_i$$

$$F(v) = 0, \quad v \geq v_i$$

In Equation (103), the quantities n, $\mathbb{K}$ and v_o represent the final values assumed by these quantities in the main filtration stage. F(v) is a function of the filtrate volume which serves as a correction term yielding the correct $d\theta/dv$ in the initial stage of the filtration. As indicated the correction term is zero beyond the initial stage when the filtrate volume is greater than v_i, denoting the upper bound of the initial stage. As mentioned above, it is presumed that the effects of the variations involved in the various quantities are localized in the initial stage.

Equation (103) can be integrated, applying the limits $v = 0$ at $\theta = 0$ and $v = v > v_i$ at $\theta = \theta$, as follows

$$\theta = \frac{n+1}{nK} \int_{v_o}^{v+v_o} (v+v_o)^{1/n} \, d(v+v_o) + \int_o^{v_i} F(v)dv \qquad (104)$$

to obtain

$$\theta = \frac{1}{K} \left[(v+v_o)^{1+1/n} - v_o^{1+1/n} \right] + \theta_o \qquad (105)$$

where the constant value represented by the integral on the right side of Equation (104) has been replaced by

$$\theta_o = \int_o^{v_i} F(v)\, dv \qquad (106)$$

Setting v equal to zero in Equation (105) yields the result that $\theta = \theta_o$, which is appropriately termed the effective time of commencement of filtration

A series expansion using the Binomial Theorem can be effected, for $v_o^2 < v^2$, to rewrite Equation (105) in the form

$$\theta = \frac{1}{K} \left[v^{1+1/n} + \frac{(n+1)v_o}{n} v^{1/n} + \frac{(n+1)}{2n^2} v^{\frac{1}{n}-1} v_o^2 \cdots - v_o^{1+1/n} \right] + \theta_o \qquad (107)$$

or, neglecting terms of the order of v_o^2,

$$\theta = \frac{1}{K} v^{1+1/n} + Nv^{1/n} + \theta_o \qquad (108)$$

where

$$N = \frac{(n+1)v_o}{nK} = v_o \left[\frac{K a_T \rho s}{p(1-ms)} \right]^{1/n} \qquad (109)$$

For a Newtonian fluid for which $n = 1$, Equation (108) yields the expected result, Equation (31), confirming the validity of its derivation.

$$\theta = \frac{1}{K} (v^2 + 2v_o v) + \theta_o \qquad (110)$$

Equation (108) for θ is of a bilinear form and a linear regression analysis of the experimental data is therefore feasible. The procedure followed is the following. First it is noted that if n is arbitrarily assigned a value near unity, values of K, N and θ_o yielding the best least squares fit to the data of the resulting equation corresponding to the value of n selected can be determined. Thus, in order to obtain the particular set of values of n, K, N and θ_o giving the best overall fit of Equation (108) to the data, one can assign n a number of different values successively in the neighbourhood of unity and compute the variance of the equation from the data for each set of coefficients determined and the corresponding n value. The set yielding the minimum variance, if one exists, gives the equation with the best fit. It is also found interesting and useful for comparison purposes to repeat the analysis just described using Equation (108) with N set equal to zero corresponding to zero filter medium resistance.

Filtration at Constant Rate

Following the analysis presented earlier, in the constant rate filtration of Newtonian fluids, from Equations (34) to (36), the mass of filter cake, in constant rate filtration, can be represented by the following relationship:

$$w = \frac{\rho s v}{1 - m s} = \frac{\rho s (q_1 \theta + v_o)}{1 - m s} \qquad (24)$$

Hence, Equation (95) after rearrangement and combination with Equation (21) yields

$$(p - p_1) = \frac{K \alpha_T \rho s q_1^{n+1}}{1 - m s} (\theta + \theta_c) = \lambda q_1^{n+1} (\theta + \theta_c) \qquad (111)$$

where λ is given by

$$\lambda = \frac{K a_T \rho s}{1 - m s} \tag{112}$$

The quantities λ and n, respectively, are expressed as functions of $(p - p_1)$ suggested by the results of study of constant pressure filtration which are presented in the next chapter, as follows:

$$\lambda = \lambda_o (p - p_1)^{r_o} \tag{113}$$

and

$$n = n_1 + m_o \log (p - p_1) \tag{114}$$

It is not necessary to be concerned by the fact that Equation (113) predicts $\lambda = 0$ at $p - p_1 = 0$ since it is only required that the relationships give good representations of the actual behaviour in the interval beyond the initial period of the constant rate filtration, that is, for $\theta > \theta_i$.

Making the substitutions indicated by Equations (113) and (114) in Equation (111) and taking the logarithm of both sides yields

$$\log (p - p_1) = \log \lambda_o q_1^{1+n_1} + (r_o + m_o \log q_1) \log (p - p_1) + \log (\theta + \theta_c) \tag{115}$$

or, finally,

$$\log (\theta + \theta_c) = A \log (p - p_1) - \log B \tag{116}$$

where

$$A = 1 - r_o - m_o \log q_1 \tag{117}$$

and

$$B = \lambda_o q_1^{1+n_1} \tag{118}$$

Equations (116) to (118) are consistent with Equations (41) and (42) derived for constant rate filtration of Newtonian fluids.

Equation (116) suggests that a log-log plot of the constant rate filtration data collected in the main filtration stage should yield a straight line with slope $A = 1 - r_o - m_o$ and value of the abscissa at $(p - p_1) = 1$ determined by $\log \lambda_o q_1^{1+n_1}$ when plotted as $(\theta + \theta_c)$ versus $(p - p_1)$. Since experimental data usually provide the overall pressure drop p and the time θ, as well as the quantity $(\theta + \theta_c)$, the pressure drop $(p - p_1)$ which is not known must be estimated. A tentative value of p_1 can be found by plotting θ versus p on linear graph paper, passing a smooth curve through the points, and extrapolating the curve to the pressure axis, where $\theta = 0$. The tentative result thus found can be used to prepare a plot of $(p - p_1)$ versus $(\theta + \theta_c)$ on log-log graph paper. If the line so obtained is linear then the tentative value of p_1 can be taken as final. If the line is curved, additional approximations for p_1 can be made until a straight line results. A digital computer can be used to advantage where the algorithm involves selecting the value of p_1 giving the best fit of the curve to the data. The requirement for achieving the best fit is that the variance between the calculated curve and the data, corresponding to the final p_1 value selected, is a minimum.

CHAPTER IV

EXPERIMENTAL DETAILS

This chapter deals with the materials used for the experiments, preparation of Natrosol solutions, experimental apparatus, and the procedure of conducting the experiments.

Experimental Materials

Newtonian filtration runs at constant pressure and constant rate were conducted with different initial periods using aqueous slurries containing 2.5 per cent calcium carbonate (C-62, Fisher Scientific Co.) by weight. These runs served the purpose of verifying the performance of the experimental set up and provided the necessary data to establish the effectiveness of the time correction applied to eliminate the ambiguity in the initial stage of filtration.

The non-Newtonian fluids investigated were aqueous solutions of different grades of hydroxyethyl cellulose (Natrosol 250 G and 250 HR, Hercules Powder Co., Wilmington, Del.) at varying concentrations. Natrosol has been described as a linear polymer with only a slight degree of chain branching but with a more restricted rotation about the connecting bonds[57]. Natrosol 250 is a nonionic water-soluble hydroxyethyl ether of cellulose produced in six different viscosity types designated HH, H, M, G, J and L to fit its varied uses as thickener, protective colloid, binder, stabilizer, suspending agent and film former. Like sodium-carboxymethyl cellulose (Na- CMC) it is a cellulose ether but it differs in being nonionic and its solutions are unaffected by cations.

Table (I) gives product specifications and typical properties for the six viscosity types. A rapid dissolving grade, designated with a "R", is available in all viscosity types. Natrosol 250 HR, used in some of these experiments, is one such rapidly dissolving grade of viscosity type designated by H.

The viscosities obtainable using the six types of Natrosol 250 at various concentrations are shown in Fig. 2. This information was provided by the manufacturer which helped in choosing the concentrations of the solutions used in the present experiments. Viscosities presented in this figure were determined at 25°C with a Brookfield viscometer[72].

The higher viscosity types with more efficient thickening action are generally used in paint manufacture, textile printing pastes and inks, and adhesives. The lower viscosity types are protective colloids in such applications as vinyl-type polymerizations, pigment dispersions, electroplating solutions and cosmetics. As a binder, stabilizer, or suspending agent, Natrosol 250 in the medium to low range is used in ceramics, refractory compositions, coloured pencil leads, plastic and tile adhesives: or in surface coatings for textile sizing, paper applications, and glass fiber sizing.

The basic difference between Natrosol 250 G and Natrosol 250 HR is their belonging to two different viscosity types. The former one is classified as the lower viscosity type whereas the latter one falls in the region of higher viscosity types. As already pointed out, Natrosol 250 HR is a rapid-dissolving grade. Added to this, solutions of Natrosol HR are reported to have exhibited viscoelastic behaviour[57], on the contrary, the solutions of Natrosol G do not

TABLE I

SPECIFICATIONS AND TYPICAL PROPERTIES

Viscosity Limits Of Water Solutions

Viscosity Type	Brookfield Viscosity At 25° C. At Varying Concentrations (cps.) 1%	2%	5%
HH	3,000-4,000	>75,000	-
H	1,500-2,500	>25,000	-
M	-	4,500-6,500	-
G	-	150-400	-
J	-	-	150-400
L	-	-	75-150

All viscosity types conform to the following additional specifications:

Ash (calculated as Na_2SO_4), %	4 max.
pH	6.5-8.5
Color	white to slight tan
Moisture (as packed), %	5 max.
Particle size: passing U. S. #40 mesh, %	90 min.
Bulk density, g./ml.	0.55-0.75

Other useful properties which are typical of Natrosol 250 are:

Refractive index at 25° C. (2 % in water solution)	1.336
Specific gravity at 25/25° C. (solid)	1.45-1.60
Bulking value, gal./lb. (2 % in water solution)	0.12

Toxicity

Testing to date has shown no evidence of toxicity or irritation due to handling Natrosol, or exposure to Natrosol dusts.

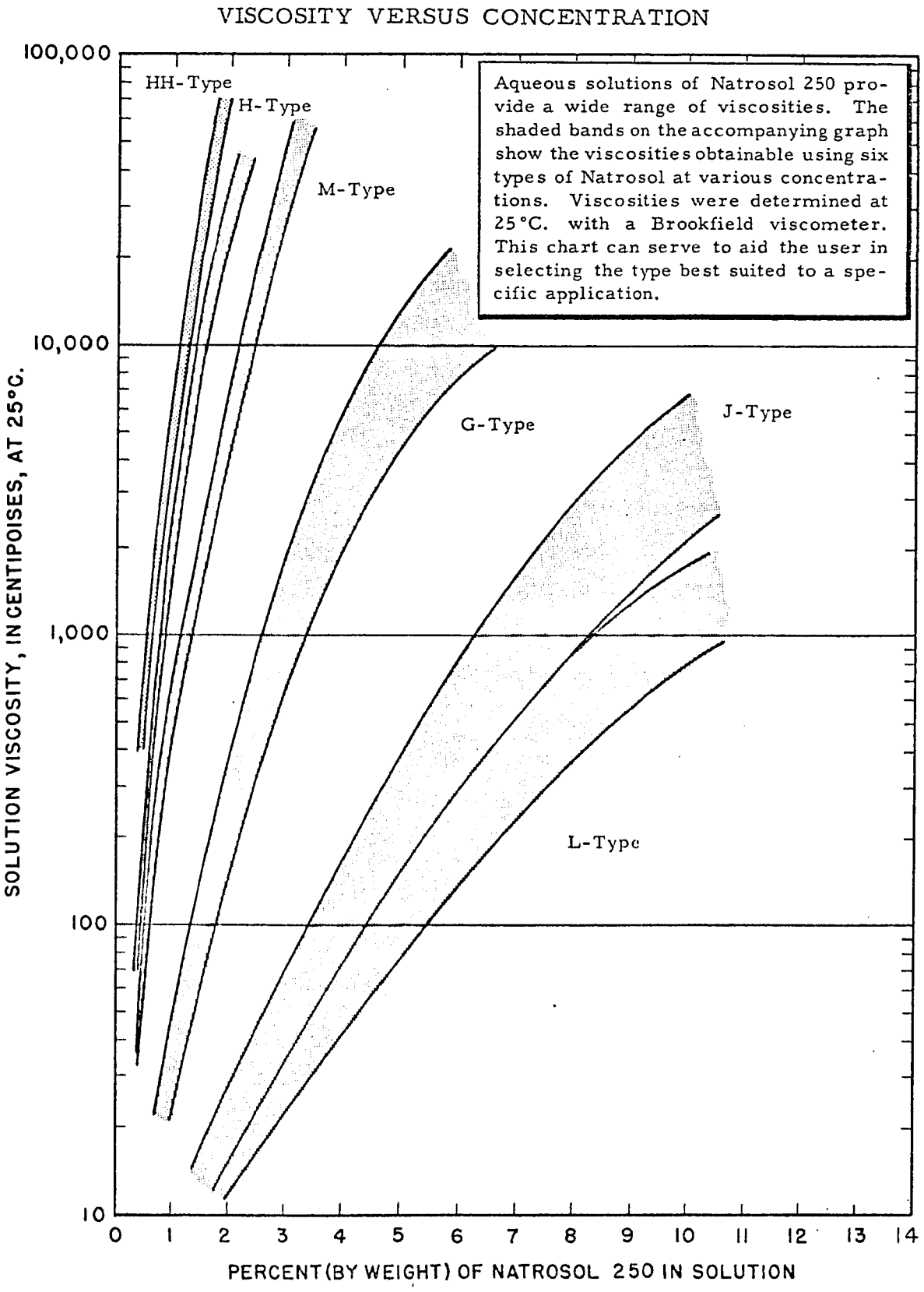

Fig. 2 Plot of viscosity versus concentration for Natrosol 250 solutions.

seem to possess such viscoelastic characteristics. More about this behaviour is discussed in a later part of the thesis while analysing the experimental results.

The structure of the cellulose molecule, showing its chain composed of anhydroglucose units, is presented in Figure 3A. Each anhydroglucose unit contains three hydroxyls capable of reaction. By treating cellulose with sodium hydroxide and reacting with ethylene oxide, hydroxyethyl groups are introduced to yield a hydroxyethyl ether. The reaction product is purified and ground to a fine white powder.

The number of reactive hydroxyl groups, possessed by each anhydroglucose unit in the cellulose, substituted in any reaction is known as the "degree of substitution" Theoretically, all three hydroxyls can be substituted. Hydroxyethyl groups can be introduced into the cellulose molecules in two ways. First, ethylene oxide reacts at the hydroxyls in the cellulose chain. Second, ethylene oxide, reacting at previously substituted hydroxyls, can polymerize to form a side chain. The average number of moles of ethylene oxide that becomes attached to each anhydroglucose unit in cellulose, in the two ways described, is called moles of substitutent combined, or M. S.

Natrosol is produced in three degress of substitution, 1. 8, 2. 5, and 3. 0, designated respectively as Natrosol 180, Natrosol 250, and Natrosol 300. In reacting ethylene oxide with cellulose to form the hydroxyethyl ether of cellulose, solubiility in water is achieved as the degree of substitution is increased. By selecting appropriate reaction conditions and moles of substituent, complete and quick solubility in water is obtained. Natrosol 250 which has optimum

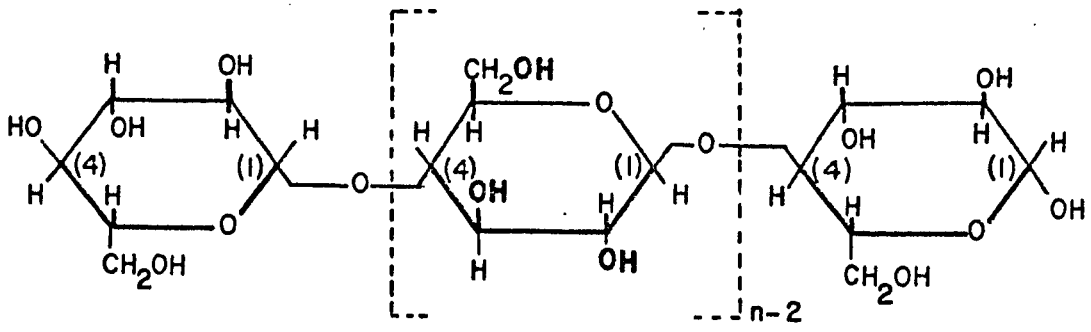

Fig 3A STRUCTURE OF CELLULOSE

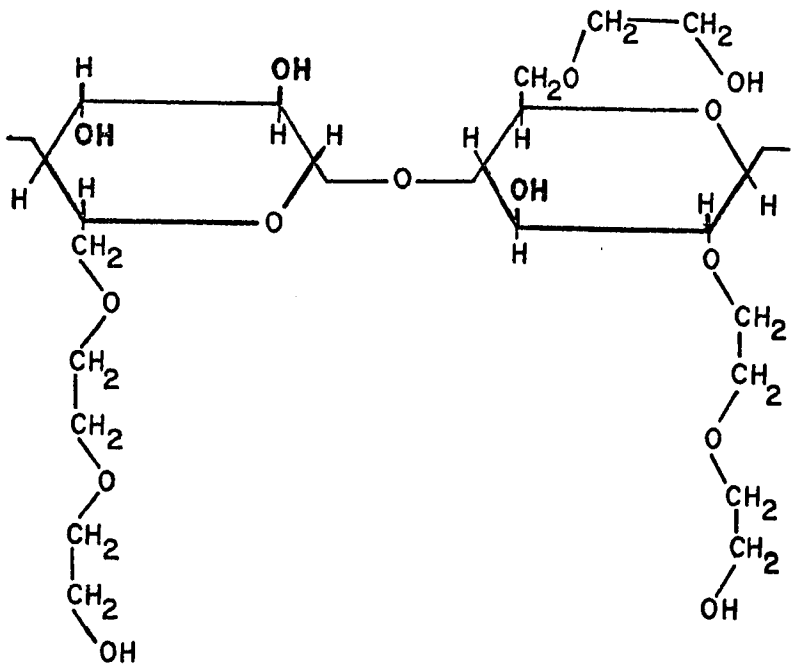

Fig 3B IDEALIZED STRUCTURE OF NATROSOL 250

solubility in water, has an M. S. of 2. 5. An idealized structure of Natrosol 250 is shown in Figure 3B. Dilute solutions of Natrosol 250 G and Natrosol 250 HR were used for the experimental work reported here. It is believed that cellulose derivatives do not possess a spherical symmetry in solution but rather a slightly extended rod configuration due to the stiffness of the chain. There is no definite information about the molecular weight of these polymers. According to Goring[78], the molecular weight should be comparable to that of CMC which is in the range of 15×10^4 to 35×10^4. Hence, the high molecular weight Natrosol solutions will extend the "degree of non-Newtonianness".

Natrosol can absorb moisture from the atmosphere as do other water soluble or finely divided materials. The amount of moisture absorbed depends on initial moisture content of Natrosol and on the relative humidity of the surrounding air. As packed by the manufacturer (Hercules Co.), the moisture content of all grades of Natrosol did not exceed the maximum of 5 per cent by weight. On long storage, the moisture content of this chemical tends to reach an equilibrium level that varies with the humidity of the surrounding atmosphere. To keep it at the original moisture content, Natrosol was stored in tightly closed containers and in dry atmosphere as recommended by the manufacturer.

PREPARATION OF SOLUTIONS

Natrosol is readily soluble in either cold or hot water. However, as with most water-soluble thickeners the particles have a tendency to agglomerate or lump when they are first wet with water. Thus, the time required to achieve complete solution of Natrosol is usually governed by the degree of lumping which is allowed to develop

during the solution process. In general, the low-viscosity types are more easily dissolved than those of the high-viscosity types. The R-grade solves the problem of lumping and slow dissolving by dispersing more quickly, and helps the user to obtain the solutions more readily.

The following procedure was used for easiest and more efficient preparation of solutions of Natrosol. Solutions of desired concentration were prepared by gradually dissolving the polymer material in a known amount of hot water which was continuously agitated by a mechanical stirrer. Natrosol was sifted slowly into the vortex of this vigorously agitated water. The rate of addition was slow enough for the particles to separate in water without lump formation. Agitation was continued until all of the swollen or gelatinized particles were dissolved to yield a clear and smooth solution. The time taken for dissolution varied from 20 to 80 minutes depending on the desired concentration, initial temperature of hot water and the intensity of agitation.

When using Natrosol 250 HR, the preparation of solutions was much simpler. In this grade, the hydration rate has been inhibited so that when dispersed in water the particles separate and form instantaneous, lump free dispersions. The special processing to which this chemical is subjected during the process of production retards surface gelation and causes particles to swell and dissolve rather than agglomerate into lumps. Hence, by simply adding R-grade to water, stirring sufficiently to secure even distribution, and allowing the mixture to stand for the complete hydration while maintaining sufficient stirring to prevent settling, clear, smooth, and viscous solutions were easily obtained within a short time. The R-grade contributes this ease of dispersion in conventional equipment

and eliminates the need either for presolution processing or complex heating and cooling operations.

The concentrations of solutions used in the present investigations were 0.6%, 0.8%, and 1.0% by weight in the case of Natrosol 250 G and 0.1%, 0.2%, and 0.3% by weight in the case of Natrosol 250 HR. Densities of these polymer solutions were determined by weighing known volume of solutions in a pycnometer at 25°C. These values are presented in a tabular form in Appendix A.

Given below are some of the common properties of Natrosol 250 solutions:

1. Water solutions of Natrosol 250 are smooth, nongrainy, and clear.
2. Solutions are nonthixotropic and flow smoothly. Their viscosities do not increase on standing.
3. Viscosity-concentration relationships for all viscosity types are substantially linear. This permits wide latitude in use.
4. Solution viscosities decrease regularly as their temperature is raised and regain viscosity on cooling. Thus, solutions show no tendency to gel on heating, even at the boiling point.
5. Natrosol being a nonionic polymer, its solutions show outstanding tolerance to high concentrations of dissolved salts. Solutions also undergo little viscosity change over the pH range of 2.5 to 10.5.
6. Natrosol solutions possess surface-active properties. This contributes to their utility as stabilizers and protective colloids.
7. Natrosol solutions have demonstrated excellent compatibility with a wide variety of natural and synthetic water-soluble gums.

and also with natural and synthetic latexes such as poly vinyl acetate. styrene-butadiene, acrylic and alkyd emulsions.

8. Solutions possess greater viscosity stability in the pH range of 6. 5 to 8. 0. Under acid conditions, solutions may suffer some decrease in viscosity due to acid hydrolysis. This is common to all water-soluble polymers and is accelerated by high temperature and high acidity. Under highly alkaline conditions, some oxidative degradation may occur to reduce viscosity. This may be inhibited by the use of an antioxidant such as hydroquinone.
9. Films cast from solutions of Natrosol are strong, clear and possess excellent flexibility.

Even though Natrosol 250 is more resistant to microbiological degradation than natural gums and colloids, a water-soluble preservative is recommended by the manufacturer if the solutions are to be stored. Water-soluble fungicides such as Formalin, Dowicide A or B, phenyl mercuric acetate (PMA), or Methyl Parasept are suitable. It is recommended that preservatives be added at the time of solution makeup. In the absence of a preservative, solutions may degrade with subsequent decrease in viscosity and appearance of haze. To avoid the microbiological degradation, fresh solutions of desired concentration were prepared on the day on which experiments were to be conducted. The possibility and extent of mechanical degradation of the polymer molecules in the solution during pumping and filtration was verified and the relevant details are given in the chapter in which the discussion of results is presented. A capillary tube viscometer was used to characterize the flow behaviour of these polymer solutions. The details of the viscometer construction and operation are given in the later part of this chapter.

Twill filter cloth (T. Shriver Co.) of following specifications was used as a filter medium to carry out the investigations reported here.

style	type	plies	count	weight, ounces/sq. yd.
3627	Twill	3 x 3	36 x 30	15.5

As mentioned earlier in the theoretical section, the resistance offered to flow by the filter medium varies from experiment to experiment even for the same sludge and filter. Also, used filter cloth offers more resistance than a fresh one. To maintain the consistency, fresh filter cloth was used for every filtration run conducted in this laboratory.

Usually, error analysis is not performed for the filtration experiments. In any case, the plots of variance versus values of n and p_1, which are typical of many prepared in the course of processing the data, give an idea of the deviations involved.

EXPERIMENTAL SET UP

Filtration Unit

The filtration equipment, shown schematically in Figure 4, included a filtration cell containing a plexiglass unit of circular cross section with an inside diameter of 2. 875 inches. The detailed sketch of filtration cell is given in Figure 5. The plexiglass unit was an assembly of two pieces at whose union the filter medium was placed. The lower section of the plexiglass unit formed a part of calming section and its transparency permitted the observation of the cake formation during a filtration run. The wall thickness of this part was chosen as 1. 325 in. to withstand the high filtration pressures to which it was exposed while conducting the experiments. The upper plexiglass section served as the receiver for the filtrate emerging from the filter septum. Provision was made in this section to measure the downstream pressure of filtration with a manometer. The volume of this section was kept at a possible minimum to enable the measurement of accumulated volume of filtrate at the earliest possible instant after the commencement of filtration. The filter medium (Twill cloth, T. Shriver Co.) was supported by a uniformly perforated brass plate to maintain the plane perpendicular to the direction of the flow. Leak proof union between the brass plate and the upper plexiglass piece was achieved by using a Teflon gasket. The plexiglass assembly was fixed to the stainless steel column, with the same inside diameter, providing the additional length for the calming section before the filtration stage. The connection between the plexiglass unit and the stainless steel column was achieved with the flange joints, making dismantling easy for cleaning purposes after a filtration run. Flange plates were kept in tact with

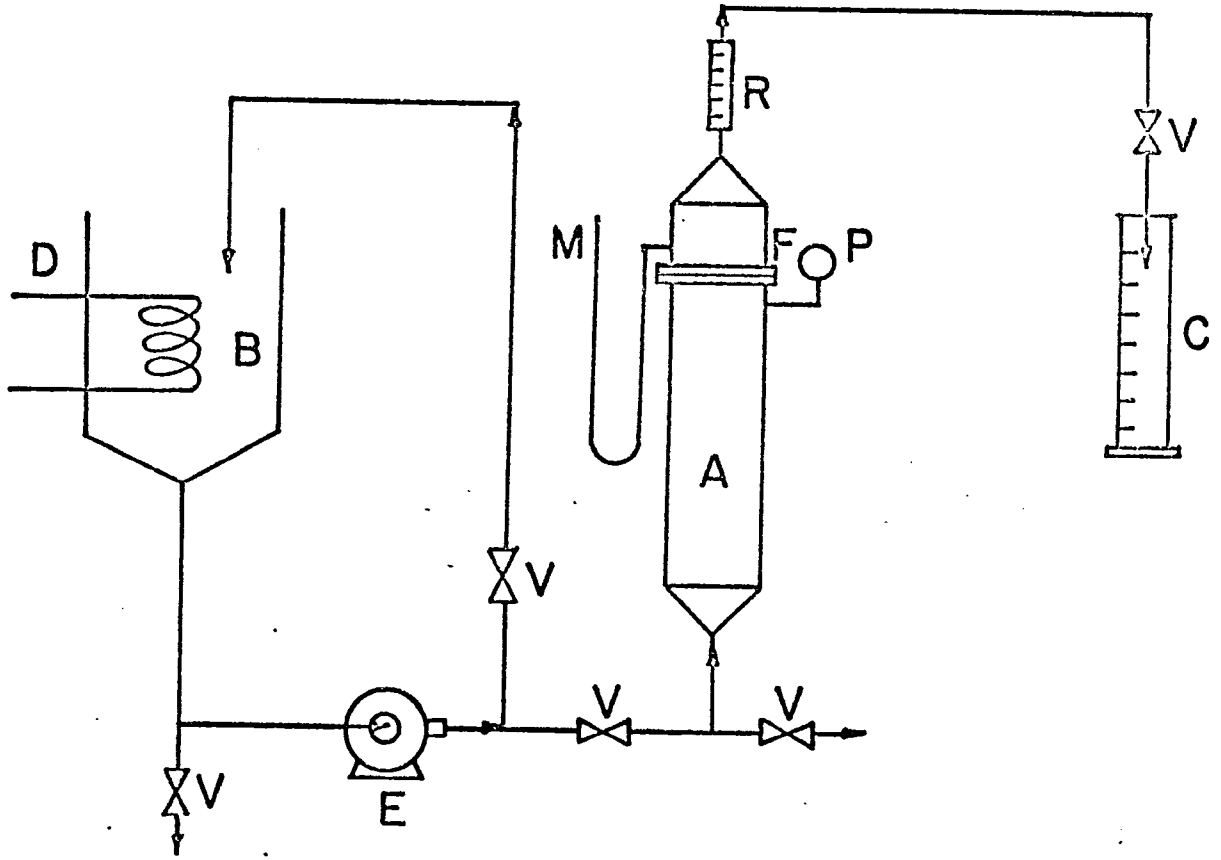

A - FILTRATION COLUMN

B - FEED TANK

C - GRADUATED CYLINDER

D - COOLING COIL

E - PUMP

F - FILTER MEDIUM

M - MANOMETER

P - PRESSURE GAUGE

R - ROTAMETER

V - VALVE

Fig. 4 Schematic diagram of filtration apparatus and flow lines.

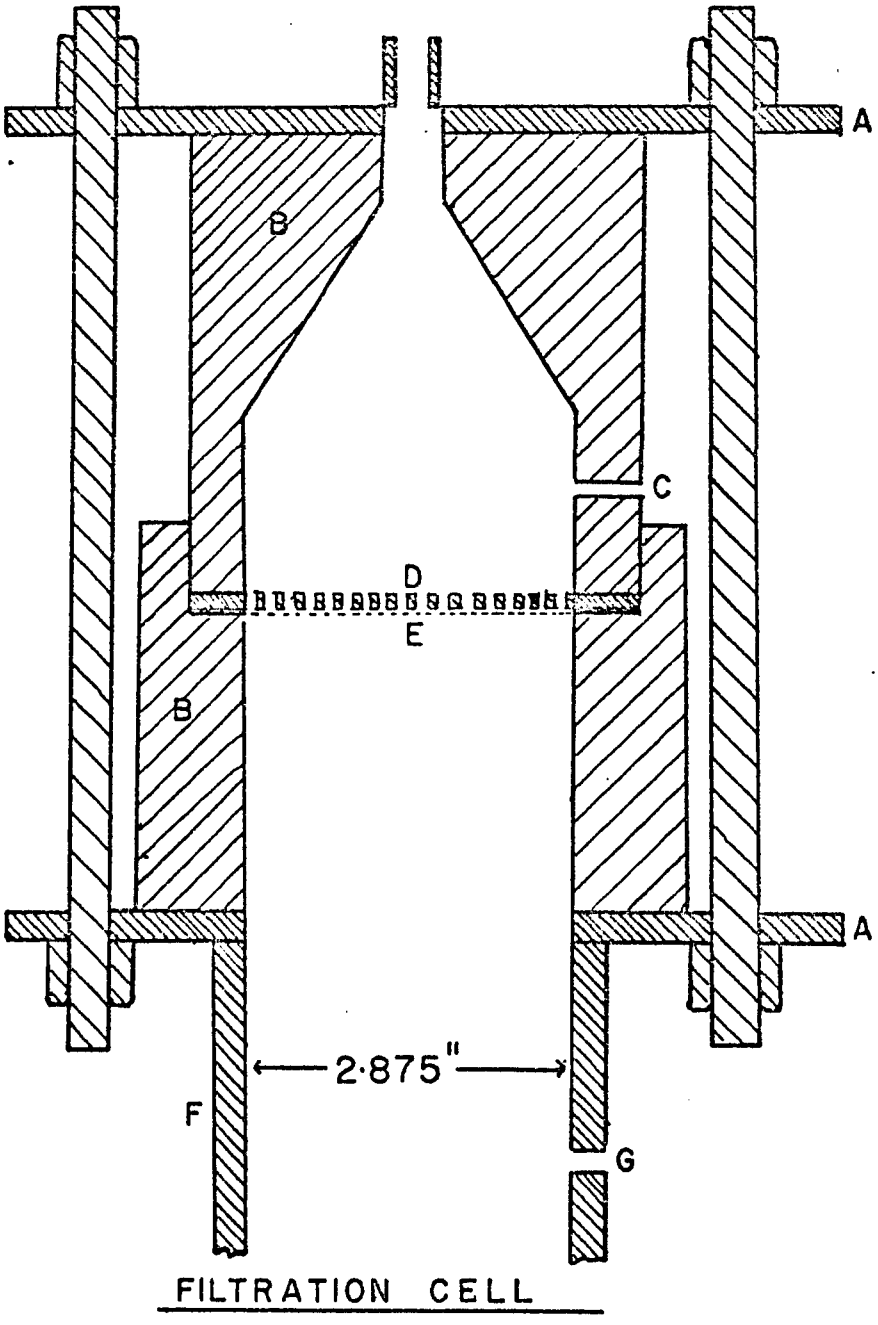

FILTRATION CELL

A– Flange plates

B– Plexi glass pieces

C– Connection to manometer

D– Perforated brass plate

E– Filter medium

F– Calming section

G– Connection to diphragm pressure gauge

Fig. 5 Detailed sketch of Filtration Cell.

the help of the nuts fitted at the ends of eight threaded steel rods placed evenly on their circumference. Teflon gaskets were used to achieve leakproof contact between the flange plates and the plexiglass assembly As mentioned earlier, the stainless steel column provided the additional length for the calming section. The limitation on the length of the calming section was imposed by the residence time of the slurry during a filtration run. The calming section of 11 inches was provided to obtain uniform velocity at the test section and at the same time to keep the settling of the particles in this section to a minimum. Calculations, based on the solids deposited during filtration and the volume of the filtrate collected, indicated that there was no appreciable amount of change in the concentration of slurry in the calming section to seriously affect the values of the quantities calculated from the filtration data. Provision was made to measure the pressure on the upstream side of filtration by connecting a diaphragm pressure gauge to the stainless steel column. The pressure gauge connections are shown in detail in Figure 6. Diaphragm gauges of different pressure ranges were used depending on the requirement of the filtration run. The capillary tube connecting the diaphragm unit to the gauge dial was two feet long and was made of flexible material. The diaphragm unit consisted of a cleanout ring which was specially designed to trap impurities that develop in the line due to the corrosive action of the process fluid. The ring could be removed and left off the line to be cleaned, while the gauge and diaphragm could be mounted directly on the line. The diaphragm unit was fitted to the calming section of the filtration unit in such a way as to facilitate the expulsion of the air present in the section connecting to the filtration unit. The pressure gauges were unmounted and cleaned of the

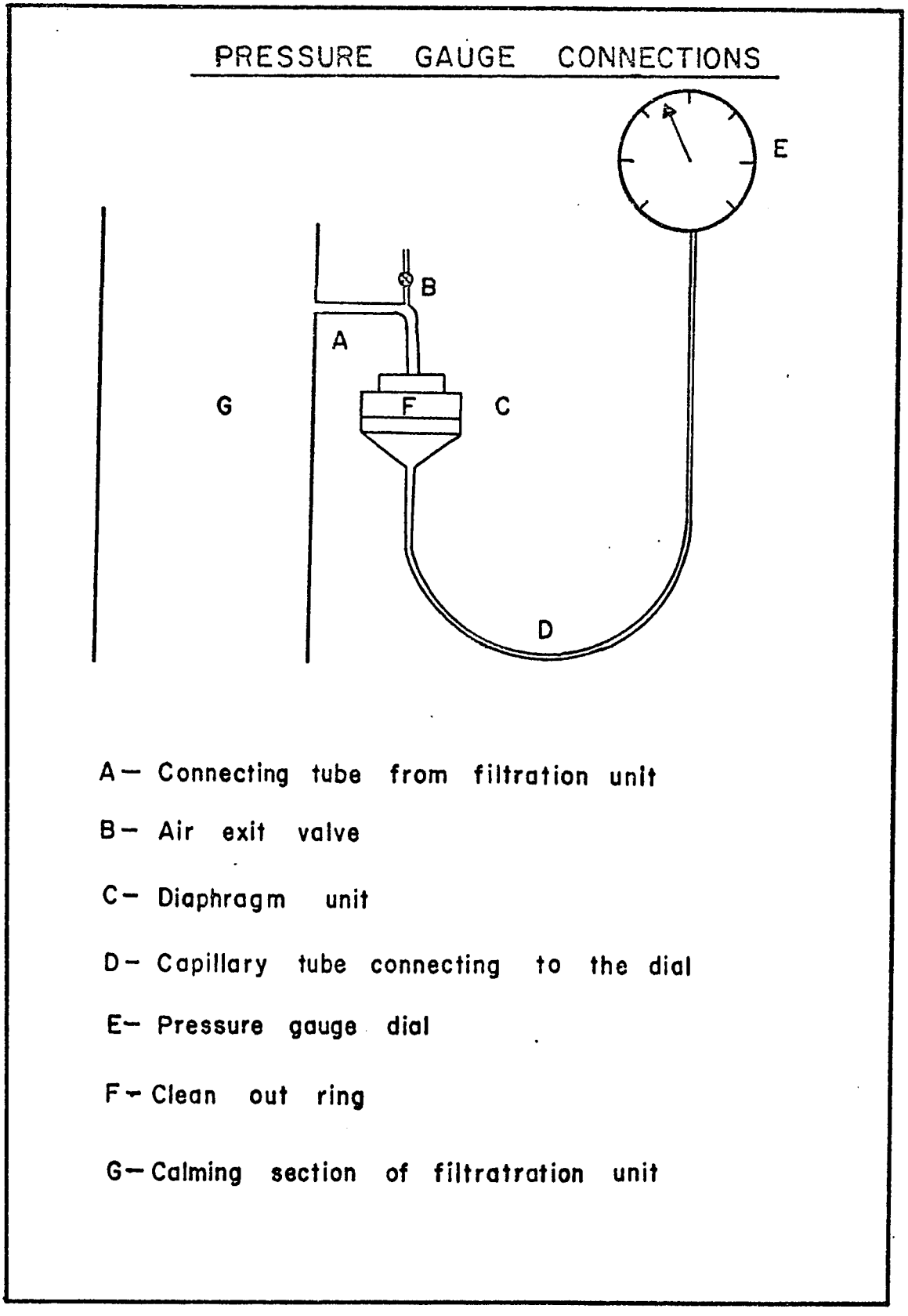

Fig. 6 .Detailed sketch of Pressure Gauge Connections.

impurities from time to time. These gauges were calibrated against the standard pressure gauges available in this laboratory.

A rotary gear pump driven by a 2-horse power motor, provided with an electronic variable speed control circuit (Boston Ratiotrol Model E300), transported the slurry to the filtration unit and developed the necessary upstream pressure. The slurry was fed to the pump from a cone bottomed stainless steel tank in which settling was kept to a minimum by recirculation via a by-pass line. A cooling coil, situated in the slurry tank, removed any heat generated in the pumping and circulation, maintaining a constant feed temperature.

A rotameter used in regulation of the flow rate in constant rate filtration was situated in the filtrate line. The filtrate was discharged into a graduated cylinder so that the volume of the filtrate could be recorded.

The performance of the filtration unit was verified with the data collected during the Newtonian filtration, which are presented in Appendices B and C. After every filtration run, the complete system was washed with hot water to remove the traces of non-Newtonian fluid completely. This procedure avoided the formation of non-Newtonian films on drying and their effect on the characteristics of the fluids used in the subsequent filtration runs.

Procedure of Conducting Filtration at Constant Pressure

This experimental procedure involved the circulation of non-Newtonian slurry until a slurry of uniform composition at the desired constant temperature was obtained. Once this requirement was fulfilled, the slurry was introduced to the filtration cell gradually,

by careful manipulation of the valve situated in the line of filtration unit. Before the slurry could reach the filter medium, placed in the plexiglass assembly, the connecting tube to the diaphragm unit was carefully filled with the slurry expelling the air present in this section. The complete expulsion of the air was indicated by the overflow of the slurry from this section after which the valve in the air expulsion line was closed. The filtration pressure was increased gradually by closing the valve in the by-pass line taking care not to rupture the filter medium. The timer was started when the first drop of filtrate was observed on the downstream side of the filter medium. Soon after the filtrate level reached the connection leading to the manometer, air in the line was carefully replaced by the filtrate and the necessary steps were taken to record the pressure on the downstream side of filtration. The filtrate was discharged into a graduated cylinder. The accumulation of filtrate volume versus time data was continued subsequent to the attainment of desired final pressure to obtain data points representative of the main filtration stage.

The temperature of the fluid was maintained at 25 ± 1°C., throughout the filtration run. The temperature of the filtrate emerging out of the unit was checked to detect if there was an appreciable change in temperature during the filtration process. The verification did not show such change in temperature which would affect the flow characteristics of the fluid. The verification was carried out at frequent intervals to the completion of the filtration run. The run was continued until a sufficient number of data points were collected.

At the completion of collecting the data, upstream pressure was decreased by manipulating the valve in the by-pass line. This act was accompanied by the closure of the valve leading to the

filtration cell. The filtrate, present in the upper section of the plexiglass assembly, was siphoned into the graduated cylinder and its volume was recorded. The flange plates were taken apart making it possible to dismantle the plexiglass assembly. The cake was carefully removed. The weights of wet and dry cake were determined. A glass petri dish was used for cake weighing to ensure that the moisture content of cake did not vary in the process of weighing. An oven maintained at 110°C was used for the purpose of drying the cake. The data collected during the constant pressure filtration of Newtonian and non-Newtonian fluids are tabulated in Appendix B.

Filtration at Constant Rate

The procedure followed to conduct the filtration run at constant rate was the same as in previous case (constant pressure run) to the stage of expelling the air from the connecting tube to diaphragm gauge. The pressure on the upstream side of filtration was increased gradually by manipulating the valves situated in the line leading to filtration unit and in the recirculation line. The timer was started when first drop of filtrate appeared on the downstream side of filter medium. Provision was made to read the downstream pressure by connecting to the manometer soon after the level reached the level of connecting tube. With the present experimental set up, filtrate rate could not be measured till the level reached the float in the rotameter. Hence, there was no indication to know if the flow of filtrate was maintained at the desired constant rate during this process. The variation in the rate during the initial stage was corrected successfully using the method of treatment suggested by Kozicki et al.[85], which was

presented earlier in the theoretical section. The flow rate was finally adjusted to the exact desired value when the rotameter was filled with the filtrate. The flow rate was subsequently maintained constant by manual valve adjustment. The variation in the filtration pressure and the accumulated volume of filtrate were recorded at convenient time intervals. The run was continued until a sufficient number of data points representative of main stage of filtration were collected. The remaining procedure to complete the run was the same as in the case of constant pressure filtration. The data collected during the constant rate filtration of Newtonian and non-Newtonian fluids are presented in tabular form in Appendix C.

Viscometer

In the present investigations, a laboratory designed and constructed capillary tube viscometer was utilized to determine the flow curves for the dilute Natrosol solutions. The schematic diagram of this experimental set up is shown in Figure 7. The viscometer consisted of a stainless steel reservoir with an inside diameter of 2.875 inches and a height of 13.4 inches. The lower portion of the viscometer was welded to a flange joint making dismantling easy for cleaning purposes. The capillary tube was fastened to the reservoir through an internally threaded hexagonal nut welded to the lower flange. Standard sleeves and male glands for Ermeto connections were used. Provision was made for the introduction of the experimental fluid at the top of the reservoir, which was also provided with connections to lines leading to pressure gauges, for determination of the pressure within the unit. The pressure inside the viscometer was measured by means of a USG test gauge with an accuracy of (a) 0.2% scale range for first twenty per cent of the range, (b) 0.5% of indicated reading for remainder of the dial range in the pressure ranges employed (10 to 350 psig). The compressed air displacing the fluid drained from the reservoir, during a measurement, was introduced tangentially at the top from the side of the reservoir to prevent bubble and foam formation resulting from direct impingement of the gas jet into the liquid. The major portion of the capillary tube was situated inside the viscometer to achieve a uniform temperature along the length of the capillary. The temperature rise due to possible viscous heat dissipation accompanying the flow through

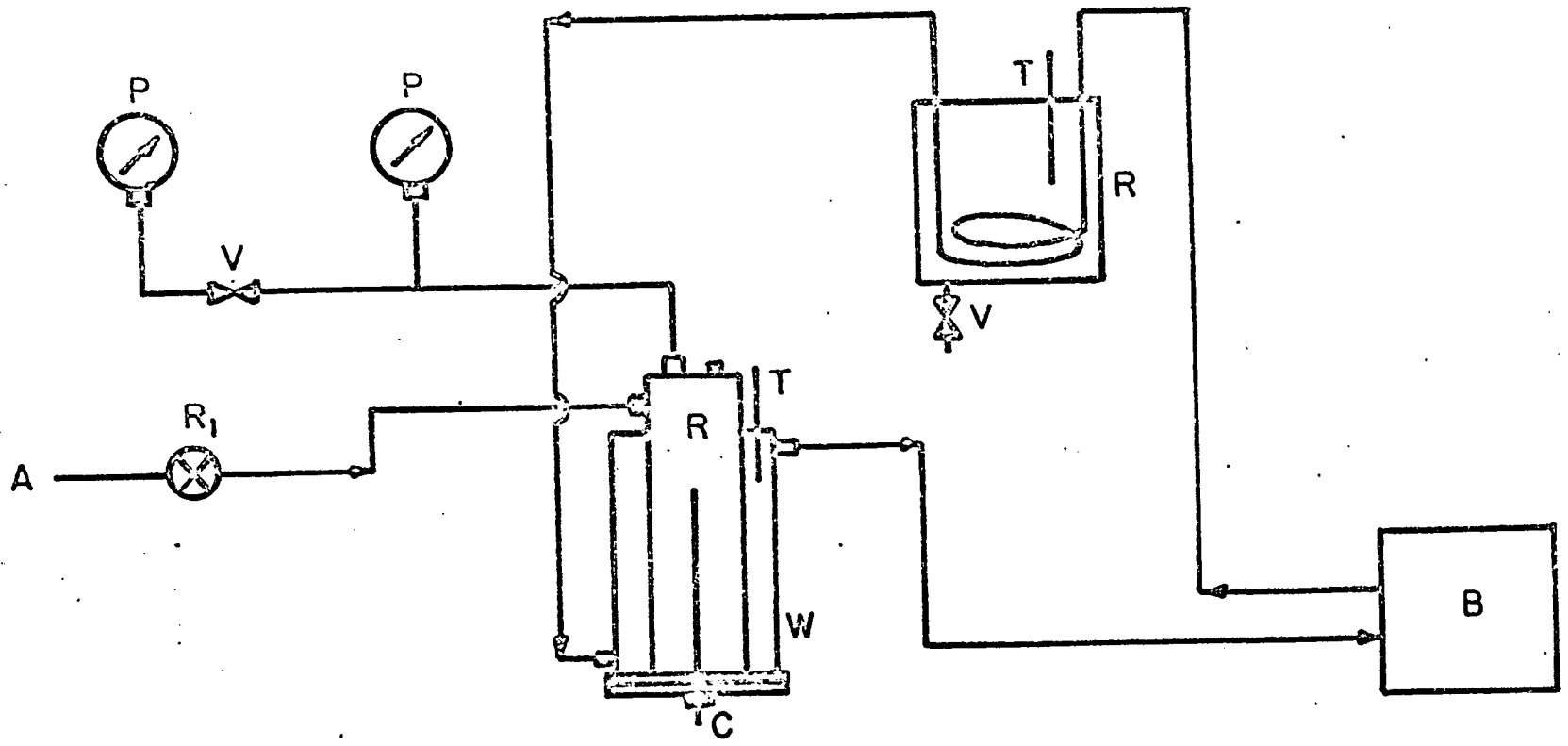

A - COMPRESSED AIR

B - CONST. TEMP. WATER BATH

C - CAPILLARY TUBE

P - PRESSURE GAUGES

R_1 - PRESSURE REGULATOR

R - FLUID RESERVOIRS

T - THERMOMETERS

V - VALVES

W - WATER JACKET

Fig. 7 Schematic diagram of viscometric apparatus.

the capillary was measured and found to be negligible. Water from a constant temperature bath (Precision Scientific Co., Chicago, Ill.) was circulated through the jacket surrounding the viscometer assembly and through a reservoir holding additional experimental fluid. All measurements were conducted at a constant temperature of 25 $\pm$ 0.1°C. The constant temperature circulating system was fitted with an adjustable micro-set thermoregulator which gave a control sensitivity of $\pm$ 0.01°C., over the entire range.

Several capillary tubes over a wide range of lengths and diameters were employed in the present study. The specifications of these tubes are given in Appendix A. Hypodermic needle tubing of type 304 stainless steel, supplied by Superior Tube Co., were used. The range of lengths of different diameter tubes varied from 17 cms. to 46 cms. The lengths were measured by a micrometer. The diameter range used in the present work was from 0.0578 cm. to 0.014 cm. The deviations in diameter, provided by the manufacturer, were reported as -10.5% to +5.26%. Two Newtonian fluids, distilled water and ethylene glycol (99.93% pure, Fisher Scientific Co.), were used to calibrate the tubes. Two sets of experimental data with different tubes were taken on each fluid. In the distilled water calibration, the deviations obtained from the manufacturer's reported diameters ranged from 3.88% to -2.35%. With ethylene glycol, the deviations obtained were from +9.35% to +0.77%. Some of the tubes were also calibrated by Filled Microscope probe method. The deviation from the reported values found by this method was about the same as that for distilled water and ethylene glycol. All the deviations were within the range given by the manufacturer. It was decided

to use the calibrated diameter obtained with distilled water since they appeared to be most accurate. Since the tubes were flexible because of the lengths used, they were enclosed by protective stainless steel tubes. These were welded near one end of the capillary tube. The L/D ratios employed were in the range of 400 to 1,100. The high ratios were intended to minimize entrance effects sufficiently to render them insignificant.

The procedure of conducting the experimental run on the viscometer was simple. The non-Newtonian fluid, whose flow characteristics were to be determined, was filled in the reservoir through the feed hole. After the fluid attaining the desired temperature (25° C.), pressure in the rheometer was increased to the desired level with the help of the pressure regulator. This pressure in the viscometer was maintained constant till three liquid smaples were collected over a measured time interval to find out the volumetric flow rate. The samples were weighed and the volumetric flow rate was calculated from the weight rate of flow. The procedure of collecting the samples was repeated at five other different pressures. The experimental fluid was filled in the reservoir whenever it was necessary. The same procedure was repeated at different pressures with different tubes with all the solutions used in filtration. The viscometric data collected with these polymer solutions and their analyses are given elsewhere[79]. A sample calculation of the viscometric results is presented in Appendix A.

On completion of taking the viscometric measurements with a non-Newtonian fluid, the fluid reservoirs and capillary tubes

were thoroughly washed with hot water to remove the last traces of experimental fluid from the equipment.

The equipment was standardized with two Newtonian fluids, distilled water and ethylene glycol, before conducting runs with experimental fluids. The shear rate versus shear stress curve shown in the Figure 8, indicates no wall effects for ethylene glycol and a slope of unity confirming the proper performance of the viscometer. The viscometric measurements for non-Newtonian fluids were carried out in the pressure range used for filtration with the intention to determine the flow characteristics under similar shear stress conditions existing in filtration. The way, in which the flow curves, obtained from viscometric measurements, were used to determine the average value of consistency index of fluid applicable for filtration calculations, is given in the chapter dealing with the discussion of results.

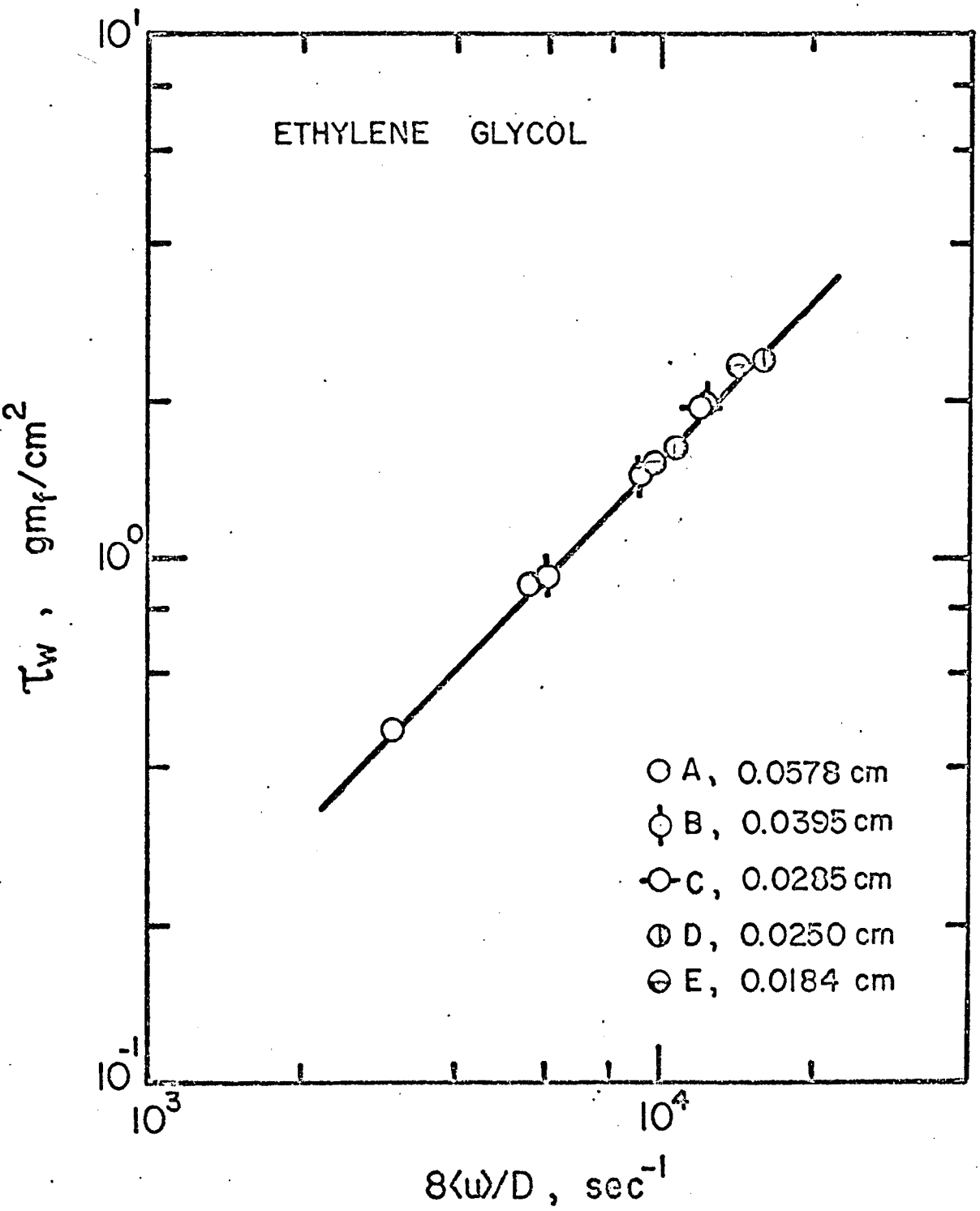

Fig. 8 Flow curve for ethylene glycol at 25°C for tubes of different diameter.

CHAPTER V

RESULTS AND DISCUSSION

NEWTONIAN FILTRATION

(i) Newtonian Filtration at Constant Pressure

A plot of data collected in three filtration runs, using aqueous slurries of calcium carbonate, conducted at a constant pressure of 50 psi, with varying time intervals used to attain the final pressure in each case, is given in Figure 9. The data are plotted as time of filtration θ versus the filtration volume per unit area of filtration. Three different curves are obtained for three runs because of the different initial periods. The initial periods are classified as falling in three categories, short, intermediate. or long, depending on the relative rates of variation of pressure with time from zero gauge pressure at the commencement of the filtration to the final desired value. The runs in which the adjustment to the final pressure was made instantaneously are designated as the runs with short initial periods. Least square fitting of Equation (31) separately to the set of data corresponding to each run was performed using a digital computer (IBM 360). The program used for these computational purposes is given in Appendix D along with the sample calculation of constant pressure filtration data. Since the initial periods of the individual runs conducted at the same pressure are different, as a result of different pressure time history to which each run was subjected, the θ_o value characterizing the initial periods of individual runs obtained by the method of least squares fitting is not the same. After applying the necessary time correction to each run, the data is plotted as effective time of filtration $(\theta - \theta_o)$ versus filtrate volume

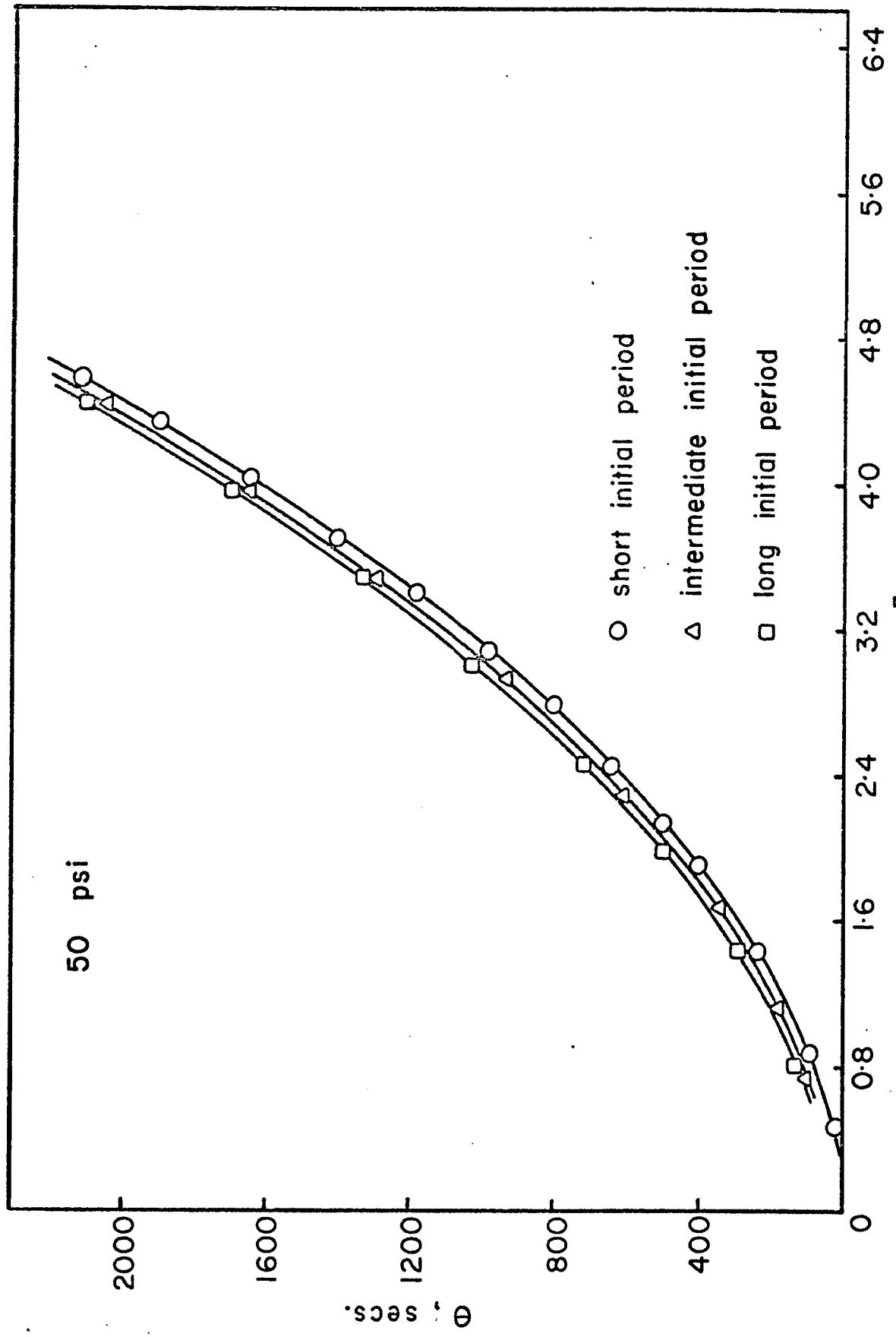

Fig. 9 Plot of time θ versus cumulative filtrate volume per unit area v for constant pressure run conducted at 50 psi with aqueous slurry containing 2.5% $CaCO_3$.

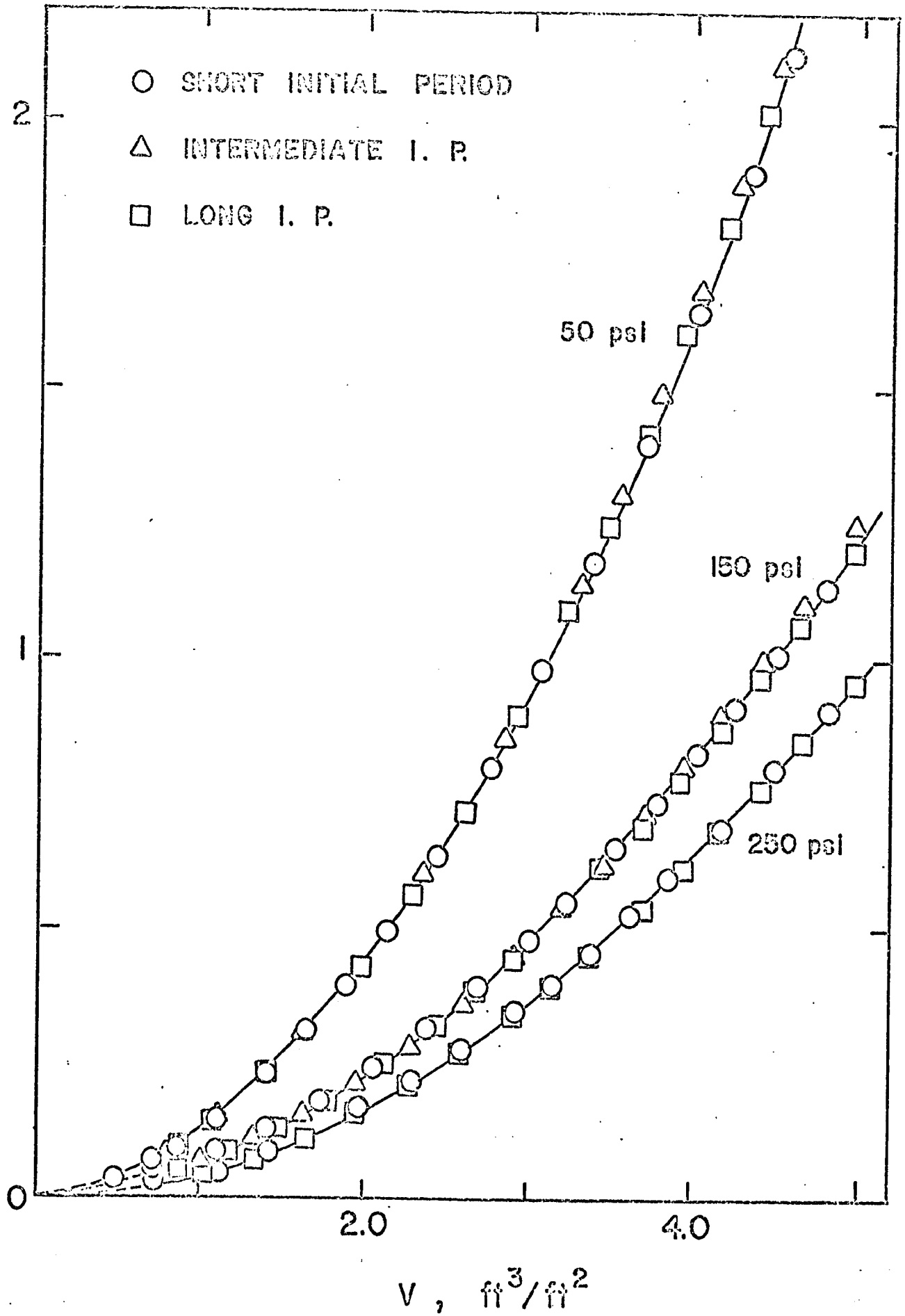

Fig. 10 Plot of v versus $(\theta - \theta_o)$ for various constant pressure filtrati

per unit area of filtration v, and is shown in Figure 10. Also included in this figure are the processed data collected during the filtration conducted at constant pressures of 150 and 250 psi.

The data points, constituting three different curves in Figure 9 representing three filtration runs at the same pressure, fall on a single curve in Figure 10, demonstrating the success of θ_o in characterization of the effect of the initial stage of filtration. Further, it exhibits the considerable success with which the parabolic relationship, developed for the main stage of constant pressure filtration, correlates the experimental data obtained in the constant pressure runs which were subjected to drastically different initial stages of filtration.

The ease with which the resistances α and R_m are determined from the coefficients of Equation (31) fitted to the data compared with the method involving the evaluation of the quantity $d\theta/dv$ is obvious.

Table II(a) summarizes values determined for the various pertinent filter medium and cake characteristics computed separately for each individual run from the coefficients of Equation (31) fitted separately to the data of each run. It is noted that the magnitude of the effective time of commencement of filtration θ_o, which characterizes the initial stage of the filtration, increases with an increase in the time taken to attain the final pressure, for all pressures used.

The negative value for θ_o determined for the filtration at the constant pressure of 150 lb_f/sq. in. prompts an inquiry into the likelihood of obtaining a negative value. Therefore, the function F(v) in Equation (28) should be examined more closely.

$$F(v) = (d\theta/dv)_i - (d\theta/dv)_m \qquad (119)$$

where the subscripts i and m refer to the initial and the extrapolated main stages of the filtration, respectively.

Referring to Equation (28), the above equation can be written

$$F(v) = 2v\left(\frac{1}{K_i} - \frac{1}{K_m}\right) + 2\left(\frac{v_{oi}}{K_i} - \frac{v_{om}}{K_m}\right) \qquad (120)$$

and utilizing Equations (26) and (27) expanded to

$$F(v) = \frac{v\mu\rho}{g_c p}\left(\frac{a_i}{\frac{1}{s} - m_i} - \frac{a_m}{\frac{1}{s} - m_m}\right) + \frac{\mu}{g_c p}\left(R_{mi} - R_{mm}\right) \qquad (121)$$

Assuming the medium resistance to be the same in both stages, $R_{mi} = R_{mm}$, the above equation simplifies to

$$F(v) = \frac{v\mu\rho\left[a_i\left(\frac{1}{s} - m_m\right) - a_m\left(\frac{1}{s} - m_i\right)\right]}{g_c p\left(\frac{1}{s} - m_i\right)\left(\frac{1}{s} - m_m\right)} \qquad (122)$$

Since, $m_i \geq m_m$ and $a_i \leq a_m$, we thus conclude that it is possible for the term in the brackets and consequently F(v) and θ_o to be negative.

Table II(a) points up quite clearly the undesirability of commencing the filtration instantly at the final pressure and the advantages to be gained by adjusting to the final pressure gradually. It is noted that the filter medium resistance decreases quite markedly with an increase in the time taken to adjust to the final pressure, characterized by increasing θ_o values. The exceptions to this rule are characterized by the fact that a lower than expected medium resistance is offset by a greater than expected specific cake resistance. Generally speaking, although the cake resistance at a particular pressure is relatively constant by comparison with the

TABLE II

Filter Medium and Cake Characteristics

(a) Resistances computed from experimental data in the form of θ versus v for each filtration run.

p psi	Initial Period	θ_o sec	$K \times 10^2$	$v_o \times 10^2$	$\alpha \times 10^{-10}$ ft/lb$_m$	$R_m \times 10^{-9}$ ft^{-1}
50	Short	3.5	1.06	13.87	4.40	10.12
	Intermediate	20.5	1.00	7.25	4.64	5.58
	Long	40.8	1.02	9.08	4.57	6.88
150	Short	- 5.8	2.36	37.06	5.94	36.35
	Intermediate	25.9	2.06	9.54	6.81	10.72
	Long	47.1	2.22	20.71	6.29	21.52
250	Short	8.8	2.69	11.60	8.70	16.62
	Long	42.7	2.60	1.46	9.02	2.17

(b) Resistances computed from $(\theta - \theta_o)$ versus v data (Figure 10)

p psi	m	$K \times 10^2$	$v_o \times 10^2$	$\alpha \times 10^{-10}$ ft/lb$_m$	$R_m \times 10^{-9}$ ft^{-1}
50	2.3615	1.03	10.67	4.53	8.01
150	2.2021	2.18	17.59	6.44	18.69
250	2.1143	2.64	6.19	8.86	9.03

variations observed in the medium resistance, which is strongly dependent on the pressure-time history of the initial period, the fact that the initial period of the filtration can also affect the specific cake resistance to some extent,is noteworthy. In particular, it is clear that the effect of the initial period cannot be overlooked entirely in accounting for observed discrepancies between experimentally determined values of the specific cake resistance α.

The final values of the cake resistance α, presented in Table II(b), are of the same magnitude as those reported by McMillen and Webber[95], who conducted the filtration experiments with calcium carbonate of different particle sizes. As shown in Figure 11, the cake resistance α is amenable to an empirical correlation in terms of a power function of pressure given by $\alpha = r_o p^{n_o}$. The points indicated by the crosses represent the average values of α computed using all the data points determined at each pressure in the form of $(\theta - \theta_o)$ versus v and the appropriate θ_o values. This correlation is in agreement with the assumption implied in Equation (39) and supports the findings of Luke[42] and Coimbra[41], that the filtration resistance may be expressed as a power function of the pressure drop. The values of the empirical constants corresponding to the dashed line are included in the figure. The value of n_o, a quantitative measure of compressibility is 0.42 indicating that the sludge is slightly compressible. n_o is commonly called the compressibility coefficient.

The filter bed characteristics computed from the $(\theta - \theta_o)$ versus v relationships (Figure 10) for the three pressure drops are presented in Table II(b). It is noticed that the moisture ratio m during the main filtration stage determined experimentally varies inversely with the pressure. This is not unexpected, and is

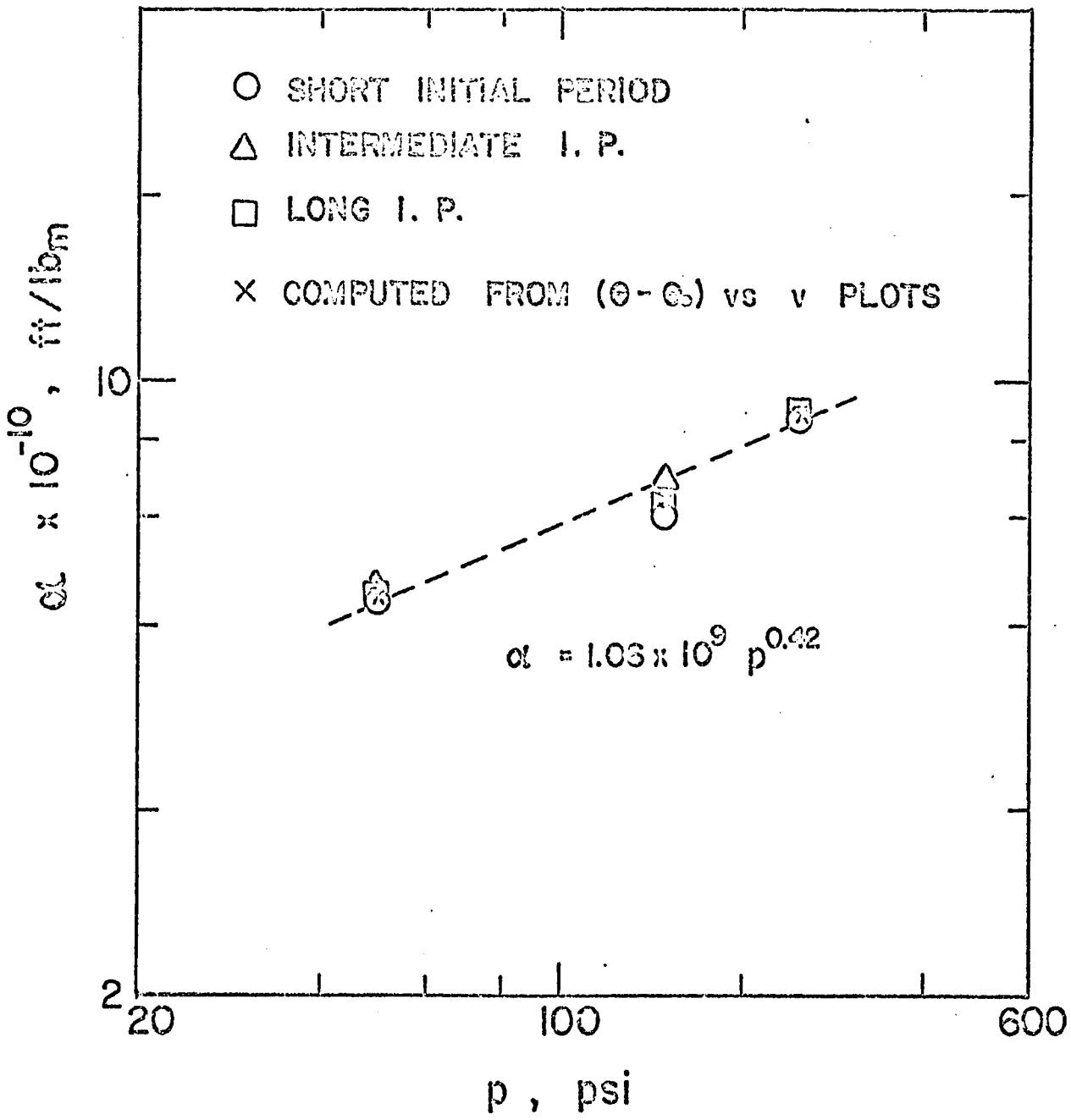

Fig. 11 Plot of average specific filtration resistance α versus pressure p.

attributable to squeezing more liquid out of the pores of the cake at higher pressures, and results in reduced voidage and the formation of more compact cake. It is also observed that the moisture ratio m can be expressed as a power function of pressure drop given by the equation $m = 4.52\ (p)^{-0.072}$.

(ii) Newtonian Filtration at Constant Rate

The results for four constant rate filtration runs, conducted with aqueous slurries containing 2.5% calcium carbonate by weight, are reported in this section. This number of runs is sufficient to illustrate the effect of the initial period of the constant rate filtration. Three of these runs were made at the same rate, $q_1 = 3.29 \times 10^{-3}$ ft/sec.

Figure 12 shows a plot of the filtrate volume V versus θ, determined for each run. The three runs conducted at the same constant rate are represented by the three parallel straight lines. It is noted that none of these lines in the plot passes through the origin when extrapolated back to time equal to zero, as a result of the effect of the initial stage of filtration. The initial periods for three of the runs are characterized by negative values of the effective initial volume of the filtrate V_o, determined as V - intercepts in this plot. Hence, for these runs, the average filtrate rate in the initial stage of the filtration was lower than the final rate of the constant rate period. It may be expected that the effective initial volume will usually be negative in practice, since, it may be desirable to adjust the filtration rate gradually during the initial stage to the desired rate. The numerical values of the effective initial filtrate volumes and the equivalent time corrections for the runs are indicated in Figure 12.

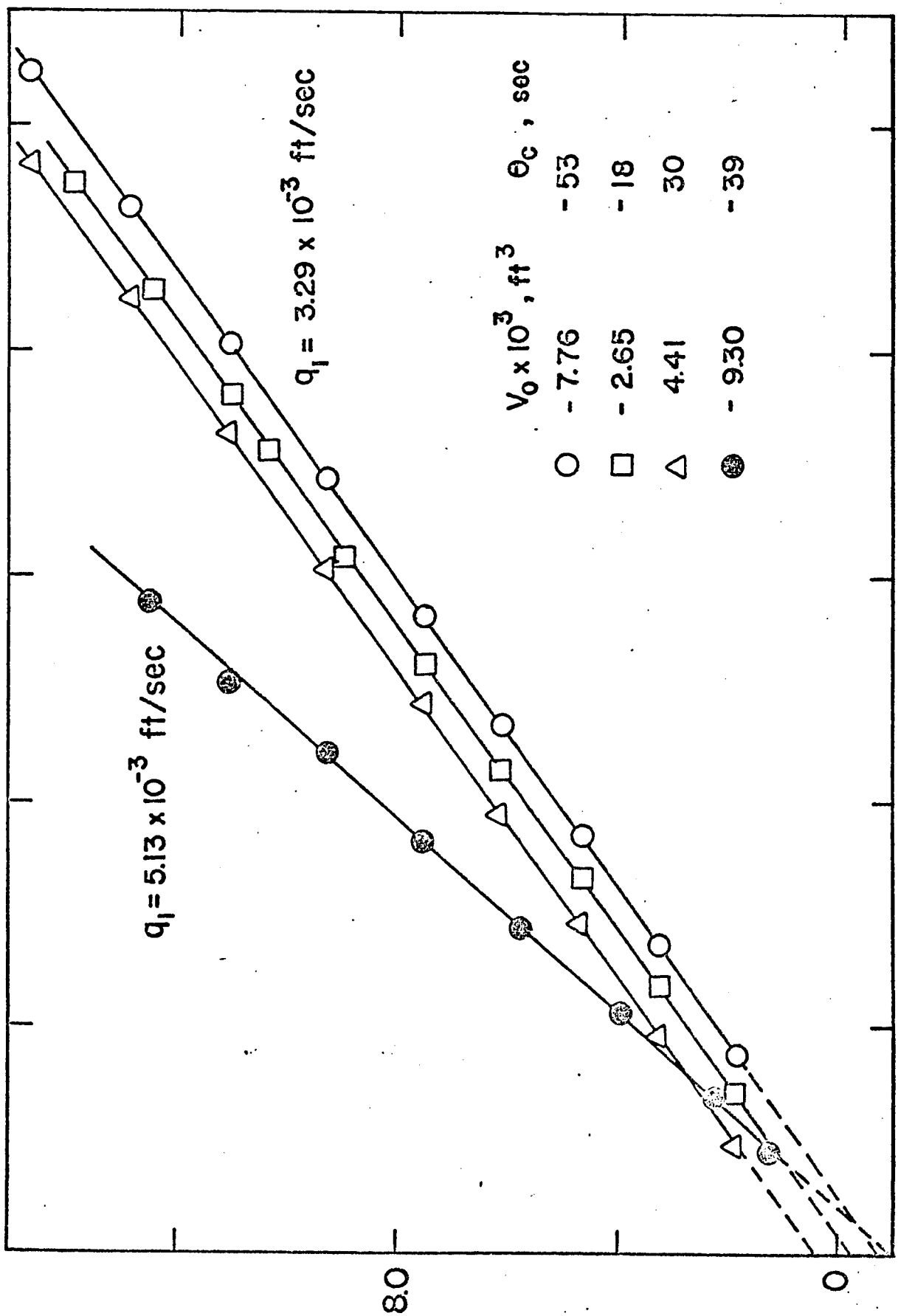

Fig. 12 Plot of v versus θ for four constant rate runs with Newtonian slurries.

The value of p_1 in each case is determined utilizing a digital computer (IBM 360) following the procedure given earlier in the theoretical section. The program used for these computational purposes is given in Appendix E along with a sample calculation of constant rate filtration data. Figure 13 presents the experimental constant rate filtration data processed and plotted in the usual manner as θ versus $(p - p_1)$ on log-log graph paper. The lowest curve depicts the data for the run conducted at the higher filtrate rate. The upper three curves represent the data obtained in the three runs conducted at the same constant rate. The absence of a unique relationship, which is attributable to the effect of the initial period, is clearly indicated by the separation of the upper curves determined at the same rate. One thus sees that the curves obtained at a particular rate are functions of the time parameter $\theta_c = v_o/q_1$, specified for each run in the figure, which characterizes the initial stage of the filtration, as suggested by Equation (41).

In Figure 14, the same experimental data are shown replotted as $(\theta + \theta_c)$ versus $(p - p_1)$ on a log-log plot, in accordance with Equation (41). The three sets of data collected at the same constant rate, $q_1 = 3.29 \times 10^{-3}$ ft/sec, are now superimposed on a single curve, the upper curve in the figure. The lower curve is a similar plot of the data collected at the higher rate, $q_1 = 5.13 \times 10^{-3}$ ft/sec. The effective initial volume $v_o = V_o/A$, required in the evaluation of the time correction parameter, $\theta_c = v_o/q_1$, appearing in the ordinate of Figure 14, was computed from a knowledge of the V-intercepts of the curves in Figure 12 and the filtrate rate in the constant rate period. The existence of a unique relationship between $(p - p_1)$ and $(\theta + \theta_c)$ suggested by Equation (41) for filtration runs at the same constant rate is confirmed by Figure 14.

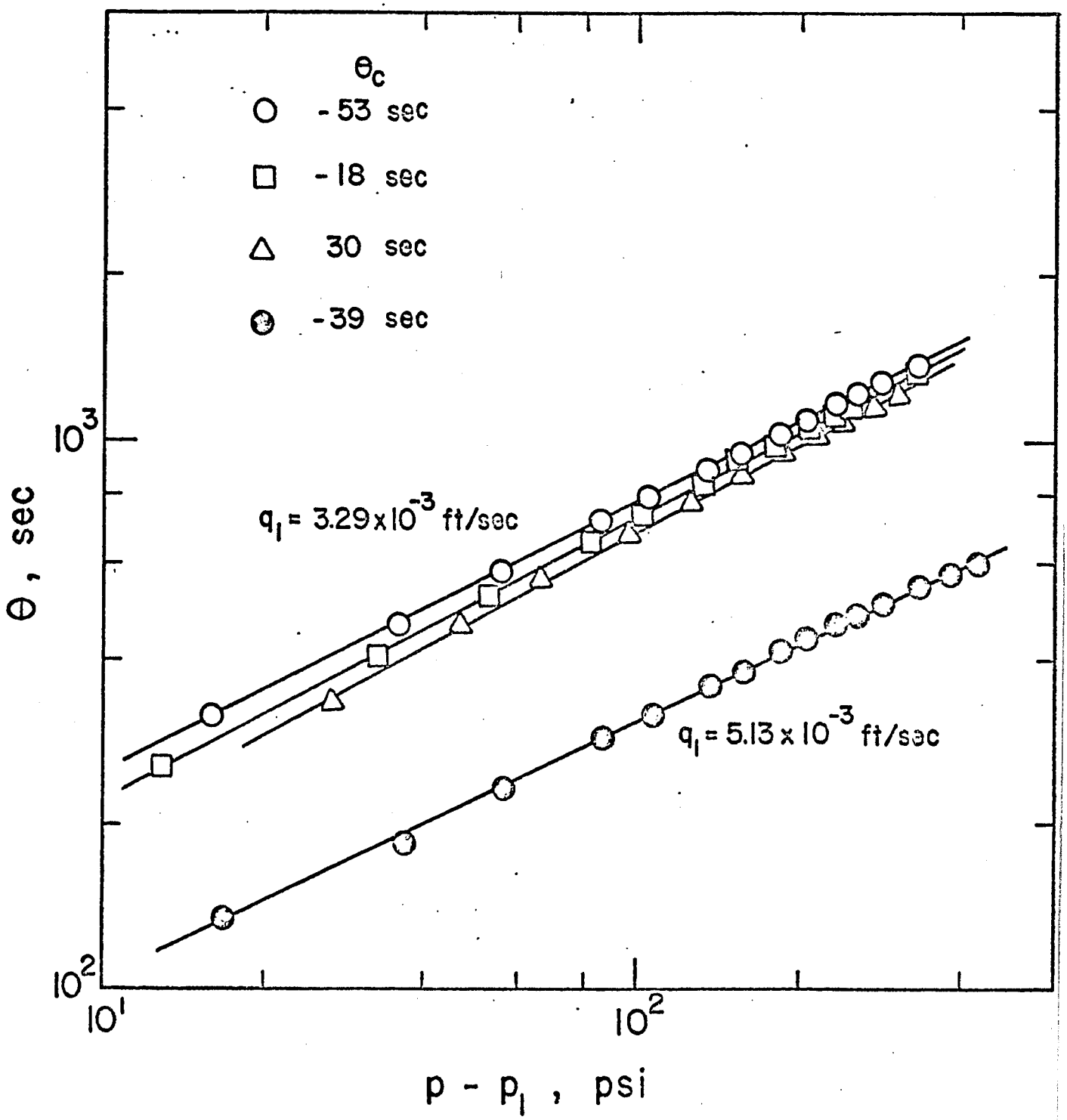

Fig. 13 Traditional plot of constant rate data as θ versus $(p - p_1)$

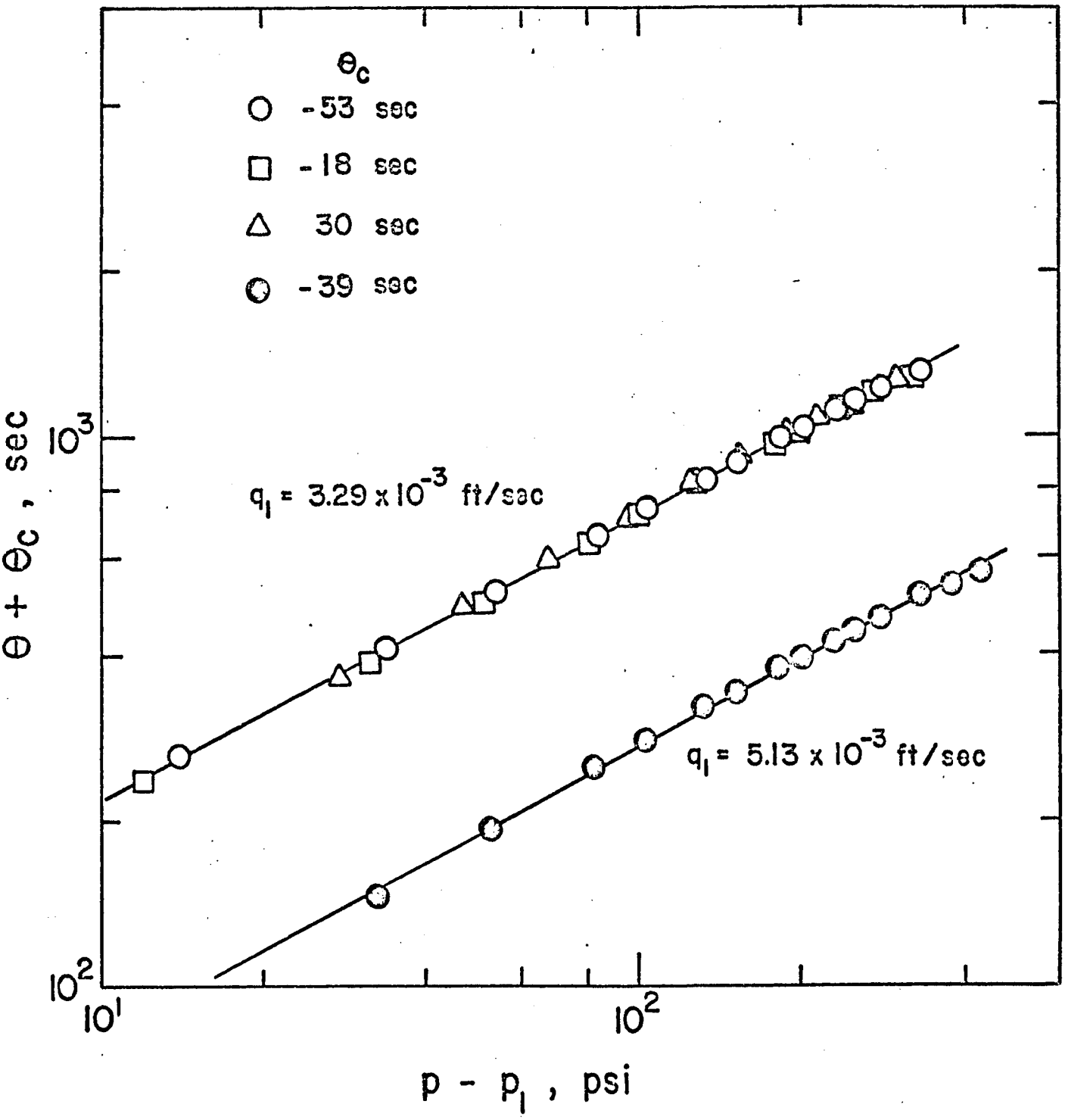

Fig. 14 Constant rate data replotted as $(\theta + \theta_c)$ versus $(p - p_1)$.

The variance of the experimental data points and the calculated values using Equation (41) is illustrated in Figure 15. The assumed p_1 value in the abscissa identifies the assumed p_1 and the corresponding $(1 - n_o)$ and log K_r values yielded by least squares fitting of Equation (41), with p_1 equal to the assumed value, to the data, as described in the analysis. Three curves determined for the three runs conducted at the same constant rate are shown. The pressure at the filter medium and cake interface p_1 is determined finally, for each run, as the value of p_1 corresponding to the minimum variance. The values determined for each run are indicated beside the corresponding curves in the figure together with the values of the time correction θ_c determined for each run. With the K_r value known, the filtration resistance coefficient r_o could be readily determined utilizing Equation (42).

Table III(a) summarizes values determined for the various pertinent filter medium and cake characteristics by the previous method in which no allowance was made for the effect of the initial transient stage of the filtration in the evaluation of the various quantities. The wide disparity in the individual n_o and r_o values determined for each of the three runs conducted at the same rate is clearly seen in quantitative terms.

Similar information computed by the method presently proposed for resolving constant rate filtration data is presented in Table III(b). The values of n_o and r_o for the three runs at the same rate, also computed individually for each run, are now seen to be in excellent agreement. The large difference resulting in the values of n_o and r_o when the correction for the effect of the initial stage is made in the analysis of filtration at higher rate is also noteworthy. A simple relationship is indicated in Table III between the pressure p_1 at the

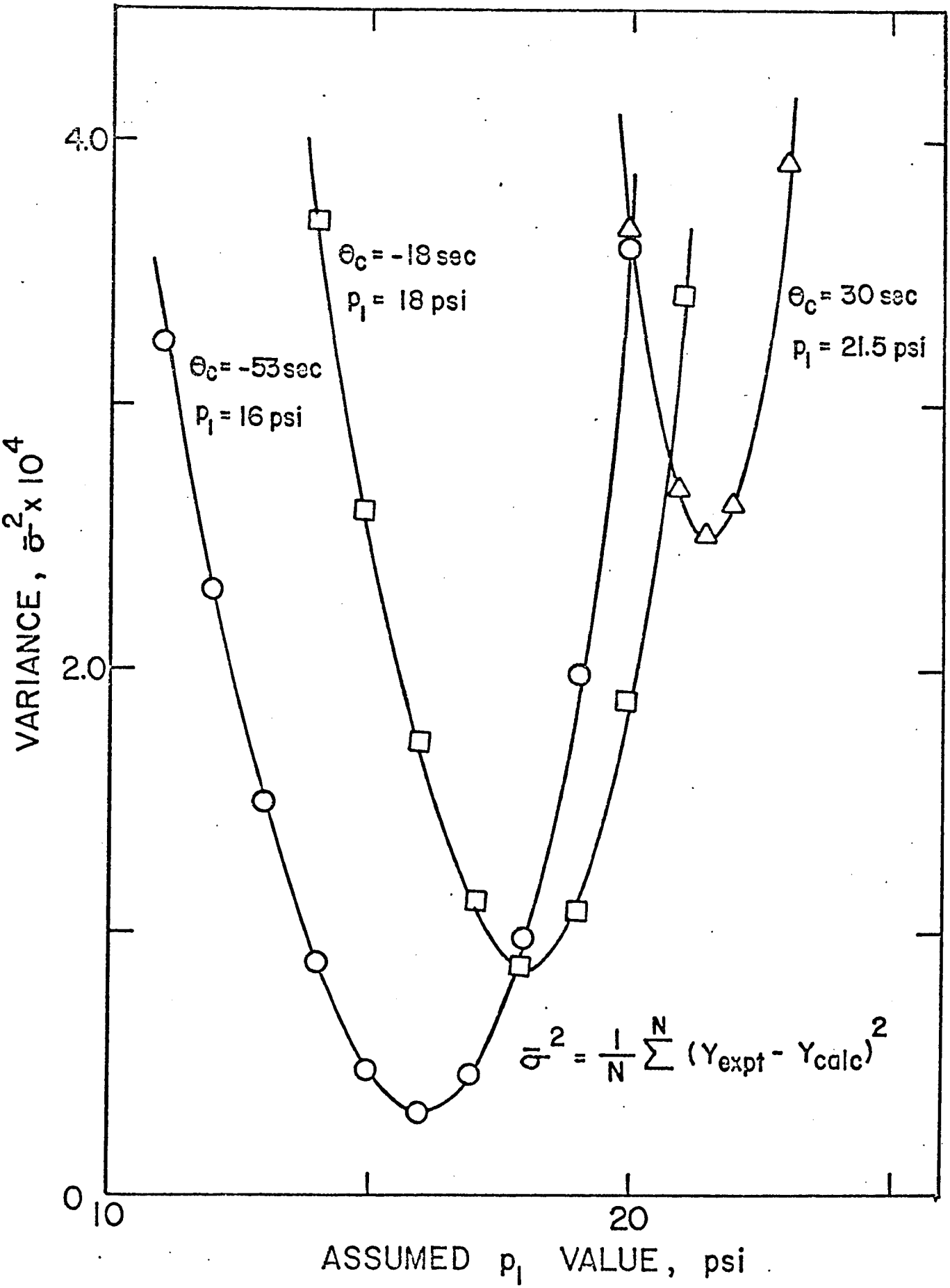

Fig. 15 Variation of the variance with the value assumed for p_1 for Newtonian slurries.

TABLE III

Filter Medium and Cake Characteristics

(a) Without Correction for Initial Period

$q_1 \times 10^3$ ft/sec	θ_c sec	p_1 psi	n_o	K_r	$r_o \times 10^{-8}$	$R_m \times 10^{-10}$ ft^{-1}
3.29	-53	14	0.515	0.135	4.10	3.28
3.29	-18	17	0.497	0.1745	5.30	3.98
3.29	30	23	0.479	0.211	6.40	5.40
5.13	-39	13	0.526	0.304	3.80	1.96

(b) Computed by Present Method

3.29	-53	16	0.489	0.1848	5.61	3.74
3.29	-18	18	0.491	0.1855	5.64	4.20
3.29	30	21.5	0.491	0.1852	5.63	5.02
5.13	-39	17	0.483	0.515	6.45	2.56

cake-medium interface and the time correction θ_c. The relationship seems to be independent of the filtrate rate q_1 of the constant rate period. Thus, the introduction of the time correction concept also affords a simple and convenient means of quantitatively relating the pressure at the medium p_1 to the flow history of the initial stage of the filtration.

Table IV presents the values of the cake resistance obtained from constant pressure and constant rate filtration data for comparison purposes. In the case of constant pressure filtration, α is represented as a power function of the total pressure drop, whereas in the case of constant rate filtration α is represented as a power function of the pressure drop across the cake. Giving proper consideration for the difference in the treatment, the agreement between the values of the cake resistance is seen to be satisfactory.

TABLE IV

PRESSURE DROP psi	CAKE RESISTANCE $\alpha \times 10^{-10}$ ft./lb m.	
	FROM Constant Pressure Filtration	FROM Constant Rate Filtration
50	4.53	4.50
150	6.44	7.35
250	8.86	9.89

NON-NEWTONIAN FILTRATION

(i) Filtration of Natrosol 250 G Solutions at Constant Pressure

Figure 16 shows the shear stress-shear rate curves obtained for the three Natrosol 250 G Solutions (0.6, 0.8 and 1.0 per cent by weight), investigated utilizing a capillary viscometer. The detailed procedure used for the analysis of the flow curves obtained with non-Newtonian fluids exhibiting anomalous surface effects was presented in a recent paper[74]. The flow behaviour index n of the fluids, corresponding to the slope of the tangent at a point on a curve in Figure 16, which is not constant, varied with the shear stress or shear rate in the range 0.6 - 1.0, for the three solutions. The values of the flow behaviour index and the maximum consistency index of these solutions are tabulated in Appendix A. The flow curves shown were utilized in the subsequent determination of the fluid consistency index K, corresponding to a particular value of the flow behaviour index characterizing the fluid, in the constant pressure filtration.

The possibility and extent of mechanical degradation of the polymer molecules in solution during filtration was investigated by conducting viscometric measurements of the filtrate before and after filtration for two runs conducted at constant pressures of 150 and 200 psi, respectively, using 0.6% Natrosol G Solution. Figure 17 shows typical flow curve for the 0.6% Natrosol G Solution plotted as the shear stress at the wall τ_w versus $8\langle u\rangle/D$ obtained with a capillary of 0.0395 cm diameter and at the temperature of 25°C. Similar curves were also obtained with different capillary diameters. It is clearly seen that the viscometric data collected before and after the filtration run fall on a single curve, characteristic of the capillary diameter, indicating that the mechanical degradation of polymer

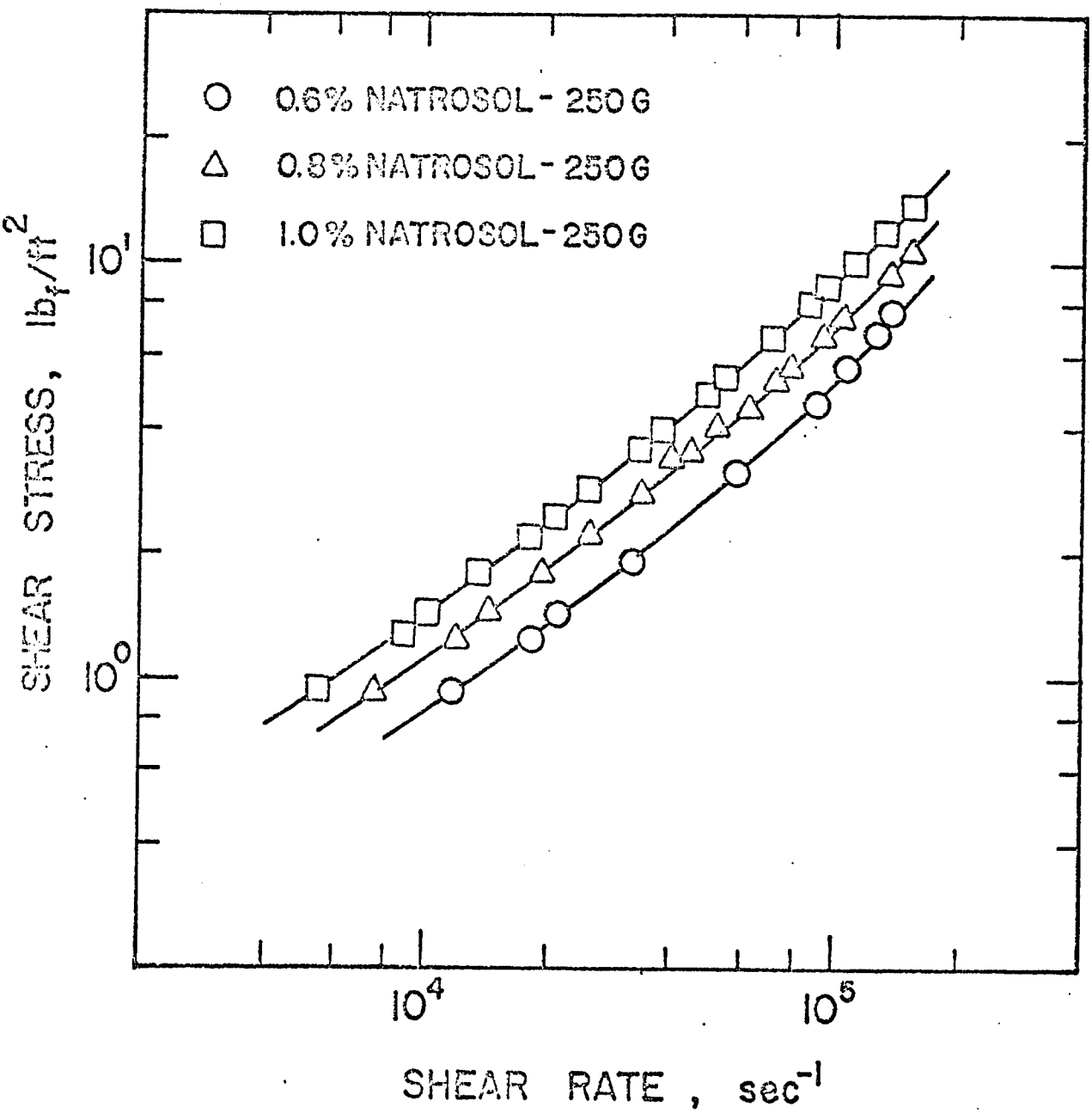

Fig. 16 Shear stress versus shear rate plots for three Natrosol 250 G solutions of different concentrations at 25° C.

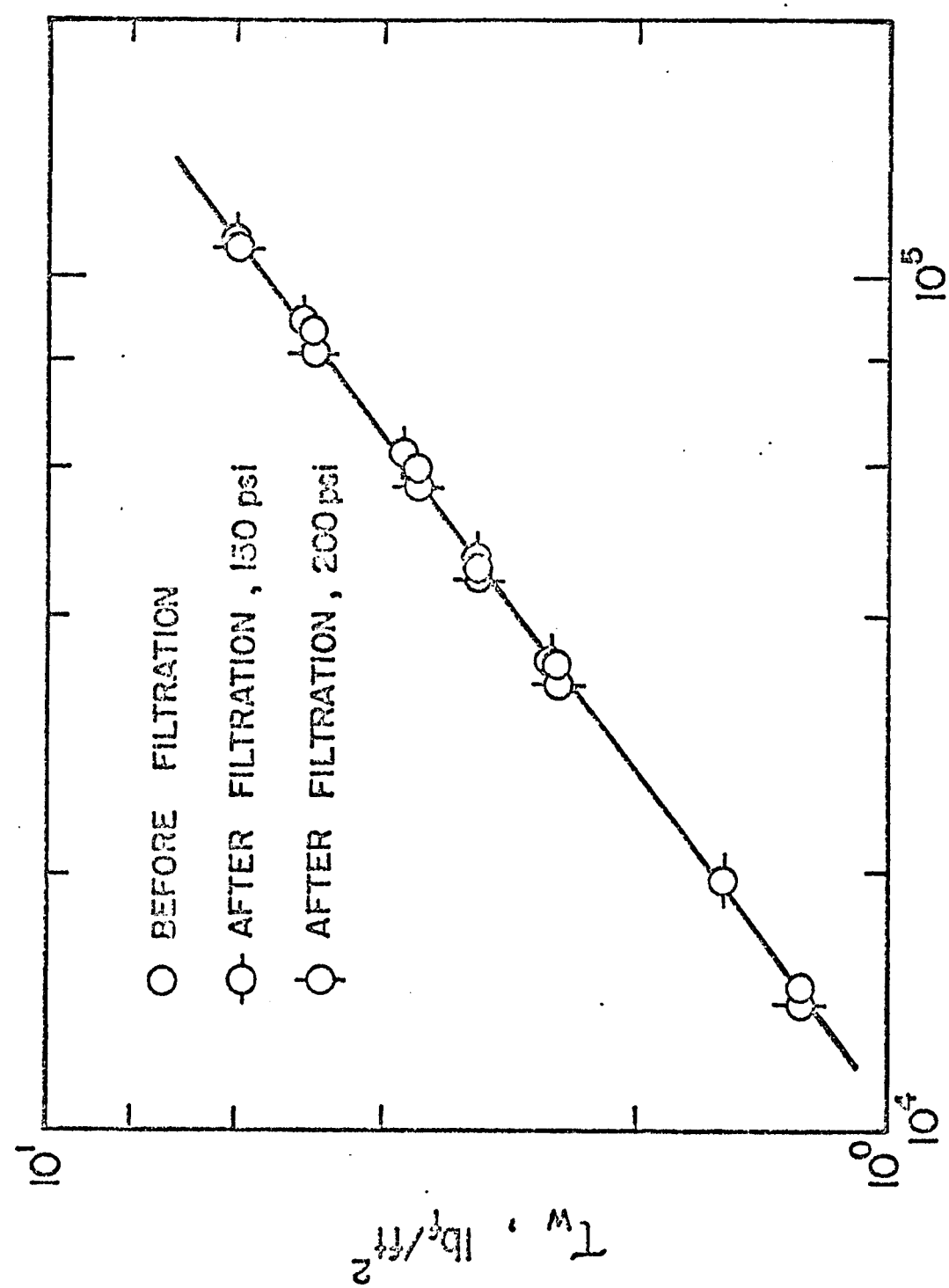

Fig. 17 Flow curve determined for 0.6% Natrosol 250 G solution before and after filtration.

molecules during these constant pressure filtration runs was insufficient to have an appreciable effect on the viscous flow properties of the fluid.

Equation (108) was fitted to the filtration data collected at constant pressure employing the method of least squares as outlined in the analysis. A digital computer (IBM 360) was utilized for this purpose. The program used for the computation is given in Appendix D along with the sample calculation of the experimental results of non-Newtonian fluids. Briefly, the criterion was to determine for each constant pressure run the characteristic value of the index n and corresponding coefficients K, N and θ_o in Equation (108) yielding the minimum variance between values predicted by Equation (108) and the experimental data. In Figures 18 and 19, the variation of the computed variance σ^{-2} with the value of the index n, using the corresponding applicable values of K, N and θ_o in Equation (108), is illustrated by the lower solid curve for slurries comprising 2. 5 per cent by weight of calcium carbonate in 1. 0% Natrosol 250 G solution, filtered at pressure of 250 and 350 psig, respectively. Similar plots were obtained for all solution concentrations and filtration pressures employed.

The upper parabolic-shaped curves in Figures 18 and 19 represent the variation of the computed variance with the assumed value of the flow behaviour index n for N equal to zero in Equation (108), corresponding to zero filter medium resistance. As noted, the lower curves in the same figures show the variation of the variance with the index n when the coefficient N in Equation (108) is retained, which involves the evaluation of the filter medium resistance. The interesting observation is made that the curves found for zero filter medium resistance yield definite minima at the points at which

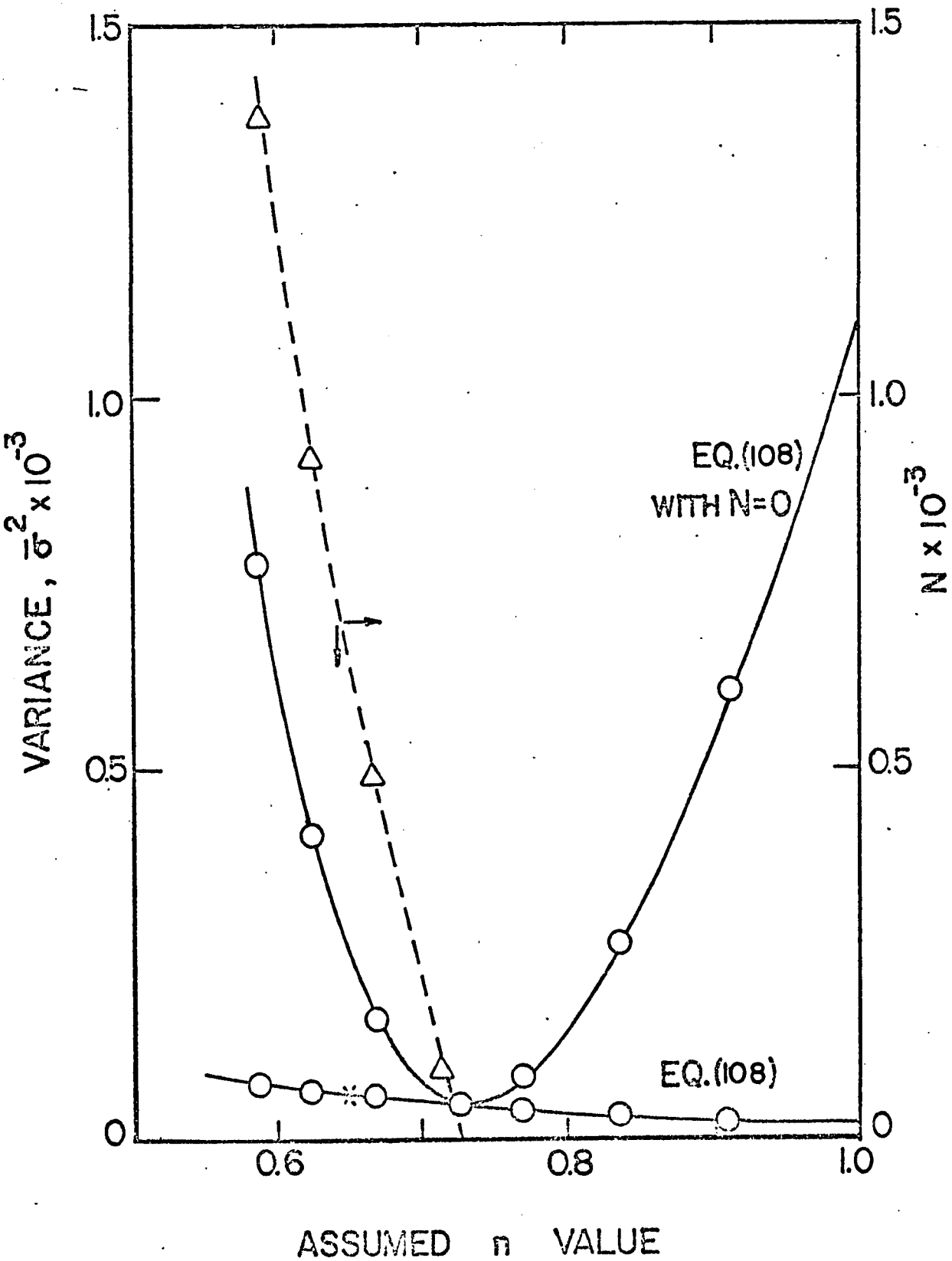

Fig. 18 Variation of the variance and the coefficient N (in Equation 108) with the assumed n value for 2.5% $CaCO_3$ slurry in 1.0% Natrosol 250 G solution at pressure of filtration of 250 psig.

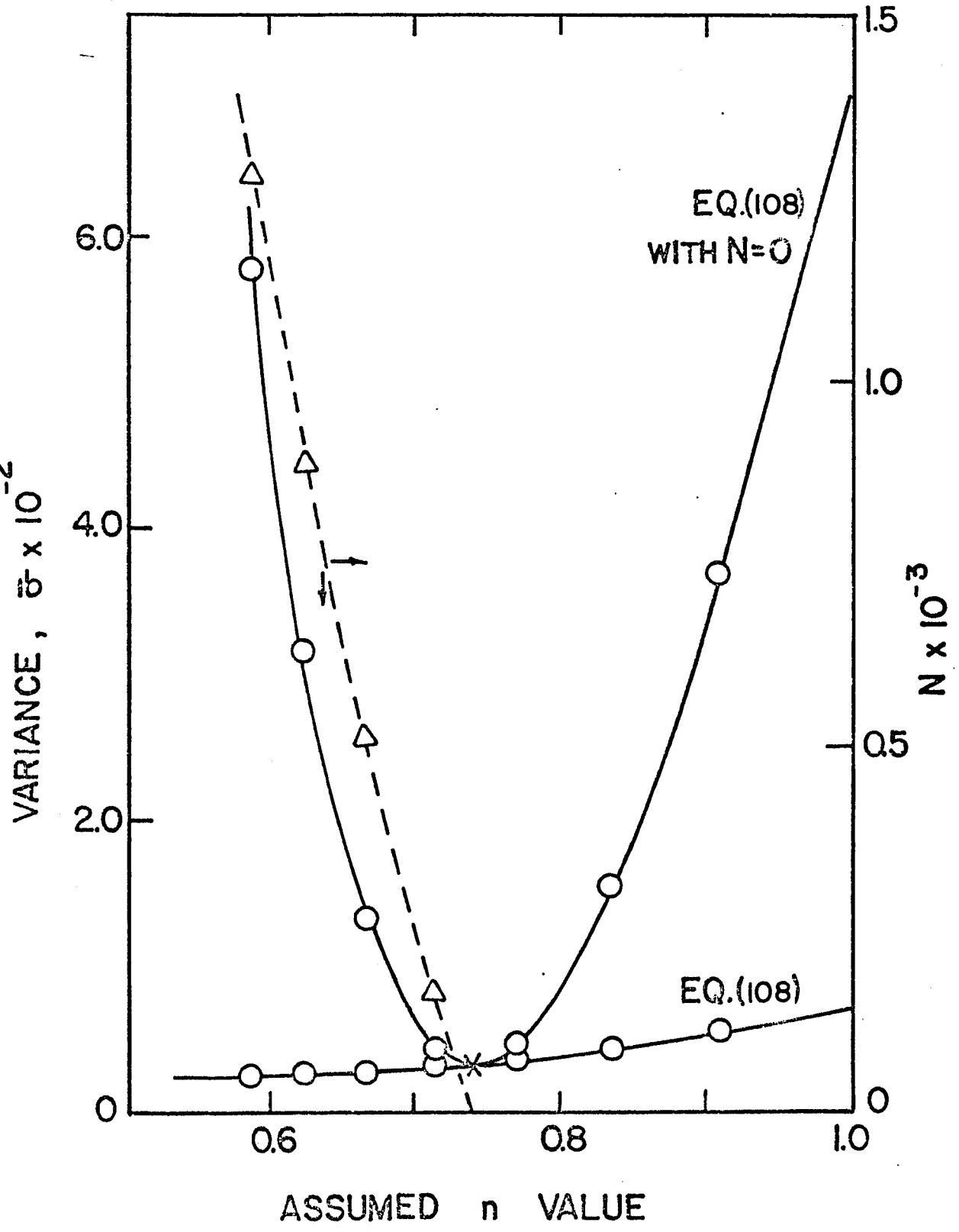

Fig. 19 Variation of the variance and the coefficient N (in Equation 108) with the assumed n value for 2.5% $CaCO_3$ slurry in 1.0% Natrosol 250 G solution at pressure of filtration of 350 psig.

these curves are tangent to the lower curves. It is also seen from the lower curves that the variance does not change significantly with the choice of n, in using Equation (108). It is thus concluded that Equation (108) is capable of giving a good fit of the experimental data over a wide range of possible n values.

The dashed curve in each figure shows the variation of the applicable value of N used in evaluation of the lower curve. As expected, the n-intercept of the dashed curve is also the value of n corresponding to the minimum of the parabolic curve, which also explains why the two curves touch tangentially at the minimum of the former curve. The negative portions of the N versus n curves are not included in the figures since negative values of N, corresponding to negative filter medium resistance, are physically inconceivable. It is also noted that the lower curves in Figures 18 and 19 represent the locii of minima of the family of parabolic-shaped curves with N = constant.

On the other hand, as noted, the three parameter equation resulting when the filter medium resistance is equated to zero in Equation (108) yields a minimum variance and an obvious best fit at a particular value of n. This suggests that constant pressure filtration measurements conducted with non-Newtonian fluids do not provide sufficient information to yield both the value of the characteristic exponent n in the filtration and the filter medium resistance. In order to obtain the value of the flow behaviour index n characterizing the non-Newtonian flow behaviour of the fluid during the filtration, one must assign N some value based on a knowledge of the filter medium resistance. The value of zero, based on a filter medium resistance of zero, which is not unreasonable, is seen to give a reasonable value for n in both cases represented by Figures 18 and 19.

It seems that a more reasonable assumption is to set v_o, which is presumed to be a function of the pressure drop only, equal to the value obtained in filtration of a slurry of a Newtonian fluid (water) using the same slurry concentration and pressure. This was done in the present work. Utilizing this information, in conjunction with Equations (108) and (109), the final n values were thus arrived at by a trial and error procedure. The points denoted by the cross marks in the figures give the variance and final applicable n values obtained by this method for these two runs.

Figure 20 presents the characteristic n values, determined for the constant pressure runs conducted, plotted as a function of the filtration pressure with the concentration of the polymer in the solution and the slurry concentration as parameters. It is seen that the flow behaviour index n is amenable to a simple linear correlation in a semi-logarithmic plot representable by the function

$$n = m_o \log p + n_1 \tag{123}$$

It is noted that the flow behaviour index increases with the filtration pressure. The numerical values of n and K computed from the experimental data are tabulated in Table V. Since the fluid consistency index K was not amenable to evaluation from the filtration data alone, as indicated by Equation (101), the values of K were determined from the results of capillary tube viscometer measurements on the fluids, after establishing the appropriate characteristic n values from the filtration data, with the aid of Figure 16. The use of Figure 16 also enables one to establish the characteristic shear stress $\bar{\tau}_w$ inside the filter cake for the particular constant pressure filtration run.

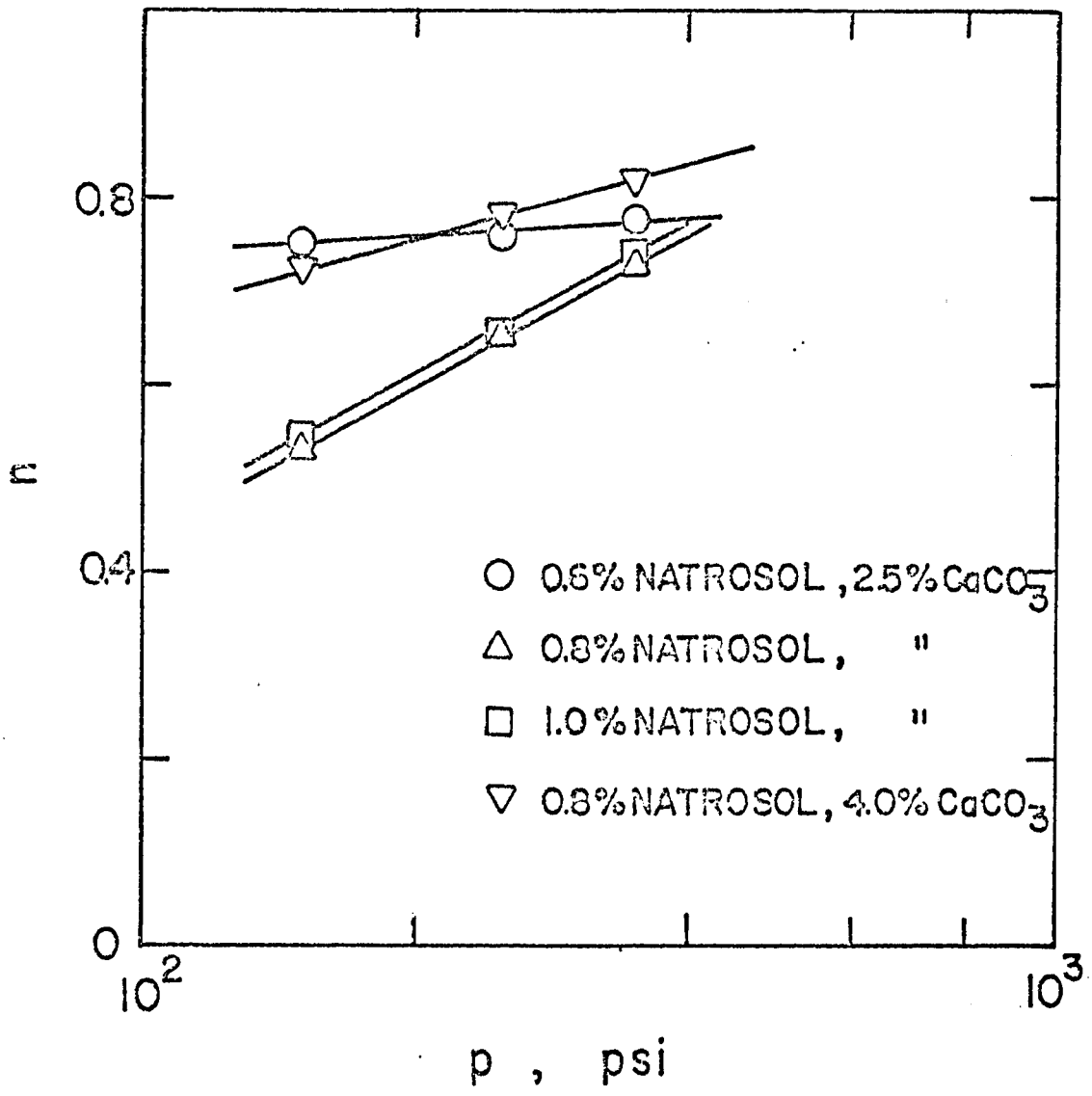

Fig. 20 Plot of the characteristic value of the flow behaviour index n versus pressure p for various slurries of Natrosol G solutions.

TABLE V

Characteristic Values of n and K for Natrosol 250 G Solutions at Various Constant Pressure Filtrations

Natrosol Concentration wt. %	Slurry Concentration wt. %	p psi	n	K $lb_f - sec^n/ft^2$
0.6%	2.5% $CaCO_3$	150	0.750	8.0×10^{-4}
		250	0.756	7.8×10^{-4}
		350	0.775	6.65×10^{-4}
0.8%	2.5% $CaCO_3$	150	0.530	7.6×10^{-3}
		250	0.655	2.62×10^{-3}
		350	0.725	1.42×10^{-3}
1.0%	2.5% $CaCO_3$	150	0.545	8.4×10^{-3}
		250	0.650	3.58×10^{-3}
		350	0.740	1.64×10^{-3}
0.8%	4.0% $CaCO_3$	150	0.725	1.42×10^{-3}
		250	0.788	7.57×10^{-4}
		350	0.814	5.70×10^{-4}

Figures 21 to 24 show the plots of the data collected in a series of filtration runs conducted at constant pressures of 150, 250 and 350 lb_f/sq. in. with slurries containing different weight fractions of $CaCO_3$ in Natrosol 250 G solutions. The data are plotted as filtrate volume per unit area v versus effective time of filtration $(\theta - \theta_o)$. The θ_o values, characterizing the initial periods of the filtration runs, are those resulting from the least squares fitting of Equation (108) to the experimental data and which correspond to the particular characteristic value of the flow behaviour index n determined for each constant pressure run. The curves drawn through the data points at each pressure are plots of Equation (108) using the values of n and the parametric coefficients obtained by the least squares fitting procedure described. As seen from Equation (108), the curves pass through the origin. The figures demonstrate the considerable success with which the relationship for the main stage of constant pressure filtration of non-Newtonian fluids, Equation (108), correlates the experimental data which are characterized by different initial stages of filtration as seen by the different values of the θ_o in Table VI. As expected, the effective time of filtration $(\theta - \theta_o)$ required to collect a given filtrate volume increases with decreasing pressure and increasing polymer solution concentration. However, it is not greatly dependent on the slurry concentration, which may be seen by comparison of Figures 22 and 24. The time required to collect the same volume of filtrate is substantially the same for two different slurry concentrations (2.5 versus 4.0 per cent $CaCO_3$) pressure drop.

The present investigation demonstrates the ease with which the filter bed characteristics can be determined by evaluation of the coefficients of Equation (108) which yield the best fit of the experimental data consistent with physical reality. Table VI summarizes the various

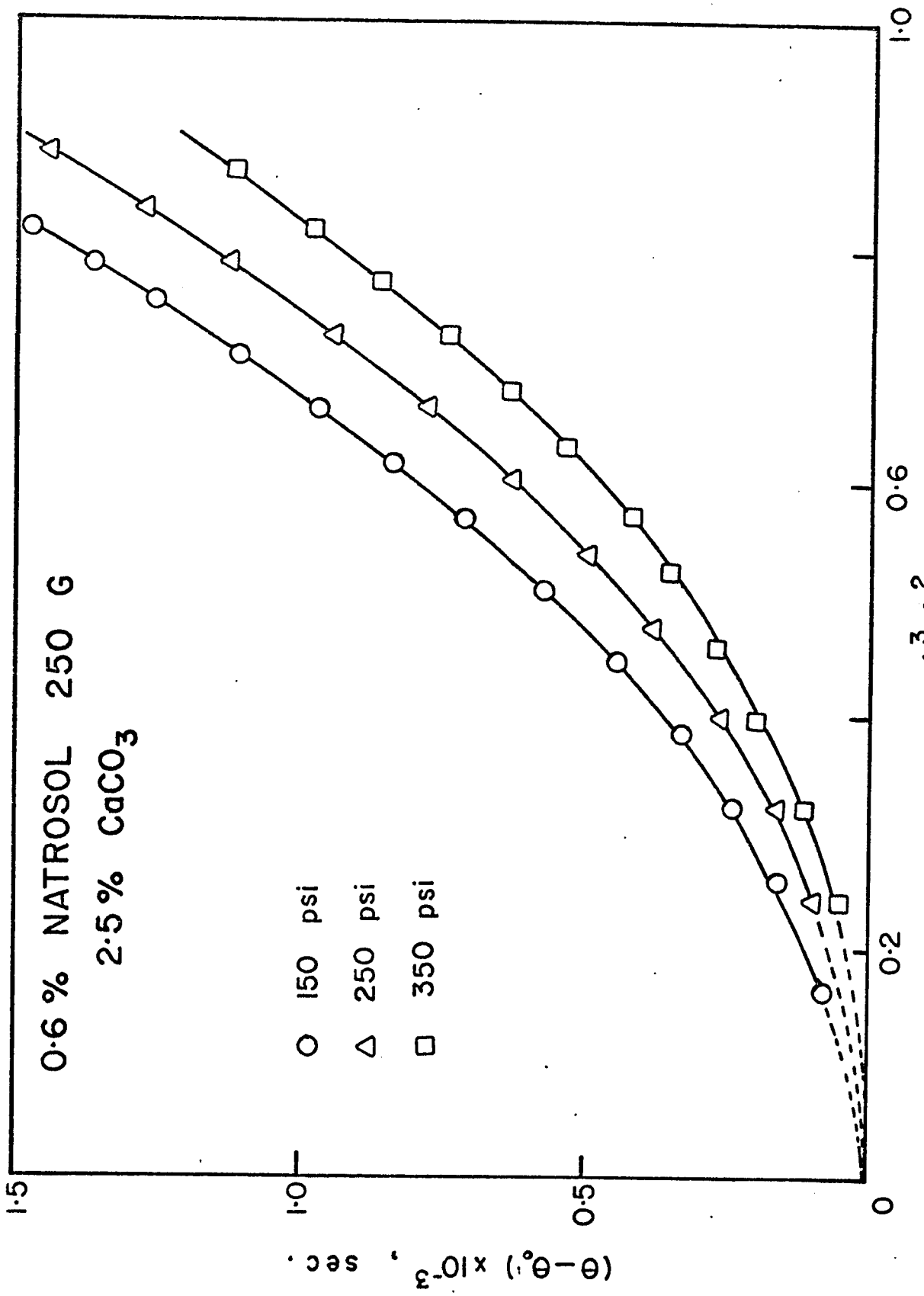

Fig. 21 Plot of v versus ($\theta - \theta_o$) for 2.5% $CaCO_3$ slurry in 0.6% Natrosol 250 G solution at various filtration pressures.

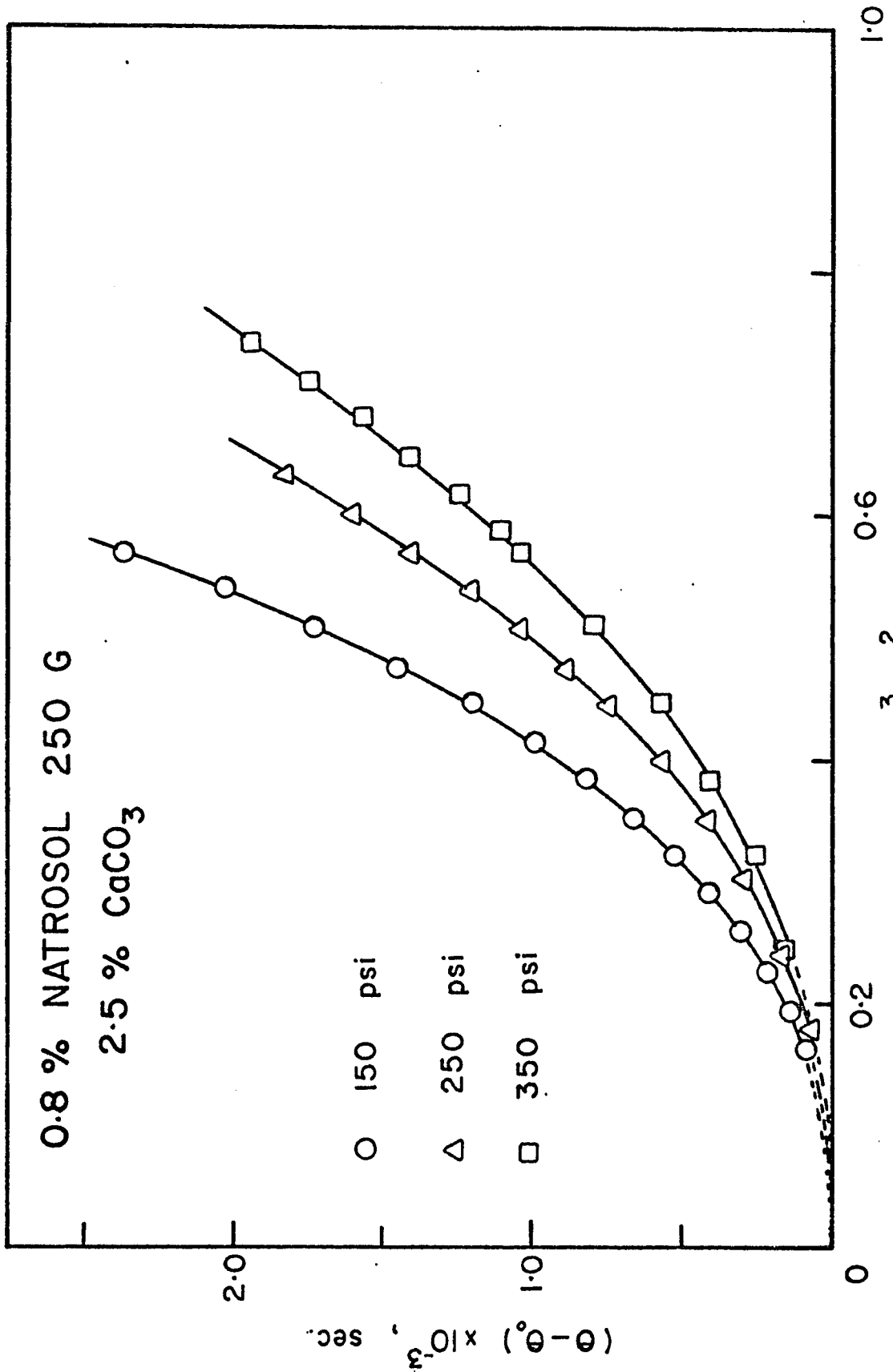

Fig. 22 Plot of v versus $(\theta - \theta_o)$ for 2.5% $CaCO_3$ slurry in 0.8% Natrosol 250 G solution at various filtration pressures.

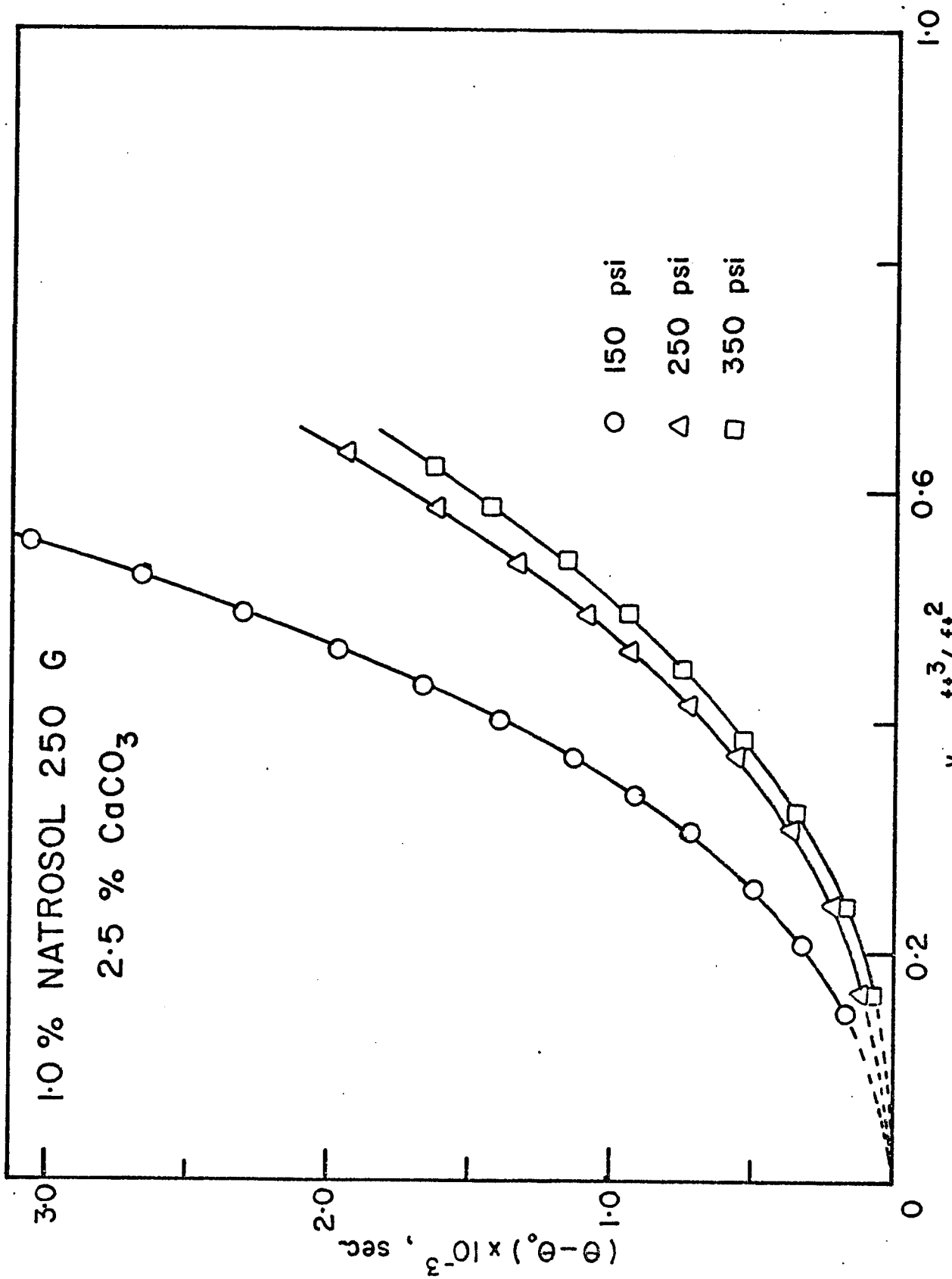

Fig. 23 Plot of v versus ($\theta - \theta_o$) for 2.5% $CaCO_3$ slurry in 1.0% Natrosol 250 G solution at various filtration pressures.

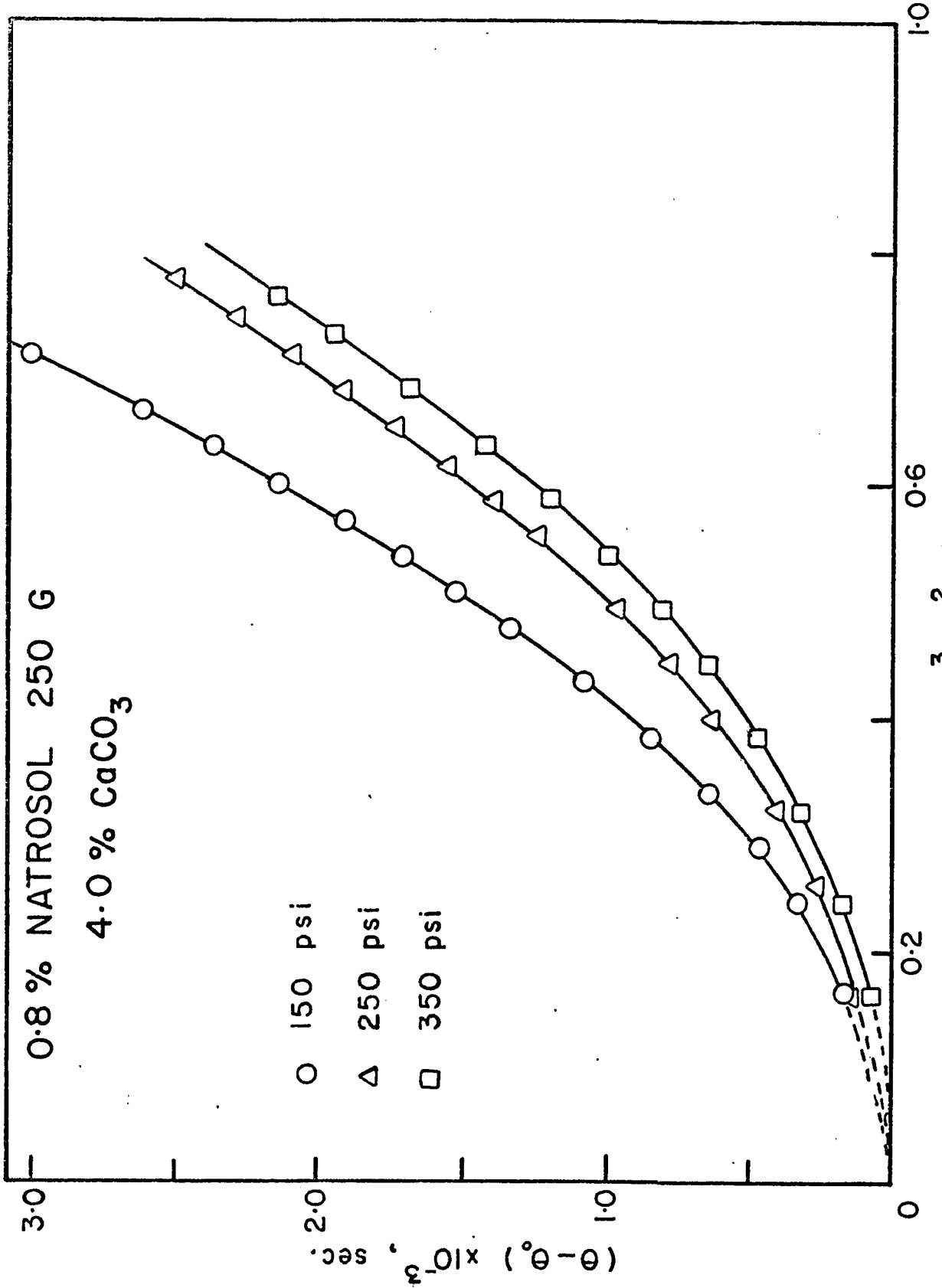

Fig. 24 Plot of v versus ($\theta - \theta_o$) for 4.0% $CaCO_3$ in 0.8% Natrosol 250 G solution at various filtration pressures.

TABLE VI

Filter Medium and Cake Characteristics

Natrosol Concentration wt. %	Slurry Concentration wt. %	p psi	θ_o sec	v_o	K x 10^4	R_m x 10^{-9} $1/ft^n$	α_T x 10^{-9} ft^{2-n}/lb_m	J_{Rn}
0.6%	2.5% $CaCO_3$	150	31	0.176	6.12	2.29	7.88	0.123
		250	27	0.062	5.95	1.50	14.7	0.166
		350	93	0.0	6.52	0.0	26.2	0.192
0.8%	2.5% $CaCO_3$	150	73	0.176	1.02	0.115	0.394	0.006
		250	34	0.062	1.74	0.453	4.44	0.050
		350	22	0.0	2.57	0.0	16.3	0.120
1.0%	2.5% $CaCO_3$	150	- 5	0.176	1.01	0.120	0.412	0.006
		250	20	0.062	1.93	0.295	2.89	0.033
		350	58	0.0	2.01	0.0	19.2	0.141
0.8%	4.0% $CaCO_3$	150	- 5	0.176	2.19	2.25	4.69	0.073
		250	8	0.062	2.60	3.81	22.6	0.255
		350	37	0.0	2.54	0.0	53.5	0.392

pertinent filter medium and cake characteristics determined for the filtration runs conducted at the various constant pressures using various polymer solution and slurry concentrations. It is interesting to note that 10 out of 12 values of the θ_o given in Table VI are positive indicating short initial period of filtration in all these cases. This may be attributable to the instantaneous adjustment to the final desired pressure in constnat pressure filtration of these polymer solutions. It is noted that two of the θ_o values are negative. The possibility of obtaining a negative value for the effective time of commencement fo filtration θ_o may be shown on the basis of the difference in the cake resistance α_T and the moisture ratio m existing in the initial and main stages of the filtration. A rigorous analytical proof of this was presented in the earlier part dealing with the constant pressure filtration of slurries of Newtonian fluids.

As mentioned earlier, in the evaluation of the characteristic n values, it was deemed preferable to assume the same v_o values as determined from measurements conducted at the same pressure with a Newtonian fluid (water) using a 2. 5 per cent slurry concentration. Since separate values were not available for the 4. 0% slurry concentration, these values were also applied to the data for the 4. 0% slurry of $CaCO_3$ in preference to simply equating the filter medium resistance to zero. A value of v_o equal to zero, corresponding to a ratio of R_m to α_T equal to zero, was found for the highest pressure drop (350 psig) used in present investigation.

As in the case of a slurry of a Newtonian fluid, the cake resistance α_T could be represented by a power function of the pressure drop, used for a moderately compressible sludge, given by $\alpha_T = r_o p^{n_o}$, as shown in Figure 25(a). In the present case, it is also found that the cake resistance α_T depends on the slurry and polymer solution

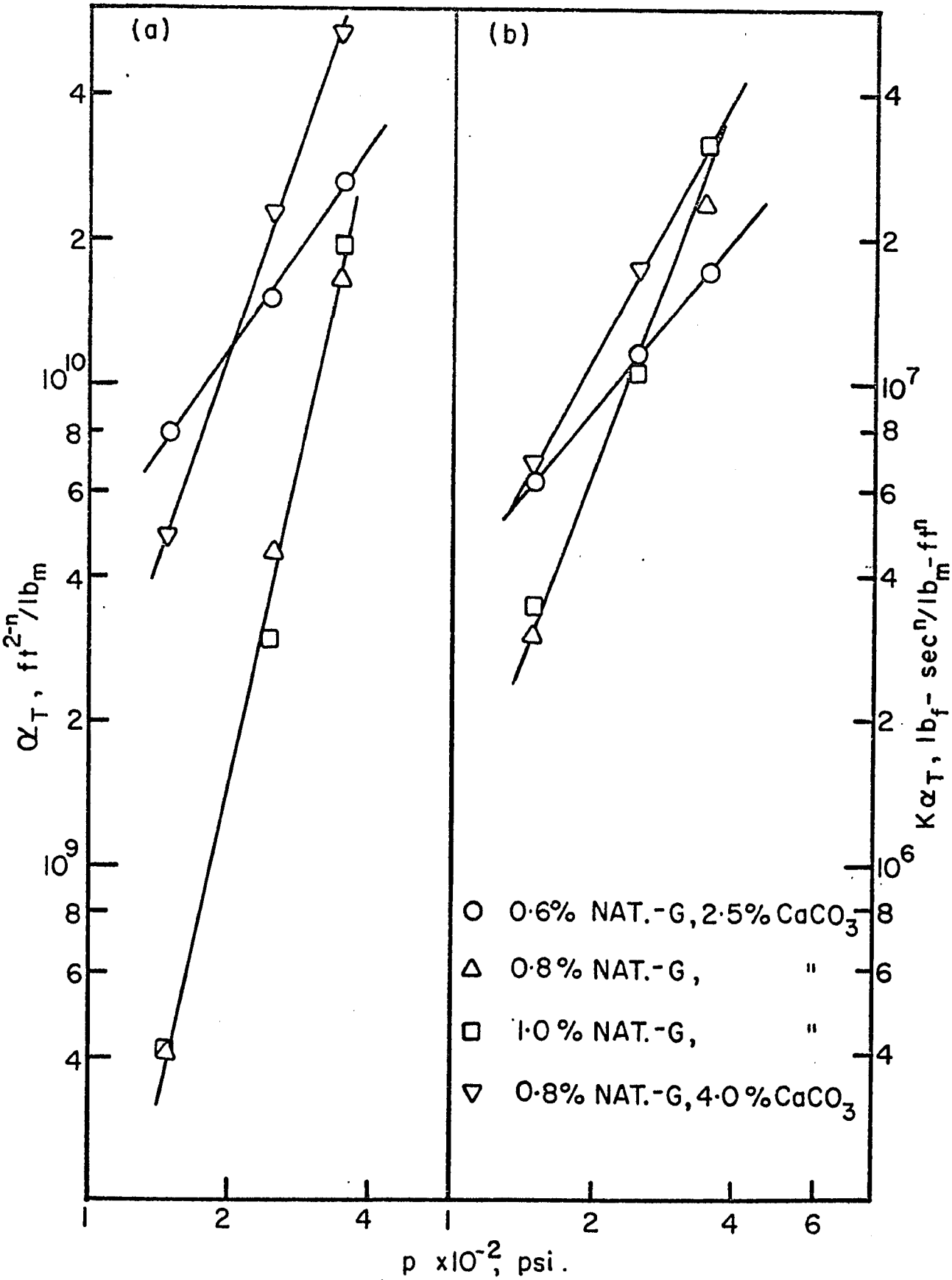

Fig. 25(a) Plot of α_T versus p for various slurries of Natrosol G solutions.

Fig. 25(b) Plot of $K\alpha_T$ versus p for various slurries of Natrosol G solutions.

concentration, since $\alpha_T = J_{Rn}$, and J_{Rn}, in general, is a function of p, n and the slurry concentration. Since α_R is a function of the pressure drop only, one might make use of the α_R value obtained with the Newtonian data to obtain an estimate of the magnitude of J_{Rn}. The computed values of J_{Rn} are markedly lower than unity for all slurries and pressures. This may be attributable to the existence of surface effects in addition to the dependence of J_{Rn} on the value of flow behaviour index and its variation throughout the thickness of the cake. It is interesting and noteworthy that the filter cake resistance for the non-Newtonian slurry is considerably lower than that found for the Newtonian slurry filtered at the same constant pressure. Thus, it appears that the viscous behaviour of the non-Newtonian fluid plays a predominant role in the resistance to flow during the filtration operation.

As shown in Figure 25, the slope n_o obtained in the α_T versus p correlation is greater than unity for all slurries. This is not an indication of the compressibility of the cake as in the case of Newtonian filtration. In view of the value of compressibility coefficient obtained during Newtonian filtration, the high dependency of α_T on p may be due to the additional contribution of the variation of n with p. Further, although α_T, in general, is a function of the polymer concentration of the solution as well as of the pressure of the filtration, in this instance, the α_T and p relationships for the 0.8% and 1.0% Natrosol 250 G slurries containing 2.5% $CaCO_3$ can be represented by the same relation. The same data are shown plotted as $K \alpha_T$ versus p in Figure 25 which gives the slurry and polymer solution concentrations for both figures, utilizing the K values corresponding to each characteristic n value determined with the aid of the viscometer data. It is found that the quantity $K \alpha_T$ can also be expressed as a power function of the pressure drop, with concentration as the parameter.

(ii) Filtration of Natrosol 250 G Solutions at Constant Rate

The results for a series of constant rate filtration runs, conducted with slurries containing 2.5 per cent by weight calcium carbonate in Natrosol 250 G solutions of three different concentrations (0.6, 0.8 and 1.0 per cent weight fraction), are reported and discussed in this section.

The effective initial volume of filtrate v_o was evaluated as the v-intercept of the straight line obtained in v versus θ plot for each individual run. Values of v_o for different flow rates and solution concentrations are presented in Table VII. A positive value of v_i corresponds to a faster average initial rate of filtrate relative to the desired constant rate of filtrate q_1 in the main stage of filtration. It is noticed that some of the values are zero, corresponding to the effective initial rate of filtrate equal to q_1. Hence, correction in the initial transient stage of filtration is not necessary in these instances. After applying the necessary time correction, the constant rate filtration data obtained with slurries of three Natrosol solutions are plotted as the effective time of filtration $(\theta + \theta_c)$ versus the pressure drop across the cake $(p - p_1)$, with flow rate q_1 as the parameter. Figures 26 to 28 represent these data plotted in accordance with the Equation (116).

The values of slope A, and intercept B of these lines, along with the values of pressure at the filter medium and cake interface p_1 are given in Table VII. These values were obtained by fitting Equation (116) to the filtration data collected at different constant rates employing the method of least squares as outlined earlier. The slope A and intercept B in Equation (116) were used subsequently in the determination of the characteristic value of the flow behaviour

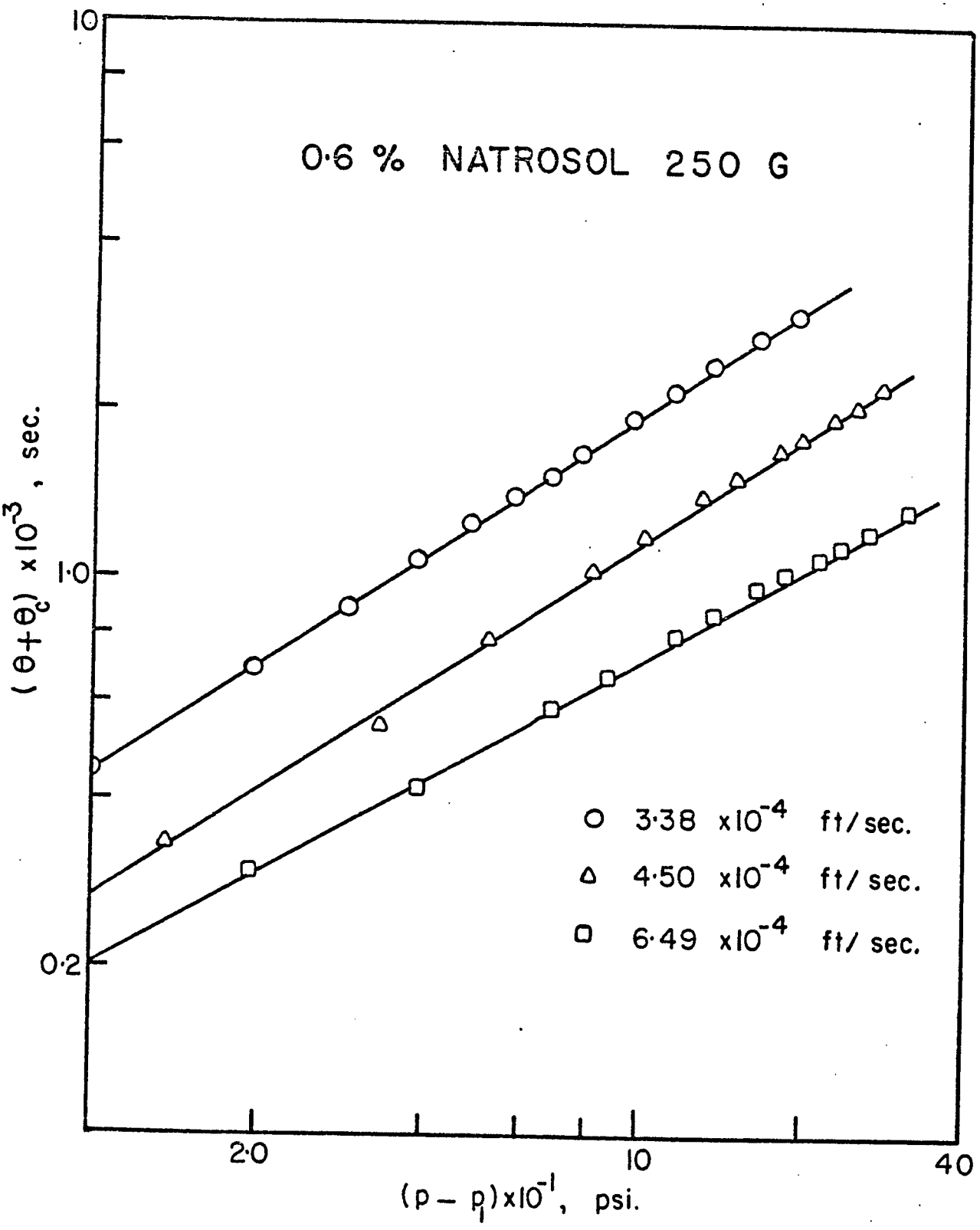

Fig. 26 Plot of $(\vartheta + \theta_c)$ versus the $(p - p_1)$ for 0.6% Natrosol 250 G solution at various constant rates of filtrate.

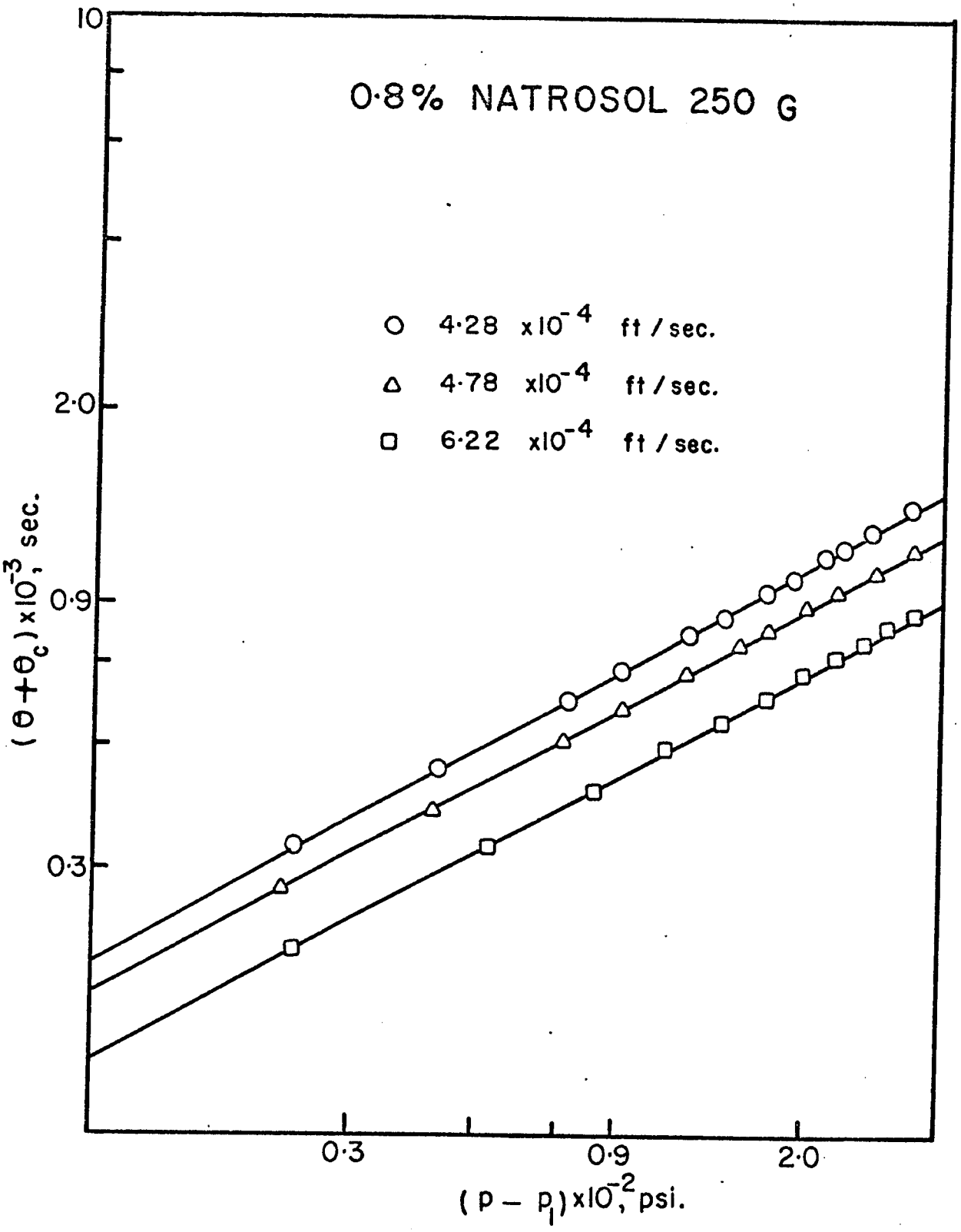

Fig. 27 Plot of $(\theta + \theta_c)$ versus $(p - p_1)$ for 0.8% Natrosol 250 G solution at various constant rates of filtrate.

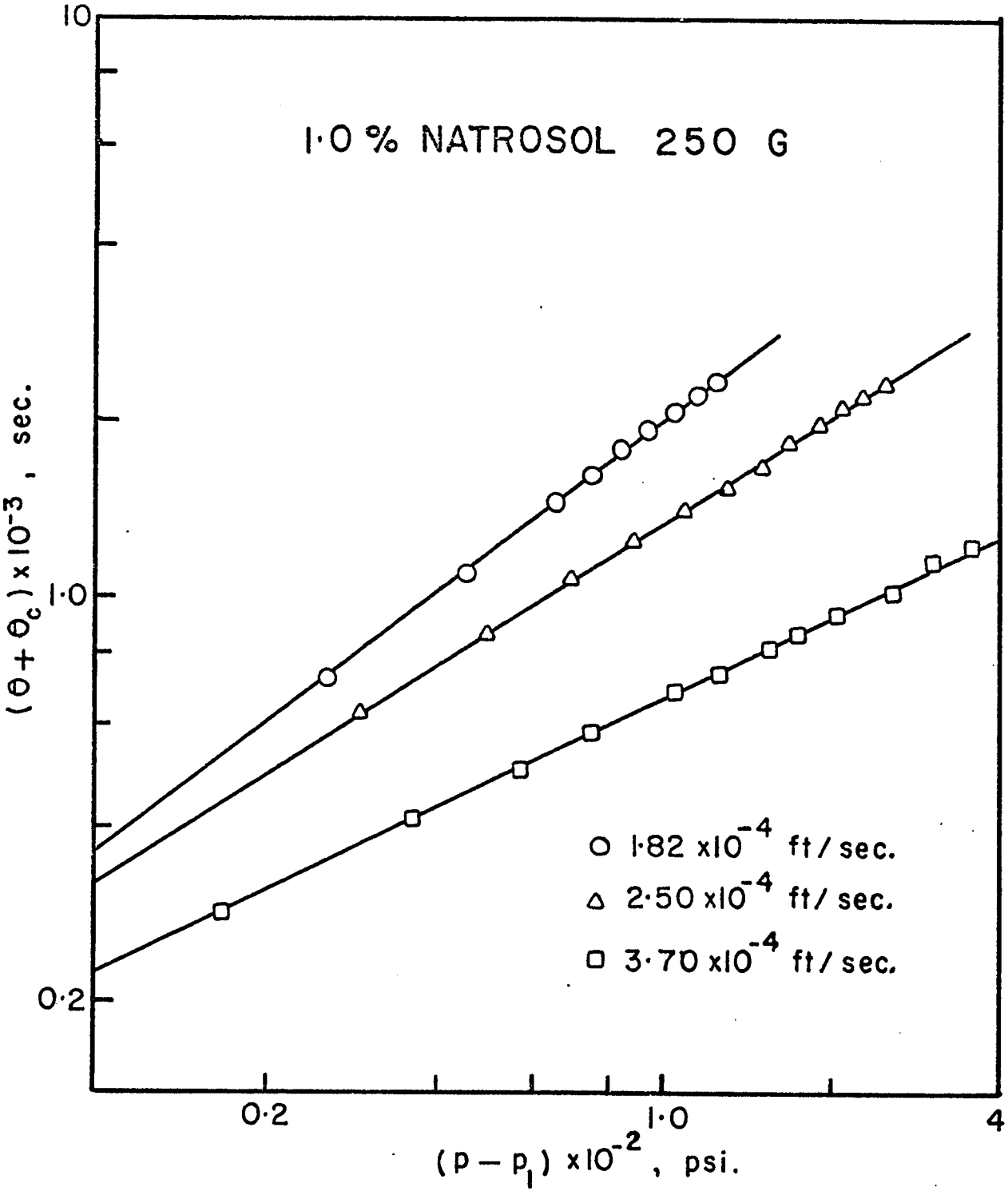

Fig. 28 Plot of $(\theta + \theta_c)$ versus $(p - p_1)$ for 1.0% Natrosol 250 G solution at various constant rates of filtrate.

TABLE VII

Values of p_1, v_o, A and B For Various Constant Rate Filtration Runs With Natrosol G Solutions

Natrosol Concentration	$q_1 \times 10^4$ ft./sec.	p_1 psi	$v_o \times 10^2$ $ft.^3/ft.^2$	A	B
0.6%	3.38	20	3.96	0.5770	0.1234
	4.50	16	1.58	0.5502	0.1550
	6.49	30	0.00	0.5380	0.2460
0.8%	4.28	26	0.00	0.5366	0.2440
	4.78	26	4.74	0.5305	0.2678
	6.22	26	0.00	0.5351	0.3686
1.0%	1.82	14	2.76	0.7374	0.5560
	2.50	20	5.91	0.6106	0.2582
	3.70	43	0.00	0.4701	0.1368

index n and the resistance term λ. Figures 26 to 29 demonstrate the considerable success with which the relationship developed for the main stage of constant rate filtration correlates the experimental data obtained with Natrosol G solutions.

According to Equation (117), the slope A obtained from the $(\theta + \theta_c)$ versus $(p - p_1)$ correlation for each constant rate when plotted against log q_1 should yield a straight line with a slope of m_o and an intercept of $(1 - r_o)$. Similarly Equation (118) suggests a linear correlation between the intercept B and the filtrate rate q_1 when plotted on a log-log paper. The slope and intercept of the B versus q_1 plot determine the n_1 and λ_o values respectively. The success with which these relationships can correlate the experimental data is illustrated by Figures 29 and 30, which show the plots of A and B versus q_1 for the three Natrosol solutions. With the values of λ_o, r_o, m_o, and n_1 known, the resistance term λ and the characteristic value of the flow behaviour index n could be readily determined utilizing Equations (113) and (114).

Table VIII presents the characteristic values of the flow behaviour index n and the corresponding m_o and n_1 values calculated from the constant rate data for the three Natrosol G solutions. The n values are presented at three different pressure drops; namely 150, 250 and 350 psi, in order to facilitate the comparison with those determined from the constant pressure data. Values of n obtained from the constant pressure filtration are also tabulated in the same table. It is seen that the characteristic value of n obtained from constant rate filtration are slightly higher than those obtained from constant pressure filtration. However, it is instructive to note that the comparison between the two sets of n values is not strictly valid since in constant rate filtration, n is represented by a logarthmic function of pressure

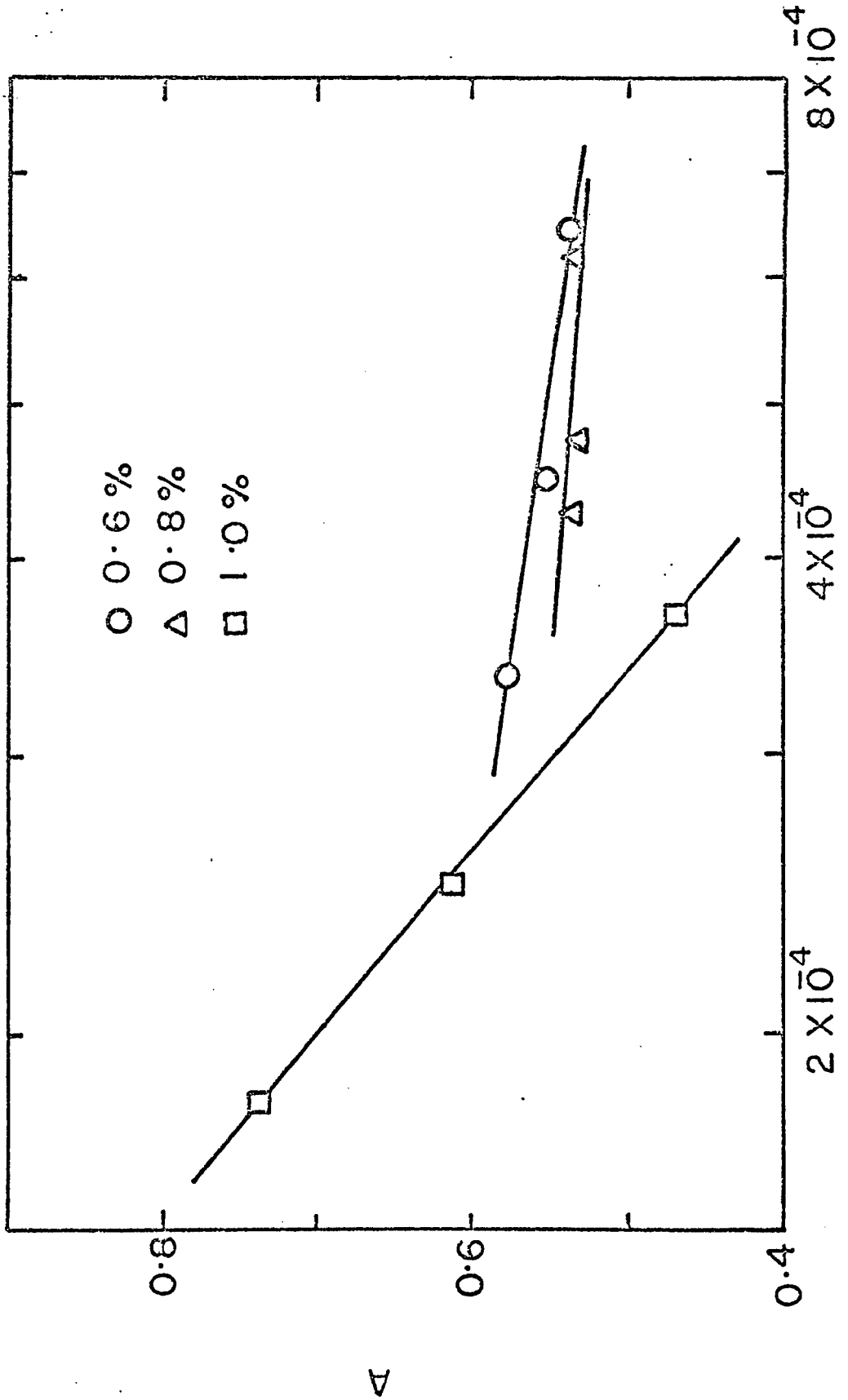

Fig. 29 Plot of the coefficient A versus flow rate q_l for different Natrosol G solution concentrations.

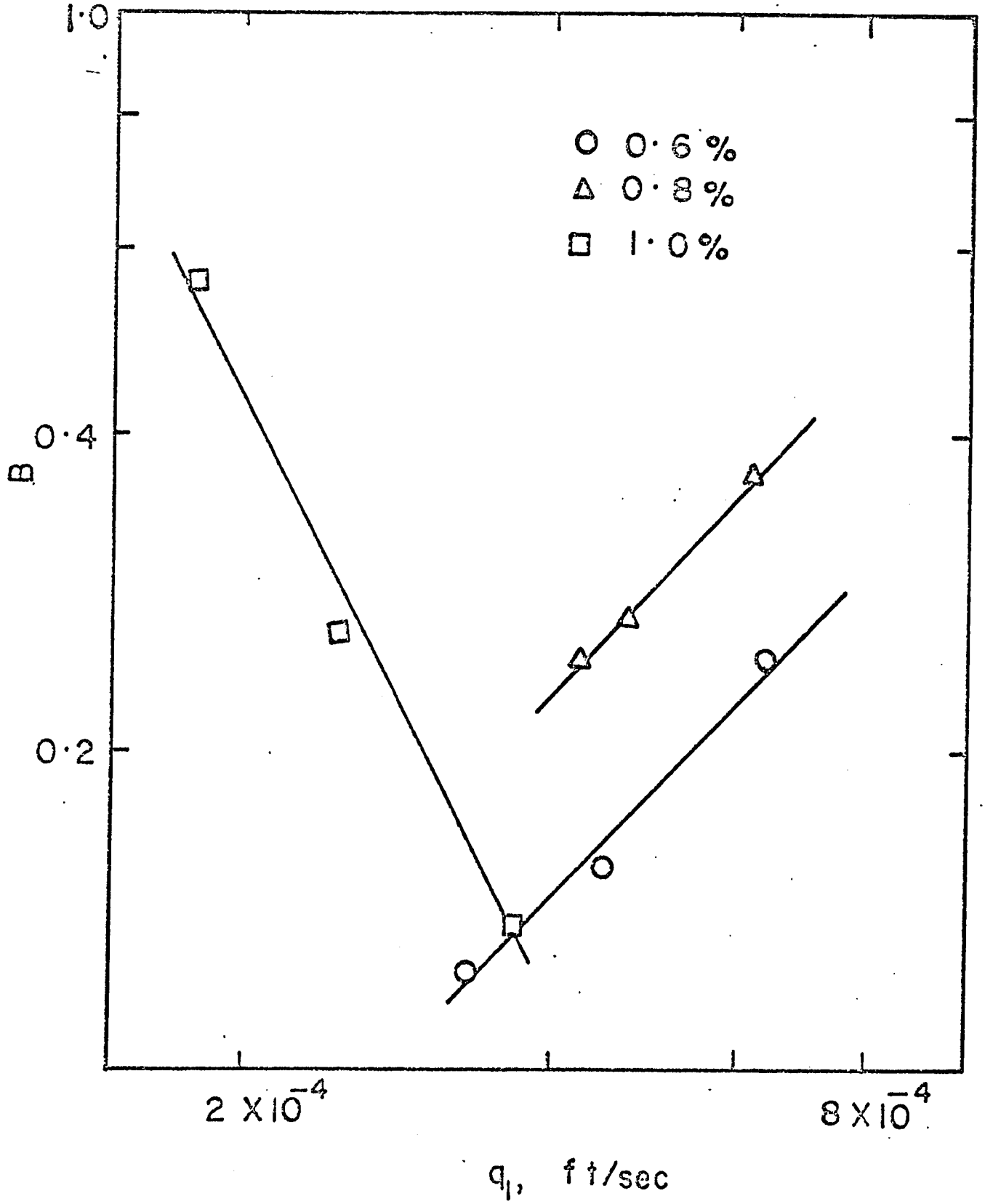

Fig. 30 Plot of the coefficient B versus flow rate q_1 for different Natrosol G solution concentrations.

TABLE VIII

Characteristic Values of n for Natrosol 250 G Solutions from Filtration

Natrosol Concentration Wt. %	m_o	n_1	Value of n at 150 psi	Value of n at 250 psi	Value of n at 350 psi
0.6%	0.155	0.065	0.736	0.774	0.795
			(0.750)*	(0.756)	(0.775)
0.8%	0.140	0.100	0.706	0.740	0.760
			(0.530)	(0.655)	(0.725)
1.0%	0.820	-2.892	0.658	0.851	0.978
			(0.545)	(0.650)	(0.740)

* Values of n in parentheses were determined from Constant Pressure Filtration Data.

drop across the cake $(p - p_1)$, while in the constant pressure filtration, n is a logarithmic function of total pressure drop p. All the characteristic values of n determined from both constant rate and constant pressure filtrations lie within the range of the flow behaviour index obtained with the viscometer measurements.

Values of λ calculated from both constant rate and constant pressure filtrations for various Natrosol G solutions at three different pressure drops are given in Table IX. It must also be emphasized that in the constant rate filtration, λ is represented as a power function of $(p - p_1)$, whereas in constant pressure filtration it is expressed as a power function of p. In spite of this difference, it is noticed that values obtained from constant rate and constant pressure agree favourably for 0.6% and 0.8% Natrosol solutions. It is observed that for 1.0% Natrosol solution, the resistance term λ is a strong function of pressure drop in the case of constant rate filtration resulting in larger values of λ.

TABLE IX

Values of λ Calculated From Filtration Data For Natrosol 250 G Solutions

Natrosol Concentration Wt. %	r_o	λ_o	$\lambda \times 10^{-7}$ at 150 psi	at 250 psi	at 350 psi
0.6%	0.970	9.24×10^{2}	1.451	2.40	3.324
			(1.05)*	(1.865)	(2.820)
0.8%	0.925	1.225×10^{3}	1.275	2.01	2.744
			(0.489)	(1.918)	(3.78)
1.0%	3.342	4.465×10^{-7}	13.75	73.0	218.2
			(0.575)	(1.602)	(5.17)

* Values of in parenthesis were determined from constant pressure filtration data.

(iii) Filtration of Natrosol 250 HR Solutions at Constant Pressure

The results for a series of constant pressure filtration runs conducted with slurries comprising 2.5 per cent by weight calcium carbonate in Natrosol HR solutions of different concentrations namely 0.1%, 0.2%, and 0.3%, are reported in this section. Viscometric data collected for these solutions utilizing a stainless steel capillary tube viscometer are presented elsewhere[79].

Equation (108) was fitted to the filtration data collected at constant pressure employing the method of least squares as done in processing the data collected with Natrosol G solutions. The criterian was to determine for each constant pressure run the characteristic value of the flow behaviour index n and corresponding coefficient K, N, and θ_o in Equation (108) yielding the minimum variance between values predicted by Equation (108) and the experimental data. The values of n, θ_o, N and 1/K computed from constant pressure runs for three concentrations of Natrosol HR solution are presented in Table X. For the run conducted with 0.2% Natrosol HR solution at the constant pressure of 200 psi, no minimum variance with respect to n could be obtained in the range of n from 0.4 to 1.6. It is observed from the values of n in the Table X, for 0.1% Natrosol HR solution the variation of n with respect to the pressure is of very small order. By the help of two runs reported for 0.2% Natrosol HR solution a slightly increasing trend for n with pressure drop is noted. In case of 0.3% solution, the linear relation between the values of n and pressure drop can be noticed from the Table as well as from the Figure 31, which shows the variation of n with pressure drop for different concentrations. This figure indicates existance of no definite relationship between the values of flow bheaviour index n and pressure drop. With the aim of achieving a correlation between the specific

TABLE X

Constant Pressure Filtration With HR Solutions

$$\theta = A+B\left(\frac{V}{A}\right)^{D-1} + C\left(\frac{V}{A}\right)^{D} = A+B\left(\frac{V}{A}\right)^{1/n} + C\left(\frac{V}{A}\right)^{\frac{n+1}{n}}$$

P_{psi}	n	θ_o	N	1/K
0.1% HR Solution				
150	0.5208	14.99	1054.0	-101.60
200	0.5076	48.00	695.4	-102.128
250	0.5319	45.34	425.1	- 29.854
0.2% HR Solution				
150	0.4130	698.25	-8325	2.037×10^4
250	-	-	-	-
350	0.500	78.115	954.06	1.209×10^3
0.3% HR Solution				
150	0.4201	-144.3	9488	-4.567×10^3
200	0.4560	19.43	3580	-4.07×10^2
300	0.5128	14.00	1651	2.262×10^3

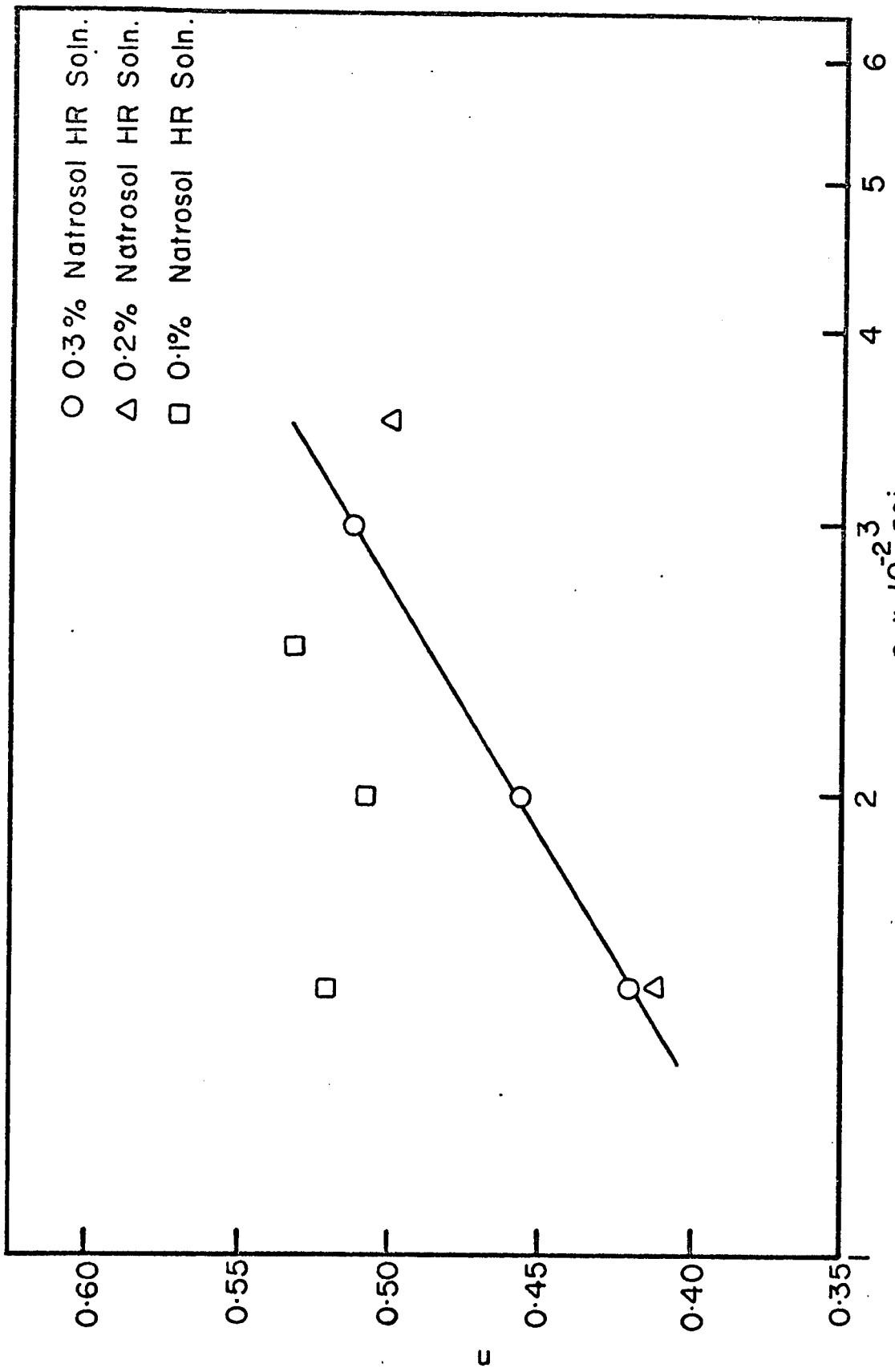

Fig. 31 Plot of the characteristic value of the flow behaviour index n versus pressure p for various slurries of Natrosol HR solutions.

cake resistance and the pressure drop, the values of the coefficients obtained in the computation are analysed. A careful observation of the Table X reveals the negative values for N in some cases and negative values for 1/K in some other cases suggesting negative filter medium resistance in the former case and negative specific cake resistance in the latter case. Negative filter medium resistance and negative cake resistance are physically inconceivable.

In view of this difficulty, an alternative method was tried to fit the experimental data to Equation (108) assuming the filter medium resistance to be zero, which may not be unreasonable at the pressure drops maintained in these experiments. In Figures 32 to 37, the parabolic shaped curves represent the variation of the computed variance with the assumed values of flow behaviour index n for N equal to zero in Equation (108) corresponding to zero filter medium resistance. The values of n, θ_o, N and 1/K obtained in this computation are given in Table XI. θ_o values obtained from computation to characterize the initial stage of filtration were utilized to transform the data into the form of effective time of filtration. The data are plotted in Figures 38 to 40, as effective time of filtration $(\theta - \theta_o)$ versus volume of filtrate per unit area of filtration for three Natrosol HR concentrations. The curves obtained for the runs conducted with care and precision at different constant pressures, demonstrate the reliability of the data collected. From the Table XI, it can be noticed that for 0.1% Natrosol HR solution the values of flow behaviour index n are more than unity. The values do not look to be convincing when compared to the values obtained at other concentrations and cast a doubt on their validity when their values are more than one. Figure 41 shows the attempt that was made to find the correlation between the values of flow behaviour index n and pressure drop at which

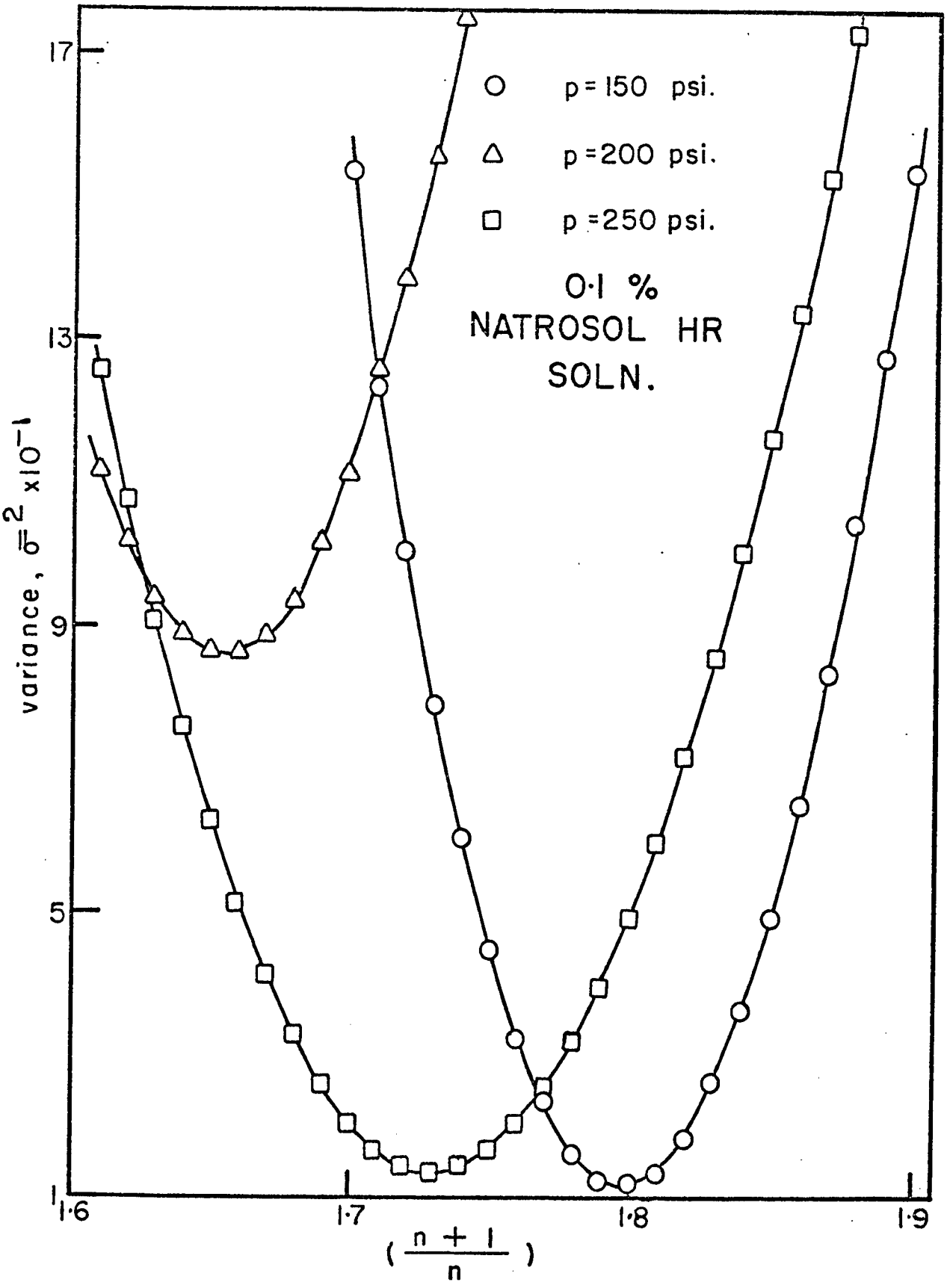

Fig. 32 Variation of the variance with assumed $(\frac{n+1}{n})$ values for 2.5% $CaCO_3$ slurry in 0.1% Natrosol HR solution at various pressures.

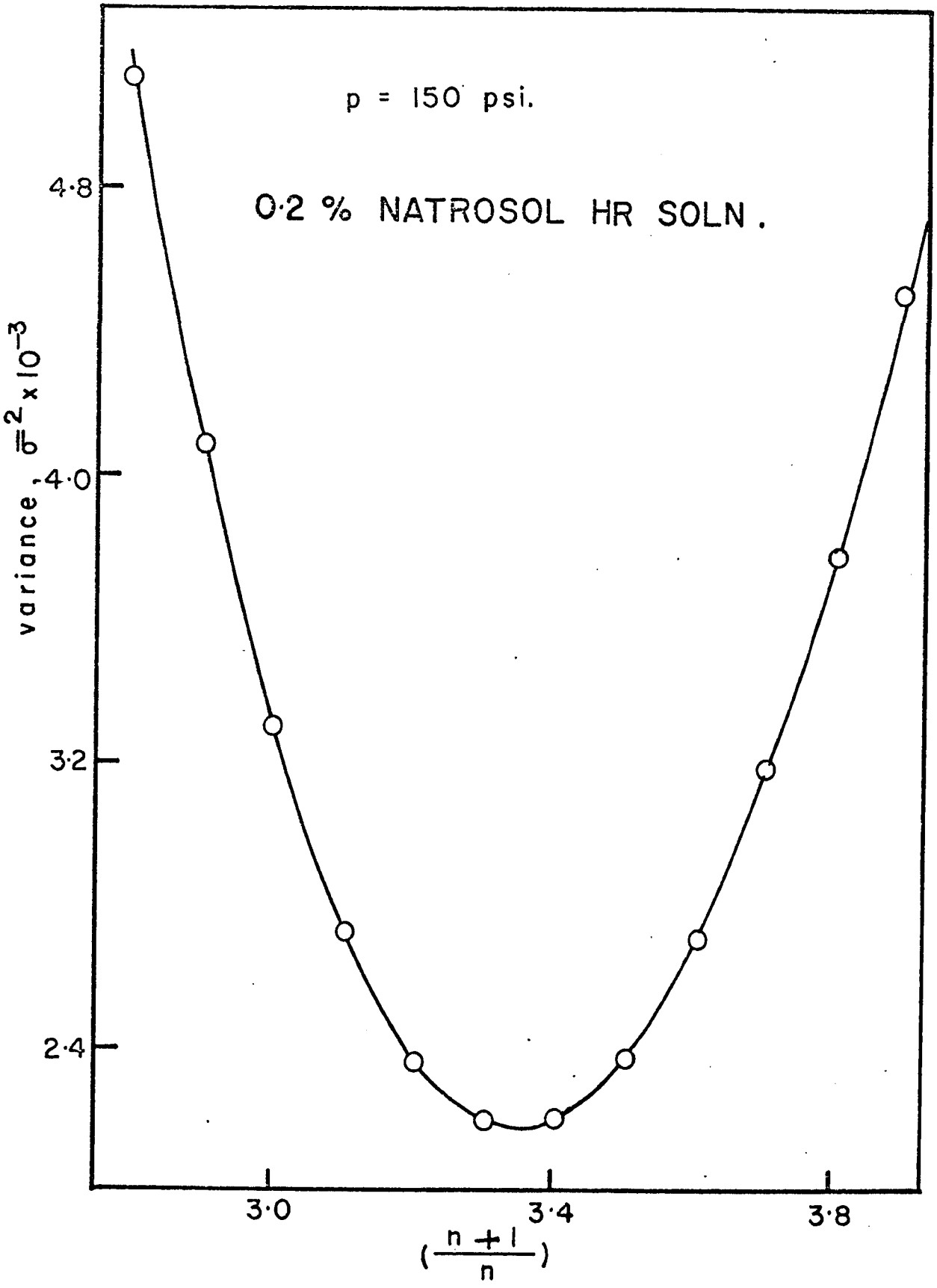

Fig. 33 Variation of the variance with assumed $(\frac{n+1}{n})$ values for 2.5% $CaCO_3$ slurry in 0.2% Natrosol HR solution at filtration pressure of 150 psi.

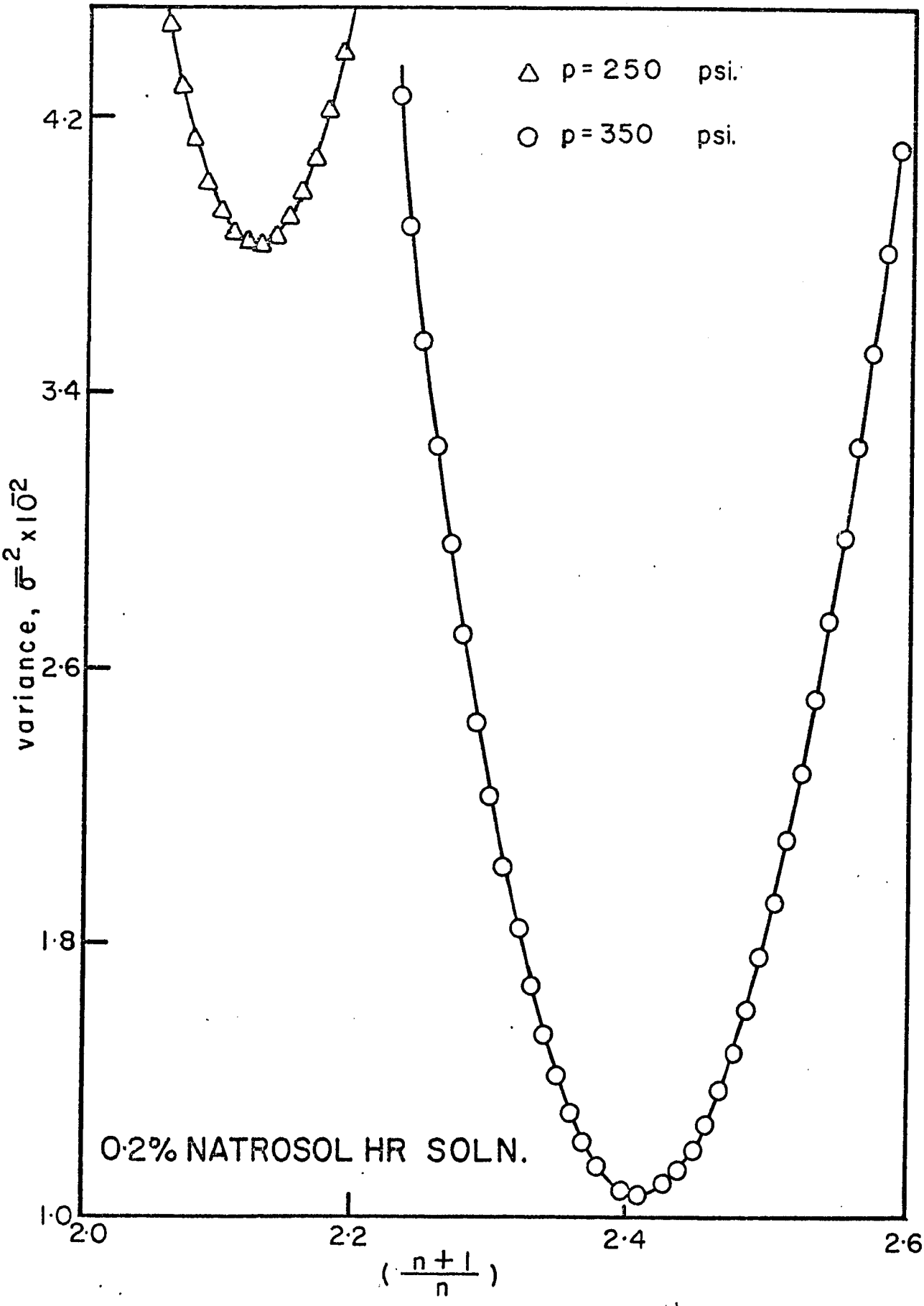

Fig. 34 Variation of the variance with assumed $(\frac{n+1}{n})$ values for 2.5% $CaCO_3$ slurry in 0.2% Natrosol HR solution at 250 and 350 psi.

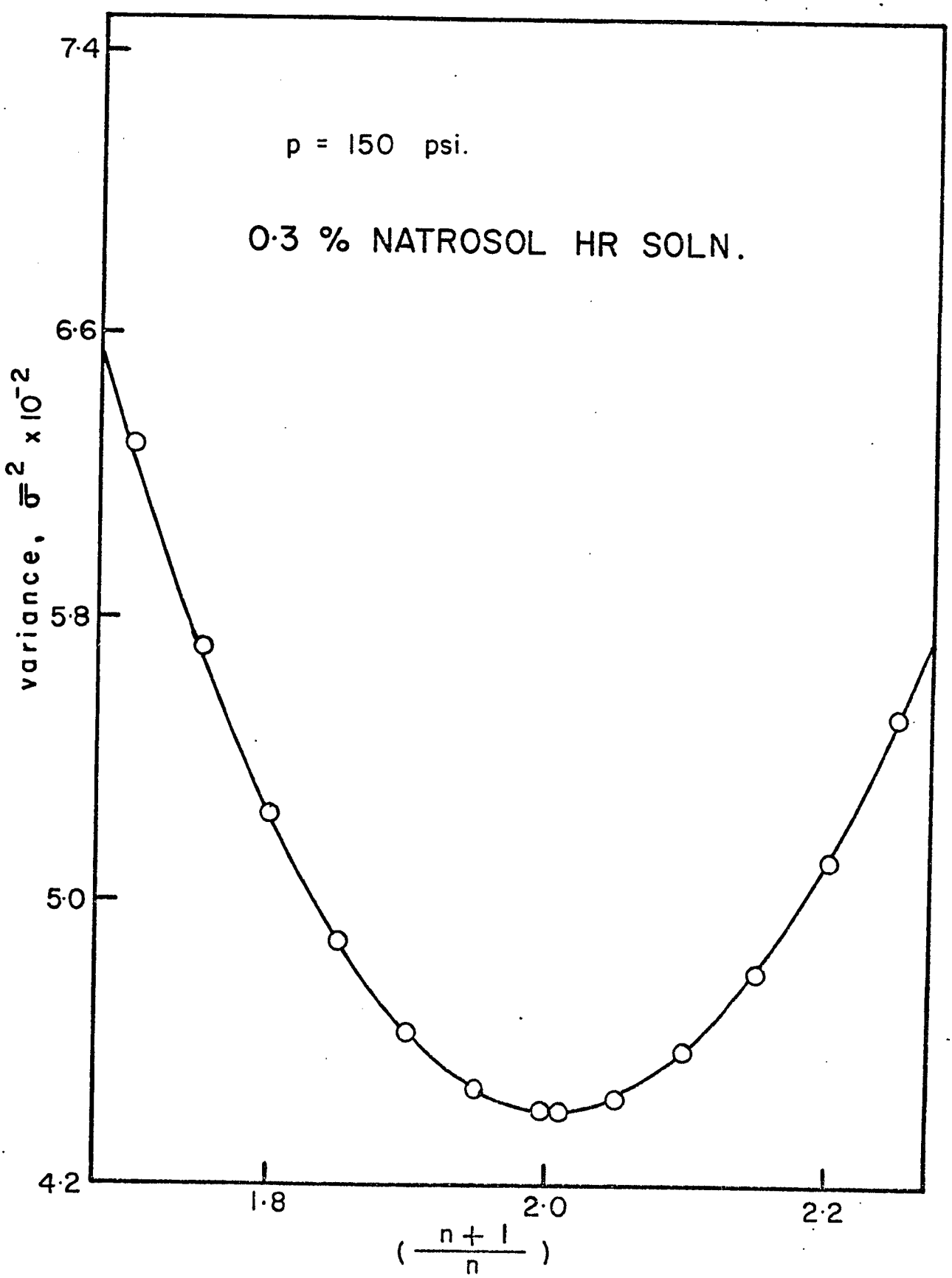

Fig. 35 Variation of the variance with assumed $(\frac{n+1}{n})$ values for 2.5% $CaCO_3$ slurry in 0.3% Natrosol HR solution at 150 psi.

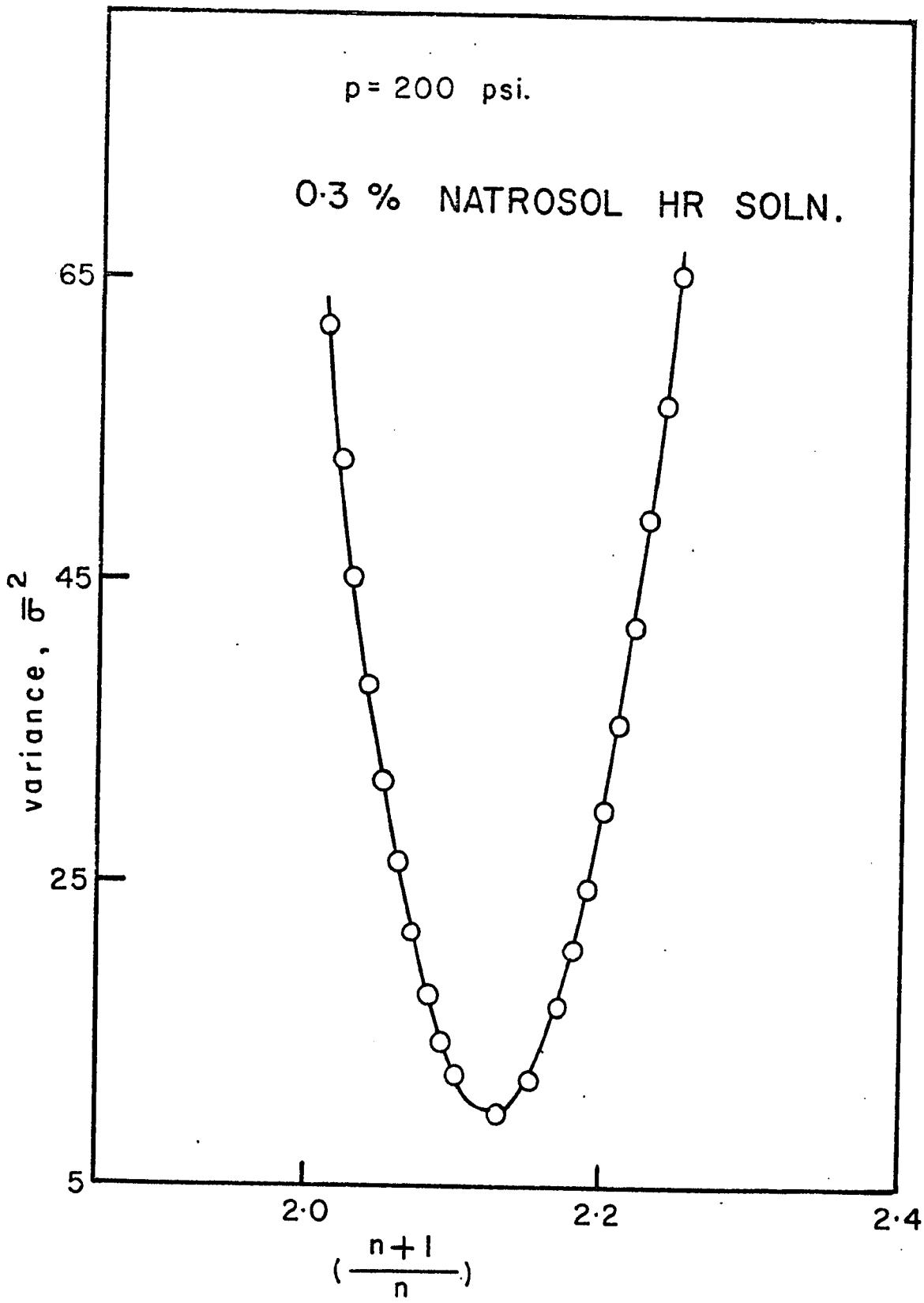

Fig. 36 Variation of the variance with assumed $(\frac{n+1}{n})$ values for 2.5% $CaCO_3$ slurry in 0.3% Natrosol HR solution at 200 psi.

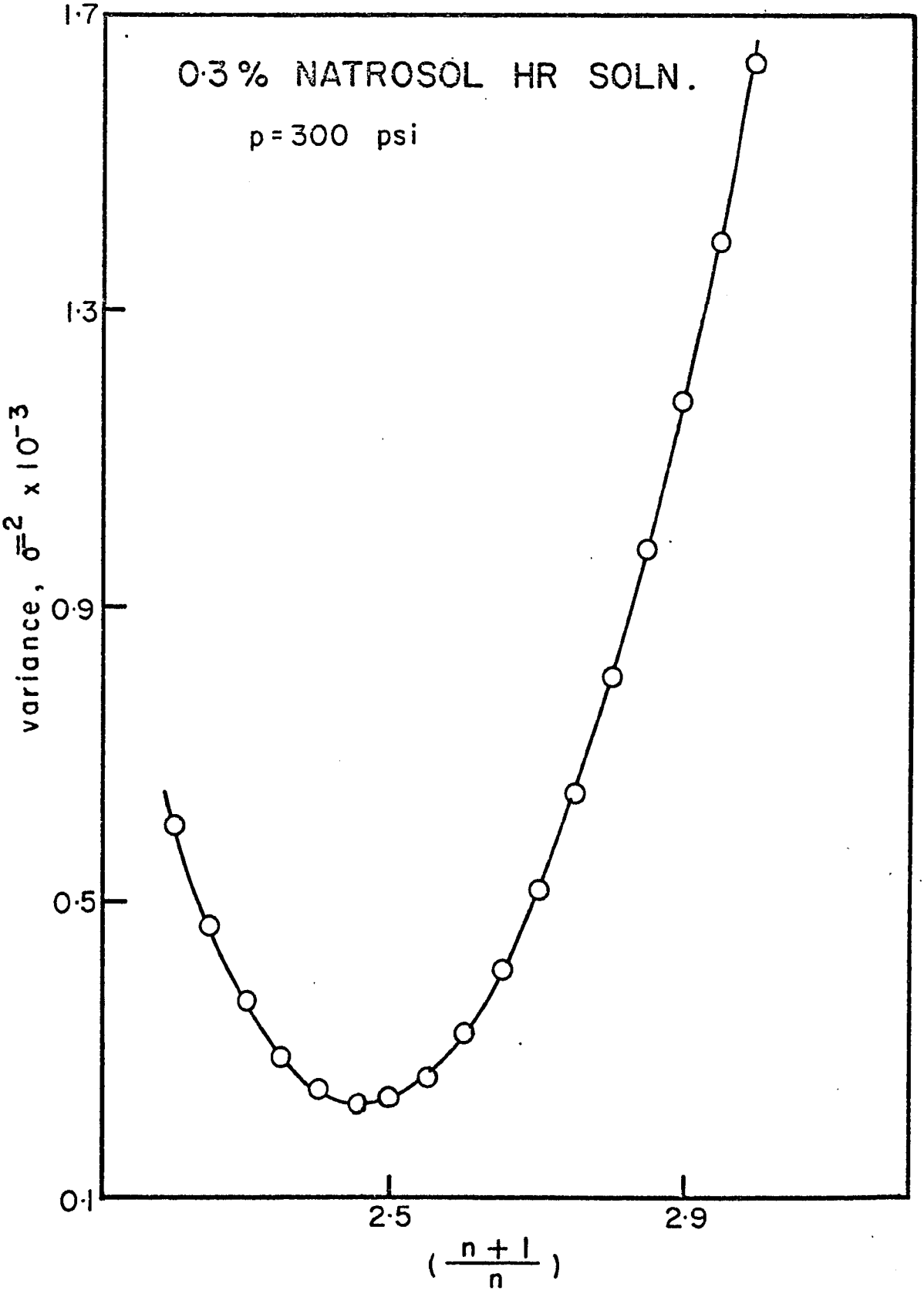

Fig. 37 Variation of the variance with assumed $(\frac{n+1}{n})$ values for 2.5% $CaCO_3$ slurry in 0.3% Natrosol HR solution at 300 psi.

TABLE XI

Constant Pressure Filtration With HR Solutions

$$\theta = A + C\left(\frac{V}{A}\right)^{D} = A + C\left(\frac{V}{A}\right)^{\frac{n+1}{n}} \quad \text{and} \quad B = 0$$

0.1% HR Solution

p	D	n	θ_o	N	1/K
150	1.7975	1.2539	9.25	0	9.559×10^2
200	1.655	1.5267	19.4	0	6.253×10^2
250	1.7300	1.3698	33.37	0	4.09×10^2
0.2% HR Solution					
150	3.3400	0.4273	114.37	0	0.666×10^3
250	2.1300	0.8849	39.9	0	2.581×10^3
350	2.405	0.7117	52.89	0	2.162×10^3
0.3% HR Solution					
150	2.0100	0.990	-193.14	0	5.765×10^3
200	2.1300	0.8849	17.91	0	3.242×10^3
300	2.4600	0.6849	38.54	0	3.823×10^3

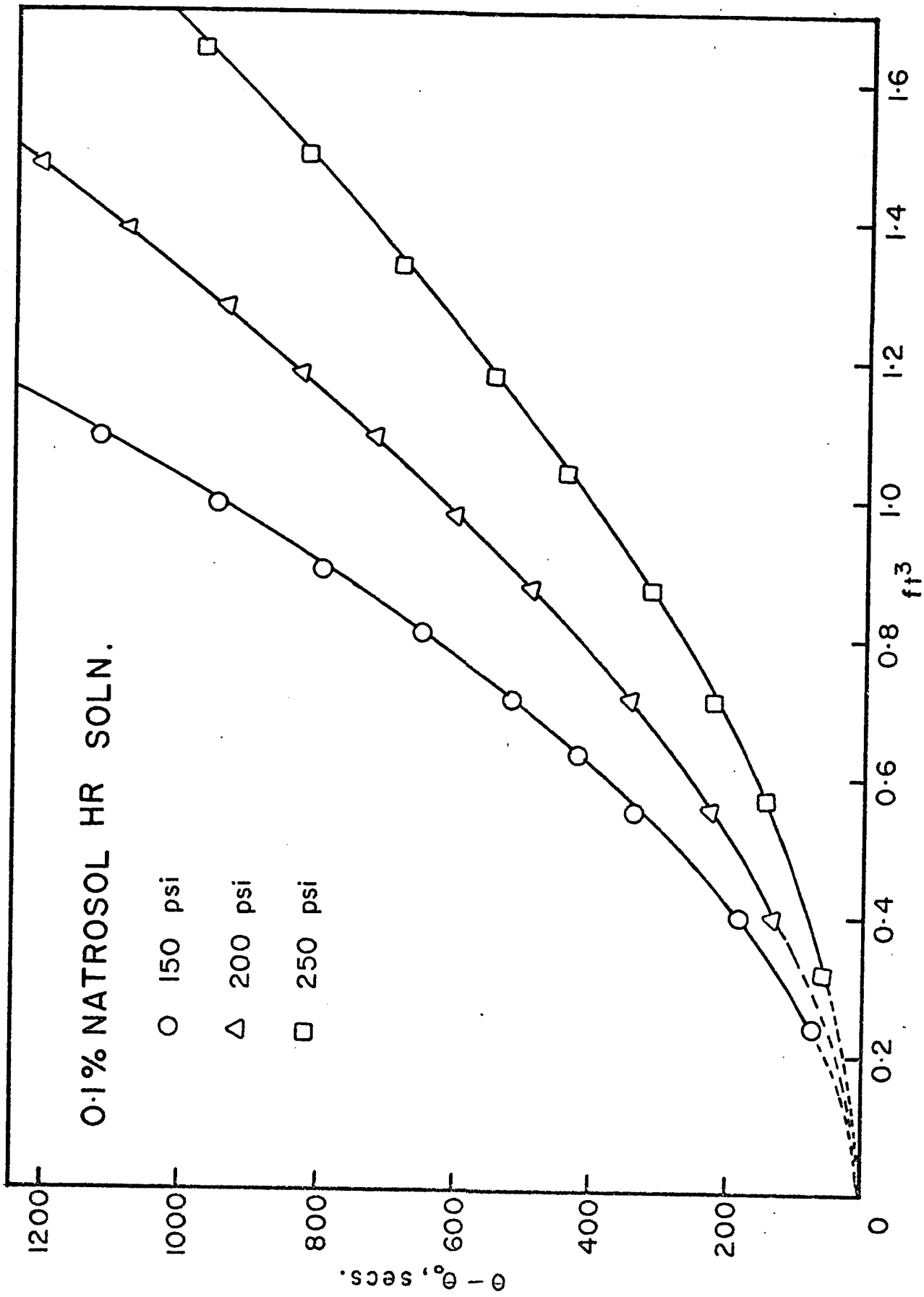

Fig. 38 Plot of $(\theta - \theta_0)$ versus v for 0.1% Natrosol HR solution at various filtration pressures

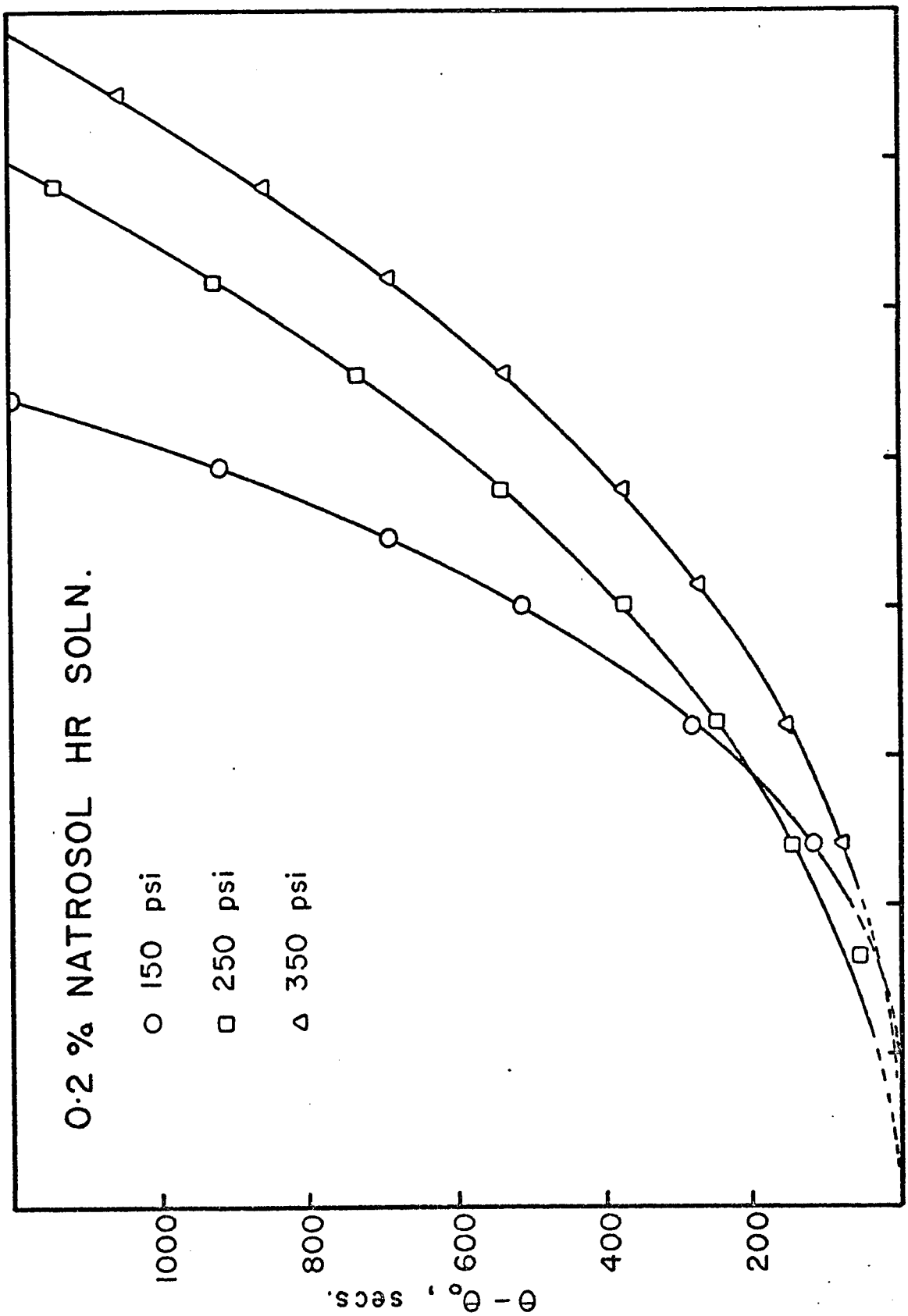

Fig. 39 Plot of $(\theta - \theta_o)$ versus v for 0.2% Natrosol HR solution at various filtration pressures.

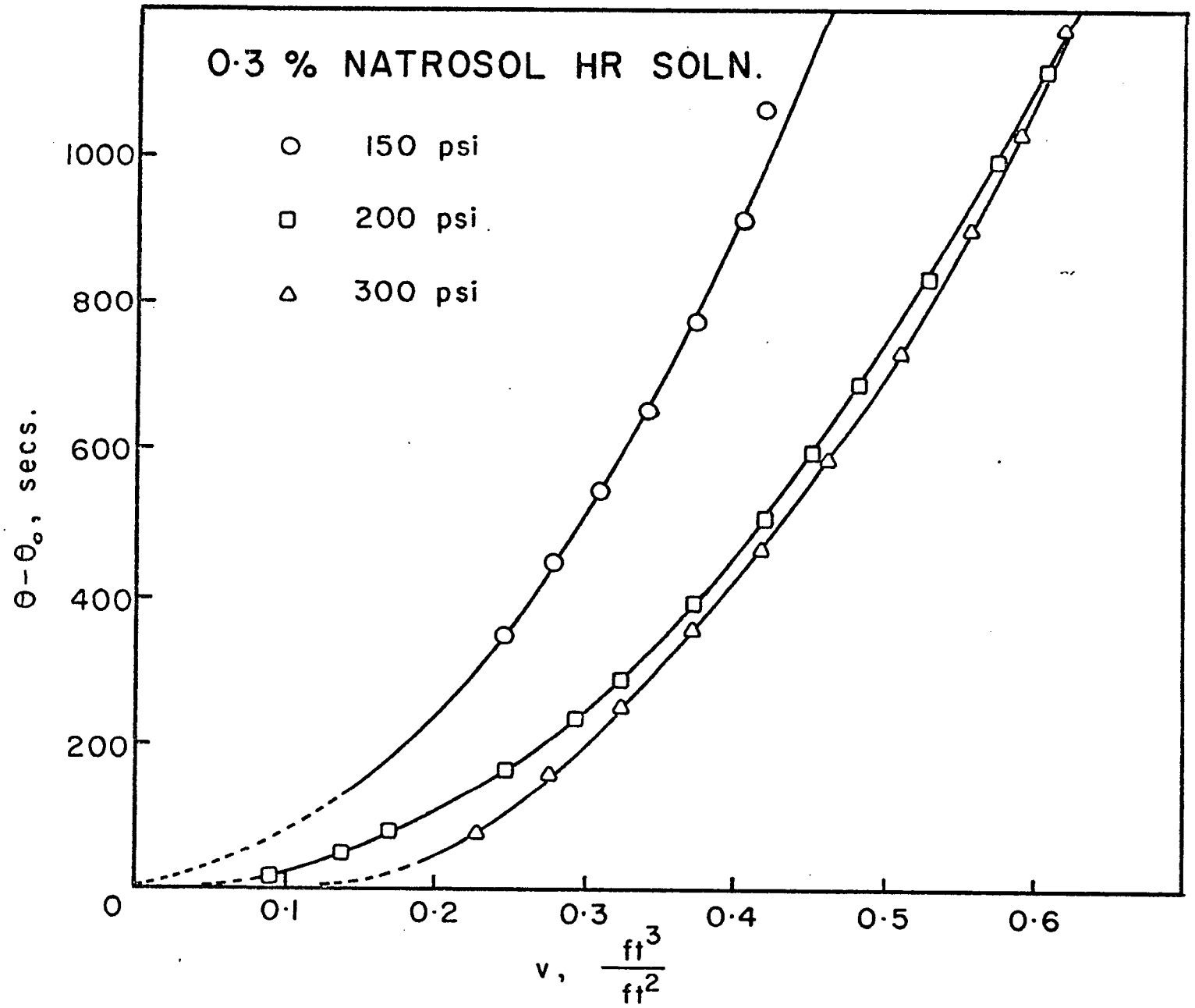

Fig. 40 Plot of ($\theta - \theta_o$) versus v for 0.3% Natrosol HR solution at various filtration pressures.

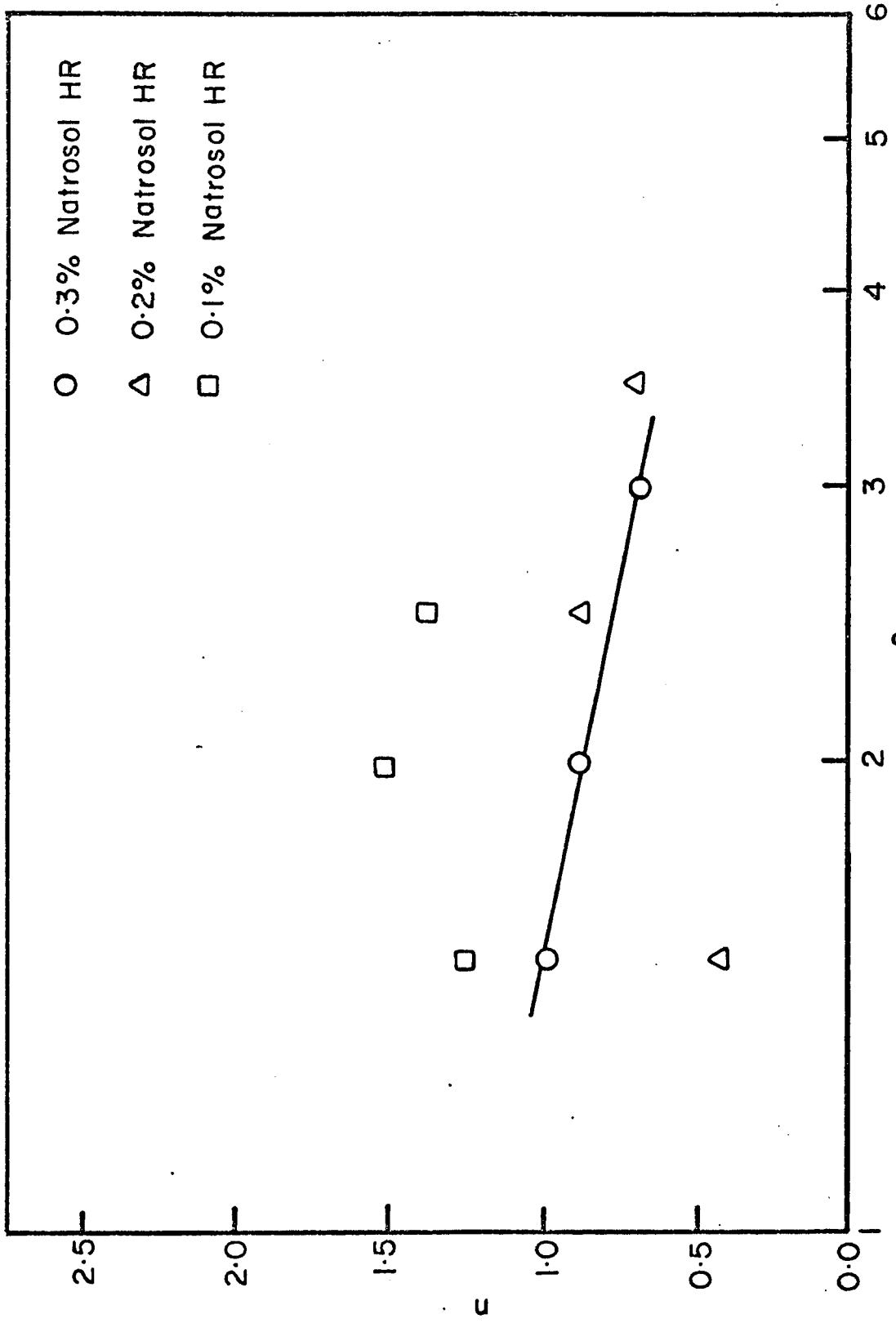

Fig. 41 n versus p correlation obtained for Natrosol HR solutions at various concentrations.

filtration was conducted. No reasonable correlation could be proposed because of the indefinite variation of n with pressure drop.

These failures may be attributable to the viscoelastic behaviour of Natrosol HR solutions which does not allow the flow model used in the derivation of the theory to characterize the fluid. Before drawing any definite conclusions, the results of filtration runs at constant rate with Natrosol HR solutions are considered in the next section.

(iv) Filtration of Natrosol 250 HR Solutions at Constant Rate

The results reported here are from the data collected during the conduction of constant rate filtration runs with slurries of calcium carbonate in Natrosol HR solutions of different concentrations (0.1, 0.2 and 0.3 per cent by weight). The data were processed basically in the same way as done in the case of data collected with Natrosol G solutions. The effective volume of filtrate v_o was evaluated as the v-intercept of the straight line obtained in v versus θ plot, for each individual run. Values of v_o for different flow rates and solution concentrations are tabulated in Table XII. After treating the data to account for the discrepancies in the initial stage of filtration (applying the necessary time correction to each run), Equation (116) was fitted to the experimental data for various values of pressure drop across the filter medium p_1, to yield the minimum variance by the method of least squares. Figures 42 to 50 exhibit the variation of the computed variance with respect to the values of pressure drop across the medium p_1. Once the value of p_1 in each case was determined, the data were plotted as the effective time of filtration $(\theta + \theta_c)$ versus the pressure drop across the cake $(p - p_1)$. These are given in Figures 51 to 53 for various solution concentrations. The lines in the figures illustrate the validity of the experimental data and the success with which a linear relationship could be achieved for the variables plotted. An attempt was made to determine the values of the specific cake resistance and flow behaviour index for these solutions utilizing the constant rate filtration data. The slopes, A, of the filtration runs conducted at different rates for the same concentration were plotted against log q_1 according to Equation (117) in Figure 54, to yield the values of r_o and m_o from the intercept and slope of this plot, respectively. On a log-log graph paper, the

TABLE XII

Values of p_1, v_o, A and B for Various Constant Rate Filtration Runs With Natrosol HR Solutions

Natrosol Concentration Wt. %	$q_1 \times 10^4$ ft./sec.	p_1 psi	$v_o \times 10^2$ $ft.^3/ft.^2$	A	B
0.1%	8.4612	17.5	-2.034	0.5906	2.57
	9.9309	15.8	-5.476	0.5455	2.482
	12.786	27.7	-49.46	0.4460	4.01
	13.926	31.7	-16.200	0.4473	6.33
0.2%	3.9150	20.8	+2.738	0.5299	6.32
	5.1060	18.8	+2.344	0.5828	2.378
	7.0235	21.6	4.460	0.4989	3.280
	8.5684	31.7	-0.705	0.4914	2.255
0.3%	2.2433	24.2	3.910	0.5572	6.56
	2.7029	30.0	3.360	0.4982	8.86
	3.5314	27.3	0.313	0.4908	6.54
	3.9690	39.2	-1.107	0.4435	8.05
	5.6877	34.0	-7.048	0.3255	15.31

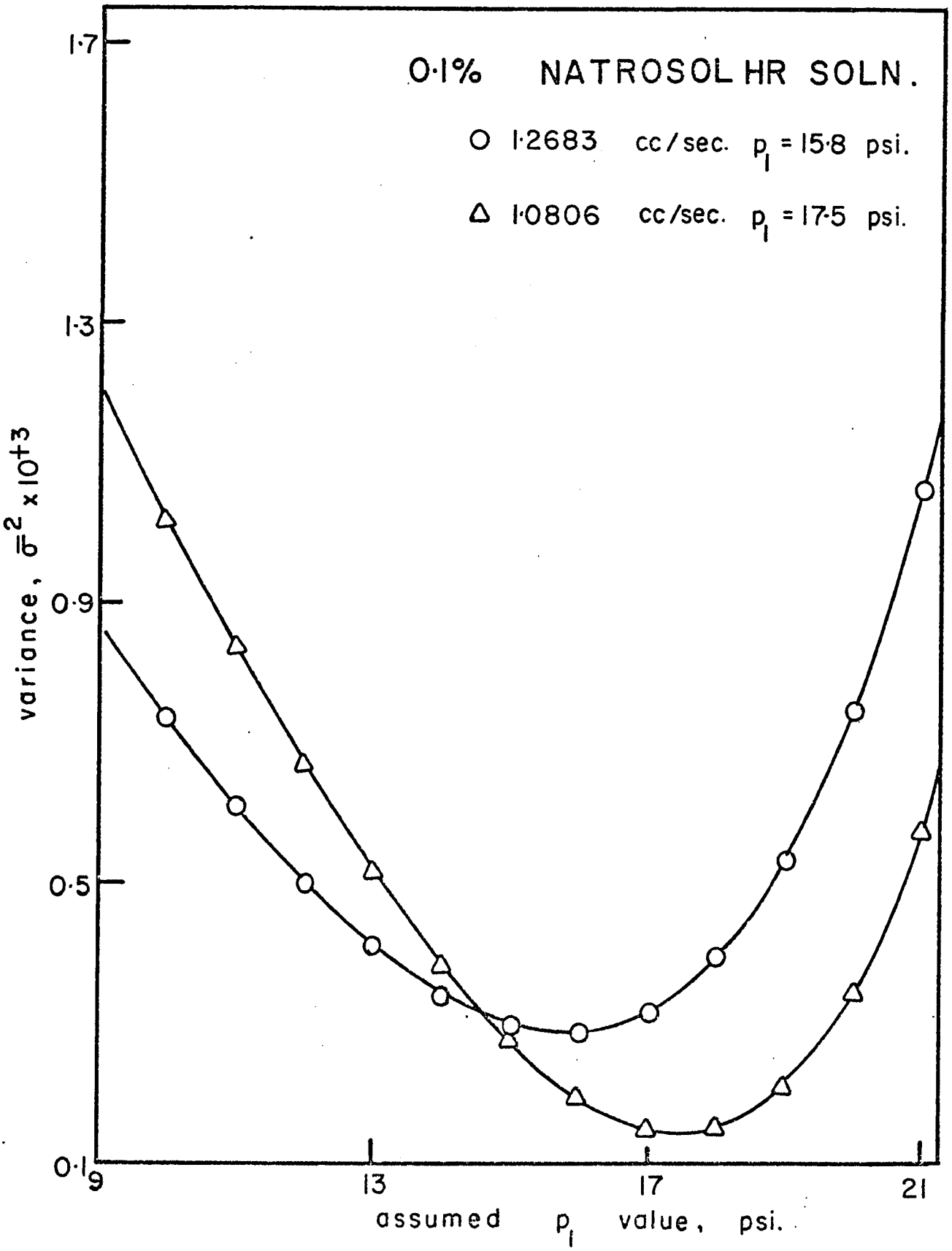

Fig. 42 Variation of variance with assumed p_1 values for slurries containing 0.1% Natrosol HR solutions.

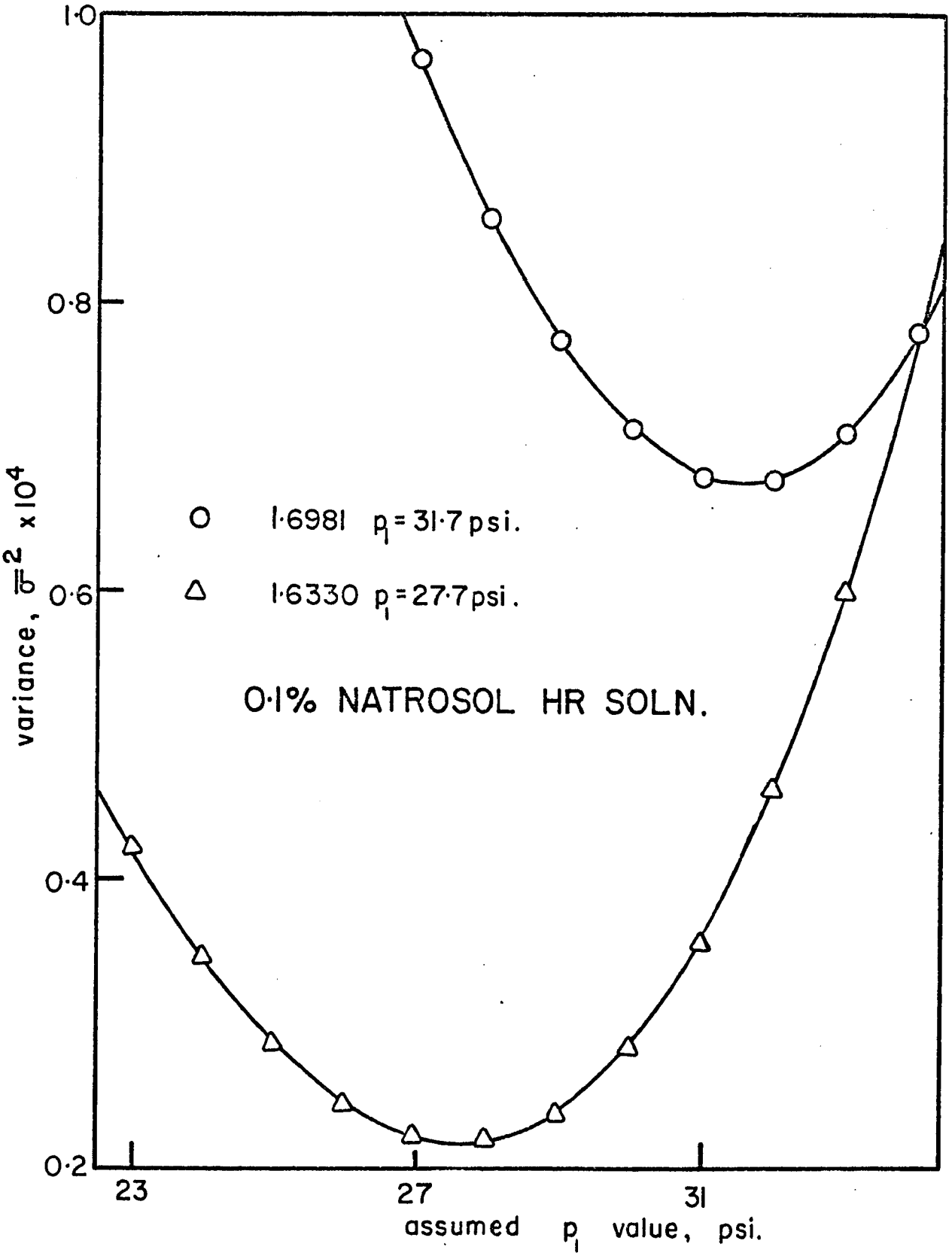

Fig. 43 Variation of variance with assumed p_1 values for slurries containing 0.1% Natrosol HR solutions.

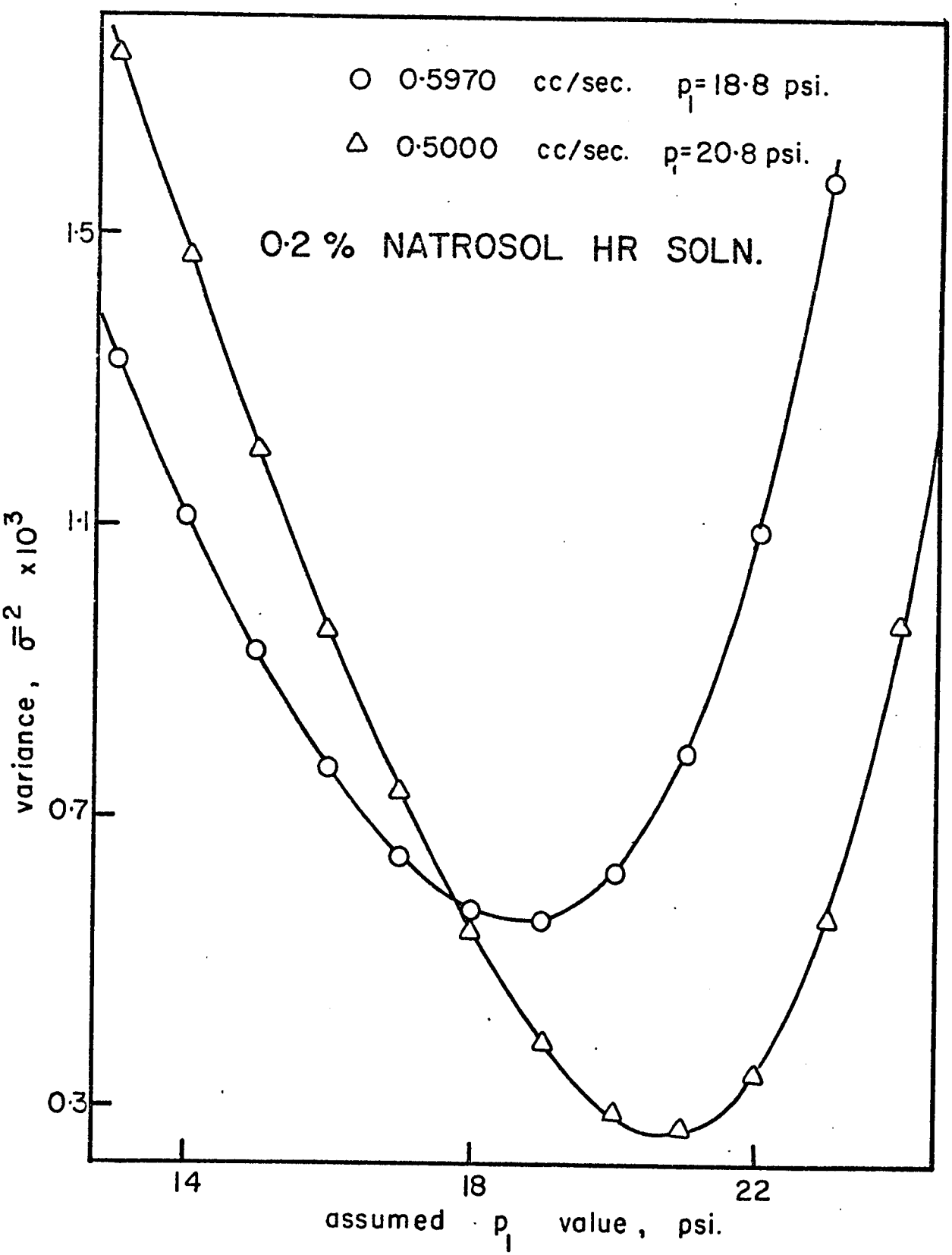

Fig. 44 Variation of variance with assumed p_1 values for slurries containing 0.2% Natrosol HR solutions.

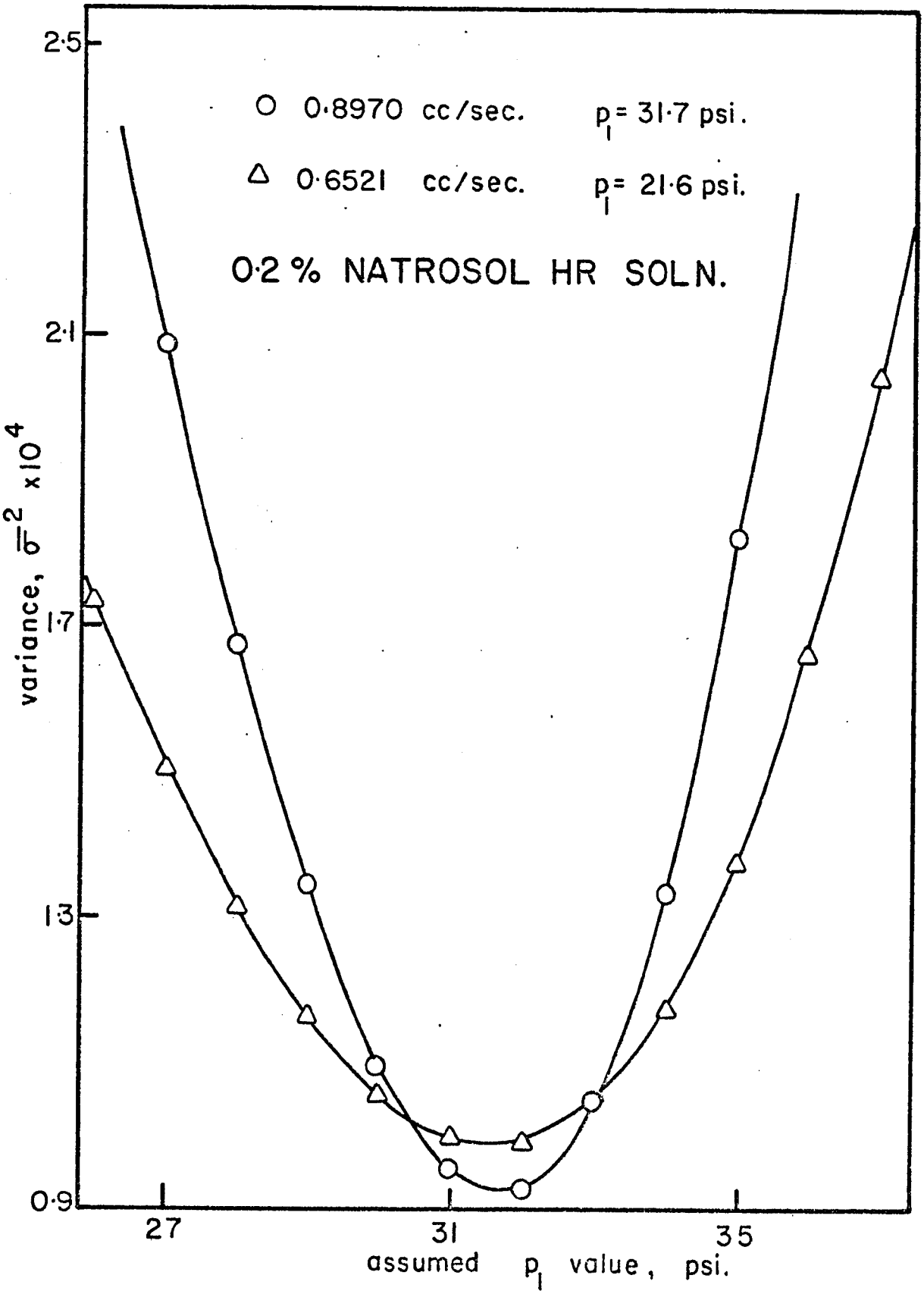

Fig. 45 Variation of variance with assumed p_1 values for slurries containing 0.2% Natrosol HR solutions.

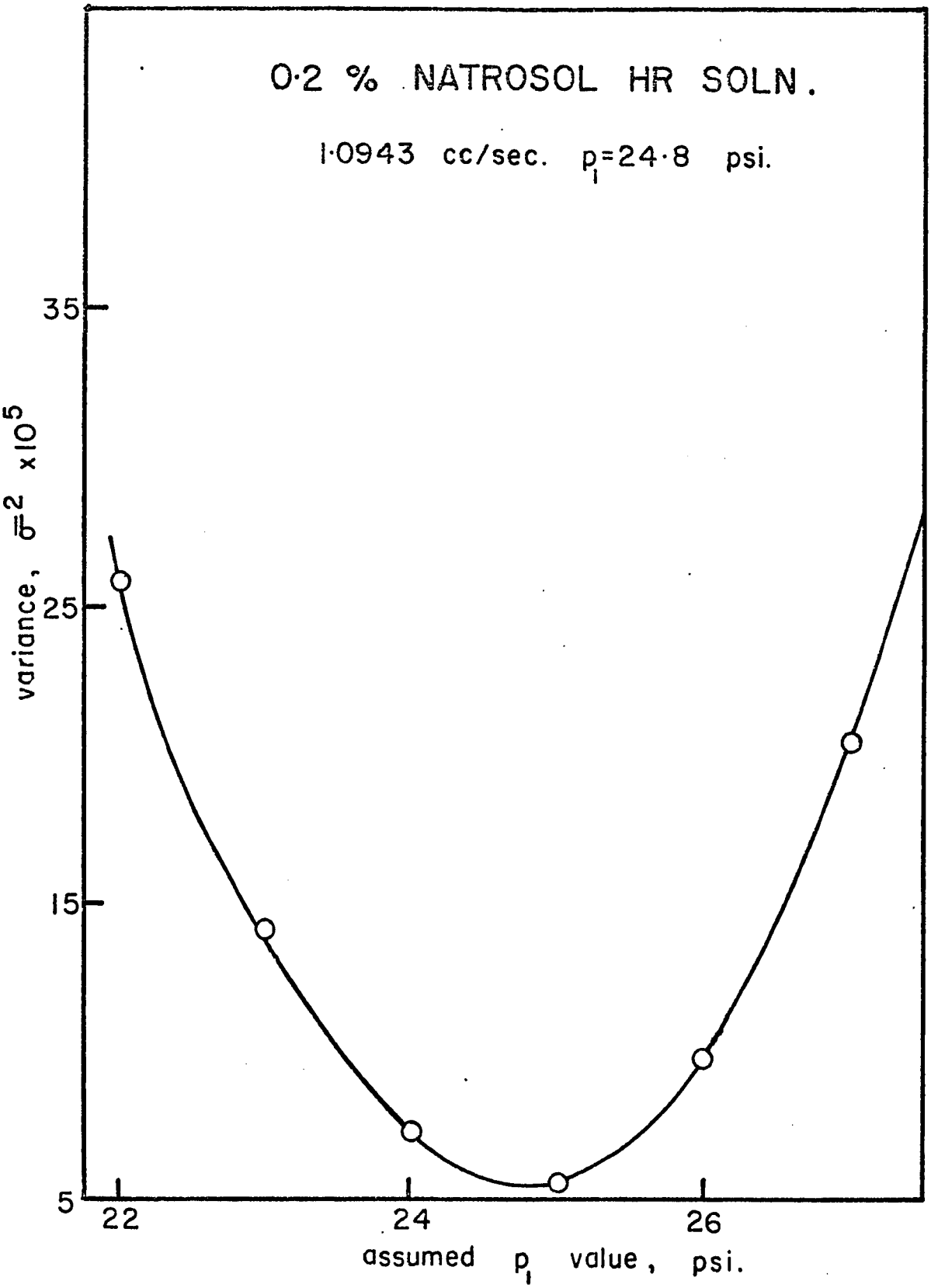

Fig. 46 Variation of variance with assumed p_1 values for slurries containing 0.2% Natrosol HR solutions.

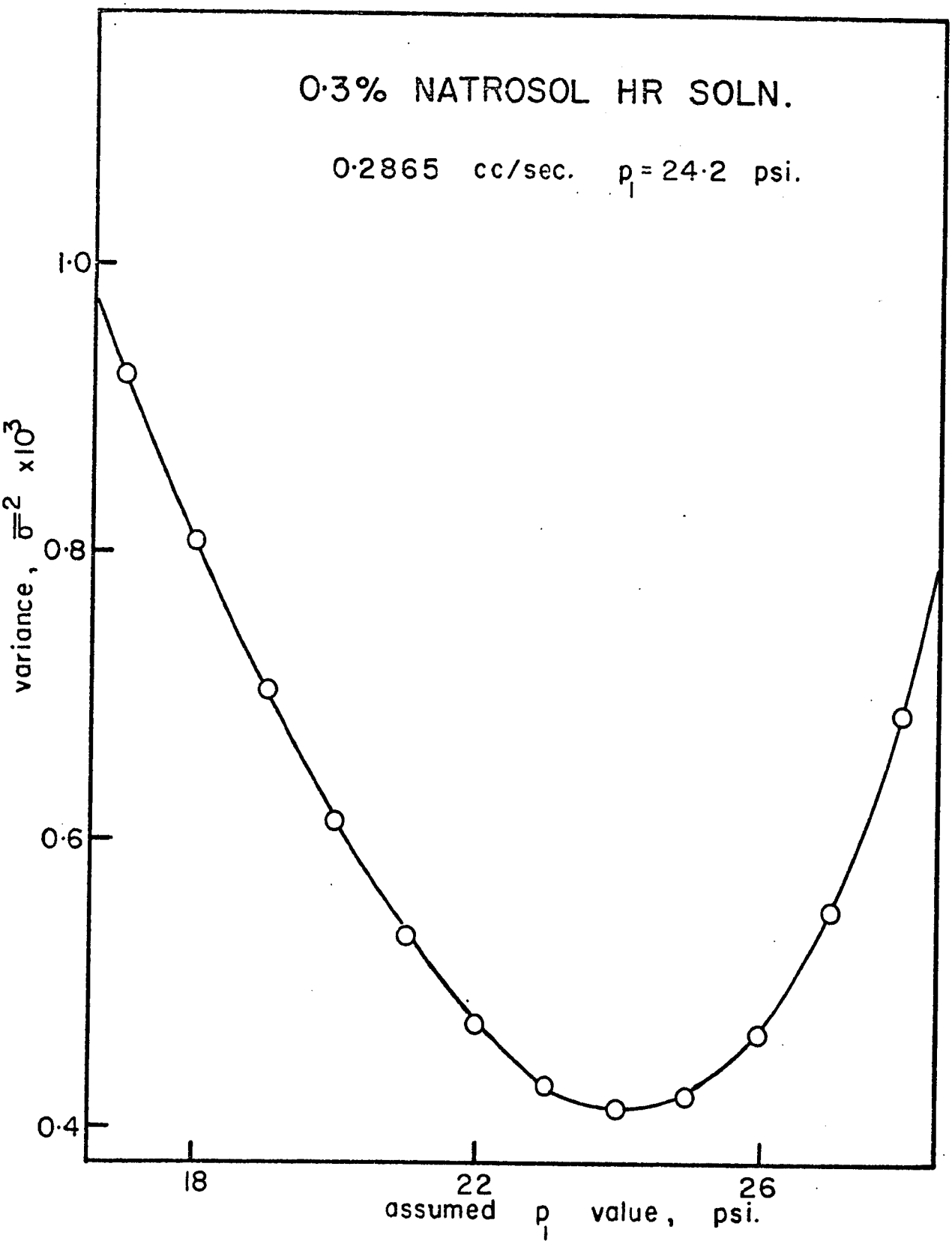

Fig. 47 Variation of variance with assumed p_1 values for slurries containing 0.3% Natrosol HR solutions.

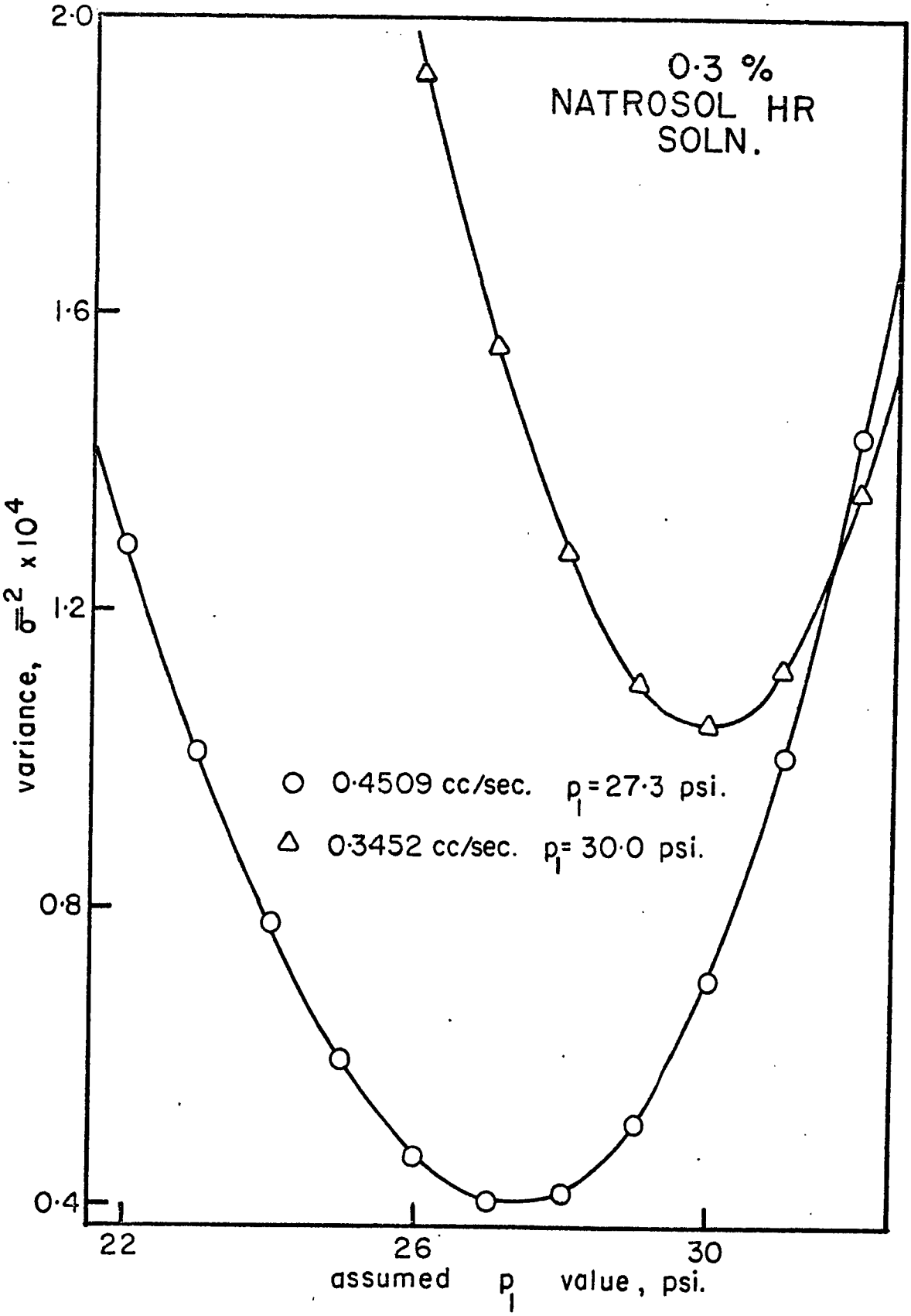

Fig. 48 Variation of variance with assumed p_1 values for slurries containing 0.3% Natrosol HR solutions.

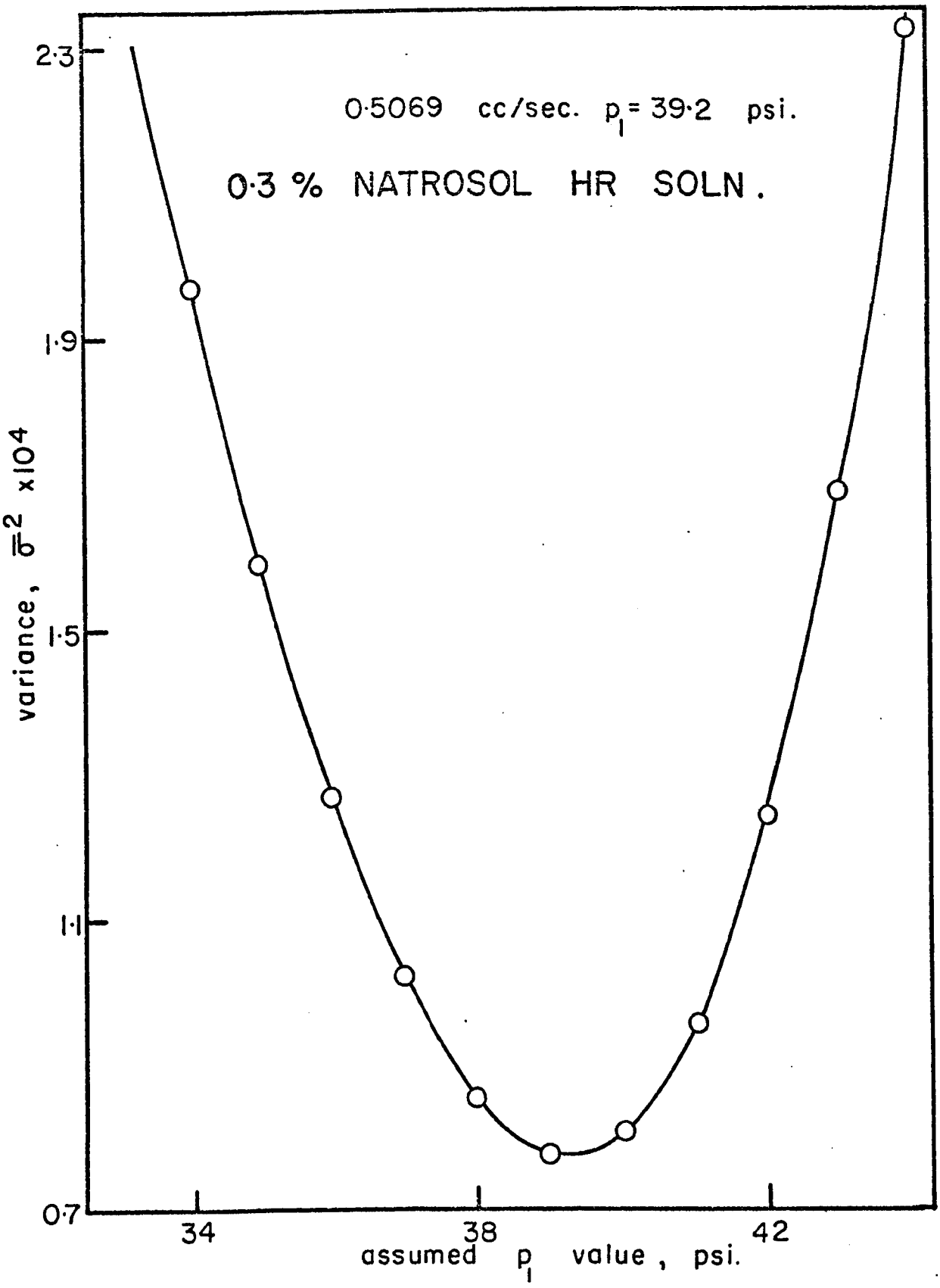

Fig. 49 Variation of variance with assumed p_1 values for slurries containing 0. 3% Natrosol HR solutions.

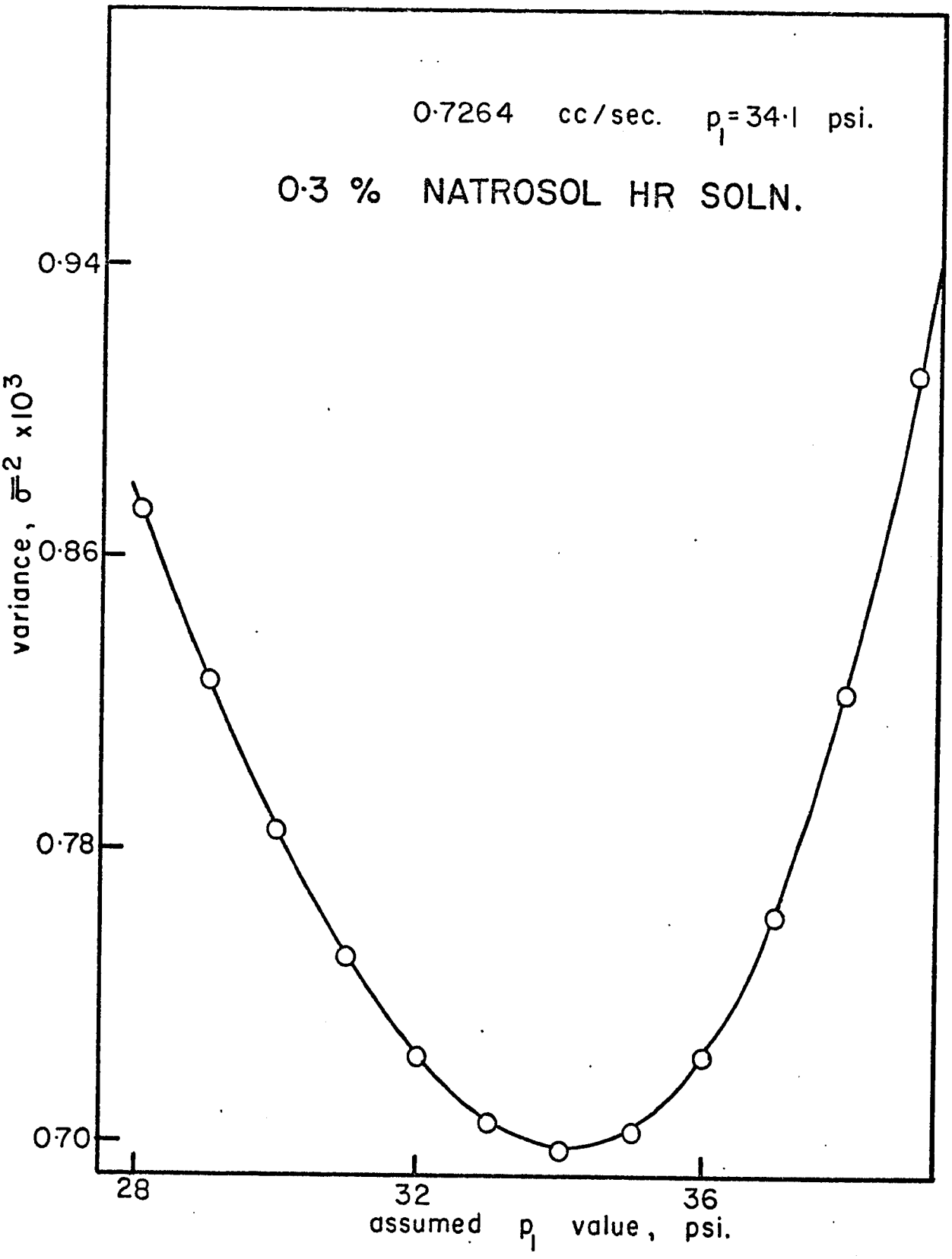

Fig. 50 Variation of variance with assumed p_1 values for slurries containing 0.3% Natrosol HR solutions.

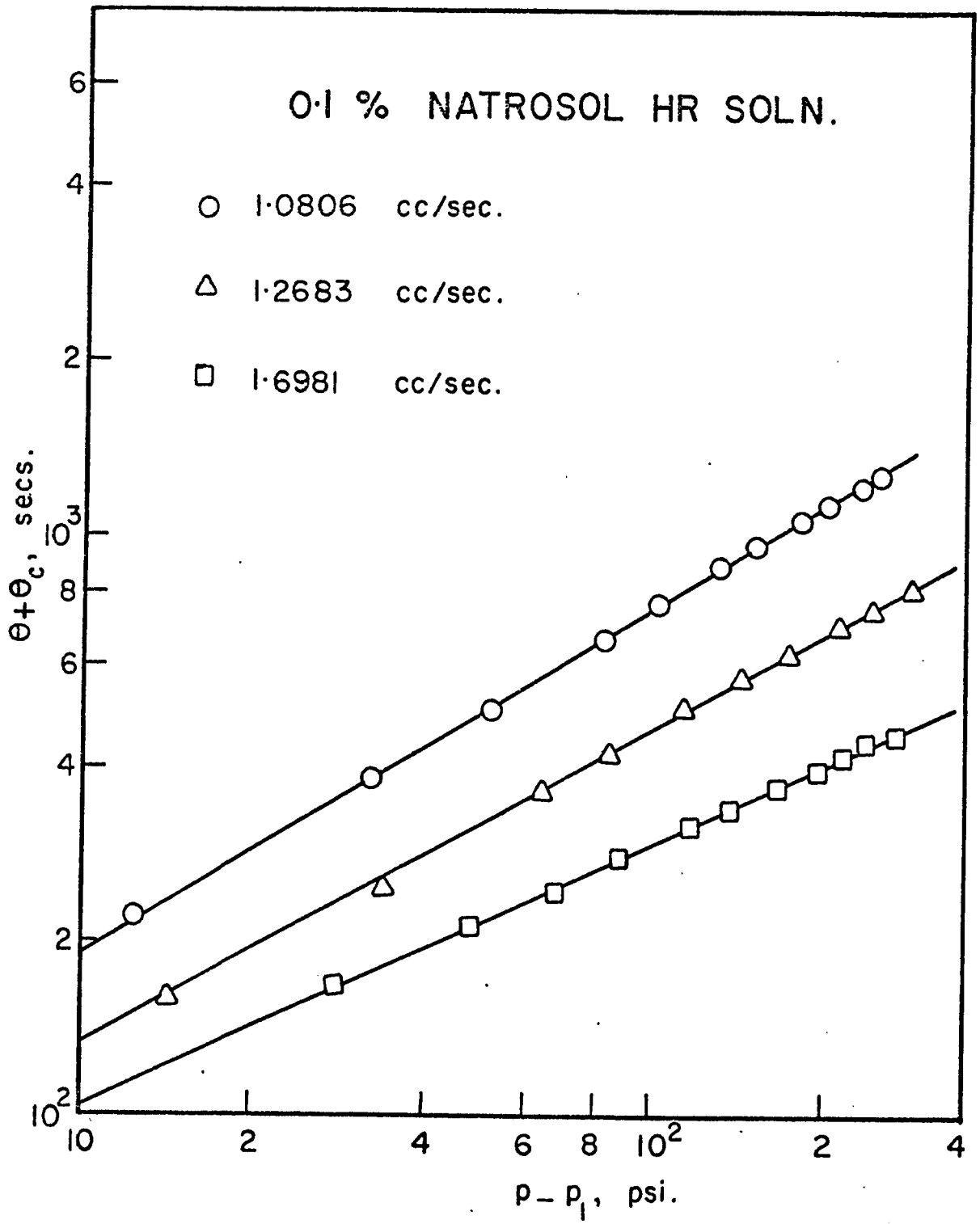

Fig. 51 Plot of $(\theta + \theta_c)$ versus $(p-p_1)$ for 0.1% Natrosol HR solutions at various constant rates of filtrate.

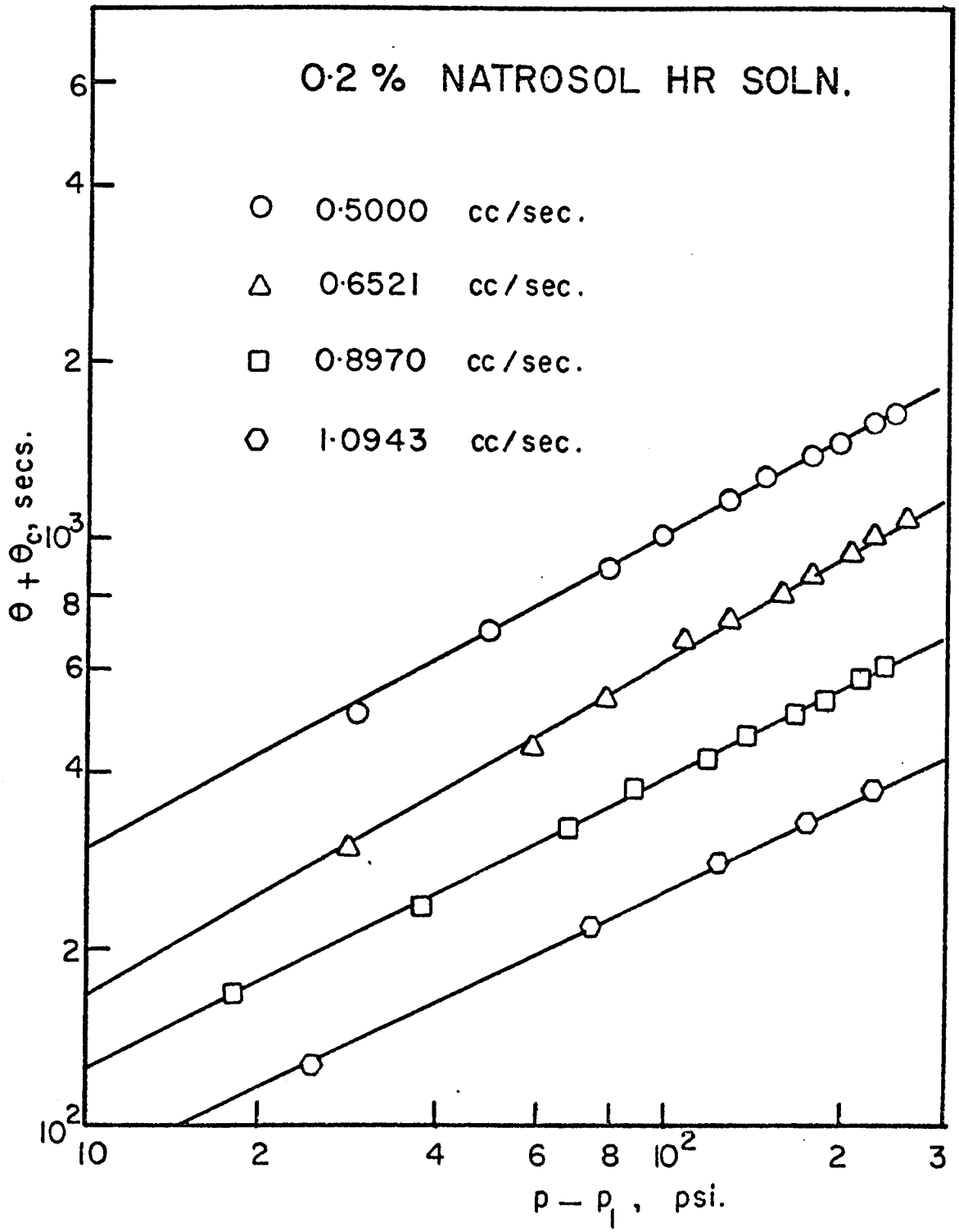

Fig. 52 Plot of $(\theta + \theta_c)$ versus $(p - p_1)$ for 0.2% Natrosol HR solutions at various constant rates of filtrate.

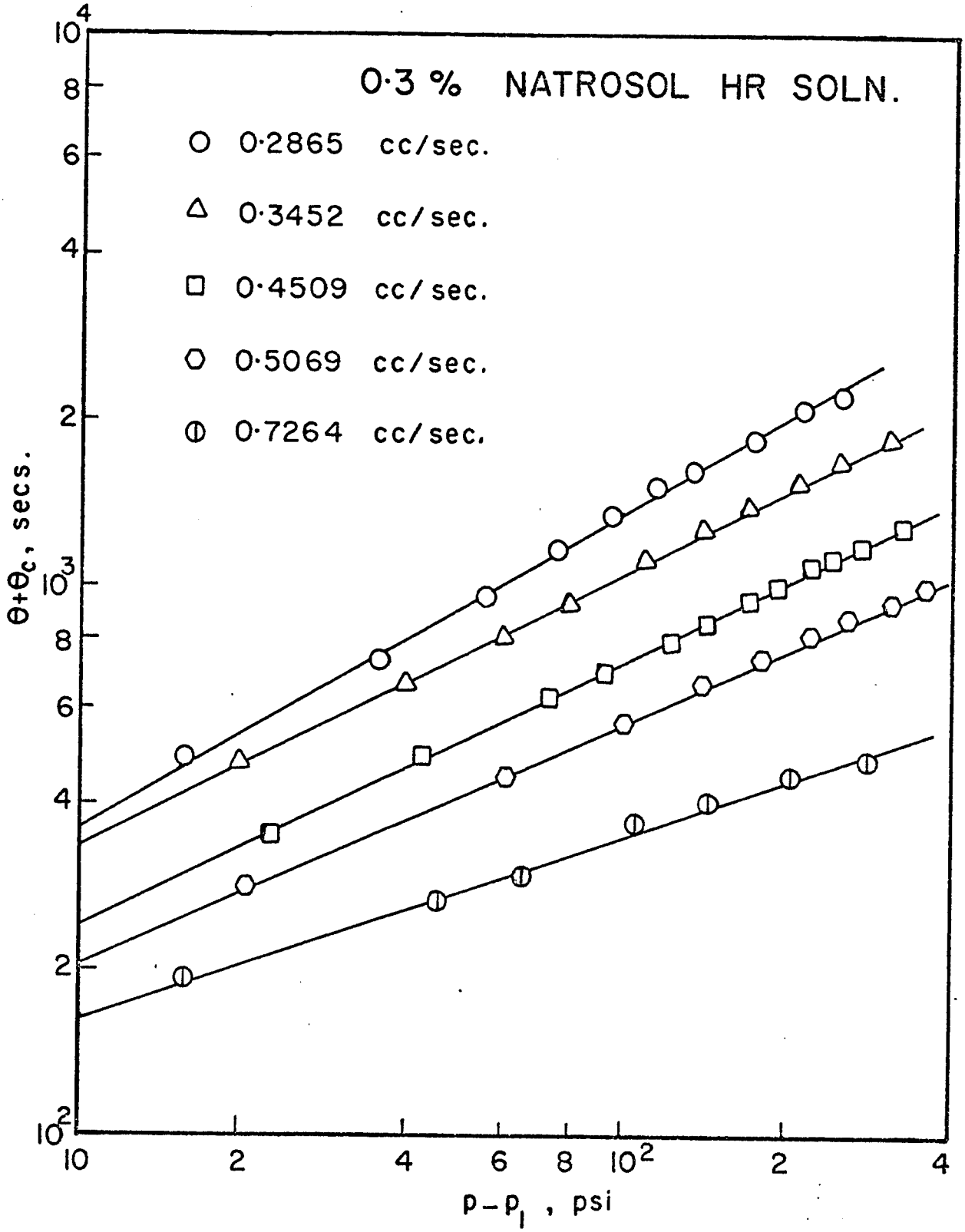

Fig. 53 Plot of $(\theta + \theta_c)$ versus $(p - p_1)$ for 0.3% Natrosol HR solutions at various constant rates of filtrate.

intercept of the lines obtained in the plot of $(\theta + \theta_c)$ versus log q_1, was plotted against q_1 according to Equation (118). Further, Equations (113) and (114) were to be used to determine the values of the specific cake resistance and the flow behaviour index n. The attempted correlation could not be obtained because of the widely scattered points in Figures 54 and 55 suggesting no definite trend to be established. This might again be attributable to the predominant viscoelastic behaviour of these Natrosol HR solutions. This confirms the failure of Ostwald de Waele model (pseudo plastic) to characterize the flow bheaviour of these Natrosol HR solutions in the shear stress region encountered in the filtration experiments.

Similar to the observations presented here, a peculiar behaviour of Natrosol HR solutions was reported by Sadowski[57] during the studies conducted on packed beds. This fluid was designated by him as possessing apparent power law behaviour. During his studies pertaining to the non-Newtonian flow through packed beds, Sadowski encountered the same difficulty of large deviation from the correlation. The data for Natrosol 250 H solutions agreed with the generalised Darcy law at the lowest value of $N_{Re, eff.}$ but the friction factor was consistently too high for $N_{Re, eff.} > 0.1$. It was further believed that the departure from the correlation was so as to suggest that it was a result of a failure in the theoretical development rather than a result of experimental error. This was attributed to not decreasing of the effective coefficient of viscosity with an increasing rate of shear as rapidly as the flow model would predict. Sadowski further believed that if the coefficient of viscosity did indeed have a different dependence on shear rate for flow in packed beds, it was a consequence of the complex geometry of the bed. The possibility that the effect of the third invariant, III, was significant for this

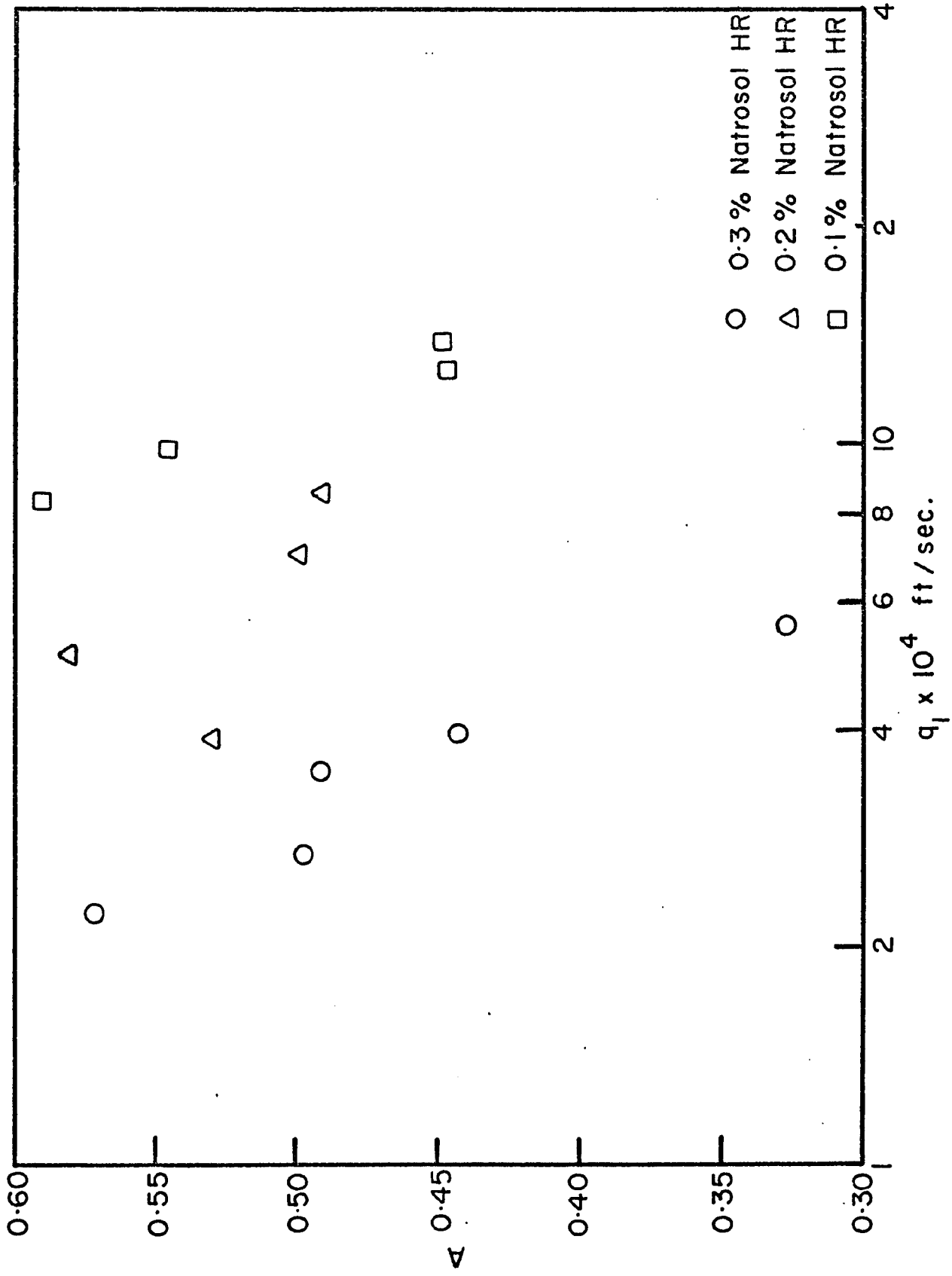

Fig. 54 Plot of coefficient A versus q_1 for Natrosol HR solutions of various concentrations.

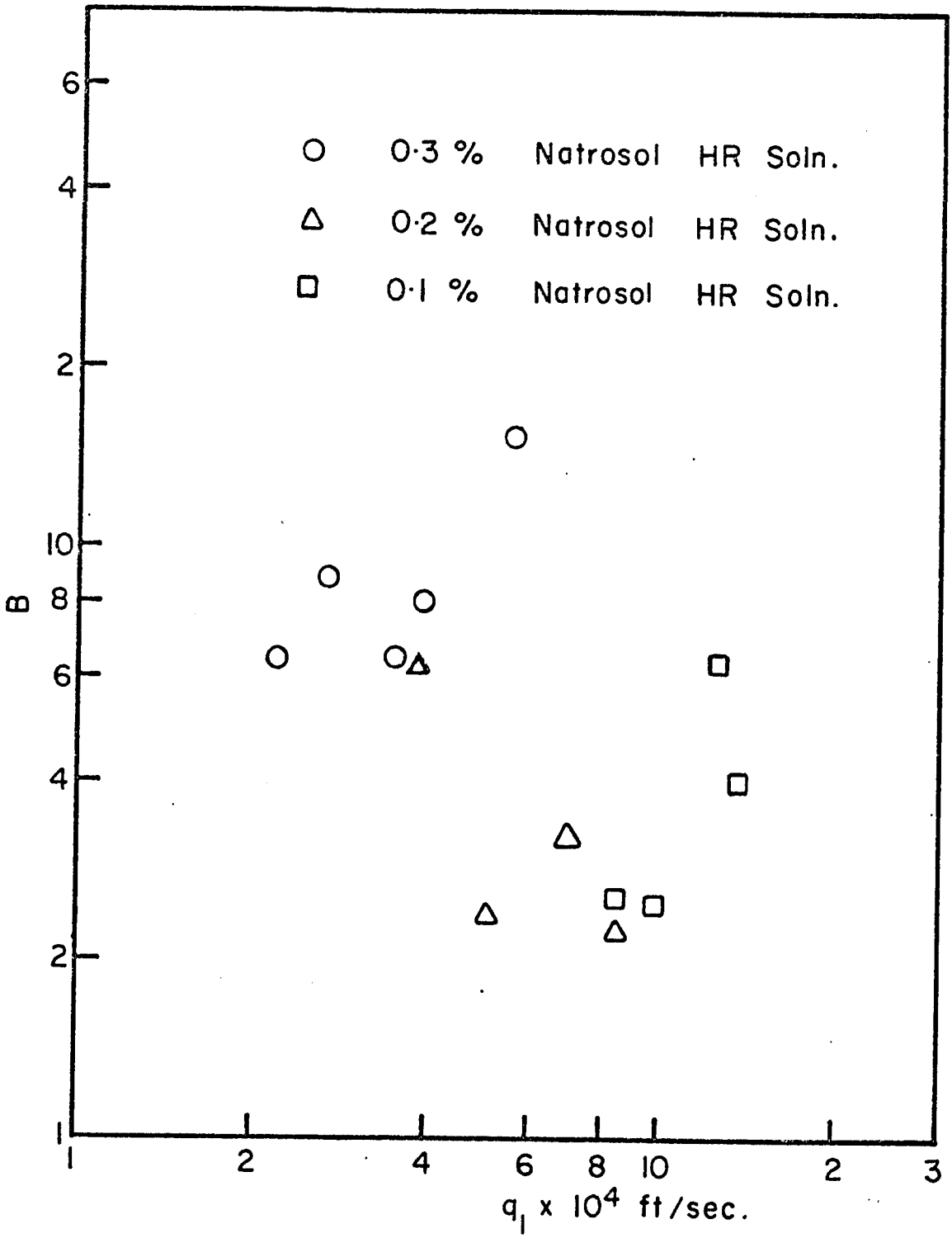

Fig. 55 Plot of coefficient B versus q_1 for Natrosol HR solutions of various concentrations.

geometry was doubtful. Slattery and Bird[67] had given sufficient reason to believe that the effect of third invariant would not account for the observed deviations. The geometry must affect the flow in some other manner.

The flow behaviour of Natrosol HR solution depends upon the cake internal geometry since it is this geometry which conditions the flow patterns of the fluids. A porous medium may be visualised as made up of innumerable flow constrictions and expansions with inter connecting curved pore channels. An eventual volume of fluid will alternately suffer accelerations and decelerations as it proceeds through the bed. This alternating, or oscillating, behaviour becomes more manifest as the average fluid velocity increases. It is this locally unsteady state phenomenon which, in all probability, leads to the observed deviations. For polymeric materials, a phenomenon which appears in those experiments in which the material is subjected to an oscillatory behaviour but not in those experiments of steady flow would suggest to the investigator[57] that viscoelastic behaviour may be present.

Dodge and Metzner[80] found that Carboxy Methyl Cellulose (CMC) behaves in an anomalous manner (with respect to their correlation) for turbulent flow conditions. They suggested tentatively, as did Metzner, Houghton, Sailor and White[81] for jet experiments, that this fluid was viscoelastic in behaviour. Meter and McEachern[82] have found that CMC and Natrosol solutions did exhibit normal pressures in a cone - and - plate apparatus. These experiments would indicate that an additional parameter, related to the viscoelastic properties of the fluids, may be necessary to correlate filtration data with Natrosol HR solutions. This suggests the necessity of an attempt to derive the filtration equations for these fluids with a different fluid model to

characterize the flow behaviour of Natrosol HR solutions. Recently Sutterby[83] proposed a new three parameter viscosity model to fit the data collected with Natrosol HR solutions in a better way than the previous models. The Sutterby model gives the viscosity as

$$\eta = \eta_o \left[\frac{arc\ Sin\ h\ (B\gamma)}{(B\gamma)}\right]^A$$

in which η_o, A and B are positive parameters. Parameter η_o has the units of viscosity; A is dimensionless; B is characteristic time.

Using these three parameter models, performing the integation to arrive at the final filtration equation is extremely difficult if not impossible. Hence, filtration theory has to be developed considerably to account for its viscoelastic behaviour, before the data collected with Natrosol HR solutions can be processed.

CHAPTER VI

SUMMARY AND CONCLUSIONS

Experimental results obtained from the data collected during the filtration of slurries of calcium carbonate in water and Natrosol 250 G and HR solutions at constant pressure and constant rate were presented and discussed. The importance and effect of transient behaviour in the initial stage of constant pressure and constant rate filtration was demonstrated and the necessary time correction was applied to the data collected in all the experiments. The theory of filtration developed in this laboratory, which took into account the variation of superficial velocity of the liquid through the cake and the velocity of the particles of the cake associated with cake compaction, was utilized to correlate the experimental data with considerable success.

Results obtained from the data collected during constant pressure filtration of Newtonian fluids indicated that the refinement of the analysis proposed in this laboratory, in which restrictions and conditions imposed in previous developments had been removed, provided an additional means of processing and interpretation of the data. The parabolic relationship developed for the main stage of constant pressure filtration successfully correlated the data obtained from the constant pressure runs which were subjected to drastically different initial stages of filtration. Cake and filter medium resistances α and R_m were determined with relative ease and accuracy from the coefficients of Equation (31) fitted to the data than by the conventional method involving the evaluation of the quantity $(\frac{d\theta}{dv})$. The effect of the initial stage of filtration on various filtration characteristics was

determined by the analysis of the experimental data. In this regard, it was observed that the initial period of the filtration also effected the values of specific cake resistance. Filter medium resistance decreased quite markedly with an increase in the time taken to adjust to the final pressure, characterized by increasing θ_o values. Cake resistance α was amenable to an empirical correlation in terms of a power function of pressure. Further, the moisture ratio of the cake, m, could also be expressed as a power function of pressure.

Utilizing the experimental data obtained during the constant rate filtration of Newtonian slurries, it was confirmed that a unique relationship existed between $(p - p_1)$ and $(\theta + \theta_c)$ as suggested by Equation (41). The importance and effect of transient behaviour in the initial stage of constant rate filtration was established. In spite of the difference in treatment, reasonable agreement was observed between the values of α obtained from the results of constant pressure and constant rate filtration of Newtonian slurries.

The characteristic value of the flow behaviour index of the polymer solution n and the filter medium resistance R_m could not be determined simultaneously from constant pressure filtration data alone. The evaluation of either one of these quantities was dependent upon a priori knowledge of the other quantity. The characteristic value of the flow behaviour index of the fluid inside the filter cake was amenable to a simple linear correlation in a semi logarithmic plot for Natrosol G solutions. This could be represented by the following equation

$$n = m_o \log p + n_1$$

The relationship developed for the main stage of constant pressure filtration of non-Newtonian (power law) fluids correlated the experimental data obtained using Natrosol 250 G solutions with considerable success. The effective time of filtration $(\theta - \theta_o)$ required to collect a given filtrate volume increased with decreasing pressure and increasing polymer solution concentration. The filter bed characteristics could be determined by evaluation of the coefficients of Equation (108) which yielded best fit of the experimental data consistent with physical reality. In line with the results obtained from the filtration of Newtonian fluids, a_T could be represented by a power function of pressure. Further, it could be inferred that the cake resistance a_T was dependent upon the slurry and polymer solution concentration. It was interesting to note that the viscous behaviour of the non-Newtonian fluid played a predominant role in the resistance to flow during the filtration operation. The quantity $K\, a_T$ could also be expressed as a power function of pressure with solution concentration as the parameter.

The proposed relationships successfully correlated the experimental data obtained during constant rate filtration of Natrosol G solutions. Utilizing the relationships presented, values of n and λ could be determined from the experimental data. The functional relationships between the characteristic quantities n and λ and the pressure drop resulting from the constant pressure filtration could be applied to constant rate filtration of Natrosol G solutions satisfactorily.

Attempts were made to correlate the data obtained from the filtration of Natrosol HR solutions at constant pressure and constant rate utilizing the relationships developed. Viscoelastic behaviour

of Natrosol HR solution appeared to be responsible for the failure to achieve the correlation. The results obtained indicated the correctness of the experimental data. Development of the filtration theory, using a different rheological model incorporating a characteristic time parameter to account for the viscoelastic behaviour, was felt necessary to enable the evaluation of cake and filter medium characteristics for the filtration of Natrosol HR solutions.

REFERENCES

1. Kozicki, W., Tiu, C., and Rao, A. R. K., Can. J. Chem. Eng., 46, 313 (1968).

2. Ruth, B. F., Ind. Eng. Chem., 27, 708 (1935).

3. Tiller, F. M., and Huang, C. J., Ind. Eng. Chem., 53, 529 (1961).

4. Tiller, F. M., and Shirato, M., A. I. Ch. E. J., 10, 61 (1964).

5. Shirato, M., Sambuichi, M., Kato, H., and Aragaki, T., Chem. Eng. (Japan), 31, 359 (1967), from Reference (53).

6. Shirato, M., Sambuichi, M., Kato, H., and Aragaki, T., A. I. Ch. E. J., 15, 405 (1969).

7. Almy, C., and Lewis, W. K., J. Ind. Eng. Chem., 4, 528 (1912).

8. Sperry, D. R., Chem. Met. Eng., 15, 198 (1916).

9. Sperry, D. R., Chem. Met. Eng., 17, 161 (1917).

10. Baker, F. P., J. Ind. Eng. Chem., 13, 610 (1921).

11. Sperry, D. R., J. Ind. Eng. Chem., 13, 1163 (1921).

12. Waterman, H. I., and Gilse, J. P. M. Van, Rec. Trav. Chim., 43, 757 (1924).

13. Ruth, B. F., Montonna, R. E., and Montillon, G. H., Ind. Eng. Chem., 23, 850 (1931).

14. Ruth, B. F., Montonna, R. E., and Montillon, G. H., Ind. Eng. Chem., 25, 76 (1933).

15. Ruth, B. F., Montonna, R. E., and Montillon, G. H., Ind. Eng. Chem., 25, 153 (1933).

16. Ruth, B. F., Ind. Eng. Chem., 27, 806 (1935).

17. Carman, P. C., Trans. Inst. Chem. Engrs. (London), 16, 168 (1938).

18. Kozeny, J., and Sitzber, Akad., Wiss. Wien, Math. naturw. klasse, Abt., IIa, 136, 271 (1927), from Reference (17).

19. Carman, P. C., Trans. Inst. Chem. Engrs. (London), 15, 150 (1937).

20. Sullivan, R. R., and Hertel, K. L., J. Appl. Phys., 11, 725 (1940).

21. Sullivan, R. R., J. Appl. Phys., 12, 503 (1941).

22. Sullivan, R. R., J. Appl. Phys., 13, 725 (1942).

23. Coulson, J. M., Trans. Inst. Chem. Engrs. (London), 27, 237 (1949).

24. Carman, P. C., J. Soc. Chem. Ind., 57, 225 (1938).

25. Carman, P. C., J. Soc. Chem. Ind., 58, 1 (1939).

26. Fair, G. M., and Hatch, L. P., J. Am. Water Works Assoc., 25, 1551 (1933).

27. Hatch, L. P., J. Appl. Mech., 7, A109 (1940).

28. Lea, F. M., and Nurse, R. W., "Symposium on particle size analysis", Suppliment to Trans. Inst. Chem. Engrs. (London), 25 (1947).

29. Blaine, R. L., A. S. T. M. Bull., 108, 17 (1941).

30. Bloomfield, A. L., Trans. Inst. Chem. Engrs. (London), 3, 38 (1928).

31. Heertjes, P. M., Research, 3, 254 (1950).

32. Miller, S. A., Chem. Eng. Progr., 47, 497 (1951).

33. Ruth, B. F., Ind. Eng. Chem., 38, 564 (1946).

34. Grace, H. P., Chem. Eng. Progr., 49, 303 (1953).

35. Booth, F., Proc. Roy. Soc. (London), 203A, 533 (1950).

36. Elton, G. A. H., Proc. Roy. Soc. (London), A194, 259, 275 (1948); A197, 568 (1949).

37. Dobry, A., J. Chim. Phys., 47, 402 (1950).

38. Grace, H. P., Chem. Eng. Progr., 49, 367 (1953).

39. Tiller, F. M., Chem. Eng. Progr., 49, 467 (1953).

40. Tiller, F. M., Chem. Eng. Progr., 51, 282 (1955).

41. Coimbra, A. L., M. S. Thesis, Vanderbilt University (1949).

42. Luke, C. D., "Constant pressure-Constant rate filtration", paper presented at the Cleveland meeting of the Am. Inst. Chem. Engrs., Cleveland (Dec. 1952).

43. Kottwitz, F. A., and Boylan, D. R., A. I. Ch. E. J., 4, 175 (1958).

44. Tiller, F. M., A. I. Ch. E. J., 4, 170 (1958).

45. Tiller, F. M., and Cooper, H. R., A. I. Ch. E. J., 6, 595 (1960).

46. Shirato, M., Sambuichi, M., and Okamura, S., A. I. Ch. E. J., 9, 599 (1963).

47. Tiller, F. M., and Cooper, H., A.I. Ch. E. J., 8, 445 (1962).

48. Shirato, M., and Sambuichi, M., Kagaku Kogaku (Abridged edition) (Chem. Eng. Japan), 2, 6 (1964).

49. Shirato, M., Sambuichi, M., and Murase, T., Memoirs of Faculty of Engineering, Nagoya University, 16, 68 (1964).

50. Brenner, H., A. I. Ch. E. J., 7, 667 (1961).

51. Shirato, M., Murase, T., Hirate, H., and Miura, M., Kagaku Kogaku (Abridged edition) (Chem. Eng. Japan) 4, 194 (1966).

52. Shirato, M., and Kobayashi, K., Memoirs of the Faculty of Engineering, Nagoya University, 19, (1967).

53. Shirato, M., Murase, T., and Kobayashi, K., "Filtration and Separation", (1968).

54. Shirato, M., and Kobayashi, K., Symposium on Filtration Part II, 64th National meeting, New Orleans, Louisiana, March 16-20, 1969.

55. Kozicki, W., Hsu, C.J., and Tiu, C., Chem. Eng. Sci., 22, 487 (1967).

56. Tiu, C., M.A.Sc. Thesis, University of Ottawa (1965).

57. Sadowski, T.J., Ph. D. Thesis, University of Wisconsin (1963).

58. Christopher, R.H., and Middleman, S., Ind. Eng. Chem. (Fund.), 4, 422 (1965).

59. McKinley, R.M., Jolins, H.O., Harris, W.W., and Greenkorn, R.A., A.I.Ch.E.J., 12, 17 (1966).

60. Savins, J.G., "Non-Newtonian Flow through Porous Media", ACS/IEC State of the art Symposium, Carnegie Institution, Washington, D.C., June 9-11, 1969.

61. McCabe and Smith, "Unit operations of Chemical Engineering", McGraw-Hill Inc., New York (1967).

62. Reiner, M., "Deformation, Strain and Flow", Interscience, New York, (1960).

63. Bird, R.B., Steward, W.E., and Lightfoot, E.N., "Transport Phenomena", J. Wiley, New York (1960).

64. Prager, W., Phys. of Fluids, 4, 1477 (1961).

65. Eringen, A.C., "Nonlinear theory of continuous media", McGraw-Hill, New York (1962).

66. Leigh, D.C., Phys. of Fluids, 5, 501 (1962).

67. Slattery, J.C., and Bird, R.B., Chem. Eng. Sci., 16, 231 (1961).

68. Gee, R.E., and Lyon, J.B., Ind. Eng. Chem., 49, 956 (1957).

69. Oldroyd, J.G., Proc. Roy. Soc. (London), A218, 122 (1953).

70. Frohlich, H., and Sack, R., Proc. Roy. Soc., (London), A185, 415 (1946).

71. Skelland, A. H., "Non-Newtonian Flow and Heat Transfer", J. Wiley, New York (1967).

72. Wilkinson, W. L., "Non-Newtonian Fluids", Pergamon Press, New York (1960).

73. Oldroyd, J. G., J. Colloid Sci., 4, 333 (1949).

74. Kozicki, W., Pasari, S. N., Rao, A. R. K., and Tiu, C., Chem. Eng. Sci., 25, 41 (1970).

75. Kozicki, W., Hsu, C. J., and Tiu, C., Chem. Eng. Sci., 22, 487 (1967).

76. Metzner, A. B., and Reed, J. C., A. I. Ch. E. J., 1, 439 (1955).

77. Longwell, P. A., "Mechanics of fluid flow", McGraw-Hill, New York (1966).

78. Goring, D. A., and Sitaramaiah, G., Polymer, 4, 7 (1963).

79. Pasari, S. N., M. A. Sc. Thesis, University of Ottawa (1969).

80. Dodge, D. W., and Metzner, A. B., A. I. Ch. E. J., 5, 189 (1959).

81. Metzner, A. B., Houghton, W. T., Sailor, R. A., and White, J. L., Trans. Soc. Rheol., 5, 133 (1961).

82. Meter, D. M., Ph. D. Thesis, University of Wisconsin (1963).

83. Sutterby, J. L., A. I. Ch. E. J., 12, 63 (1966).

84. Kozikci, W., Rao, A. R. K., and Tiu, C., Can. J. Chem. Eng., in press.

85. Kozicki, W., Rao, A. R. K., and Tiu, C., Ind. Eng. Chem., in press.

86. Kozicki, W., Rao, A. R. K., and Tiu, C., Chem. Eng. Sci., Submitted for publication.

87. Scheidegger, A. E., "The physics of flow through porous media", McMillan Co., New York (1957).

88. Kozeny, J. S., - Bev. Weiner Akad. Abt. IIa, 136, 271 (1927a).

89. Brooks, C. S., and Purcell, W. R., Trans. A. I. M. E., 195, 289 (1952).

90. Burdine, N. T., Gournay, L. S., and Reicherty, P. P., Trans. A. I. M. E., 189, 195 (1950).

91. Collins, R. E., "Flow of fluids through porous materials", Reinhold Publishing Corporation, N. Y., (1961).

92. Richardson, J. G., Kerver, J. K., Hafford, J. A., and Osoba, J. S., Trans. A. I. M. E., 195, 187 (1952).

93. Glasstone, S., "Textbook of physical chemistry", D. Van Nostrand Co., New York, (1946).

94. Perry, J. H., "Chemical Engineers' Handbook", McGraw Hill, New York, (1963).

95. McMillen, E. L., and Webber, H. A., Trans. A. I. Ch. E., 34, 213 (1938).

APPENDIX A

I. DENSITIES OF POLYMER SOLUTIONS USED

(i) Densities of Natrosol 250 G Solutions

Concentration Wt %	Density gm/cm^3
0.6	1.01159
0.8	1.01633
1.0	1.01695

(ii) Densities of Natrosol 250 HR Solutions

Concentration Wt %	Density gm/cm^3
0.1	1.01438
0.2	1.01494
0.3	1.01507

II. CAPILLARY TUBE SPECIFICATIONS

CAPILLARY	LENGTH, L in cm	CALI. DIAM., D in cm	L/D
A	22.96	0.0578	397.23
A_1	45.40	0.0578	785.47
B	22.90	0.0395	579.74
C	23.00	0.0285	807.01
C_1	17.95	0.0285	629.82
D	20.37	0.0250	814.80
D_1	22.28	0.0250	891.20
E	20.66	0.0184	1,122.82

III. SAMPLE CALCULATIONS OF VISCOMETRIC DATA

(i) The Calculation of Shear Strees Versus $\frac{8\langle U\rangle}{D}$ For The Flow of 1.0% Natrosol 250 G Solution

Density of the solution at 25° C = 1.0169 gm/c. c.

The diameter of capillary tube = 0.0578 cm.

Pressure drop across the capillary tube = 40 psi

Flow rate of the solution = 0.5321 gm/sec.

$$\frac{8\langle U\rangle}{D} = \frac{32W}{\pi \rho D^3}$$

$$= \frac{32 \times 0.5321}{3.1428 \times 1.0169 \times (0.0578)^3} \text{ sec}^{-1}$$

$$= 2.7590 \times 10^4 \text{ sec}^{-1}$$

Shear stress = $\tau_w = r_h \left(-\frac{dp'}{dx}\right)$

and $\left(-\frac{dp'}{dx}\right) = \frac{\Delta P}{L} + \frac{(L+L')}{L} \rho \frac{g}{g_c} - 1.12 \rho \frac{\langle U\rangle^2}{g_c L}$

where L = Length of the tube and

L'= Height of liquid surface over the upper end of capillary.

$$\left(-\frac{dp'}{dx}\right) = \frac{40.0 \times 70.3324}{22.96} + \frac{5.5 + 22.96}{22.96} - \frac{1.12 \times 1.0169 \times 3.9542 \times 10^4}{22.96 \times 980}$$

$$= (122.5303 + 1.2395 - 2.0012) \text{ gmf/cm}^3$$

$$= 121.7686 \text{ gmf/cm}^3$$

$$\tau_w = r_H \left(-\frac{dp'}{dx}\right) = 0.0145 \times 121.7675 \text{ gmf/cm}^2$$

$$= 1.7656 \text{ gmf/cm}^2$$

(ii) Calculation of The Effective Slip Velocity At A Shear Stress of 1.7656 gmf/cm^2

The diameter of the capillary tube = 0.0578 cm

The critical shear stress for 1.0% Natrosol 250 G (Fig. 7 of Ref. 79) = 8.0 gmf/cm^2

From the Equation (B-6) in Chapter III of Ref. (79)

$$U_w = \frac{a'}{D} (\tau_w - \tau_c)$$

where a' is the modified slip coefficient and τ_c is the critical shear stress.

Value of a' is obtained from the plot of modified slip coefficient a' versus shear stress τ_w (Fig. 10 of Ref. 79).

$$a' = 0.2799 \text{ cm}^4/\text{gmf. sec.}$$

Therefore, $U_w = \frac{0.2799}{0.0578} (1.7656 - 8.0)$ cm/sec.

$$U_w = -30.1903 \text{ cm/sec.}$$

(iii) Fluid Parameters of Natrosol 250 G Solutions

Concentration Wt %	Shear Stress Range gmf/cm^2	n'	Max. K' gmf sec$^{n'}$/cm^2
0.6	0.461 - 4.641	0.739 - 0.921	4.50×10^{-4}
0.8	0.463 - 5.322	0.736 - 0.893	6.13×10^{-4}
1.0	0.464 - 6.783	0.751 - 0 959	7.11×10^{-4}

APPENDIX B

CONSTANT PRESSURE FILTRATION OF AQUEOUS SLURRIES

Slurry: 2.5% $CaCO_3$ in Water LONG INITIAL PERIOD

ΔP= 50 psi Temperature: 25° C

S. No.	Volume of Filtrate in c. c.	Time in M. S.	V Ft^3/Ft^2	θ in secs.
1	914	1-42	0.7210	102
2	1114	2-10	0.8788	130
3	1414	3-03	1.1155	183
4	1814	4-30	1.4310	270
5	2114	5-46	1.6677	346
6	2514	7-46	1.9832	466
7	2914	10-05	2.2988	605
8	3314	12-40	2.6144	760
9	3714	15-36	2.9299	936
10	4114	18-51	3.2455	1131
11	4414	21-30	3.4822	1290
12	4714	24-20	3.7188	1460
13	5014	27-29	3.9555	1649
14	5314	30-41	4.1922	1841
15	5614	34-15	4.4288	2055

CONSTANT PRESSURE FILTRATION OF AQUEOUS SLURRIES

Slurry: 2.5% $CaCO_3$ in Water

INTERMEDIATE INITIAL PERIOD

ΔP= 50 psi Temperature: 25 °C

S. No.	Volume of Filtrate in c. c.	Time in M. S.	V Ft^3/Ft^2	θ in secs.
1	1014	1-28	0.7999	88
2	1414	2-39	1.1155	159
3	1814	4-10	1.4310	250
4	2114	5-27	1.6677	327
5	2414	6-54	1.9044	414
6	2714	8-32	2.1410	512
7	3014	10-24	2.3777	624
8	3614	14-31	2.8510	871
9	3914	16-53	3.0877	1013
10	4214	19-24	3.3244	1164
11	4514	22-11	3.5610	1331
12	4814	25-12	3.7977	1512
13	5114	28-23	4.0344	1703
14	5414	31-43	4.2711	1903
15	5714	35-21	4 5077	2121

CONSTANT PRESSURE FILTRATION OF AQUEOUS SLURRIES

Slurry: 2.5% $CaCO_3$ in Water SHORT INITIAL PERIOD

ΔP= 50 psi Temperature: 25 °C

S. No.	Volume of Filtrate in c. c.	Time in M. S.	V Ft^3/Ft^2	θ in secs.
1	614	0-36	0.4843	36
2	914	1-09	0.7210	69
3	1114	1-37	0.8788	97
4	1414	2-30	1.1155	150
5	1814	3-59	1.4310	239
6	2114	5-15	1.6677	315
7	2414	6-40	1.9044	400
8	2714	8-15	2.1410	495
9	3114	10-42	2.4566	642
10	3514	13-20	2.7721	800
11	3914	16-23	3.0877	983
12	4314	19-41	3.4033	1181
13	4714	23-24	3.7188	1404
14	5114	27-28	4.0344	1648
15	5514	31-46	4.3499	1906
16	5814	35-20	4.5866	2120

CONSTANT PRESSURE FILTRATION OF AQUEOUS SLURRIES

Slurry: 2.5% $CaCO_3$ in Water

LONG INITIAL PERIOD

ΔP= 150 psi Temperature: 25° C

S. No.	Volume of Filtrate in c. c.	Time in M. S.	V Ft^3/Ft^2	θ in secs.
1	1514	2-15	1.1943	135
2	1914	2-56	1.5099	176
3	2314	3-50	1.8255	230
4	2714	4-51	2.1410	291
5	3114	6-04	2.4566	364
6	3414	7-04	2.6933	424
7	3714	8-08	2.9299	488
8	4114	9-41	3.2455	581
9	4414	10-57	3.4822	657
10	4714	12-16	3.7188	736
11	5014	13-44	3.9555	824
12	5314	15-13	4.1922	913
13	5614	16-50	4.4288	1010
14	5914	18-32	4.6655	1112
15	6314	20-54	4.9811	1254

CONSTANT PRESSURE FILTRATION OF AQUEOUS SLURRIES

Slurry: 2.5% $CaCO_3$ in Water

INTERMEDIATE INITIAL PERIOD

ΔP= 150 psi Temperature: 25° C

S. No.	Volume of Filtrate in c. c.	Time in M. S.	V Ft^3/Ft^2	θ in secs.
1	1314	1-27	1.0366	87
2	1714	2-08	1.3521	128
3	2114	2-55	1.6677	175
4	2514	3-55	1.9832	235
5	2914	5-06	2.2988	306
6	3314	6-24	2.6144	384
7	3714	7-52	2.9299	472
8	4114	9-28	3.2455	568
9	4414	10-45	3.4822	645
10	4714	12-10	3.7188	730
11	5014	13-42	3.9555	822
12	5314	15-17	4.1922	917
13	5614	17-00	4.4288	1020
14	5914	18-48	4.6655	1128
15	6314	21-18	4.9811	1278

CONSTANT PRESSURE FILTRATION OF AQUEOUS SLURRIES

Slurry: 2.5% $CaCO_3$ in Water

SHORT INITIAL PERIOD

ΔP= 150 psi Temperature: 25° C

S. No.	Volume of Filtrate in c. c.	Time in M. S.	V Ft^3/Ft^2	θ in secs.
1	800+114	0-41	0.7210	41
2	1300+114	1-23	1.1155	83
3	1700+114	2-05	1.4310	125
4	2100+114	2-56	1.7466	176
5	2500+114	3-58	2.0621	238
6	2900+114	5-07	2.3777	307
7	3300+114	6-27	2.6933	387
8	3700+114	7-53	3.0088	473
9	4000+114	9-03	3.2455	543
10	4400+114	10-42	3.5610	642
11	4700+114	12-05	3.7977	725
12	5000+114	13-35	4.0344	815
13	5300+114	15-05	4.2711	905
14	5600+114	16-41	4.5077	1001
15	6000+114	18-45	4.8233	1125

CONSTANT PRESSURE FILTRATION OF AQUEOUS SLURRIES

Slurry: 2.5% $CaCO_3$ in Water

ΔP= 250 psi Temperature: 25° C LONG INITIAL PERIOD

S. No.	Volume of Filtrate in c. c.	Time in M. S.	V Ft^3/Ft^2	θ in secs.
1	1314	1-25	1.0366	85
2	1714	1-55	1.3522	115
3	2114	2-31	1.6678	151
4	2514	3-17	1.9833	197
5	2914	4-09	2.2989	249
6	3314	5-10	2.6145	310
7	3714	6-17	2.9301	377
8	4014	7-13	3.1667	433
9	4314	8-12	3.4034	492
10	4714	9-37	3.7190	577
11	5014	10-50	3.9557	650
12	5314	12-06	4.1923	725
13	5614	13-24	4.4290	804
14	5914	14-46	4.6657	886
15	6314	16-44	4.9812	1004

CONSTANT PRESSURE FILTRATION OF AQUEOUS SLURRIES

Slurry: 2.5% $CaCO_3$ in Water

SHORT INITIAL PERIOD

ΔP= 250 psi Temperature: 25° C

S. No.	Volume of Filtrate in c. c.	Time in M. S.	V Ft^3/Ft^2	θ in secs.
1	914	0-33	0.7211	33
2	1414	1-04	1.1155	64
3	1814	1-37	1.4311	97
4	2114	2-07	1.6678	127
5	2514	2-54	1.9833	177
6	2914	3-45	2.2989	225
7	3314	4-45	2.6145	285
8	3714	5-52	2.9301	352
9	4014	6-48	3.1667	408
10	4314	7-48	3.4034	468
11	4614	8-51	3.6401	531
12	4914	10-01	3.8768	601
13	5314	11-37	4.1923	697
14	5714	13-22	4.5079	802
15	6114	15-17	4.8235	917

CONSTANT PRESSURE FILTRATION OF NATROSOL G SOLUTIONS

Slurry: 2.5% $CaCO_3$ in 0.6% Natrosol 'G' Solution

ΔP=150 psi Temperature: 25° C

S. No.	Volume of Filtrate in c. c.	Time in M. S.	V Ft^3/Ft^2	θ in secs.
1	112	1-09	0.0876	69
2	212	1-53	0.1659	113
3	332	3-13	0.2599	193
4	412	4-29	0.3225	269
5	492	6-07	0.3852	367
6	572	7-58	0.4478	478
7	652	10-09	0.5105	609
8	732	12-30	0.5731	750
9	792	14-33	0.6201	873
10	852	16-42	0.6671	1002
11	912	19-05	0.7140	1145
12	972	21-34	0.7610	1294
13	1012	23-22	0.7923	1402
14	1052	25-10	0.8237	1510
15	1112	28-15	0.8706	1695

CONSTANT PRESSURE FILTRATION OF NATROSOL G SOLUTIONS

Slurry: 2.5% $CaCO_3$ in 0.6% Natrosol 'G' Solution

ΔP: 250 psi Temperature: 25° C

S. No.	Volume of Filtrate in c. c.	Time in M. S.	V Ft^3/Ft^2	θ in secs.
1	112	0-58	0.0876	58
2	312	2-05	0.2442	125
3	412	3-13	0.3225	193
4	512	4-50	0.4008	290
5	612	6-52	0.4791	412
6	692	8-48	0.5418	528
7	772	10-57	0.6044	657
8	852	13-27	0.6671	807
9	932	16-12	0.7297	972
10	1012	19-22	0.7923	1162
11	1072	21-53	0.8393	1313
12	1132	24-38	0.8863	1478
13	1192	27-32	0.9333	1652

CONSTANT PRESSURE FILTRATION OF NATROSOL G SOLUTIONS

Slurry: 2.5% $CaCO_3$ in 0.6% Natrosol 'G' Solution

ΔP= 350 psi Temperature: 25° C

S. No.	Volume of Filtrate in c. c.	Time in M. S.	V Ft^3/Ft^2	θ in secs.
1	112	1-01	0.0876	61
2	312	2-24	0.2442	144
3	412	3-31	0.3225	211
4	512	4-52	0.4008	292
5	592	6-03	0.4635	363
6	672	7-26	0.5261	446
7	732	8-40	0.5731	520
8	812	10-34	0.6357	634
9	872	12-12	0.6827	732
10	932	13-55	0.7297	835
11	992	15-54	0.7767	954
12	1052	17-56	0.8237	1076
13	1112	20-18	0.8706	1218

CONSTANT PRESSURE FILTRATION OF NATROSOL G SOLUTIONS

Slurry: 2.5% $CaCO_3$ in 0.8% Natrosol G Solution

ΔP= 150 psi Temperature: 25° C

S. No.	Volume of Filtrate in c. c.	Time in M. S.	V Ft^3/Ft^2	θ in secs.
1	252	3-32	0.1973	212
2	292	4-50	0.2286	290
3	332	6-15	0.2599	375
4	372	7-57	0.2912	477
5	412	10-00	0.3225	600
6	452	12-10	0.3539	730
7	492	14-48	0.3852	888
8	532	17-45	0.4165	1065
9	572	21-20	0.4478	1280
10	612	25-26	0.4791	1526
11	652	30-04	0.5105	1804
12	692	35-02	0.5418	2102
13	732	40-44	0.5731	2444

CONSTANT PRESSURE FILTRATION OF NATROSOL G SOLUTIONS

Slurry: 2.5% $CaCO_3$ in 0.8% Natrosol G Solution

ΔP= 250 psi Temperature: 25° C

S. No.	Volume of Filtrate in c. c.	Time in M. S.	V Ft^3/Ft^2	θ in secs.
1	312	3-17	0.2442	197
2	392	5-29	0.3069	329
3	452	7-34	0.3539	454
4	512	10-07	0.4008	607
5	572	13-08	0.4478	788
6	612	15-26	0.4791	926
7	652	18-03	0.5105	1083
8	692	20-51	0.5418	1251
9	732	23-57	0.5731	1437
10	772	27-23	0.6044	1643
11	812	31-05	0.6357	1865

CONSTANT PRESSURE FILTRATION OF NATROSOL G SOLUTIONS

Slurry: 2.5% $CaCO_3$ in 0.8% Natrosol G Solution

ΔP = 350 psi Temperature: 25° C

S. No.	Volume of Filtrate in c. c.	Time in M. S.	V Ft^3/Ft^2	θ in secs.
1	412	4-40	0.3225	280
2	492	7-01	0.3852	421
3	572	9-58	0.4478	598
4	652	13-31	0.5105	811
5	732	17-39	0.5731	1059
6	752	18-49	0.5888	1129
7	792	21-08	0.6201	1268
8	832	23-44	0.6514	1424
9	872	26-28	0.6827	1588
10	912	29-28	0.7140	1768
11	952	32-40	0.7454	1960

CONSTANT PRESSURE FILTRATION OF NATROSOL G SOLUTIONS

Slurry: 2.5% $CaCO_3$ in 1.0% Natrosol G Solution

ΔP: 150 psi Temperature: 25° C

S. No.	Volume of Filtrate in c. c.	Time in M. S.	$\frac{V}{Ft^3/Ft^2}$	θ in secs.
1	192	2-42	0.1503	162
2	272	5-20	0.2103	320
3	332	8-09	0.2600	489
4	392	12-00	0.3070	720
5	432	15-15	0.3380	915
6	472	19-03	0.3696	1143
7	512	23-20	0.4010	1400
8	552	27-52	0.4320	1672
9	592	32-50	0.4640	1970
10	632	38-29	0.4950	2309
11	672	44-30	0.5260	2670
12	712	50-53	0.5570	3053

CONSTANT PRESSURE FILTRATION OF NATROSOL G SOLUTIONS

Slurry: 2.5% $CaCO_3$ in 1.0% Natrosol G Solution

ΔP= 250 psi Temperature: 25° C

S. No.	Volume of Filtrate in c. c.	Time in M. S.	V Ft^3/Ft^2	θ in secs.
1	212	2-04	0.1660	124
2	312	3-57	0.2441	237
3	392	6-12	0.3068	372
4	472	9-22	0.3700	562
5	532	12-27	0.4162	747
6	592	16-09	0.4640	969
7	632	18-33	0.4950	1113
8	692	22-45	0.5418	1365
9	752	27-32	0.5890	1652
10	812	32-52	0.6355	1972

CONSTANT PRESSURE FILTRATION OF NATROSOL G SOLUTIONS

Slurry: 2.5% $CaCO_3$ in 1.0% Natrosol G Solution

ΔP= 350 psi Temperature: 25° C

S. No.	Volume of Filtrate in c. c.	Time in M. S.	V Ft^3/Ft^2	θ in secs.
1	112	1-01	0.0877	61
2	212	2-10	0.1660	130
3	312	3-58	0.2441	238
4	412	6-48	0.3220	408
5	492	9-57	0.3856	597
6	572	13-37	0.4480	817
7	632	16-52	0.4950	1012
8	692	20-26	0.5418	1226
9	752	24-57	0.5890	1497
10	792	28-07	0.6200	1687

CONSTANT PRESSURE FILTRATION OF NATROSOL G SOLUTIONS

Slurry: 4% $CaCO_3$ in 0.8% Natrosol G Solution

ΔP= 150 psi Temperature: 25° C

S. No.	Volume of Filtrate in c. c.	Time in M. S.	V Ft^3/Ft^2	θ in secs.
1	312	5-29	0.2442	329
2	372	7-48	0.2912	468
3	432	10-41	0.3382	641
4	492	14-15	0.3852	855
5	552	18-02	0.4322	1082
6	612	22-14	0.4791	1334
7	652	25-24	0.5105	1524
8	692	28-19	0.5418	1699
9	732	31-52	0.5731	1912
10	772	35-41	0.6044	2141
11	812	39-30	0.6357	2370
12	852	43-36	0.6671	2616
13	912	50-05	0.7140	3005

CONSTANT PRESSURE FILTRATION OF NATROSOL G SOLUTIONS

Slurry: 4.0% $CaCO_3$ in 0.8% Natrosol G Solution

ΔP= 250 psi Temperature: 25° C

S. No.	Volume of Filtrate in c. c.	Time in M. S.	V Ft^3/Ft^2	θ in secs.
1	332	4-28	0.2599	268
2	412	6-47	0.3225	407
3	512	10-36	0.4008	636
4	572	13-16	0.4478	796
5	632	16-22	0.4948	982
6	712	21-07	0.5574	1267
7	752	23-27	0.5888	1407
8	792	26-05	0.6201	1565
9	832	28-58	0.6514	1738
10	872	32-02	0.6827	1922
11	912	35-05	0.7140	2105
12	952	38-25	0.7456	2305
13	992	41-51	0.7767	2511

CONSTANT PRESSURE FILTRATION OF NATROSOL G SOLUTIONS

Slurry: 4.0% $CaCO_3$ in 0.8% Natrosol G Solution

ΔP = 350 psi Temperature: 25° C

S. No.	Volume of Filtrate in c. c.	Time in M. S.	V Ft^3/Ft^2	θ in secs.
1	312	3-26	0.2442	206
2	412	6-01	0.3225	361
3	492	8-27	0.3852	507
4	572	11-32	0.4478	692
5	632	14-18	0.4948	858
6	692	17-20	0.5418	1040
7	752	20-47	0.5888	1247
8	812	24-33	0.6357	1473
9	872	28-40	0.6827	1720
10	932	33-10	0.7297	1990
11	972	36-19	0.7610	2179

CONSTANT PRESSURE FILTRATION OF NATROSOL HR SOLUTIONS

Slurry: 2.5% $CaCO_3$ in 0.1% HR Solution

ΔP= 150 psi Temperature: 25° C

S. No.	Volume of Filtrate in c. c.	Time in M. S.	V Ft^3/Ft^2	θ in secs.
1	112	0-22	0.0877	22
2	212	0-47	0.1660	47
3	312	1-26	0.2420	86
4	512	3-12	0.4010	192
5	712	5-43	0.5571	343
6	812	7-10	0.6360	430
7	912	8-48	0.7146	528
8	1032	11-00	0.8100	660
9	1152	13-26	0.9030	806
10	1272	16-00	0.9960	960
11	1392	18-51	1.0910	1131
12	1512	21-49	1.1830	1309
13	1612	24-26	1.2620	1466
14	1692	26-36	1.3250	1596
15	1772	28-50	1.3900	1730

CONSTANT PRESSURE FILTRATION OF NATROSOL HR SOLUTIONS

Slurry: 2.5% $CaCO_3$ in 0.1% Natrosol HR Solution

ΔP= 200 psi Temperature: 25° C

S. No.	Volume of Filtrate in c. c.	Time in M. S.	V Ft^3/Ft^2	θ in secs.
1	312	1-31	0.2420	91
2	512	2-36	0.4010	156
3	712	4-08	0.5571	248
4	912	6-05	0.7146	365
5	1112	8-30	0.8710	510
6	1252	10-23	0.9810	623
7	1392	12-24	1.090	744
8	1512	14-11	1.185	851
9	1632	16-01	1.279	961
10	1772	18-25	1.389	1105
11	1892	20-32	1.482	1232
12	2012	22-45	1.574	1365
13	2212	25-54	1.730	1554
14	2312	28-13	1.810	1693
15	2432	30-33	1.902	1833

CONSTANT PRESSURE FILTRATION OF NATROSOL HR SOLUTIONS

Slurry: 2.5% $CaCO_3$ in 0.1% Natrosol HR Solution

ΔP= 250 psi Temperature: 25° C

S. No.	Volume of Filtrate in c. c.	Time in M. S.	V Ft^3/Ft^2	θ in secs.
1	412	1-38	0.3226	98
2	712	2-59	0.5571	179
3	912	4-16	0.7146	256
4	1112	5-52	0.8710	352
5	1332	7-52	1.0420	472
6	1512	9-42	1.1830	582
7	1712	11-58	1.3400	718
8	1912	14-18	1.4980	858
9	2112	16-50	1.6510	1010
10	2312	19-32	1.8100	1172
11	2512	22-27	1.9630	1347
12	2712	25-34	2.1200	1534

CONSTANT PRESSURE FILTRATION OF NATROSOL HR SOLUTIONS

Slurry: 2.5% $CaCO_3$ in 0.2% Natrosol HR Solution

ΔP = 150 psi Temperature: 25° C

S. No.	Volume of Filtrate in c. c.	Time in M. S.	V Ft^3/Ft^2	θ in secs.
1	112	0-42	0.0877	42
2	212	1-56	0.1660	116
3	312	3-53	0.2420	233
4	412	6-37	0.3221	397
5	512	10-26	0.4010	626
6	572	13-22	0.4480	802
7	632	17-13	0.4950	1033
8	692	21-59	0.5410	1319
9	732	26-04	0.5730	1564
10	772	31-06	0.6045	1866
11	812	37-26	0.6360	2246
12	852	44-27	0.6660	2667

CONSTANT PRESSURE FILTRATION OF NATROSOL HR SOLUTIONS

Slurry: 2.5% $CaCO_3$ in 0.2% Natrosol HR Solution

ΔP= 250 psi Temperature: 25° C

S. No.	Volume of Filtrate in c. c.	Time in M. S.	V Ft^3/Ft^2	θ in secs.
1	112	0-33	0.0877	33
2	212	1-38	0.1660	98
3	312	3-03	0.2420	183
4	412	4-47	0.3221	287
5	512	6-53	0.4010	413
6	612	9-39	0.4798	579
7	712	12-48	0.5571	768
8	792	16-01	0.6200	961
9	872	19-39	0.6830	1179
10	932	22-34	0.7300	1353
11	992	25-50	0.7762	1550
12	1052	29-23	0.8250	1763
13	1112	33-27	0.8700	2007
14	1172	35-55	0.9183	2155

CONSTANT PRESSURE FILTRATION OF NATROSOL HR SOLUTIONS

Slurry: 2.5% $CaCO_3$ in 0.2% Natrosol HR Solution

ΔP= 350 psi Temperature: 25° C

S. No.	Volume of Filtrate in c. c.	Time in M. S.	V Ft^3/Ft^2	θ in secs.
1	112	0-42	0.0877	42
2	212	1-14	0.1666	74
3	312	2-10	0.2420	130
4	412	3-25	0.3221	205
5	532	5-26	0.4160	326
6	612	7-09	0.4798	429
7	712	9-48	0.5571	588
8	792	12-17	0.6200	737
9	872	15-12	0.6830	912
10	952	18-31	0.7451	1111
11	1012	21-19	0.7940	1279
12	1072	24-23	0.8410	1463
13	1112	26-44	0.8715	1604
14	1152	29-11	0.9040	1751
15	1212	33-03	0.9500	1983

CONSTANT PRESSURE FILTRATION OF NATROSOL HR SOLUTIONS

Slurry: 2.5% $CaCO_3$ in 0.3% Natrosol HR Solution

ΔP= 150 psi Temperature: 25° C

S. No.	Volume of Filtrate in c. c.	Time in M. S.	V Ft^3/Ft^2	θ in secs.
1	315	2-34	0.2464	154
2	355	4-13	0.2780	253
3	395	5-48	0.3092	348
4	435	7-38	0.3403	458
5	475	9-39	0.3720	579
6	515	12-00	0.4040	720
7	535	14-31	0.4190	871
8	615	18-45	0.4820	1125
9	635	20-09	0.4970	1209
10	675	23-28	0.5290	1408
11	695	25-15	0.5449	1515

CONSTANT PRESSURE FILTRATION OF NATROSOL HR SOLUTIONS

Slurry: 2.5% $CaCO_3$ in 0.3% Natrosol HR Solution

ΔP= 200 psi Temperature: 25° C

S. No.	Volume of Filtrate in c. c.	Time in M. S.	V Ft^3/Ft^2	θ in secs.
1	115	0-33	0.0900	33
2	175	1-07	0.1370	67
3	215	1-35	0.1682	95
4	315	3-04	0.2462	184
5	375	4-13	0.2936	253
6	415	5-08	0.3242	308
7	475	6-49	0.3720	409
8	535	8-48	0.4190	528
9	575	10-15	0.4500	615
10	615	11-46	0.4820	706
11	675	14-12	0.5290	852
12	735	16-54	0.5750	1014
13	775	18-53	0.6060	1133

CONSTANT PRESSURE FILTRATION OF NATROSOL HR SOLUTIONS

Slurry: 2.5% $CaCO_3$ in 0.3% Natrosol HR Solution

ΔP= 300 psi Temperature: 25° C

S. No.	Volume of Filtrate in c. c.	Time in M. S.	V Ft^3/Ft^2	θ in secs.
1	292	1-53	0.2285	113
2	352	3-14	0.2780	194
3	412	4-50	0.3242	290
4	472	6-39	0.3720	399
5	532	8-27	0.4190	507
6	592	10-27	0.4640	627
7	652	12-50	0.5105	770
8	712	15-42	0.5580	942
9	752	17-50	0.5898	1070
10	792	20-11	0.6200	1211
11	832	22-38	0.6520	1358
12	892	26-52	0.6990	1612
13	932	30-01	0.7300	1801
14	972	33-35	0.7610	2015

APPENDIX C

CONSTANT RATE FILTRATION OF AQUEOUS SLURRIES

Record of Variation of Pressure Drop With Time

Slurry: 2.5% $CaCO_3$ in Water θ_c = 30 secs.

Rotameter Reading: 8.0 $q_1 = 3.29 \times 10^{-3}$ Ft. Sec.$^{-1}$ Temp. = 25° C

S. No.	ΔP in psi	Time θ in M.S.	$(\theta + \theta_c)$ in secs	ΔP_c in psi
1	30	2-55	205	10
2	50	5-32	362	30
3	70	7-50	500	50
4	90	9-30	600	70
5	120	11-25	715	100
6	150	13-15	825	130
7	180	14-40	910	160
8	210	16-05	995	190
9	240	17-15	1065	220
10	270	18-20	1130	250
11	300	19-20	1190	280
12	330	20-18	1248	310

CONSTANT RATE FILTRATION OF AQUEOUS SLURRIES

Record of Volume of Filtrate Collected with Time

Slurry: 2.5% $CaCO_3$ in Water θ_c = 30 secs.

Rotameter Reading: 8.0 $q_1 = 3.29 \times 10^{-3}$ Ft. $Sec.^{-1}$ Temp.= 25° C

S. No.	Volume of Filtrate in c. c.	Time θ in M. S.	Volume of Filtrate in Litres	Time in Secs.
1	525	1-35	0.525	95
2	925	3-14	0.925	194
3	1325	4-51	1.325	291
4	1725	6-29	1.725	389
5	2125	8-06	2.125	486
6	2625	10-06	2.625	606
7	3125	12-06	3.125	726
8	3625	14-06	3.625	846
9	4125	16-06	4.125	966
10	4625	18-07	4.625	1087

CONSTANT RATE FILTRATION OF AQUEOUS SLURRIES

Record of Variation of Pressure Drop With Time

Slurry: 2.5% $CaCO_3$ in Water θ_c = - 18 secs.

Rotameter Reading: 8.0 q_l = 3.29 x 10^{-3} Ft. $Sec.^{-1}$ Temp. = 25° C

S. No.	ΔP in psi	Time θ in M.S.	$(\theta + \theta_c)$ in secs	ΔP_c in psi
1	30	4-15	237	12
2	50	6-41	383	32
3	70	8-35	497	52
4	100	10-54	636	82
5	120	12-00	702	102
6	150	13-45	807	132
7	170	14-45	867	152
8	200	16-10	952	182
9	220	17-05	1007	202
10	250	18-10	1072	232
11	270	18-56	1118	252
12	300	19-50	1172	282
13	350	21-15	1257	332

CONSTANT RATE FILTRATION OF AQUEOUS SLURRIES

Record of Volume of Filtrate Collected with Time

Slurry: 2.5% $CaCO_3$ in Water θ_c = - 18 secs.

Rotameter Reading: 8.0 $q_1 = 3.29 \times 10^{-3}$ Ft. Sec.$^{-1}$ Temp.= 25° C

S. No.	Volume of Filtrate in c. c.	Time θ in M. S.	Volume of Filtrate in Litres	Time in Secs.
1	525	2-21	0.525	141
2	925	3-57	0.925	237
3	1325	5-32	1.325	332
4	1725	7-07	1.725	427
5	2125	8-43	2.125	523
6	2525	10-18	2.525	618
7	2925	11-52	2.925	712
8	3125	12-40	3.125	760
9	3525	14-14	3.525	854
10	3925	15-47	3.925	947

CONSTANT RATE FILTRATION OF AQUEOUS SLURRIES

Record of Variation of Pressure Drop With Time

Slurry: 2.5% $CaCO_3$ in Water θ_c = - 53 secs

Rotameter Reading: 8.0 $q_1 = 3.29 \times 10^{-3}$ Ft. Sec.$^{-1}$ Temp. = 25° C

S. No.	ΔP in psi	Time θ in M.S.	$(\theta + \theta_c)$ in secs	ΔP_c in psi
1	30	5-18	265	16
2	50	7-44	411	36
3	70	9-39	526	56
4	100	11-57	664	86
5	120	13-15	742	106
6	150	14-55	842	136
7	170	15-52	899	156
8	200	17-21	988	186
9	220	18-15	1042	206
10	250	19-35	1122	236
11	270	20-18	1165	256
12	300	21-18	1225	286
13	350	22-58	1325	336

CONSTANT RATE FILTRATION OF AQUEOUS SLURRIES

Record of Volume of Filtrate Collected with Time

Slurry: 2.5% $CaCO_3$ in Water θ_c = - 53 secs.

Rotameter Reading: 8.0 $q_1 = 3.29 \times 10^{-3}$ Ft. Sec.$^{-1}$ Temp.= 25° C

S.No.	Volume of Filtrate in c.c.	Time θ in M.S.	Volume of Filtrate in Litres	Time in Secs.
1	525	2-54	0.525	174
2	925	4-33	0.925	273
3	1325	6-10	1.325	370
4	1725	7-49	1.725	469
5	2125	9-25	2.125	565
6	2625	11-26	2.625	686
7	3125	13-26	3.125	806
8	3625	15-26	3.625	926
9	4125	17-26	4.125	1046
10	4625	19-26	4.625	1166

CONSTANT RATE FILTRATION OF AQUEOUS SLURRIES

Record of Variation of Pressure Drop With Time

Slurry: 2.5% $CaCO_3$ in Water θ_c = - 39 secs.

Rotameter Reading: 12.0 $q_1 = 5.13 \times 10^{-3}$ Ft. Sec.$^{-1}$ Temp. = 25° C

S. No.	ΔP in psi	Time θ in M.S.	$(\theta + \theta_c)$ in secs	ΔP_c in psi
1	30	2-15	96	17
2	50	3-04	145	37
3	70	3-52	193	57
4	100	4-50	251	87
5	120	5-20	281	107
6	150	6-00	321	137
7	170	6-21	342	157
8	200	6-59	380	187
9	220	7-17	398	207
10	250	7-46	427	237
11	270	8-02	443	257
12	300	8-28	469	287
13	350	9-10	511	337
14	400	9-36	537	387
15	450	10-00	561	437

CONSTANT RATE FILTRATION OF AQUEOUS SLURRIES

Record of Volume of Filtrate Collected with Time

Slurry: 2.5% $CaCO_3$ in Water θ_c = - 39 secs.

Rotameter Reading: 12.0 $q_1 = 5.13 \times 10^{-3}$ Ft. Sec.$^{-1}$ Temp.= 25° C

S. No.	Volume of Filtrate in c. c.	Time θ in M. S.	Volume of Filtrate in Litres	Time in Secs.
1	325	1-30	0.325	90
2	625	2-16	0.625	136
3	1125	3-33	1.125	213
4	1625	4-48	1.625	288
5	2125	6-05	2.125	365
6	2625	7-23	2.625	443
7	3125	8-25	3.125	505
8	3525	9-38	3.525	578
9	-	-	-	-
10	-	-	-	-

CONSTANT RATE FILTRATION OF NATROSOL G SOLUTIONS

Record of Variation of Pressure Drop With Time

Slurry: 2.5% $CaCO_3$ in 0.6% Natrosol G Solution

Rotameter Reading: 4.5 $q_1 = 3.38 \times 10^{-4}$ Ft. Sec.$^{-1}$ Temp. = 25° C

S. No.	ΔP in psi	Time θ in M.S.	$(\theta + \theta_c)$ in secs	ΔP_c in psi
1	30	5-35	452	10
2	40	9-27	684	20
3	50	12-50	887	30
4	60	16-01	1078	40
5	70	19-19	1286	50
6	80	21-45	1422	60
7	90	24-01	1558	70
8	100	26-26	1703	80
9	120	29-57	1914	100
10	140	34-12	2169	120
11	160	38-20	2417	140
12	190	43-06	2703	170
13	220	47-38	2975	200

CONSTANT RATE FILTRATION OF NATROSOL G SOLUTIONS

Record of Volume of Filtrate Collected with Time

Slurry: 2.5% $CaCO_3$ in 0.6% Natrosol G Solution

Rotameter Reading: 4.5 $q_1 = 3.38 \times 10^{-4}$ Ft. Sec.$^{-1}$ Temp.= 25° C

S. No.	Volume of Filtrate in c. c.	Time θ in M. S.	Volume of Filtrate in Litres	Time in Secs.
1	225	6-37	0.225	397
2	325	10-31	0.325	631
3	405	13-36	0.405	816
4	485	16-43	0.485	1003
5	575	20-15	0.575	1215
6	655	23-17	0.655	1397
7	725	25-55	0.725	1555
8	825	29-54	0.825	1794
9	905	33-02	0.905	1982
10	1005	37-01	1.005	2221

CONSTANT RATE FILTRATION OF NATROSOL G SOLUTIONS

Record of Variation of Pressure Drop With Time

Slurry: 2.5% $CaCO_3$ in 0.6% Natrosol G Solution

Rotameter Reading: 5.0 $q_1 = 4.5 \times 10^{-4}$ Ft. Sec.$^{-1}$ Temp. = 25° C

S. No.	ΔP in psi	Time θ in M.S.	$(\theta + \theta_c)$ in secs	ΔP_c in psi
1	30	4-55	330	14
2	50	8-33	548	34
3	70	12-22	777	54
4	100	16-50	1045	84
5	120	19-30	1205	104
6	150	22-55	1410	134
7	170	24-52	1527	154
8	200	27-53	1708	184
9	220	29-29	1804	204
10	250	31-50	1945	234
11	270	33-22	2037	254
12	300	35-43	2178	284

CONSTANT RATE FILTRATION OF NATROSOL G SOLUTIONS

Record of Volume of Filtrate Collected with Time

Slurry: 2.5% $CaCO_3$ in 0.6% Natrosol G Solution

Rotameter Reading: 5.0 $q_1 = 4.5 \times 10^{-4}$ Ft. Sec.$^{-1}$ Temp.= 25° C

S. No.	Volume of Filtrate in c. c.	Time θ in M. S.	Volume of Filtrate in Litres	Time in Secs.
1	205	5-20	0.205	320
2	265	7-07	0.265	427
3	325	8-55	0.325	535
4	385	10-40	0.385	640
5	445	12-24	0.445	744
6	525	14-46	0.525	886
7	605	17-07	0.605	1027
8	675	19-06	0.675	1146
9	725	20-33	0.725	1233
10	775	22-00	0.775	1320
11	1025	29-15	1.025	1755

CONSTANT RATE FILTRATION OF NATROSOL G SOLUTIONS

Record of Variation of Pressure Drop With Time

Slurry: 2.5% $CaCO_3$ in 0.6% Natrosol G Solution

Rotameter Reading: 6.0 $q_1 = 6.49 \times 10^{-4}$ Ft. Sec.$^{-1}$ Temp. = 25° C

S. No.	ΔP in psi	Time θ in M.S.	$(\theta + \theta_c)$ in secs	ΔP_c in psi
1	50	4-57	297	20
2	70	6-55	415	40
3	100	9-45	585	70
4	120	11-05	665	90
5	150	13-15	795	120
6	170	14-25	865	140
7	200	16-05	965	170
8	220	17-00	1020	190
9	250	18-15	1095	220
10	270	18-55	1135	240
11	300	20-05	1205	270
12	350	21-45	1305	320

CONSTANT RATE FILTRATION OF NATROSOL G SOLUTIONS

Record of Volume of Filtrate Collected with Time

Slurry: 2.5% $CaCO_3$ in 0.6% Natrosol G Solution

Rotameter Reading: 6.0 $q_1 = 6.49 \times 10^{-4}$ Ft. Sec.$^{-1}$ Temp.= 25° C

S. No.	Volume of Filtrate in c. c.	Time θ in M. S.	Volume of Filtrate in Litres	Time in Secs.
1	225	4-29	0.225	269
2	305	6-11	0.305	371
3	385	7-48	0.385	468
4	465	9-26	0.465	566
5	545	11-04	0.545	664
6	625	12-41	0.625	761
7	705	14-20	0.705	860
8	785	15-56	0.785	956
9	865	17-32	0.865	1052
10	945	19-10	0.945	1150

CONSTANT RATE FILTRATION OF NATROSOL G SOLUTIONS

Record of Variation of Pressure Drop With Time

Slurry: 2.5% $CaCO_3$ in 0.8% Natrosol G Solution

Rotameter Reading: 6.0 $q_1 = 4.28 \times 10^{-4}$ Ft. Sec.$^{-1}$ Temp. = 25° C

S. No.	ΔP in psi	Time θ in M.S.	$(\theta + \theta_c)$ in secs	ΔP_c in psi
1	50	5-28	328	24
2	70	7-32	452	44
3	100	10-00	600	74
4	120	11-26	686	94
5	150	13-12	792	124
6	170	14-15	855	144
7	200	15-45	945	174
8	220	16-34	994	194
9	250	18-05	1085	224
10	270	18-57	1137	244
11	300	20-12	1212	274
12	350	22-14	1334	324

CONSTANT RATE FILTRATION OF NATROSOL G SOLUTIONS

Record of Volume of Filtrate Collected with Time

Slurry: 2.5% $CaCO_3$ in 0.8% Natrosol G Solution

Rotameter Reading: 6.0 $q_1 = 4.28 \times 10^{-4}$ Ft. Sec.$^{-1}$ Temp.= 25° C

S. No.	Volume of Filtrate in c. c.	Time θ in M. S.	Volume of Filtrate in Litres	Time in Secs.
1	205	6-20	0.205	380
2	285	8-52	0.285	532
3	365	11-19	0.365	679
4	465	14-18	0.465	858
5	575	17-37	0.575	1057
6	655	20-00	0.655	1200
7				
8				
9				
10				

CONSTANT RATE FILTRATION OF NATROSOL G SOLUTIONS

Record of Variation of Pressure Drop With Time

Slurry: 2. 5% $CaCO_3$ in 0. 8% Natrosol G Solution

Rotameter Reading: 6. 5 $q_1 = 4.78 \times 10^{-4}$ Ft. Sec.$^{-1}$ Temp. = 25° C

S. No.	ΔP in psi	Time θ in M.S.	$(\theta + \theta_c)$ in secs	ΔP_c in psi
1	50	3-00	279	24
2	70	4-45	384	44
3	100	6-55	514	74
4	120	8-05	584	94
5	150	9-35	674	124
6	180	11-13	772	154
7	200	11-55	814	174
8	230	13-10	889	204
9	260	14-12	951	234
10	300	15-30	1029	274
11	350	17-00	1119	324

CONSTANT RATE FILTRATION OF NATROSOL G SOLUTIONS

Record of Volume of Filtrate Collected with Time

Slurry: 2.5% $CaCO_3$ in 0.8% Natrosol G Solution

Rotameter Reading: 6.5 $q_1 = 4.78 \times 10^{-4}$ Ft. Sec.$^{-1}$ Temp.= 25° C

S. No.	Volume of Filtrate in c. c.	Time θ in M. S.	Volume of Filtrate in Litres	Time in Secs.
1	205	4-00	0.205	240
2	285	6-15	0.285	375
3	365	8-30	0.365	510
4	425	10-10	0.425	610
5	485	11-50	0.485	710
6	545	13-29	0.545	809
7	605	15-07	0.605	907
8	665	16-44	0.665	1004
9				
10				

CONSTANT RATE FILTRATION OF NATROSOL G SOLUTIONS

Record of Variation of Pressure Drop With Time

Slurry: 2. 5% $CaCO_3$ in 0. 8% Natrosol G Solution

Rotameter Reading: 7. 5 $q_1 = 6.22 \times 10^{-4}$ Ft. Sec.$^{-1}$ Temp. = 25° C

S. No.	ΔP in psi	Time θ in M.S.	$(\theta + \theta_c)$ in secs	ΔP_c in psi
1	50	3-35	215	24
2	80	5-34	334	54
3	110	6-58	418	84
4	140	8-19	499	114
5	170	9-20	560	144
6	200	10-18	618	174
7	230	11-20	680	204
8	260	12-07	727	234
9	290	12-58	778	264
10	320	13-45	825	294
11	350	14-24	864	324

CONSTANT RATE FILTRATION OF NATROSOL G SOLUTIONS

Record of Volume of Filtrate Collected with Time

Slurry: 2.5% $CaCO_3$ in 0.8% Natrosol G Solution

Rotameter Reading: 7.5 $q_1 = 6.22 \times 10^{-4}$ Ft. Sec.$^{-1}$ Temp.= 25° C

S. No.	Volume of Filtrate in c. c.	Time θ in M. S.	Volume of Filtrate in Litres	Time in Secs.
1	225	4-50	0.225	290
2	325	7-01	0.325	421
3	425	9-08	0.425	548
4	525	11-16	0.525	676
5	625	13-24	0.625	804
6				
7				
8				
9				
10				

CONSTANT RATE FILTRATION OF NATROSOL G SOLUTIONS

Record of Variation of Pressure Drop With Time

Slurry: 2.5% $CaCO_3$ in 1.0% Natrosol G Solution

Rotameter Reading: 5.5 $q_1 = 1.82 \times 10^{-4}$ Ft. Sec.$^{-1}$ Temp. = 25° C

S. No.	ΔP in psi	Time θ in M.S.	$(\theta + \theta_c)$ in secs	ΔP_c in psi
1	40	9-46	737	26
2	60	15-57	1108	46
3	80	21-48	1459	66
4	90	24-35	1626	76
5	100	27-22	1793	86
6	110	29-43	1934	96
7	120	32-05	2076	106
8	130	34-20	2211	116
9	140	36-21	2332	126
10				
11				
12				

CONSTANT RATE FILTRATION OF NATROSOL G SOLUTIONS

Record of Volume of Filtrate Collected with Time

Slurry: 2.5% $CaCO_3$ in 1.0% Natrosol G Solution

Rotameter Reading: 5.5 $q_1 = 1.82 \times 10^{-4}$ Ft. Sec.$^{-1}$ Temp.= 25° C

S.No.	Volume of Filtrate in c.c.	Time θ in M.S.	Volume of Filtrate in Litres	Time in Secs.
1	165	9-25	0.165	565
2	205	12-22	0.205	742
3	245	15-13	0.245	913
4	285	18-06	0.285	1086
5	325	21-00	0.325	1260
6	365	23-55	0.365	1435
7	405	26-50	0.405	1610
8				
9				
10				

CONSTANT RATE FILTRATION OF NATROSOL G SOLUTIONS

Record of Variation of Pressure Drop With Time

Slurry: 2.5% $CaCO_3$ in 1.0% Natrosol G Solution

Rotameter Reading: 6.0 $q_1 = 2.5 \times 10^{-4}$ Ft. Sec.$^{-1}$ Temp. = 25° C

S. No.	ΔP in psi	Time θ in M.S.	$(\theta + \theta_c)$ in secs	ΔP_c in psi
1	50	6-40	636	30
2	70	10-30	866	50
3	90	14-00	1076	70
4	110	16-50	1246	90
5	130	19-30	1406	110
6	150	21-45	1541	130
7	170	24-10	1686	150
8	190	26-55	1851	170
9	210	28-55	1971	190
10	230	31-10	2106	210
11	250	32-50	2206	230
12	270	34-30	2306	250

CONSTANT RATE FILTRATION OF NATROSOL G SOLUTIONS

Record of Volume of Filtrate Collected with Time

Slurry: 2.5% $CaCO_3$ in 1.0% Natrosol G Solution

Rotameter Reading: 6.0 $q_1 = 2.5 \times 10^{-4}$ Ft. Sec.$^{-1}$ Temp.= 25° C

S. No.	Volume of Filtrate in c. c.	Time θ in M. S.	Volume of Filtrate in Litres	Time in Secs.
1	205	7-39	0.205	459
2	245	9-55	0.245	595
3	285	12-24	0.285	744
4	325	14-47	0.325	887
5	365	17-06	0.365	1026
6	405	19-18	0.405	1158
7	445	21-34	0.445	1294
8	485	23-45	0.485	1425
9	545	27-04	0.545	1624
10	605	30-24	0.605	1824

CONSTANT RATE FILTRATION OF NATROSOL G SOLUTIONS

Record of Variation of Pressure Drop With Time

Slurry: 2.5% $CaCO_3$ in 1.0% Natrosol G Solution

Rotameter Reading: 7 5 $q_1 = 3.7 \times 10^{-4}$ Ft Sec^{-1} Temp. = 25° C

S. No.	ΔP in psi	Time θ in M.S.	$(\theta + \theta_c)$ in secs	ΔP_c in psi
1	60	4-47	287	17
2	80	6-55	415	37
3	100	8-25	505	57
4	120	9-45	585	77
5	150	11-25	685	107
6	170	12-15	735	127
7	200	13-35	815	157
8	220	14-20	860	177
9	250	15-37	937	207
10	300	16-58	1018	257
11	350	18-50	1130	307
12	400	20-00	1200	357

CONSTANT RATE FILTRATION OF NATROSOL G SOLUTIONS

Record of Volume of Filtrate Collected with Time

Slurry: 2.5% $CaCO_3$ in 1.0% Natrosol G Solution

Rotameter Reading: 7.5 $q_1 = 3.70 \times 10^{-4}$ Ft. Sec.$^{-1}$ Temp.= 25° C

S. No.	Volume of Filtrate in c. c.	Time θ in M. S.	Volume of Filtrate in Litres	Time in Secs.
1	225	7-46	0.225	466
2	265	9-28	0.265	568
3	305	10-52	0.305	652
4	345	12-19	0 345	739
5	385	13-44	0.385	824
6	425	15-07	0.425	907
7	465	16-33	0.465	993
8	505	17-57	0.505	1077
9	545	19-21	0.545	1161
10	585	20-47	0.585	1247

CONSTANT RATE FILTRATION OF NATROSOL HR SOLUTIONS

Record of Variation of Pressure Drop With Time

Slurry: 2.5% $CaCO_3$ in 0.1% Natrosol HR Solution

Rotameter Reading: 4.0 $q_1 = 8.46 \times 10^{-4}$ Ft. Sec^{-1} Temp. = 25° C

S. No.	ΔP in psi	Time θ in M.S.	$(\theta + \theta_c)$ in secs	ΔP_c in psi
1	30	4-05	221	12.50
2	50	6-45	381	32.5
3	70	8-45	501	52.5
4	100	11-27	663	82.5
5	120	13-12	768	102.5
6	150	15-05	881	132.5
7	170	16-25	961	152.5
8	200	18-05	1061	182.5
9	220	19-10	1126	202.5
10	250	20-22	1198	232.5
11	270	21-16	1252	252.5
12				

CONSTANT RATE FILTRATION OF NATROSOL HR SOLUTIONS

Record of Volume of Filtrate Collected with Time

Slurry: 2.5% $CaCO_3$ in 0.1% Natrosol HR Solution

Rotameter Reading: 4.0 $q_1 = 8.46 \times 10^{-4}$ Ft. Sec.$^{-1}$ Temp.= 25° C

S. No.	Volume of Filtrate in c. c.	Time θ in M. S.	Volume of Filtrate in Litres	Time in Secs.
1	125	2-23	0.125	143
2	225	3-54	0.225	234
3	325	5-27	0.325	327
4	425	6-59	0.425	419
5	525	8-31	0.525	511
6	625	10-06	0.625	606
7	725	11-37	0.725	697
8	825	13-13	0.825	793
9	925	14-46	0.925	886
10				

CONSTANT RATE FILTRATION OF NATROSOL HR SOLUTIONS

Record of Variation of Pressure Drop With Time

Slurry: 2 5% $CaCO_3$ in 0 1% Natrosol HR Solution

Rotameter Reading: 4. 5 $q_1 = 9.93 \times 10^{-4}$ Ft Sec $^{-1}$ Temp. = 25° C

S. No.	ΔP in psi	Time θ in M.S.	$(\theta + \theta_c)$ in secs	ΔP_c
1	30	3-35	160	14. 2
2	50	5-02	247	34. 2
3	80	6-58	363	64. 2
4	100	8-00	425	84. 2
5	130	9-24	509	114. 2
6	160	10-25	570	144. 2
7	190	11-24	629	174. 2
8	230	12-35	700	214. 2
9	260	13-20	745	244. 2
10	300	14-18	803	284. 2
11				
12				

CONSTANT RATE FILTRATION OF NATROSOL HR SOLUTIONS

Record of Volume of Filtrate Collected with Time

Slurry: 2.5% $CaCO_3$ in 0.1% Natrosol HR Solution

Rotameter Reading: 4.5 $q_1 = 9.93 \times 10^{-4}$ Ft. Sec.$^{-1}$ Temp.= 25° C

S.No.	Volume of Filtrate in c.c.	Time θ in M.S.	Volume of Filtrate in Litres	Time in Secs.
1	125	2-28	0.125	148
2	225	3-52	0.225	232
3	325	5-10	0.325	310
4	425	6-30	0.425	390
5	525	7-46	0.525	466
6	625	9-06	0.625	546
7	825	11-42	0.825	702
8				
9				
10				

CONSTANT RATE FILTRATION OF NATROSOL HR SOLUTIONS

Record of Variation of Pressure Drop With Time

Slurry: 2.5% $CaCO_3$ in 0.1% Natrosol HR Solution

Rotameter Reading: 5.0 $q_1 = 12.78 \times 10^{-4}$ Ft. Sec.$^{-1}$ Temp. = 25° C

S. No.	ΔP in psi	Time θ in M.S.	$(\theta + \theta_c)$ in secs	ΔP_c in psi
1	60	11-08	281	32.3
2	80	12-18	351	52.3
3	100	13-08	401	72.3
4	120	13-58	451	92.3
5	150	14-54	507	122.3
6	170	15-35	548	142.3
7	200	16-23	596	172.3
8	220	16-52	625	192.3
9	250	17-35	668	222.3
10	270	18-05	698	242.3
11	300	18-32	725	272.3
12				

CONSTANT RATE FILTRATION OF NATROSOL HR SOLUTIONS

Record of Volume of Filtrate Collected with Time

Slurry: 2.5% $CaCO_3$ in 0.1% Natrosol HR Solution

Rotameter Reading: 5.0 $q_1 = 12.78 \times 10^{-4}$ Ft. Sec.$^{-1}$ Temp.= 25° C

S. No.	Volume of Filtrate in c. c.	Time θ in M. S.	Volume of Filtrate in Litres	Time in Secs.
1	125	3-30	0.125	210
2	225	7-30	0.225	450
3	325	9-30	0.325	570
4	425	10-49	0.425	649
5	545	12-04	0.545	724
6	755	14-11	0.755	851
7	945	16-07	0.945	967
8	1125	17-56	1.125	1076
9				
10				

CONSTANT RATE FILTRATION OF NATROSOL HR SOLUTIONS

Record of Variation of Pressure Drop With Time

Slurry: 2.5% $CaCO_3$ in 0.1% Natrosol HR Solution

Rotameter Reading: 5.3 $q_1 = 13.92 \times 10^{-4}$ Ft. Sec.$^{-1}$ Temp. = 25° C

S.No.	ΔP in psi	Time θ in M.S.	$(\theta + \theta_c)$ in secs	ΔP_c in psi
1	60	4-48	166	28.3
2	80	5-32	210	48.3
3	100	6-05	243	68.3
4	120	6-40	278	88.3
5	150	7-19	317	118.3
6	170	7-41	339	138.3
7	200	8-10	368	168.3
8	230	8-35	393	198.3
9	250	8-56	414	218.3
10	270	9-20	438	238.3
11	300	9-32	450	268.3
12				

CONSTANT RATE FILTRATION OF NATROSOL HR SOLUTIONS

Record of Volume of Filtrate Collected with Time

Slurry: 2.5% $CaCO_3$ in 0.1% Natrosol HR Solution

Rotameter Reading: 5.3 $q_1 = 13.92 \times 10^{-4}$ Ft. Sec.$^{-1}$ Temp.= 25° C

S. No.	Volume of Filtrate in c. c.	Time θ in M. S.	Volume of Filtrate in Litres	Time in Secs.
1	125	3-05	0.125	185
2	245	4-26	0.245	266
3	325	5-13	0.325	313
4	425	6-07	0.425	367
5	525	7-12	0.525	432
6	645	8-22	0.645	502
7	725	9-07	0.725	547
8				
9				
10				

CONSTANT RATE FILTRATION OF NATROSOL HR SOLUTIONS

Record of Variation of Pressure Drop With Time

Slurry: 2.5% $CaCO_3$ in 0.2% Natrosol HR Solution

Rotameter Reading: 4.0 $q_1 = 3.915 \times 10^{-4}$ Ft. Sec.$^{-1}$ Temp. = 25° C

S. No.	ΔP in psi	Time θ in M.S.	$(\theta + \theta_c)$ in secs	ΔP_c in psi
1	30	3-35	285	9.2
2	50	7-15	505	29.2
3	70	10-30	700	49.2
4	100	13-50	900	79.2
5	120	15-45	1015	99.2
6	150	18-21	1171	129.2
7	170	20-10	1280	149.2
8	200	21-44	1374	179.2
9	220	23-05	1450	199.2
10	250	24-43	1553	229.2
11	270	25-42	1612	249.2
12				

CONSTANT RATE FILTRATION OF NATROSOL HR SOLUTIONS

Record of Volume of Filtrate Collected with Time

Slurry: 2.5% $CaCO_3$ in 0.2% Natrosol HR Solution

Rotameter Reading: 4.0 $q_1 = 3.915 \times 10^{-4}$ Ft. Sec.$^{-1}$ Temp.= 25° C

S. No.	Volume of Filtrate in c. c.	Time θ in M. S.	Volume of Filtrate in Litres	Time in Secs.
1	125	2-59	0.125	179
2	225	6-19	0.225	259
3	325	9-39	0.325	579
4	425	12-56	0.425	776
5	525	16-18	0.525	978
6	625	19-37	0.625	1177
7	725	22-47	0.725	1367
8	825	26-02	0.825	1562
9				
10				

CONSTANT RATE FILTRATION OF NATROSOL HR SOLUTIONS

Record of Variation of Pressure Drop With Time

Slurry: 2.5% $CaCO_3$ in 0.2% Natrosol HR Solution

Rotameter Reading: 4.3 $q_1 = 5.10 \times 10^{-4}$ Ft. Sec.$^{-1}$ Temp. = 25° C

S. No.	ΔP in psi	Time θ in M.S.	$(\theta + \theta_c)$ in secs	ΔP_c in psi
1	30	5-40	390	11.2
2	50	10-35	685	31.2
3	70	14-54	944	51.2
4	100	20-20	1270	81.2
5	150	26-42	1652	131.2
6	170	29-20	1810	151.2
7	200	30-45	1895	181.2
8				
9				
10				
11				
12				

CONSTANT RATE FILTRATION OF NATROSOL HR SOLUTIONS

Record of Volume of Filtrate Collected with Time

Slurry: 2.5% $CaCO_3$ in 0.2% Natrosol HR Solution

Rotameter Reading: 4.3 $q_1 = 5.10 \times 10^{-4}$ Ft. Sec.$^{-1}$ Temp.= 25° C

S. No.	Volume of Filtrate in c. c.	Time θ in M. S.	Volume of Filtrate in Litres	Time in Secs.
1	125	2-44	0.125	164
2	225	5-25	0.225	325
3	325	8-15	0.325	495
4	425	11-03	0.425	663
5	525	13-50	0.525	830
6	625	16-39	0.625	999
7	725	19-23	0.725	1163
8	825	22-00	0.825	1320
9	925	24-46	0.925	1486
10	1125	30-10	1.125	1810

CONSTANT RATE FILTRATION OF NATROSOL HR SOLUTIONS

Record of Variation of Pressure Drop With Time

Slurry: 2.5% $CaCO_3$ in 0.2% Natrosol HR Solution

Rotameter Reading: 4.5 $q_1 = 7.02 \times 10^{-4}$ Ft. Sec.$^{-1}$ Temp. = 25° C

S. No.	ΔP in psi	Time θ in M.S.	$(\theta + \theta_c)$ in secs	ΔP_c in psi
1	30	2-50	257	8.4
2	50	3-32	299	28.4
3	80	6-00	447	58.4
4	100	7-30	537	78.4
5	130	9-40	667	108.4
6	150	10-42	729	128.4
7	180	12-05	812	158.4
8	200	13-00	867	178.4
9	230	14-30	957	208.4
10	250	15-22	1009	228.4
11	280	16-37	1084	258.4
12				

CONSTANT RATE FILTRATION OF NATROSOL HR SOLUTIONS

Record of Volume of Filtrate Collected with Time

Slurry: 2.5% $CaCO_3$ in 0.2% Natrosol HR Solution

Rotameter Reading: 4.5 $q_1 = 7.02 \times 10^{-4}$ Ft. Sec.$^{-1}$ Temp.= 25° C

S. No.	Volume of Filtrate in c. c.	Time θ in M. S.	Volume of Filtrate in Litres	Time in Secs.
1	125	2-17	0.125	137
2	225	4-30	0.225	270
3	325	6-50	0.325	410
4	375	8-00	0.375	480
5	525	11-57	0.525	717
6	625	14-30	0.625	870
7				
8				
9				
10				

CONSTANT RATE FILTRATION OF NATROSOL HR SOLUTIONS

Record of Variation of Pressure Drop With Time

Slurry: 2.5% $CaCO_3$ in 0.2% Natrosol HR Solution

Rotameter Reading: 5.0 $q_1 = 8.57 \times 10^{-4}$ Ft. Sec.$^{-1}$ Temp. = 25° C

S. No.	ΔP in psi	Time θ in M.S.	$(\theta + \theta_c)$ in secs	ΔP_c in psi
1	50	2-57	167	18.3
2	70	4-07	237	38.3
3	100	5-32	322	68.3
4	120	6-24	374	88.3
5	150	7-12	422	118.3
6	170	7-52	462	138.3
7	200	8-34	504	168.3
8	220	9-00	530	188.3
9	250	9-47	577	218.3
10	270	10-13	603	238.3
11				
12				

CONSTANT RATE FILTRATION OF NATROSOL HR SOLUTIONS

Record of Volume of Filtrate Collected with Time

Slurry: 2.5% $CaCO_3$ in 0.2% Natrosol HR Solution

Rotameter Reading: 5.0 $q_1 = 8.57 \times 10^{-4}$ Ft. Sec.$^{-1}$ Temp.= 25° C

S. No.	Volume of Filtrate in c. c.	Time θ in M. S.	Volume of Filtrate in Litres	Time in Secs.
1	125	2-31	0.125	151
2	225	4-22	0.225	262
3	325	6-15	0.325	375
4	425	8-05	0.425	485
5	525	10-00	0.525	600
6				
7				
8				
9				
10				

CONSTANT RATE FILTRATION OF NATROSOL HR SOLUTIONS

Record of Variation of Pressure Drop With Time

Slurry: 2.5% $CaCO_3$ in 0.3% Natrosol HR Solution

Rotameter Reading: 4.3 $q_1 = 2.24 \times 10^{-4}$ Ft. Sec.$^{-1}$ Temp. = 25° C

S. No.	ΔP in psi	Time θ in M.S.	$(\theta + \theta_c)$ in secs	ΔP_c in psi
1	40	5-15	489	15.8
2	60	9-22	736	35.8
3	80	13-02	956	55.8
4	100	16-30	1164	75.8
5	120	19-27	1341	95.8
6	140	22-15	1509	115.8
7	160	24-05	1619	135.8
8	200	27-50	1844	175.8
9	240	31-12	2046	215.8
10	280	33-55	2209	255.8
11				
12				

CONSTANT RATE FILTRATION OF NATROSOL HR SOLUTIONS

Record of Volume of Filtrate Collected with Time

Slurry: 2.5% $CaCO_3$ in 0.3% Natrosol HR Solution

Rotameter Reading: 4.3 $q_1 = 2.24 \times 10^{-4}$ Ft. Sec.$^{-1}$ Temp.= 25° C

S. No.	Volume of Filtrate in c. c.	Time θ in M. S.	Volume of Filtrate in Litres	Time in Secs.
1	125	4-16	0.125	256
2	185	7-42	0.185	462
3	245	11-13	0.245	673
4	305	14-40	0.305	880
5	365	18-13	0.365	1093
6	425	21-45	0.425	1305
7				
8				
9				
10				

CONSTANT RATE FILTRATION OF NATROSOL HR SOLUTIONS

Record of Variation of Pressure Drop With Time

Slurry: 2.5% $CaCO_3$ in 0.3% Natrosol HR Solution

Rotameter Reading: 4.8 $q_l = 2.70 \times 10^{-4}$ Ft. Sec.$^{-1}$ Temp. = 25° C

S. No.	ΔP in psi	Time θ in M.S.	$(\theta + \theta_c)$ in secs	ΔP_c in psi
1	50	5-52	477	20
2	70	8-56	661	40
3	90	11-30	815	60
4	110	13-35	940	80
5	140	16-29	1114	110
6	170	19-10	1275	140
7	200	21-05	1390	170
8	240	23-30	1535	210
9	280	25-35	1660	250
10	340	28-25	1830	310
11				
12				

CONSTANT RATE FILTRATION OF NATROSOL HR SOLUTIONS

Record of Volume of Filtrate Collected with Time

Slurry: 2.5% $CaCO_3$ in 0.3% Natrosol HR Solution

Rotameter Reading: 4.8 $q_1 = 2.70 \times 10^{-4}$ Ft. Sec.$^{-1}$ Temp.= 25° C

S. No.	Volume of Filtrate in c. c.	Time θ in M. S.	Volume of Filtrate in Litres	Time in Secs.
1	175	6-20	0.175	380
2	205	7-50	0.205	470
3	245	9-45	0.245	585
4	305	12-37	0.305	757
5	365	15-32	0.365	932
6	425	18-30	0.425	1110
7	485	21-25	0.485	1285
8	545	24-17	0.545	1457
9				
10				

CONSTANT RATE FILTRATION OF NATROSOL HR SOLUTIONS

Record of Variation of Pressure Drop With Time

Slurry: 2.5% $CaCO_3$ in 0.3% Natrosol HR Solution

Rotameter Reading: 5.0 $q_l = 3.53 \times 10^{-4}$ Ft. Sec.$^{-1}$ Temp. = 25° C

S. No.	ΔP in psi	Time θ in M.S.	$(\theta + \theta_c)$ in secs	ΔP_c in psi
1	50	5-40	349	22.70
2	70	7-52	481	42.7
3	100	10-15	624	72.7
4	120	11-25	694	92.7
5	150	13-02	791	122.7
6	170	14-08	857	142.7
7	200	15-30	939	172.7
8	220	16-25	994	192.7
9	250	17-50	1079	222.7
10	270	18-35	1124	242.7
11	300	19-28	1177	272.7
12	350	21-15	1284	322.7

CONSTANT RATE FILTRATION OF NATROSOL HR SOLUTIONS

Record of Volume of Filtrate Collected with Time

Slurry: 2.5% $CaCO_3$ in 0.3% Natrosol HR Solution

Rotameter Reading: 5 0 $q_1 = 3.53 \times 10^{-4}$ Ft. Sec.$^{-1}$ Temp.= 25° C

S.No.	Volume of Filtrate in c.c.	Time θ in M.S.	Volume of Filtrate in Litres	Time in Secs.
1	125	3-45	0.125	225
2	185	6-14	0.185	374
3	245	8-39	0.245	519
4	305	11-05	0.305	665
5	365	13-14	0.365	794
6	425	15-28	0.425	928
7	485	17-44	0.485	1064
8				
9				
10				

CONSTANT RATE FILTRATION OF NATROSOL HR SOLUTIONS

Record of Variation of Pressure Drop With Time

Slurry: 2.5% $CaCO_3$ in 0.3% Natrosol HR Solution

Rotameter Reading: 5.5 $q_1 = 3.97 \times 10^{-4}$ Ft. Sec.$^{-1}$ Temp. = 25° C

S. No.	ΔP in psi	Time θ in M.S.	$(\theta - \theta_c)$ in secs	ΔP_c
1	60	5-08	282	20.8
2	100	7-55	449	60.8
3	140	9-46	560	100.8
4	180	11-27	661	140.8
5	220	12-40	734	180.8
6	260	13-55	809	220.8
7	300	14-55	869	260.8
8	350	16-00	934	310.8
9	400	17-00	994	360.8
10	450	17-40	1034	410.8
11				
12				

CONSTANT RATE FILTRATION OF NATROSOL HR SOLUTIONS

Record of Volume of Filtrate Collected with Time

Slurry: 2.5% $CaCO_3$ in 0.3% Natrosol HR Solution

Rotameter Reading: 5.5 $q_1 = 3.97 \times 10^{-4}$ Ft. Sec.$^{-1}$ Temp. = 25° C

S. No.	Volume of Filtrate in c. c.	Time θ in M. S.	Volume of Filtrate in Litres	Time in Secs.
1	125	4-28	0.125	268
2	185	6-22	0.185	382
3	245	8-24	0.245	504
4	305	10-25	0.305	625
5	365	12-23	0.365	743
6	425	14-18	0.425	858
7	485	16-17	0.485	977
8				
9				
10				

CONSTANT RATE FILTRATION OF NATROSOL HR SOLUTIONS

Record of Variation of Pressure Drop With Time

Slurry: 2.5% $CaCO_3$ in 0.3% Natrosol HR Solution

Rotameter Reading: 7.0 $q_1 = 5.69 \times 10^{-4}$ Ft. Sec.$^{-1}$ Temp. = 25° C

S. No.	ΔP in psi	Time θ in M.S.	$(\theta + \theta_c)$ in secs	ΔP_c in psi
1	50	5-18	194	16
2	80	6-33	269	46
3	100	7-00	296	66
4	140	8-15	371	106
5	180	8-50	406	146
6	240	9-35	451	206
7	320	10-00	476	286
8				
9				
10				
11				
12				

CONSTANT RATE FILTRATION OF NATROSOL HR SOLUTIONS

Record of Volume of Filtrate Collected with Time

Slurry: 2.5% $CaCO_3$ in 0.3% Natrosol HR Solution

Rotameter Reading: 7.0 $q_1 = 5.69 \times 10^{-4}$ Ft. Sec.$^{-1}$ Temp.= 25° C

S.No.	Volume of Filtrate in c.c.	Time θ in M.S.	Volume of Filtrate in Litres	Time in Secs.
1	125	3-47	0.125	227
2	225	7-16	0.225	436
3	305	9-11	0.305	551
4	365	10-24	0.365	624
5				
6				
7				
8				
9				
10				

APPENDIX D

SAMPLE CALCULATION OF CONSTANT PRESSURE FILTRATION DATA

The following is the program used to fit the constant pressure filtration data to Equation (108) by the method of least squares utilizing a digital Computer IBM 360. The form of equation used in the computation is

$$Y = A + B(X)^{D-1} + C(X)^{D}$$

The notation used in computation is explained below in terms of notation used in Equation (108).

$A = \theta_o$ $\qquad$ $D = \frac{n+1}{n}$

$B = N$ $\qquad$ $Y = \theta$

$C = \frac{1}{K}$ $\qquad$ $X = v$

****

```
      Dimension Y(20), X(20), D(74)
      Double Precision Y, X, D, SUMXD1, SUMXD, SUMY, SUMX22,
        SUMX21, SMXD1Y, SUMX2D, SUMXDY, W11, W12, W13,
        W14, W21, W22, W23, W24, W31, W32, W33, W34, TERM,
        RES1, RES2, A, B, C
      DATA D/2.00, 2.01, 2.02, 2.03, 2.04, 2.05, 2.06, 2.07,
        2.08, 2.09, 2.10, 2.11, 2.12, 2.13, 2.14, 2.15, 2.16, 2.17,
        2.18, 2.19, 2.20, 2.21, 2.22, 2.23, 2.24, 2.25, 2.26, 2.27,
        2.28, 2.29, 2.30, 2.31, 2.32, 2.33, 2.34, 2.35, 2.36,
        2.37, 2.38, 2.39, 2.40, 2.41, 2.42, 2.43, 2.44, 2.45, 2.46,
        2.47, 2.48, 2.49, 2.50, 2.51, 2.52, 2.53, 2.54, 2.55, 2.56,
        2.57, 2.58, 2.59, 2.60, 2.61, 2.62, 2.63, 2.64, 2.65, 2.66,
        2.67, 2.68, 2.69, 2.70, 2.71, 2.72, 2.73/
C******Constant Pressure Filtration Using Nitrosol Solutions
```

```
      Do 50 ITest = 1, 36
      Read (1, 10)N, IPSI, Conc
10    Format (12, 13, F4. 2)
      Read (1, 2) (Y(J), X(J), J=1, N)
2     Format (F6. 0, F8. 4)
      Write (3, 40)IPSI, Conc, N
40    Format (1Hl, 5X, 'Constant Pressure Filtration', 'Deltap=',
      I3, 2X, 'Concentration=', F4. 2, 5X, 'Data Points=', I2////)
      Write (3, 8)
8     Format (5X, ' The Data Points Are : Y and X for Theta and V/A')
      Write (3, 2) (Y(J), X(J), J=1, N)
      Do 80 K=1, 74
      SUMXDl=0. 0
      SUMXD=0. 0
      SUMY=0. 0
      SUMX22=0. 0
      SUMX21=0. 0
      SUMXDlY=0. 0
      SUMX2D=0. 0
      SUMXDY=0. 0
      SUMX22=0. 0
      SUMX21=0. 0
      DO 70 J=1, N
      SUMXDl=SUMXDl+( X(J)**(D(K)-1))
      SUMXD=SUMXD+(X(J)**D(K))
      SUMY=SUMY+Y(J)
      SUMX22=SUMX22+(X(J)**(2*D(K)-2. 1))
      SUMX21=SUMX21+(X(J)**(2*D(K)-1. ))
      SMXDlY=SMXDlY+((X(J)**(D(K)-1))*Y(J))
      SUMX2D=SUMX2D+( X(J)**(2*D(K)))
```

```
      SUMXDY=SUMXDY+((X(J)**D(K))*Y(J))
70    CONTINUE
      W11=N
      W12=SUMXD1
      W13=SUMXD
      W14=SUMY
      W21=SUMXD1
      W22=SUMX22
      W23=SUMX21
      W24=SMXD1Y
      W31=SUMXD
      W32=SUMX21
      W33=SUMX2D
      W34=SUMXDY
      DENOM=W11*(W22*W33-W32*W23)-W12*(W21*W33-W31*W23)
        +W13*(W21*W32-W31*W22)
      A=(W14*(W22*W33-W32*W23)-W12*(W24*W33-W34*W23)
        +W13*(W24*W32-W34*W22))/DENOM
      B=(W11*(W24*W33-W34*W23)-W14*(W21*W33-W31*W23)
        +W13*(W21*W34-W31*W24))/DENOM
      C=(W11*(W22*W34-W32*W24)-W12*(W21*W34-W31*W24)
        +W14*(W21*W32-W31*W22))/DENOM
      RES1=0.0
      RES2=0.0
      DO 90 J=1,N
      TERM=Y(J)-(A+B*(X(J)**(D(K)-1)+(C*(X(J)**D(K))))
      RES1=RES1+TERM
      RES2=RES2+TERM*TERM
90    CONTINUE
```

```
      RES1=RES1/N
      RES2=RES2/N
      WRITE (3,100)D(K), A, B, C, RES1, RES2
100   FORMAT (1HO, 5X, 'D=', F5.2, 2X, 'A=', 1PD13.5,2X, 'B=',
        1PD13.5,2X,
      'C=', 1PD13.5,2X, 'RES1=', 1PD13.5,2X, 'RES2=', 1PD15.8)
80    CONTINUE
50    CONTINUE
      RETURN
      END
```

****

The run conducted at 250 psi with 1.0% Natrosol G solution containing 2.5% $CaCO_3$ is chosen for the sample calculation.

The values of A. B. C and D obtained from computation by fitting the data to the equation with minimum variance are given below.

$A = 20$, $B = 6.5835 \times 10^2$, $C = 5.15304 \times 10^3$,

and $D = 2.54$

(i) Calculation of 'n' and 'θ_o'

$$A = \theta_o = 20 \text{ secs}$$

$$D = \frac{n+1}{n} = 1 + \frac{1}{n} = 2.54$$

$$n = \frac{1}{(D-1)} = \frac{1}{1.54} = 0.650$$

$$n = 0.650$$

(ii) Calculation of α_T

$$K = \frac{1}{C} = \frac{1}{5.153 \times 10^3} = 1.93 \times 10^{-4}$$

Mass fraction of solids in slurry - S = 0.025

Density of 1.0% Natrosol G Solution = 1.01695 gm/c. c.

= 1.01695 x 62.4 lb m/c ft.

Ratio of mass of wet to dry cake $m = 2.1143$

Pressure drop $p = 250$ psi $= 250 \times 144$ psf.

$\mathbb{K}$ is related to α_T by the Equation (101)

as $$\mathbb{K} = \left(\frac{n+1}{n}\right)\left[\frac{p(1-ms)}{K\alpha_T \rho s}\right]^{1/n}$$

$$\alpha_T = \left[\left(\frac{n+1}{n}\right)\frac{1}{\mathbb{K}}\right]^{n}\left[\frac{p(1-ms)}{K\rho s}\right]$$

From viscometric data at $n = 0.65$

$$K = 3.58 \times 10^{-3} \text{ lbf - sec}^n/\text{ft}^2$$

substituting these values into equation for α_T

$$\alpha_T = \left(\frac{2.54}{1.93} \times 10^4\right)^{0.65}\left[\frac{250 \times 144\ (1 - 2.1143 \times 0.025)}{3.58 \times 10^{-3} \times 1.0169 \times 62.4 \times 0.025}\right]$$

$$\alpha_T = 2.89 \times 10^9 \quad \frac{\text{Ft}^{2-n}}{\text{lbm}}$$

(iii) Calculation of Rm

From Equation (102) Rm is given by

$$Rm = \frac{V_o\ \alpha_T\ \rho\ s}{(1 - ms)}$$

value of V_o from Newtonian filtration $= 0.062$

$$Rm = \frac{0.062 \times 2.89 \times 10^9 \times 1.0169 \times 62.4 \times 0.025}{(1 - 2.1143 \times 0.025)}$$

$$Rm = 0.295 \times 10^9\ \text{Ft}^{-n}$$

(iv) Calculation of J_{Rn}

J_{Rn} is given by the equation

$$J_{Rn} = \frac{\alpha_T}{\alpha_R}$$

The value of α_R from Newtonian filtration under the same condition of pressure is 8.86×10^{10}.

$$\alpha_T = 2.89 \times 10^9$$

$$J_{Rn} = \frac{2.89 \times 10^9}{8.86 \times 10^{10}}$$

$$J_{Rn} = 0.033$$

(v) Calculation of λ from K

$$\lambda = \frac{K \alpha_T \rho s}{(1 - ms)}$$

But $$K = \left(\frac{n+1}{n}\right)\left[\frac{p(1-ms)}{K \alpha_T \rho s}\right]^{1/n}$$

Therefore $$K = \left(\frac{n+1}{n}\right)\left[\frac{p}{\lambda}\right]^{1/n}$$

Hence $$\lambda = p\left(\frac{n+1}{n}\ \frac{1}{K}\right)^n$$

here, $n = 0.65, \frac{n+1}{n} = 2.54$

$K = 1.93 \times 10^{-4}$ and $p = 250 \times 144$

$$\lambda = 250 \times 144 \left(2.54 \times \frac{10^4}{1.93}\right)^{0.65}$$

$$\lambda = 1.602 \times 10^7 \ \frac{\text{lbf. sec}^n}{\text{ft}^{3+n}}$$

APPENDIX E

SAMPLE CALCULATION OF CONSTANT RATE FILTRATION DATA

(i) Calculation of θ_c

The data collected during the constant rate filtration run conducted with 0.6% Natrosol G Solution at the velocity of 3.38 ft./sec. is chosen for the sample calculation.

Volumetric flow rate = V = 0.428 cc/sec.

Initial volume = V_o = 50 cc

so time correction to be applied $\theta_c = \frac{50}{0.428}$

θ_c = 117 secs.

(ii) Determination of p_1

The computer program utilized to determine proper p_1 yielding minimum variance in the plot of $(\theta + \theta_c)$ versus $(p - p_1)$ is given on the next page.

```
      Dimension THETA(20), DP(20), Y(20), X(20), DPM(50)
      DATA DPM/1. 0, 2. 0, 3. 0, 4. 0, 5. 0, 6. 0, 7. 0, 8. 0, 9. 0, 10. 0, 11. 0,
       12. 0, 13. 0, 14. 0, 15. 0, 16. 0, 17. 0, 18. 0, 19. 0, 20. 0, 21, 0, 22. 0,
       23. 0, 24. 0, 25. 0, 26. 0, 27. 0, 28. 0, 29. 0, 30. 0, 31. 0, 32. 0, 33. 0, 34. 0,
         35. 0, 36. 0, 37. 0, 38. 0, 39. 0, 40. 0, 41. 0, 42. 0, 43. 0, 44. 0, 45. 0,
         46. 0, 47. 0, 48. 0, 49. 0/
C     Constant Rate Filtration of Natrosol Solutions.
1     READ (1, 10) N, FLOW, CONC
10    FORMAT (6X, I2, F6. 4, F4. 2)
      IF (N. EQ. 0) GO TO 80
      WRITE (3, 11) N, FLOW, CONC
11    FORMAT (1H1, 5X, 'CONSTANT RATE FILTARION'2X, 'DATA
        POINTS=', I2,
       2X, 'FLOW RATE=', F6. 4 2X, 'CONCENTRATION=', F4. 2/)
      READ(1 20)(THETA(J), DP(J), J=1, N)
20    FORMAT (6X, F5. 0, F4. 0)
      WRITE(3, 20)(THETA(J), DP(J), J=1, N)
      DO 50 K=1, 49
      DO 30 J=1, N
      Y(J)=ALOG(THETA(J))
      X(J)=ALOG(DP(J)-DPM(K))
30    CONTINUE
      SIGMAX=0. 0
      SIGMAY=0. 0
      SUMXY=0. 0
      SUMX2=0. 0
      SUMY2=0. 0
      DO 60 J=1, N
      SIGMAX=SIGMAX+X(J)
      SIGMAY=SIGMAY+Y(J)
```

```
      SUMXY=SUMXY+Y(J)*X(J)
      SUMX2=SUMX2+X(J)**2
      SUMY2=SUMY2+Y(J)**2
60    CONTINUE
      DENOM=N*SUMX2-SIGMAX**2
      A=(SIGMAY*SUMX2-SIGMAX*SUMXY)/DENOM
      B=(N*SUMXY-SIGMAY*SIGMAX)/DENOM
      RES1=0.0
      RES2=0.0
      DO 70 J=1,N
      TERM=Y(J)-(A+B*X(J))
      RES1=RES1+TERM
      RES2=RES2+TERM*TERM
70    CONTINUE
      RES1=RES1/N
      RES2=RES2/N
      WRITE (3.100) DPM(K), A, B, RES2
100   FORMAT (5X,'DPM=', F5.2, 2X,'A=', E12.6 2X,'B=', E12.6.2X,
        'RES2=',
       E12.6)
50    CONTINUE
      GO TO 1
80    RETURN
      END
```

****

For the run conducted with 0.6% Natrosol G Solution at the velocity of 3.38×10^{-4} ft/sec, the value of p_1 is 26.0 psi.

(iii) Calculation of 'n' and λ

Data collected during the constant rate filtration runs conducted with 0.6% Natrosol G Solution are chosen for calculation in this case.

After plotting the data according to Equations (117) and (118), the following values for m_o, r_o, n_1 and λ_o are obtained.

$$m_o = 0.155$$
$$r_o = 0.9695$$
$$n_1 = 0.065$$
$$\lambda_o = 9.24 \times 10^2$$

As per the Equation (114) n at 150 psi is given by

$$n = n_1 + m_o \log (p - p_1)$$

$$n = 0.065 + 0.155 \log (150 \times 144)$$

$$n = 0.065 + 0.671$$

Finally, $n = 0.736$

According to Equation (113), λ at 150 psi is given by

$$\lambda = \lambda_o (p - p_1)^{r_o}$$

$$\lambda = 9.24 \times 10^2 (150 \times 144)^{0.9695}$$

$$\lambda = 1.451 \times 10^7 \ \frac{\text{lbf sec}^n}{\text{ft}^{3+n}}$$